

AD-A094 003

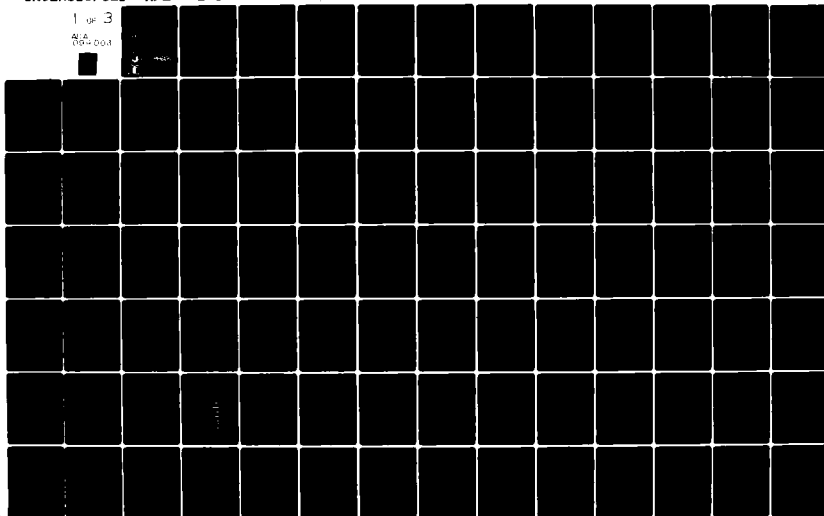
AIR FORCE ENGINEERING AND SERVICES CENTER TYNDALL AF--ETC F/6 13/2
ANALYSIS FOR THE ACCURACY DEFINITION OF THE AIR QUALITY ASSESS--ETC(U)
MAR 80 R J YAMARTINO; L A CONLEY; D M ROTE
AFESC/ESL-TR-80-19-VOL-2

UNCLASSIFIED

NL

1 of 3

AIA
00-001



19/1 42 / ESL-TR-8Q-19-1

AD A094003

**ANALYSIS FOR THE ACCURACY DEFINITION
OF THE AIR QUALITY ASSESSMENT MODEL
(AQAM) AT WILLIAMS AIR FORCE BASE,
ARIZONA
VOLUME II. APPENDICES.**

2

R. J. YAMARTINO, L. A. COMLEY, D. M. ROTE
ARGONNE NATIONAL LABORATORY
9700 SOUTH CASS AVENUE
ARGONNE, ILLINOIS 60439

LEVEL II

MARCH 1980

FINAL REPORT

JULY 1976 - MARCH 1980

DTIC
ELECTE
OCT 28 1980
S D E

APPROVED FOR PUBLIC RELEASE; DISTRIBUTION UNLIMITED

DDC FILE COPY



**ENGINEERING AND SERVICES LABORATORY
AIR FORCE ENGINEERING AND SERVICES CENTER
TYNDALL AIR FORCE BASE, FLORIDA 32403**

377-33 80 62

NOTICE

Please do not request copies of this report from
HQ AFESC/RD (Engineering and Services Laboratory).
Additional copies may be purchased from:

National Technical Information Service
5285 Port Royal Road
Springfield, Virginia 22161

Federal Government agencies and their contractors
registered with Defense Technical Information Center
should direct requests for copies of this report to:

Defense Technical Information Center
Cameron Station
Alexandria, Virginia 22314

UNCLASSIFIED

SECURITY CLASSIFICATION OF THIS PAGE (When Data Entered)

an attempt was made to select an isolated base from urban background emissions, the background concentration had to be accounted for in the analysis. Concentrations in the air base vicinity were extremely low when compared with background concentrations resulting from urban transport. Without the background concentration adjustments, the AQAM model tended to underpredict the pollutant concentrations. The results also indicate that AQAM is especially accurate in simulating the potential worst case airbase concentrations associated with morning hours, low wind speeds, stable atmospheric conditions, and high activity.

A

UNCLASSIFIED

SECURITY CLASSIFICATION OF THIS PAGE (When Data Entered)

PREFACE

This final report was prepared by the Energy and Environmental Systems Division of Argonne National Laboratory (ANL) under contract to USAF Engineering and Services Center, Tyndall AFB, Florida. This volume contains the supporting information and data required by the analyses presented in Volume I. The work was accomplished under Job Order Number 19009004. Lt Col Peter A. Crowley, Majors Dennis F. Naugle and Joseph B. Hotten, and Captain Harold A. Scott were the Air Force project officers.

Contributions were made by many others including Mr Edward P. Durphy, while at the University of New Mexico, Civil Engineering Research Facility (CERF) and subsequently as a statistical consultant to ANL, and Mr Karl F. Zeller, while EPA project officer.

Northrop Environmental Services provided the ambient measurement data used throughout this report.

The authors are also grateful to the following people for their technical assistance: Mr John Connolly, EPA/EMSL; Lt Blair Thisted, USAF; Ms Polly Brown, ANL; Ms Lyn Deacon, ANL; Dr Kenneth Brubaker, ANL; and Mr Simon Bremer, ANL.

A special thanks is given to Ms Louise Benson, Ms Patricia Traczyk, Ms Sally Vargo, and Ms Linda Wulf for typing this and the numerous draft manuscripts.

This report has been reviewed by the Public Affairs Office and is releasable to the National Technical Information Service (NTIS). At NTIS it will be available to the general public and foreign nationals.

This report has been reviewed and is approved for publication.

Harold A. Scott Jr
HAROLD A. SCOTT JR., Capt, USAF
Air Quality Research Engineer

Emil C. Frein
EMIL C. FREIN, Lt Col, USAF
Chief, Environics Division

Robert E. Brandon
ROBERT E. BRANDON, GS-15
Dep Dir, Engrg & Services
Laboratory

Accession For	
NTIS Class	<input checked="" type="checkbox"/>
DDC TAB	<input type="checkbox"/>
Unannounced	<input type="checkbox"/>
Justification	
By _____	
Distribution / _____	
Availability Codes	
Dist.	Available/or special
A	

TABLE OF CONTENTS

Appendix	Title	Page
APPENDIX A:	THE WILLIAMS AFB AIR QUALITY STUDY	1
1	INTRODUCTION.	1
2	MONITORING LOCATIONS AND STATION RATIONALE.	1
3	AIR QUALITY MONITORING STATION DESCRIPTION.	1
4	PRIMARY DATA FLOW	2
	a Aerometric and Meteorological Data	2
	b Emissions Data	2
5	THE AEROMETRIC DATA	3
	a Frequency Distributions.	3
	b Statistical Summaries.	3
	c Cumulative Distributions	4
	REFERENCES	4
APPENDIX B:	METEOROLOGICAL DATA: PROCESSING AND ASSUMPTIONS	46
1	INTRODUCTION.	46
2	METEOROLOGICAL DATA	46
3	STABILITY CLASS INDEX AS DETERMINED BY EPA METHOD	47
4	STABILITY CLASS INDEX AS DETERMINED BY ANL METHOD	51
5	MIXING DEPTH, DIRECT MEASUREMENT BY ACOUSTIC SOUNDER.	51
6	DEVELOPMENT OF A MIXING DEPTH ALGORITHM	51
	REFERENCES	64
APPENDIX C:	SOURCE EMISSIONS INVENTORY PROGRAM: INPUT MODIFICATIONS	65
1	INTRODUCTION.	65
2	NAMELIST DATA, REASSIGNED PROGRAM DATA.	65
3	DATA SET 4, AIRBASE AIRCRAFT AND RUNWAY TOTALS.	66
4	DATA SET 5, AIRCRAFT ACTIVITY	66
5	DATA SET 6, AIRCRAFT PARKING AREAS.	66
6	DATA SET 7, AIRCRAFT TAXIWAY PATH SEGMENTS.	67
7	DATA SET 8, AIRCRAFT RUNWAY INFORMATION	67
8	AEROSPACE GROUND EQUIPMENT EMISSIONS.	67
9	DATA SET 10, AIRCRAFT REFUELING, SPILLAGE, AND VENTING TOTALS	67
10	DATA SET 13, TRAINING FIRE POINT SOURCES.	68
	REFERENCES	68
APPENDIX D:	AIRCRAFT OPERATIONS DATA	81
1	OBJECTIVE.	81
2	BASE OPERATIONS.	81
3	DATA ACQUISITION AND REDUCTION OF AIRCRAFT TIME-IN-MODE.	81

TABLE OF CONTENTS (Cont'd)

Appendix	Title	Page
4	DETAILED AIRCRAFT ACTIVITY AT WILLIAMS AFB FOR THE PERIOD 1 JUNE 1976-30 JUNE 1977	92
	a Aircraft Mix at Williams Air Force Base.	92
	b Classification of Aircraft at Williams Air Force Base.	92
	c Definitions for Aircraft Activity Operations at WAFB	95
	d Edits to the Aircraft Activity Data Base	97
	e Full Traffic Count on Airbase Runways.	97
	f Touch-and-Go Training Flights.	101
	g Summary Report of Aircraft Activities WAFB for the Period 1 June 1976-30 June 1977	102
	REFERENCES	106
APPENDIX E: ESSAY: VERIFICATION OF SHORT-TERM AIR QUALITY MODELS USING THE GAUSSIAN DISPERSION APPROACH BY KARL ZELLER, EPA . 125		
1	INTRODUCTION.	125
2	RECOMMENDED VERIFICATION APPROACH	126
	a Discussion of Data Base.	126
	b Comparisons for Analysis	126
	c Cumulative Frequency Distributions and Error Limits.	127
	d Percent Error Distribution	129
	e Emission Submodel Adjustment	133
	f Model Verification Discussion.	135
3	CONCLUSIONS	135
	ACKNOWLEDGMENT	135
	REFERENCES	135
APPENDIX F: STATISTICAL ANALYSIS OF AIR POLLUTION DATA AND THE VALIDATION OF THE AQAM 137		
1	INTRODUCTION.	137
2	PAST AIRPORT AIR POLLUTION AND MODEL VALIDATION PROGRAMS.	137
3	DESCRIPTIVE STATISTICS AND DISTRIBUTIONAL CONSIDERATIONS.	141
4	TIME SERIES METHODS	144
5	MULTIPLE LINEAR REGRESSION ANALYSIS	147
6	RECOMMENDATIONS	149
	REFERENCES	150
	BIBLIOGRAPHY	155

TABLE OF CONTENTS (Cont'd)

Appendix	Title	Page
APPENDIX G:	STATION-BY-STATION COMPARISON OF MEASURED AND COMPUTED CONCENTRATIONS.	157
APPENDIX H:	ANALYSIS OF HIGHER REPETITION RATE DATA.	192
1	INTRODUCTION.	192
2	INDEPENDENCE OF COMPUTED HOURLY QUANTITIES FROM SAMPLING FREQUENCY. . .	193
3	THE EFFECT OF SCAN RATE ON THE AVERAGE VERTICAL WIND SPEED AND THE STANDARD DEVIATION.	198
4	THE STANDARD DEVIATION OF THE WIND DIRECTION AS A FUNCTION OF SAMPLING TIME	199
5	MEAN SQUARE EDDY VELOCITIES AND FILTERING OF THE RAPID SCAN DATA. . .	201
6	APPROXIMATE EQUATIONS RELATING VARIOUS COMPUTED PARAMETERS.	208
APPENDIX I:	PRELIMINARY TIME SERIES ANALYSIS	231
1	INTRODUCTION.	231
2	CONCLUSIONS AND RECOMMENDATIONS	233
	REFERENCES	235

LIST OF FIGURES

Figure	Title	Page
A-1	Locations of the Five Ambient Air Quality Monitoring Trailers	5
A-2	Primary Data Flow	6
A-3	Frequency Distribution for Hourly Average NO.	7
A-4	Frequency Distribution for Hourly Average NO _x	8
A-5	Frequency Distribution for Hourly Average CH ₄	9
A-6	Frequency Distribution for Hourly Average THC	10
A-7	Frequency Distribution for Hourly Average CO.	11
A-8	Frequency Distribution for Hourly Average b _{SCAT}	12
A-9	Frequency Distribution for Hourly Average NO ₂	13
A-10	Frequency Distribution for Hourly Average NMHC.	14
A-11	Frequency Distribution for Hourly Average Wind Speeds	15
A-12	Frequency Distribution for Hourly Average Wind Directions	16
A-13	Cumulative Frequency Distributions of Hourly Average NO Concentrations at Williams AFB: June 1976-June 1977.	17
A-14	Cumulative Frequency Distributions of Hourly Average NO _x Concentrations at Williams AFB: June 1976-June 1977.	18
A-15	Cumulative Frequency Distributions of Hourly Average NO ₂ Concentrations at Williams AFB: June 1976-June 1977.	19
A-16	Cumulative Frequency Distributions of Hourly Average CO Concentrations at Williams AFB: June 1976-June 1977.	20
A-17	Cumulative Frequency Distributions of Hourly Average CH ₄ Concentrations at Williams AFB: June 1976-June 1977.	21
A-18	Cumulative Frequency Distributions of Hourly Average THC Concentrations at Williams AFB: June 1976-June 1977.	22
A-19	Cumulative Frequency Distributions of Hourly Average NMHC Concentrations at Williams AFB: June 1976-June 1977.	23
A-20	Cumulative Frequency Distributions of Hourly Average Scattering Coefficients at Williams AFB	24
B-1	The Behavior of EPA Stability Index When Restricted to Changes of One Class per Hour	48
B-2	The Behavior of EPA Stability Index for Unrestricted Hourly Class Changes.	49
B-3	Frequency Distribution of Acoustic Sounder Measurements by Hour	55
B-4	Frequency Distribution of Acoustic Sounder Measurements by Month.	56
B-5	Scatter Plot of Acoustic Sounder Measured Lid Height vs Nozaki's Theoretical Model Predictions for Daytime Hours.	57
B-6	Average Daytime Depth of M ₁₂ of Layer by Acoustic Sounder.	61

LIST OF FIGURES (Cont'd)

Figure	Title	Page
B-7	Average Daytime Depth of Mixed Layer by Nozaki.	62
B-8	Mixing Depth: A Comparison of Observations vs a Theoretical Model	63
C-1	Point Source Locations Relative to Taxiways, Runways and Ambient Air Monitors.	69
C-2	Petroleum Storage Tank Locations Relative to Taxiways, Runways, and Ambient Air Monitors	70
C-3	Evaporative Hydrocarbon Source Locations Relative to Taxiways, Runways, and Ambient Air Monitors	71
C-4	Tank Truck Parking Locations Relative to Taxiways, Runways, and Ambient Air Monitors	72
C-5	Vehicle Parking Locations Relative to Taxiways, Runways, and Ambient Air Monitors.	73
C-6	Space Heating Source Locations Relative to Taxiways, Runways, and Ambient Air Monitors	74
C-7	Non-Aircraft Line Source Locations Relative to Taxiways, Runways, and Ambient Air Monitors	75
C-8	Environ Source Locations Relative to Williams Air Force Base, AZ.	76
C-9	Aircraft Parking Areas Relative to Taxiways, Runways, and Ambient Air Monitors.	77
C-10	Airbase Taxiway Segments Relative to Airbase Runway Configuration	78
D-1	Aircraft Squadrons at Williams Air Force Base	79
D-2	Locations of Taxiway Segments and Pad Areas	80
E-1	Cumulative Frequency Distribution for Site #X during Periods of <u>Y</u> Wind Direction	129
E-2	Delta Concentration: in this Example, 77-31, or 46% of the Time, the Difference between Observed and Predicted was within $\pm 20 \text{ ng/m}^3$	130
E-3	Error Limit Diagram	131
E-4	Percent Error Distribution.	132
E-5	Percent Error - Cumulative Frequency Diagram.	134
G-1a	Cumulative Frequency Distributions of CO at Station 1	157
G-1b	Cumulative Frequency Distributions of CO at Station 2	158
G-1c	Cumulative Frequency Distributions of CO at Station 3.	159
G-1d	Cumulative Frequency Distributions of CO at Station 4.	160
G-1e	Cumulative Frequency Distributions of CO at Station 5.	161

LIST OF FIGURES (Cont'd)

Figure	Title	Page
G-2a	Cumulative Frequency Distributions of THC at Station 1.	162
G-2b	Cumulative Frequency Distributions of THC at Station 2.	163
G-2c	Cumulative Frequency Distributions of THC at Station 3.	164
G-2d	Cumulative Frequency Distributions of THC at Station 4.	165
G-2e	Cumulative Frequency Distributions of THC at Station 5.	166
G-3a	Cumulative Frequency Distributions of NMHC at Station 1.	167
G-3b	Cumulative Frequency Distributions of NMHC at Station 2.	168
G-3c	Cumulative Frequency Distributions of NMHC at Station 3.	169
G-3d	Cumulative Frequency Distributions of NMHC at Station 4.	170
G-3e	Cumulative Frequency Distributions of NMHC at Station 5.	171
G-4a	Cumulative Frequency Distributions of NO _x at Station 1.	172
G-4b	Cumulative Frequency Distributions of NO _x at Station 2.	173
G-4c	Cumulative Frequency Distributions of NO _x at Station 3.	174
G-4d	Cumulative Frequency Distributions of NO _x at Station 4.	175
G-4e	Cumulative Frequency Distributions of NO _x at Station 5.	176
G-5a	Frequency Distribution of Log (AQAM II/Observation) for the Upper ~10% of Observed CO Concentration at Station 1.	177
G-5b	Frequency Distribution of Log (AQAM II/Observation) for the Upper ~10% of Observed CO Concentration at Station 2.	178
G-5c	Frequency Distribution of Log (AQAM II/Observation) for the Upper ~10% of Observed CO Concentration at Station 3.	179
G-5d	Frequency Distribution of Log (AQAM II/Observation) for the Upper ~10% of Observed CO Concentration at Station 4.	180
G-5e	Frequency Distribution of Log (AQAM II/Observation) for the Upper ~10% of Observed CO Concentration at Station 5.	181
G-6a	Frequency Distribution of Log (AQAM II/Observation) for the Upper ~10% of Observed NMHC Concentrations at Station 1.	182
G-6b	Frequency Distribution of Log (AQAM II/Observation) for the Upper ~10% of Observed NMHC Concentrations at Station 2.	183
G-6c	Frequency Distribution of Log (AQAM II/Observation) for the Upper ~10% of Observed NMHC Concentrations at Station 3.	184
G-6d	Frequency Distribution of Log (AQAM II/Observation) for the Upper ~10% of Observed NMHC Concentrations at Station 4.	185
G-6e	Frequency Distribution of Log (AQAM II/Observation) for the Upper ~10% of Observed NMHC Concentrations at Station 5.	186
G-7a	Frequency Distribution of Log (AQAM II/Observation) for the Upper ~10% of Observed CO ₂ Concentrations at Station 1.	187

LIST OF FIGURES (Cont'd)

Figure	Title	Page
G-7b	Frequency Distribution of Log (AQAM 11/Observation) for the Upper $\approx 10\%$ of Observed NO_x Concentrations at Station 1.	188
G-7c	Frequency Distribution of Log (AQAM 11/Observation) for the Upper $\approx 10\%$ of Observed NO_x Concentrations at Station 3.	189
G-7d	Frequency Distribution of Log (AQAM 11/Observation) for the Upper $\approx 10\%$ of Observed NO_x Concentrations at Station 4.	190
G-7e	Frequency Distribution of Log (AQAM 11/Observation) for the Upper $\approx 10\%$ of Observed NO_x Concentrations at Station 5.	191
H-1	Definition of Coordinates	212
H-2	Synthesized Three-Stage, Butterworth, Low-Pass Prototype Values of Components Chosen to Give $f_c = 1.67 \times 10^{-3}$ Hz or $T_c = 10$ min.	212
H-3	Frequency Response of 3-Stage Low-Pass Butterworth Filter	213
H-4	Filtered Wind Speed for Day 146, Hour 1650-1750	213
H-5	Filtered Wind Direction for Day 146, Hour 1650-1750	215
H-6	Filtered Wind Speed for Day 145, Hour 1200-1300	216
H-7	Filtered Wind Direction for Day 145, Hour 1200-1300	217
H-8	Calculated Eq. (H-31) versus Observed σ_θ : Global Values.	218
H-9	Calculated Eq. (H-31) versus Observed σ_θ : Average of Minute Values.	219
H-10	Calculated Eq. (H-31) versus Observed σ_θ : Minute Values.	220
H-11	Calculated Eq. (H-32) versus Observed σ_θ : Average of Minute Values.	221
H-12	Calculated Eq. (H-33) versus Observed σ_θ : Average of Minute Values.	222
I-1	Time Series for Observed CO Concentrations at Station 2 During August 1976	236
I-2	Frequency Spectrum for the Time Series of Observed CO Concentrations at Station 2	237
I-3	Integrated Spectral Density for Observed CO Concentrations at Station 2	238
I-4	Time Series for Observed NO_x Concentrations at Station 2 During August 1976	239
I-5	Frequency Spectrum for the Time Series of Observed NO_x Concentrations at Station 2	240
I-6	Coherence versus Periodicity of the Station 2 Observed CO and NO_x Time Series	241

LIST OF FIGURES (Cont'd)

Figure	Title	Page
1-7	Time Series for Aircraft CO Emission Rates on All Ground-Level Lines Based on Actual Hourly Aircraft Operations for August 1976	242
1-8	Frequency Spectrum for the Time Series of Aircraft CO Emission Rates	243
1-9	Coherence vs Periodicity of the Observed CO at Station 2 and the Aircraft CO Emission Rate Time Series	244

LIST OF TABLES

Table	Title	Page
A-1	Siting Rationale	25
A-2	Aircraft Activity Data Format	26
A-3	Minimum, Maximum, and Threshold Concentration Values.	27
A-4	Williams AFB Data for the Period June 1, 1976 to June 30, 1977.	28
A-5	Williams AFB Data Summary for the Month of June, 1976	29
A-6	Williams AFB Data Summary for the Month of July, 1976	30
A-7	Williams AFB Data Summary for the Month of August, 1976	31
A-8	Williams AFB Data Summary for the Month of September, 1976.	32
A-9	Williams AFB Data Summary for the Month of October, 1976.	33
A-10	Williams AFB Data Summary for the Month of November, 1976	34
A-11	Williams AFB Data Summary for the Month of December, 1976	35
A-12	Williams AFB Data Summary for the Month of January, 1977.	36
A-13	Williams AFB Data Summary for the Month of February, 1977	37
A-14	Williams AFB Data Summary for the Month of March, 1977.	38
A-15	Williams AFB Data Summary for the Month of April, 1977.	39
A-16	Williams AFB Data Summary for the Month of May, 1977.	40
A-17	Williams AFB Data Summary for the Month of June, 1977	41
A-18	Cumulative Frequency Percentile Concentrations (PPM) for WAFB Hourly NO Data: June 1976-June 1977	42
A-19	Cumulative Frequency Percentile Concentrations (PPM) for WAFB Hourly NO _x Data: June 1976-June 1977.	42
A-20	Cumulative Frequency Percentile Concentrations (PPM) for WAFB Hourly NO ₂ Data: June 1976-June 1977.	43
A-21	Cumulative Frequency Percentile Concentrations (PPM) for WAFB Hourly CO Data: June 1976-June 1977	43
A-22	Cumulative Frequency Percentile Concentrations (PPM) for WAFB Hourly CH ₄ Data: June 1976-June 1977.	44
A-23	Cumulative Frequency Percentile Concentrations (PPM) for WAFB Hourly THC Data: June 1976-June 1977.	44
A-24	Cumulative Frequency Percentile Concentrations (PPM) for WAFB Hourly NMHC Data: June 1976-June 1977	45
A-25	Cumulative Frequency Percentile Scattering Coefficients ($\times 10^{-6}$ for WAFB Hourly bSCAT Data)	45
B-1	Turner Requirement Related to Sky Cover.	51
B-2	Frequency Table of Sky Cover Codes	52

LIST OF TABLES (Cont'd)

Table	Title	Page
B-3	Insolation Classes as a Function of Solar Altitude for Cloud Cover $\leq 5/10$	52
B-4	Stability Classification Criteria	53
B-5	Acoustic Sounder Classification Codes for Williams AFB Study.	58
C-1	Engine Data (SRI)	79
C-2	Engine Data (Update).	79
C-3	Aircraft Activity (SRI)	80
C-4	Aircraft Activity (Update).	80
C-5	Aircraft Parking Area Geometries (SRI).	80
C-6	Aircraft Parking Area Geometries (Update)	81
C-7	Taxiway Segment Geometries (SRI).	81
C-8	Taxiway Segment Geometries (Update)	82
C-9	Annual Aircraft Arrivals and Departures (SRI)	83
C-10	Annual Aircraft Arrivals and Departures (Update).	83
C-11	WAFB Runway Geometries (SRI).	84
C-12	WAFB Runway Geometries (Update)	84
C-13	Aircraft Movement over Taxiway Segments	85
C-14	Service Vehicle Emissions in Kilograms per Operation (Arrival or Departure).	86
C-15	Refueling Information (JP4-Jet Fuel).	86
D-1	Schedule of Aircraft Operations	90
D-2	Time-in-Mode Data	91
D-3	Aircraft Activity Data Format	93
D-4	Monthly Summary of Aircraft Mix at WAFB	94
D-5	Classification of Transient Aircraft at WAFB.	96
D-6	Edits to Normal Operations Data at WAFB	98
D-7	Edits to Deviation Operations Data at WAFB.	100
H-1	Average Wind Direction ($\phi = \overline{WD}$)	223
H-2	Vector Mean Wind Direction ($\phi = \text{VMWD}$)	223
H-3	Standard Deviation of the Wind Direction ($\phi = \sigma_{\theta}$)	224
H-4	Average Wind Speed ($\phi = \overline{WS}$)	224
H-5	Vector Mean Wind Speed ($\phi = \text{VMWS}$)	225
H-6	Standard Deviation of the Wind Speed ($\phi = \sigma_w$)	225
H-7	Hourly Average WS ($\phi = \overline{WS}$)	225

LIST OF TABLES (Cont'd)

Table	Title	Page
H-8	Hourly Average NO_x ($\Phi = \overline{\text{NO}_x}$)	226
H-9	Standard Deviation of the Vertical Wind Speed ($\Phi = \sigma_w$)	226
H-10	Average Vertical Wind Speed ($\Phi = \bar{w}$)	226
H-11	Calculation of p for Sampling Times of 3 min and 60 min	227
H-12	Calculation of p for Sampling Times of 10 min and 60 min	227
H-13	Calculation of p for Sampling Times of 3 min and 10 min	227
H-14	Comparison of the Actual σ_θ to the σ_θ Value Calculated from Eq. (H-11) using $\tau_S=3$ min	228
H-15	Comparison of the Actual σ_θ to the σ_θ Value Calculated from Eq. (H-11) using $\tau_S=10$ min	228
H-16	Mean Square Along Wind Eddy Velocity ($\Phi = \overline{u'^2}$)	228
H-17	Mean Square Cross Wind Eddy Velocity ($\Phi = \overline{v'^2}$)	228
H-18	Mean Square Along Wind Eddy Velocity ($\Phi = \overline{u'^2}$) Computed Using a Fixed Mean	229
H-19	Mean Square Cross Wind Eddy Velocity ($\Phi = \overline{v'^2}$) Computed Using a Fixed Mean	230

ATTACHMENTS TO APPENDIX D

A	Hourly Aircraft Activity Summary; A One-Day Example, 76-08-06.	110
B	Monthly Aircraft Activity Summary; 1 June 1976-30 June 1977.	111
C	Grand Totals of Aircraft Activity, 1 June 1976-30 June 1977.	124

APPENDIX A
THE WILLIAMS AFB AIR QUALITY STUDY

1. INTRODUCTION

This appendix begins with a brief description of the Williams AFB experiment and concludes with the presentation of statistical summaries of the data acquired during the 13-month monitoring period beginning June 1976. A considerably more extensive review of the experimental operations is contained in the paper of Sheesley et al.:^{A-1} a report issued jointly by Northrup Services, Inc. and the USEPA Environmental Monitoring and Support Laboratory.

2. MONITORING LOCATIONS AND STATION SITING RATIONALE^{A-2}

The placement of the five ambient air quality monitoring trailers is shown in Fig. A-1.* The rationale for selecting these trailer locations is provided in Table A-1.*

3. AIR QUALITY MONITORING STATION DESCRIPTION^{A-2}

Each monitoring station consists of a mobile enclosure (trailer) approximately 2.4 m wide, 4.3 m long, and 3.1 m from ground to roof. The following monitoring instruments are rack-mounted in each trailer:

1. Beckman Model 6800 Air Quality Gas Chromatograph for analysis of carbon monoxide, methane, and total hydrocarbons. The Beckman 6800 has an automatic calibration capability.
2. Monitor Labs Model 8440-R/FR/DA Dual-Chamber NO/NO_x Analyzer with teflon filter, flowmeter, molybdenum NO₂-to-NO converter and 0.05 ppm full scale lowest range option.
3. R.M. Young Co. Model 35003 Gill Propeller Vane for wind speed and direction measurements.
4. MRI Integrating Nephelometer that will be used as a measure of light scattering due to particulates.

Each trailer also has an Esterline Angus L11-028 strip chart laboratory recorder for calibration and back-up purposes.

The intake system for the above air quality instruments includes a glass ballast chamber (not in system at present) to provide a sample air residence time (ratio of volume to flow rate) of at least twice the data system interrogation rate. The chamber will allow the averaging of transient high concentrations of pollutants that might otherwise pass unobserved. In addition, the Beckman 6800 has a separate mixing chamber to allow for the

*Figures and tables appear consecutively at the end of this appendix.

five-minute instantaneous sampling rate. A separate sampling train is provided for the MRI integrating nephelometer so that the aerosol size distribution will not be distorted prior to entry into the nephelometer. A "T" was installed in the air quality sampling train so that, if necessary, air could be sampled from heights other than the fixed entry port several feet above the roof of the trailer.

4. PRIMARY DATA FLOW

a. Aerometric and Meteorological Data

During the period June 1, 1976, to June 30, 1977, the U.S. EPA/Las Vegas collected reliable data at Williams AFB on five pollutants (CO, CH₄, THC, NO, NO_x) and b-scatt plus wind speed and direction from the five-station network described briefly above. The raw data, collected at one-minute intervals, was corrected for span and zero drift before computation of the hourly average quantities required for the AQAM evaluation effort. The procedure for producing the hourly-average tape (DS III) is indicated schematically in Fig. A-2 and described in detail in the report of Sheesley et al.^{A-1}

Additional meteorological data, taken routinely by the U.S. Air Force at Williams AFB, was recorded onto coding sheets, keypunched, and stored on magnetic tape. This data set also includes mixing-depth measurements taken by the EPA with an acoustic sounder. For logistical reasons, this data set was not merged (as erroneously suggested in Fig. A-2) with the aerometric data. The format and information structure of the meteorological data tape, along with details of the acoustic sounder measurement program, are also given by Sheesley et al.^{A-1} and further described in Appendix B.

b. Emissions Data

Figure A-2 also shows the essential steps taken in the creation of the source inventory data set (DS I) and the detailed aircraft activity data set (DS II). The source inventory data set was created by running the AQAM Source Emissions Inventory Code on emissions data for Williams AFB, recently compiled and coded by SRI and checked for consistency by the Air Quality Research Division of USAF/CEEDO. Modifications to the emissions inventory are described in Appendix C. The aircraft activity data set (DS II) contains hour-by-hour tallies of aircraft operations (i.e., takeoffs, landings, touch and goes, aborts, and transient aircraft arrivals and departures) broken down according to aircraft type and runway number. This data set serves as input to that version of AQAM (i.e., AQAM II), incorporating the actual hourly aircraft emissions as opposed to the version (AQAM I) that uses the fractional apportionment of total yearly aircraft operations dictated by the AQAM Source Emissions Inventory Code.

Generation of data set DS II was accomplished by processing information on each individual aircraft operation. This information, extracted from USAF Flight Forms ATC 355, ATC 90, and TW 124 by USAF student pilots and CEEDO technicians, was coded and keypunched according to the format specified in

Table A-2. Unfortunately, all the data required to produce D5-11 was not contained in available USAF flight forms. These deficiencies originally pointed out by Duncan and Dunphy,^{A-3} required the implementation of a few simplifying assumptions; none of which are presently thought to significantly alter the space-time distribution of aircraft emissions. These deficiencies and approximations are discussed in Appendix D.

5. THE AEROMETRIC DATA

a. Frequency Distributions

As a first step, preceding more detailed analyses, one generally examines the frequency distributions of the measured quantities. Visual inspection of such distributions quickly gives one an estimate of the mean, median, standard deviation, range, and statistical nature (e.g., normal, lognormal) of the measurables and occasionally reveals systematic problems in the data. For example: an uncharacteristic bimodal shape in the station 2, October CO distribution led to the discovery of an instrument calibration problem covering a two-week period. Though the pollutant distributions for each station and month were examined during the diagnostic phase, the distributions presented in Figs. A-3 to A-8 combine all stations and months, as the subtle differences between stations and months are shown more clearly in the statistical tabulations. Distributions for the "calculated" pollutants NO_2 ($\equiv \text{NO}_x - \text{NO}$) and NMHC ($\equiv \text{THC} - \text{CH}_4$) are given in Figs. A-9 and A-10, respectively.

The meteorological variables, wind speed (Fig. A-11) and wind direction (Fig. A-12) were also investigated in this manner. Of particular interest is the greatly enhanced probability of winds from the ESE and West. Subsequent analysis of this phenomenon revealed a strong correlation between wind direction and time of day. This strong diurnal dependence of the wind direction (see Fig. A-12) is characteristic of the mountain-valley flow found in the Valley of the Sun, where Williams AFB is located.

Usefulness of the frequency distribution extends beyond the diagnostic phase to the analysis phase. For example, a detailed fit of the NO and NO_x frequency distributions, assuming only a positive concentration distribution convoluted with a Gaussian instrumental resolution function, should disclose the overall accuracy, σ , of the NO/ NO_x instrument near threshold. Visual examination of the "negative concentration" tail of these distributions suggests a σ of a few ppb.

Instrument threshold and repeatability noise might also be indicated on frequency distributions of the data. If a significant problem, the repeatability noise resolution function could be folded into the experimental data to produce frequency ideograms.

b. Statistical Summaries

Before presenting a statistical summary of the aerometric data, one first must define the range of data values that are acceptable or physically

allowable given the instrument range setting, instrument threshold and accuracy, as well as "data windows" used in the program that generated the hourly average data tape (DS III). While some discussion regarding the selection of the "data windows" is given by Sheesley et al.,^{A-1} selection of threshold concentrations C_T (such that $C_{MIN} < C < C_T$ are set equal to C_T) was based on a combination of conversations with the experimenters, instrument manufacturer's specifications, and a strong desire to avoid taking the logarithm of a number (necessary in the computation of geometric means) too close to zero. The minimum, maximum, and threshold concentrations for measured, as well as computed, pollutants are given in Table A-3.

Statistical properties of the entire 13-month data sample are given in Table A-4, and for each of the 13 months individually in Tables A-5 to A-17. In these tables, the geometric mean and geometric standard deviation should be considered meaningless when the arithmetic mean is negative.

c. Cumulative Frequency Distributions

Cumulative frequency distributions for the 13-month data sample are presented (Figs. A-13 to A-20) in logprobability format for each of the pollutants. The interesting characteristic of the logprobability plot is that a lognormal distribution transforms into a straight line that intercepts the fifty percentile point at the geometric mean and has a slope proportional to the geometric standard deviation.

These figures relate to equivalent tables (A-18 to A-25) at the end of this appendix, giving the concentrations at several useful cumulative percentile levels for each pollutant species.

REFERENCES

- A-1. Sheesley, D.C., S.J. Gordon, and M.L. Ehlert, *Williams Air Force Base Air Quality Study*, Northrop Services, Inc., Report ESC-TR-79-26 (June 1979).
- A-2. Zeller, K.F., and R.B. Evans, *Airport Air Quality and Its Control*, J. APCA, 15 (Dec. 1965).
- A-3. Duncan, D., and E.P. Dunphy, *Acquisition, Production, and Analysis of Aircraft Activity Data from Williams Air Force Base, Arizona*, letter report EE-11, final report to AFCEC/EVA (for period 8 March 1976-30 June 1976).

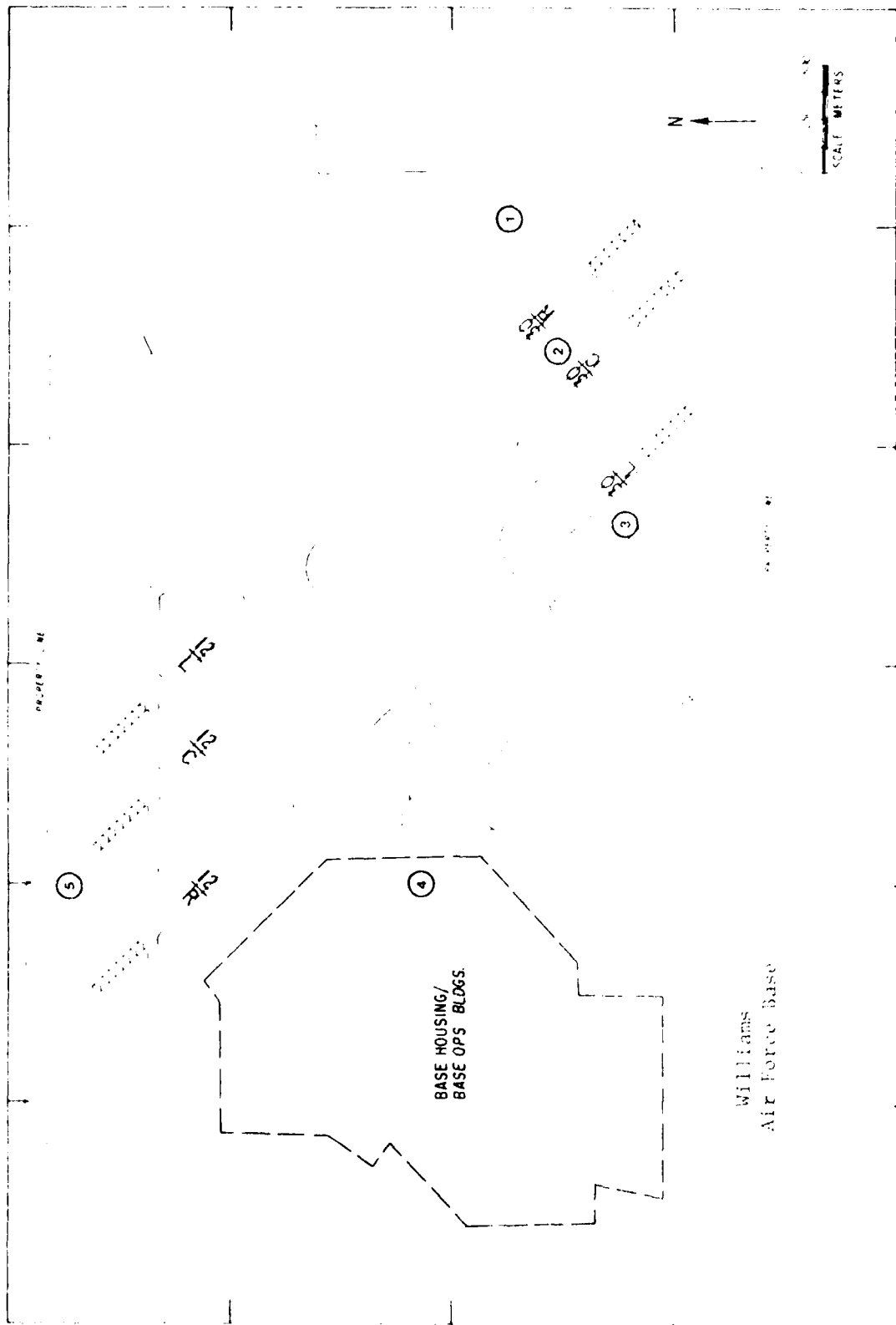


FIG. 5-1. Locations of the Five Ambient Air Quality Monitoring Trailers

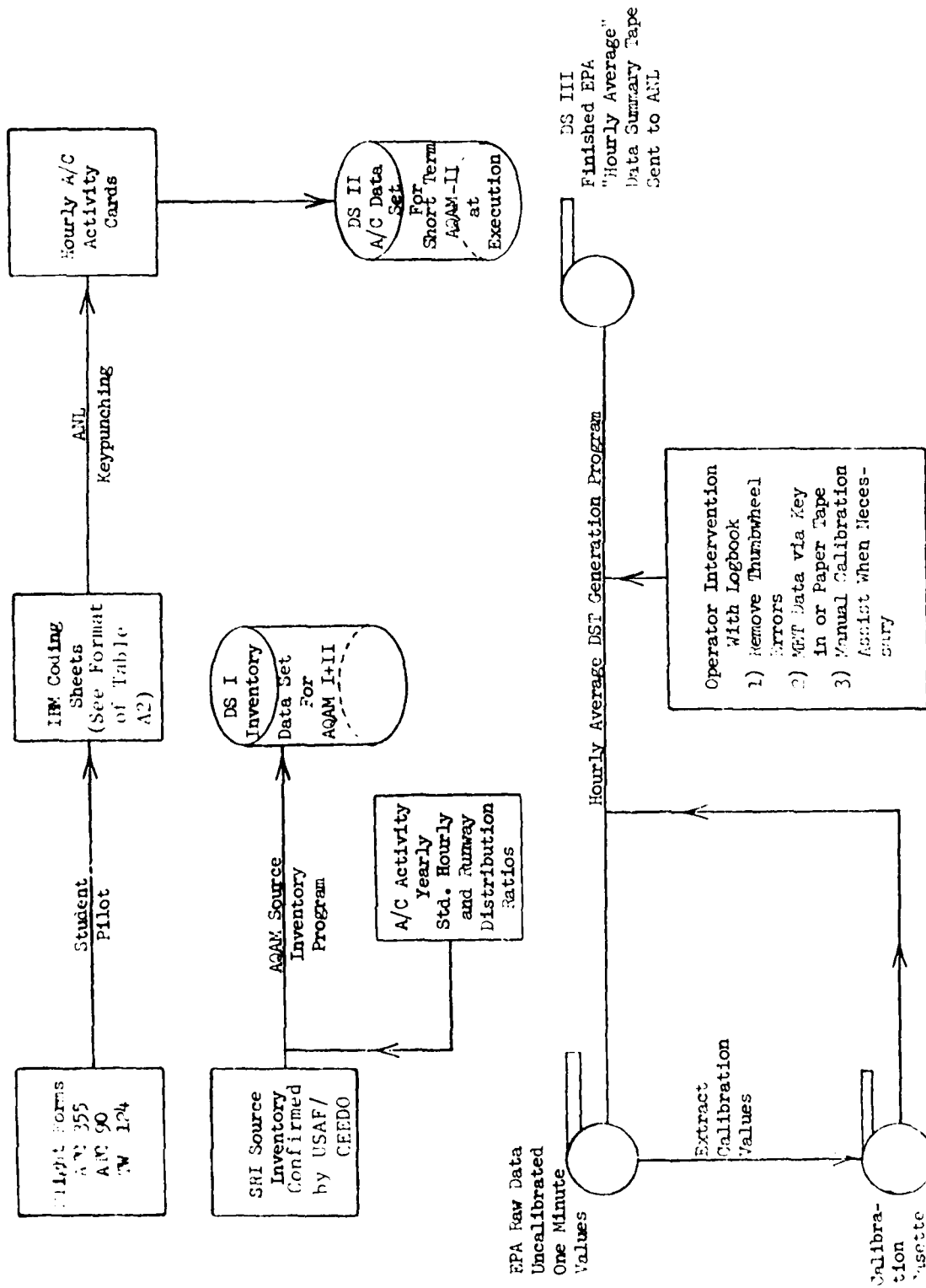


Fig. A-2. Primary Data Flow

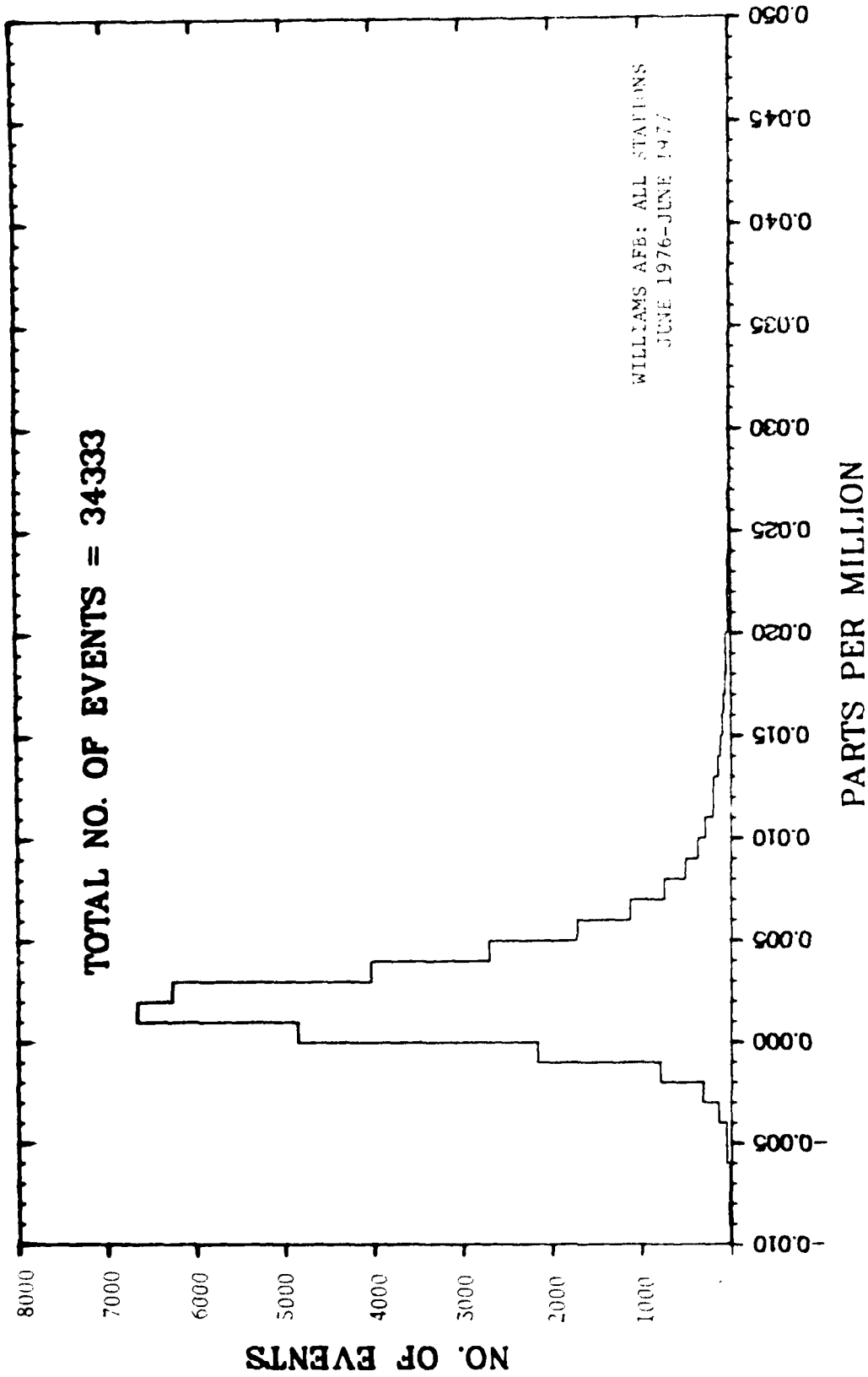


Fig. A-2. Frequency Distribution for Hourly Average 50

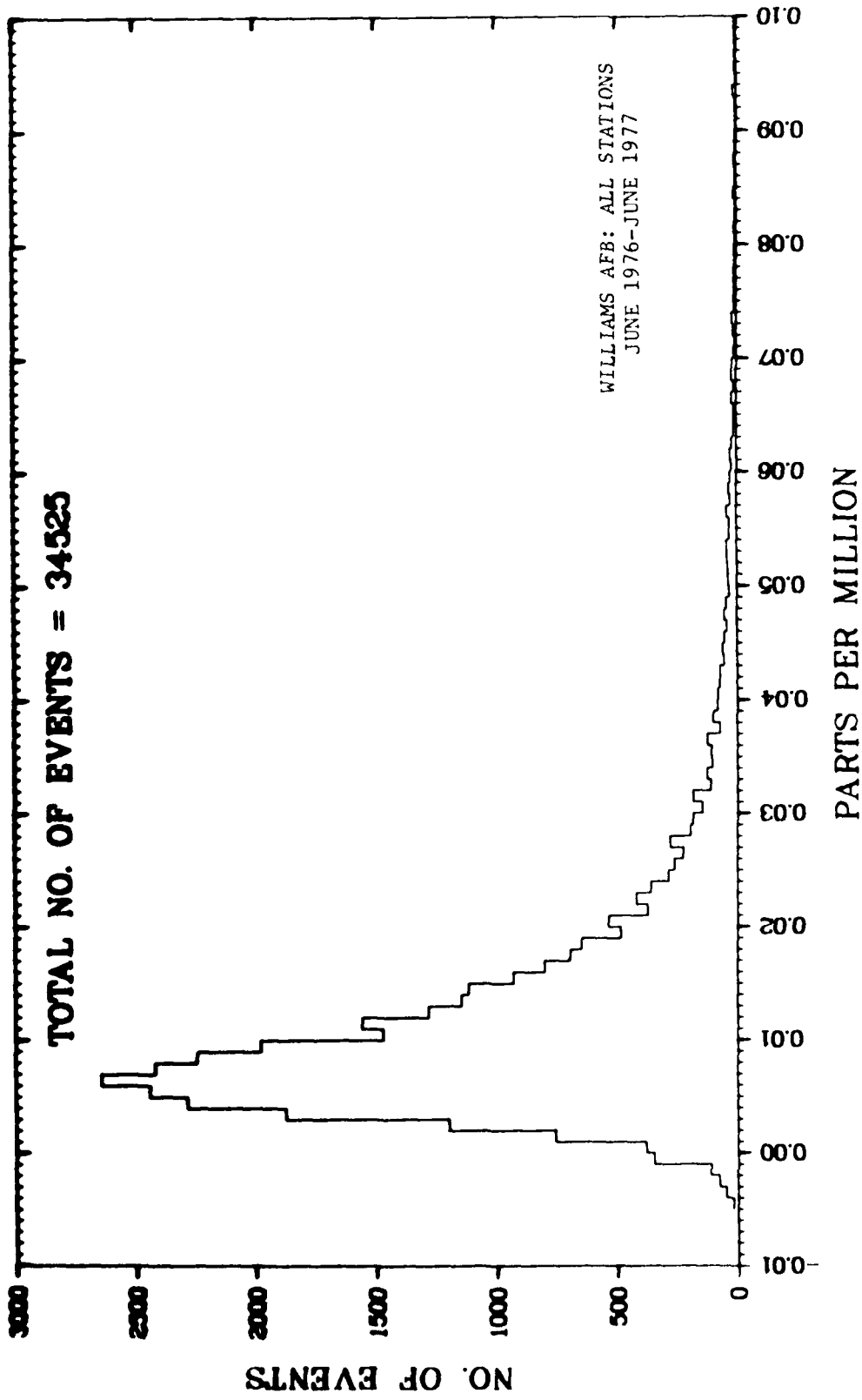


Fig. A-4. Frequency Distribution for Hourly Average NO_x

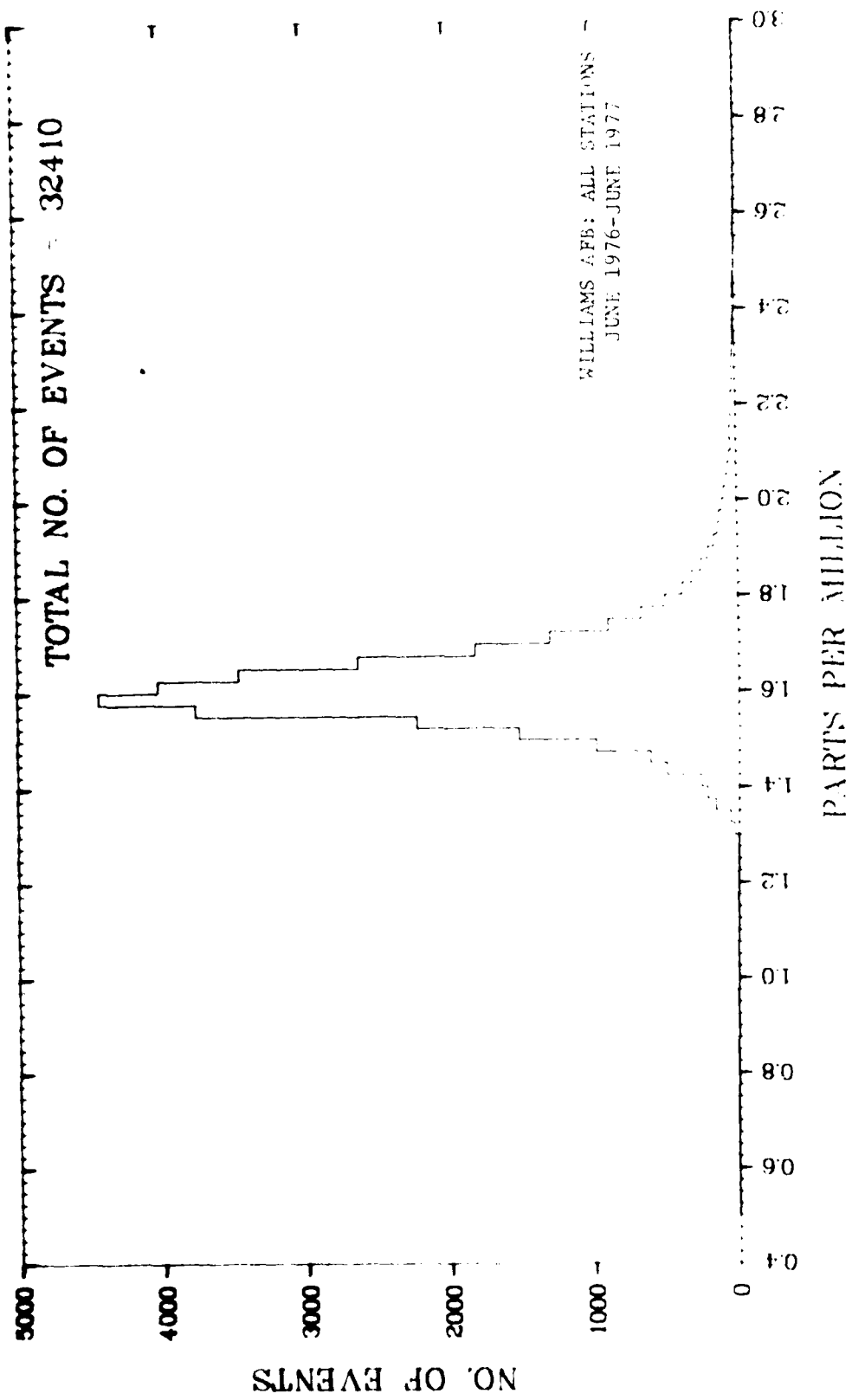


FIG. A-5. Frequency Distribution for Hourly Average CH₄

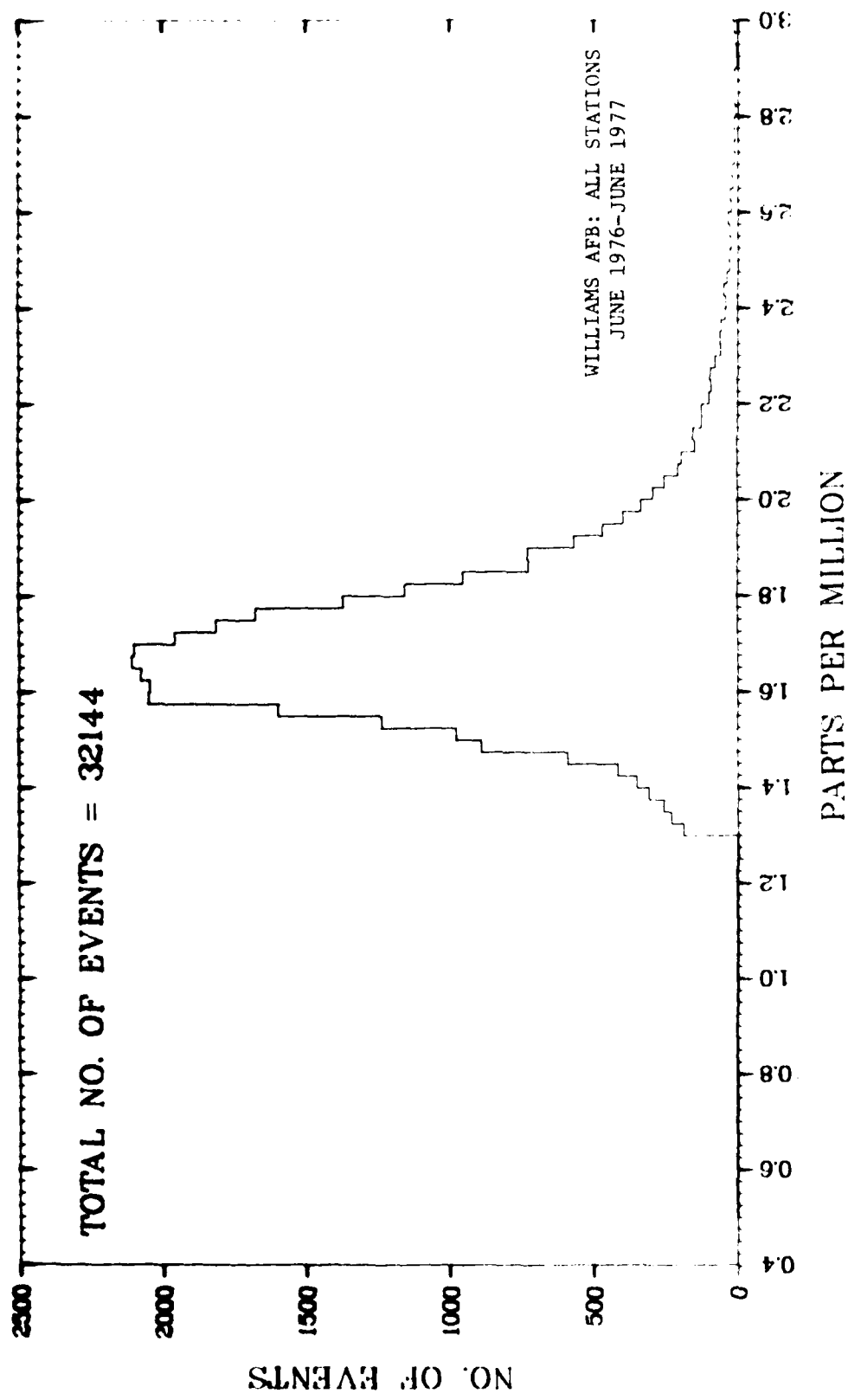


Fig. A-6. Frequency Distribution for Hourly Average THC

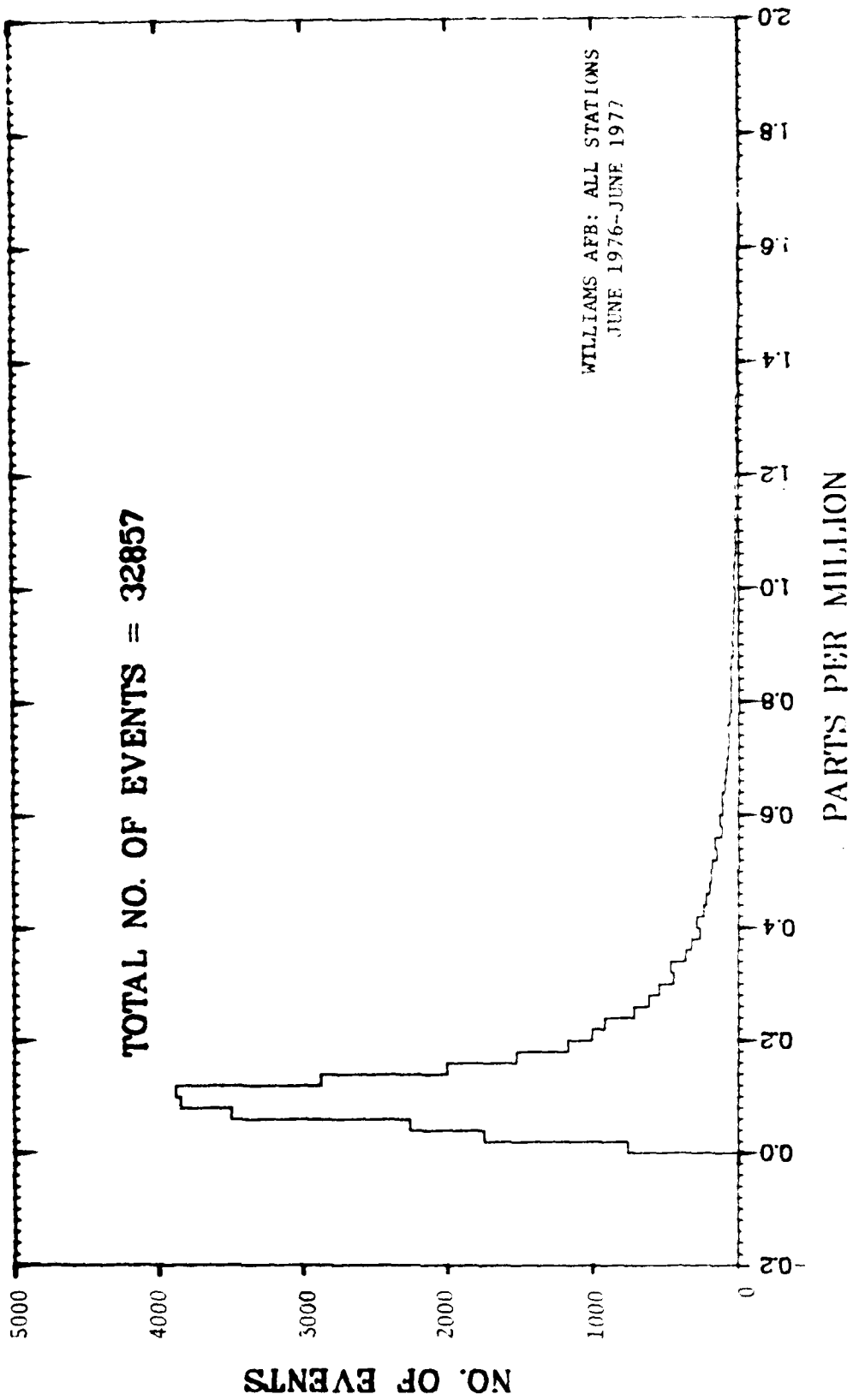


Fig. A-7. Frequency Distribution for Hourly Average CO

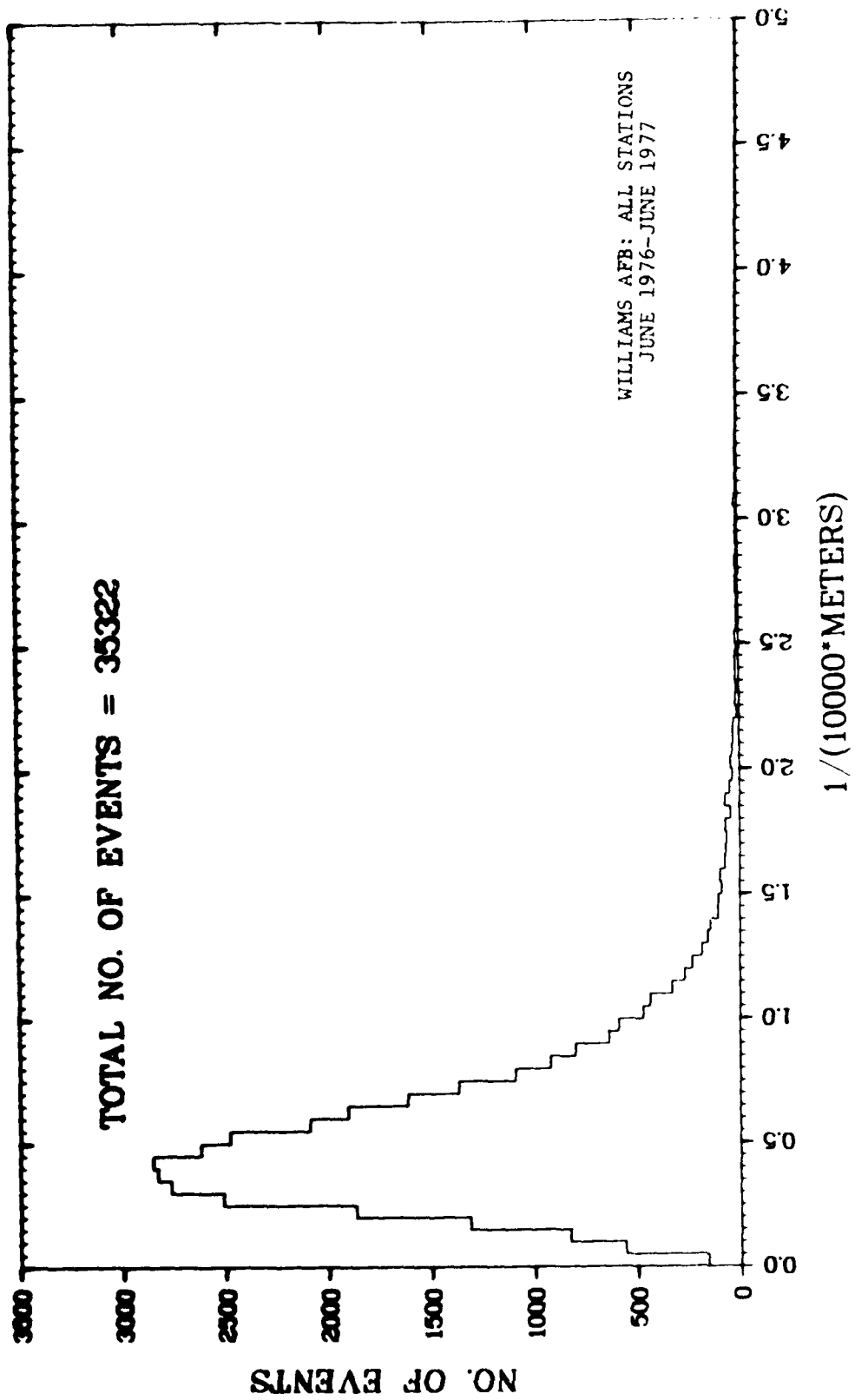


Fig. A-8. Frequency Distribution for Hourly Average b_{SCAT}

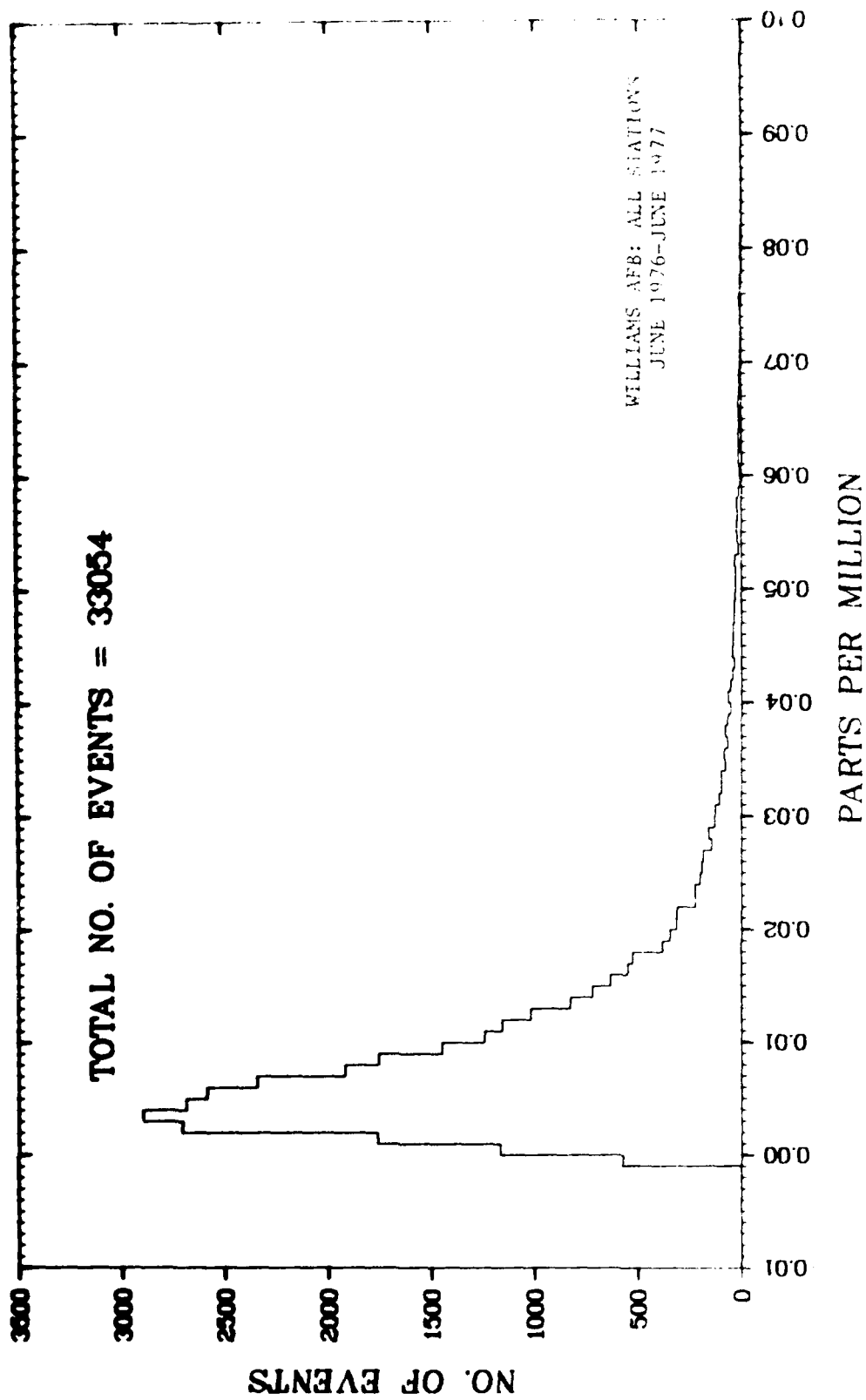


Fig. A-9. Frequency Distribution for Hourly Average NO₂

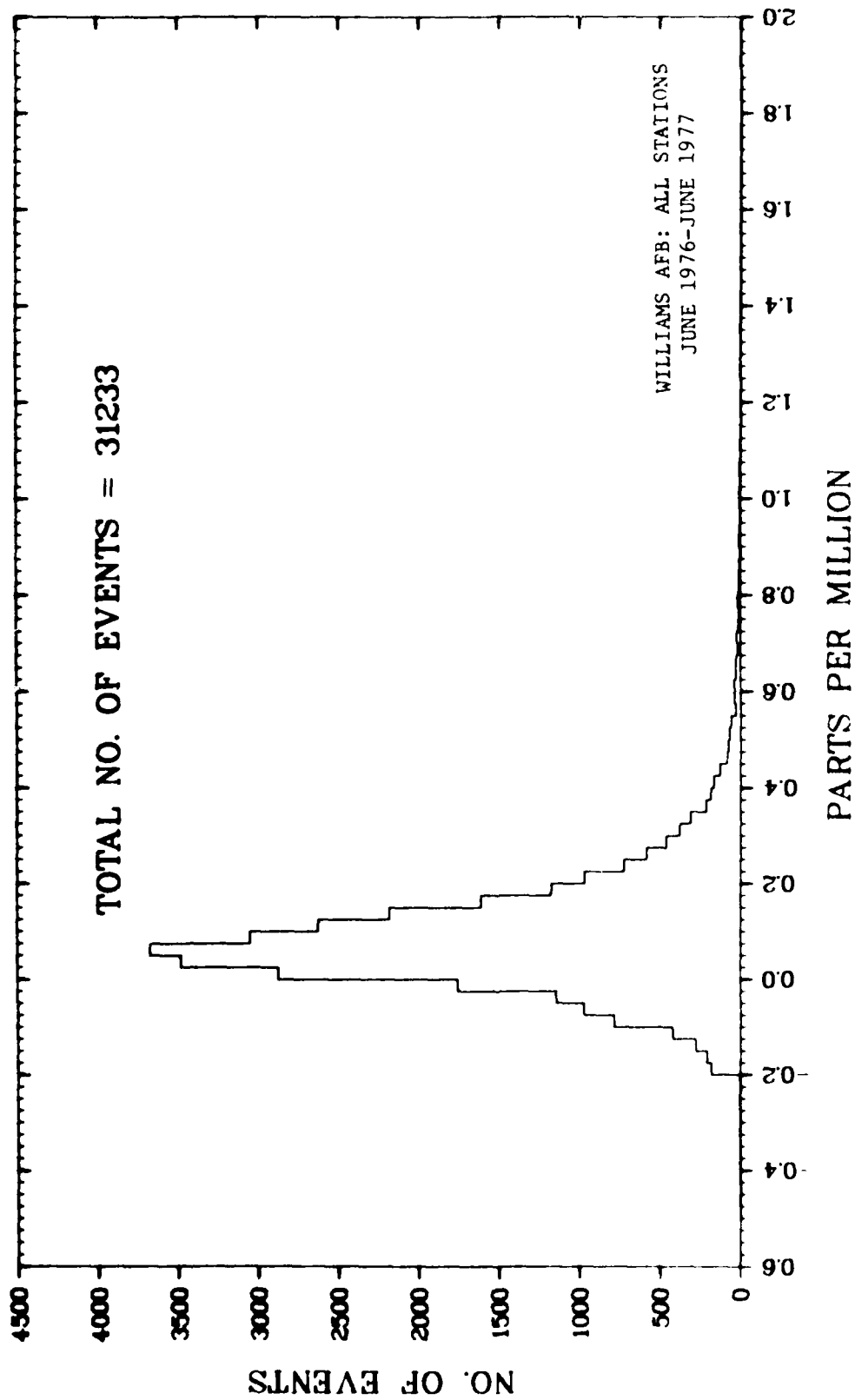


Fig. A-10. Frequency Distribution for Hourly Average NMHC

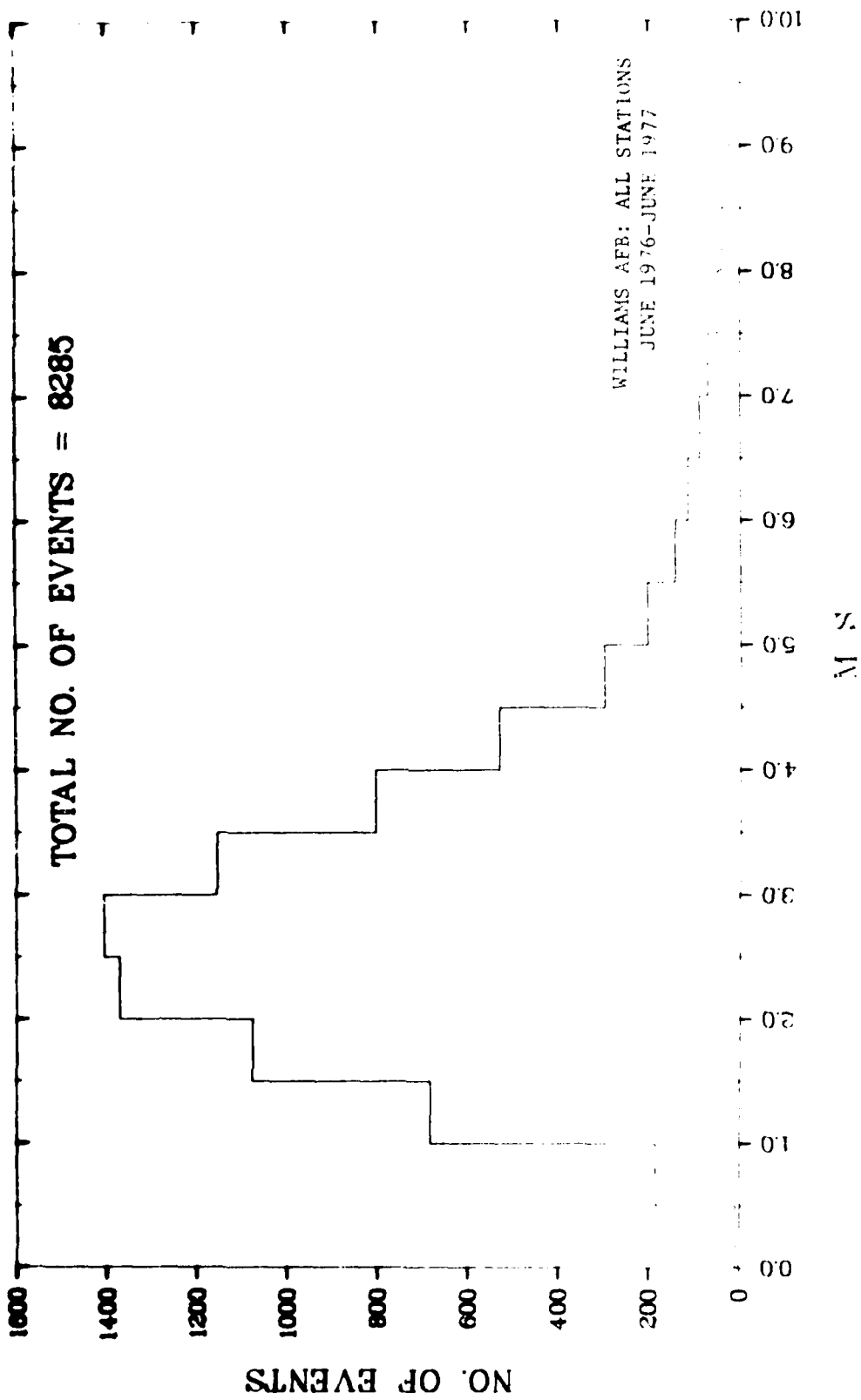


Fig. A-II. Frequency Distribution for Hourly Average Wind Speeds

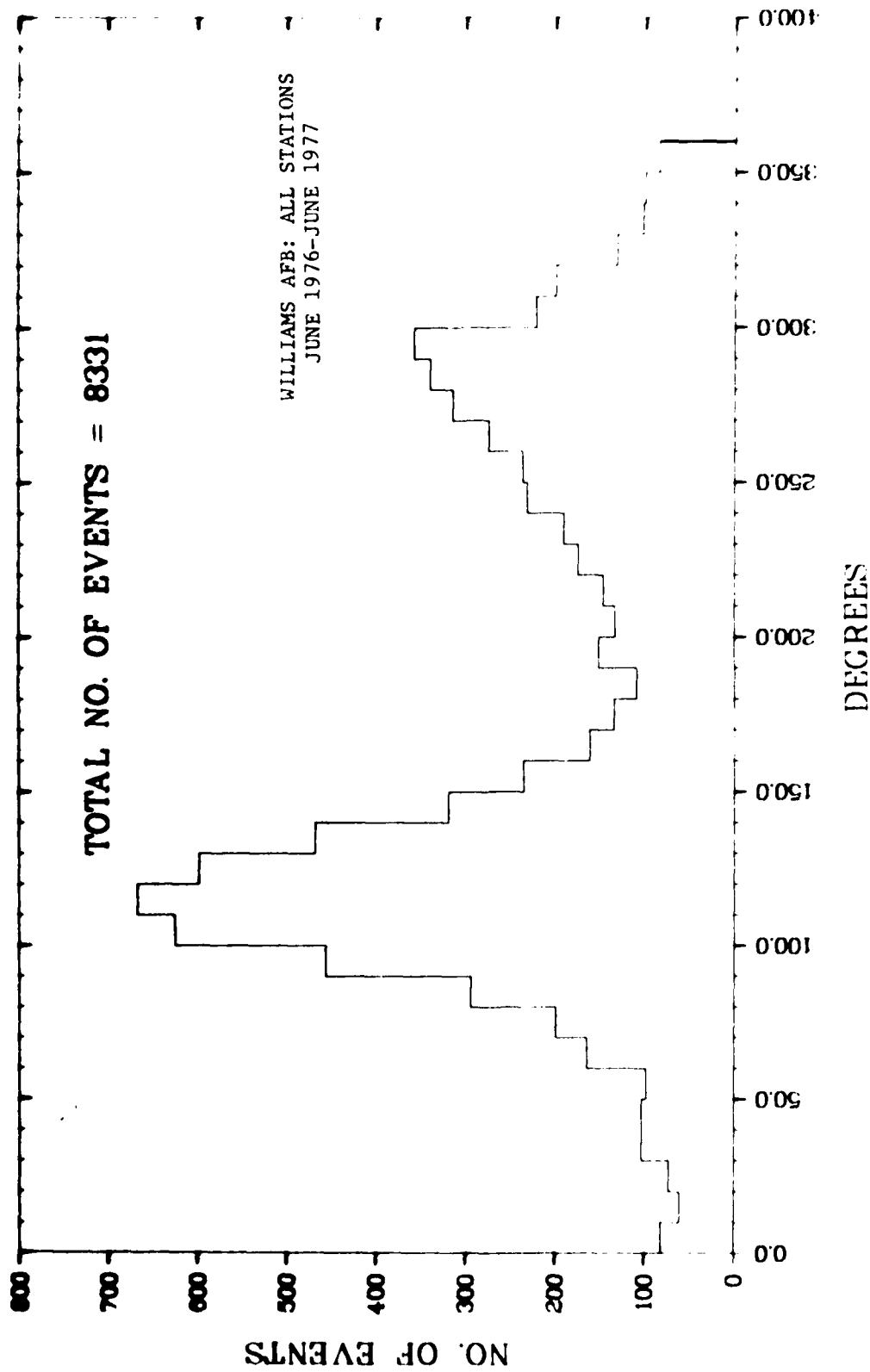


Fig. A-12. Frequency Distribution for Hourly Average Wind Directions

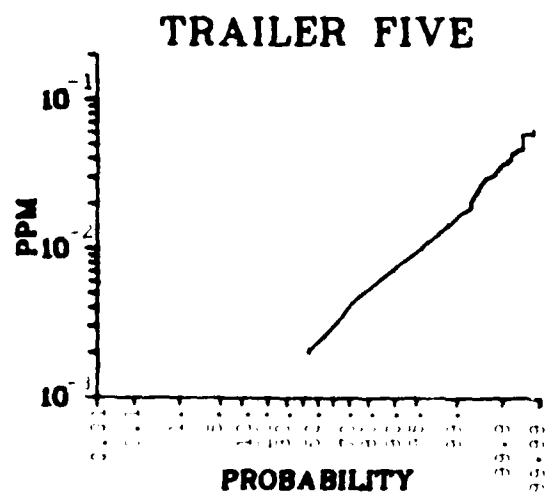
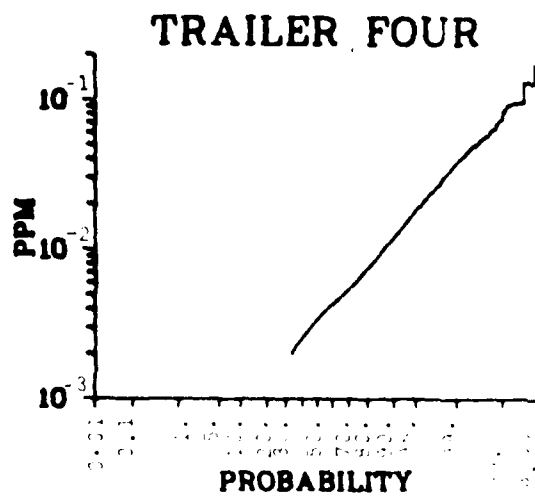
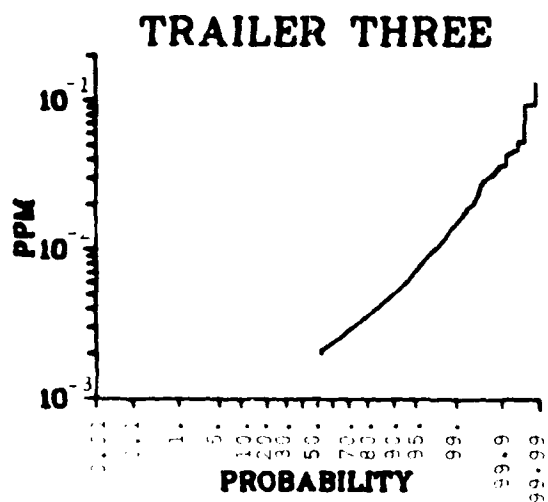
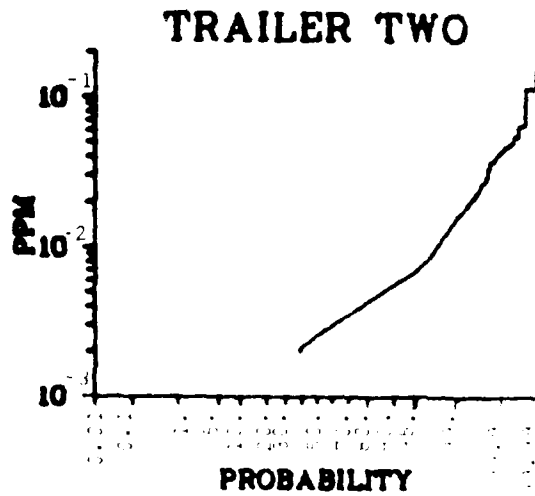
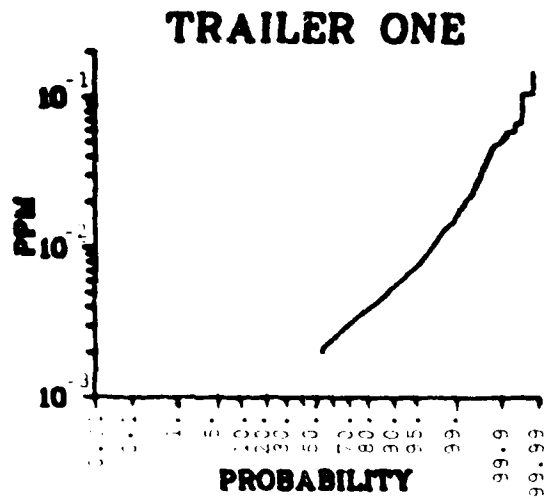


Fig. A-13

Cumulative Frequency Distributions
of Hourly Average NO Concentra-
tions at Williams AFB: June 1976 -
June 1977

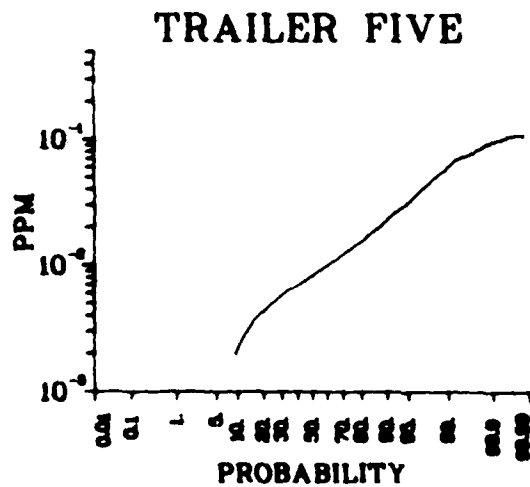
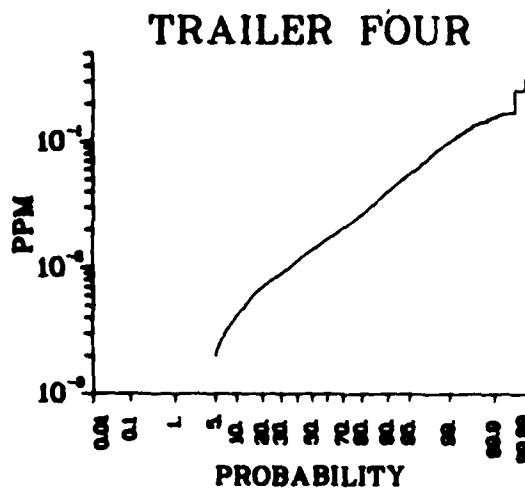
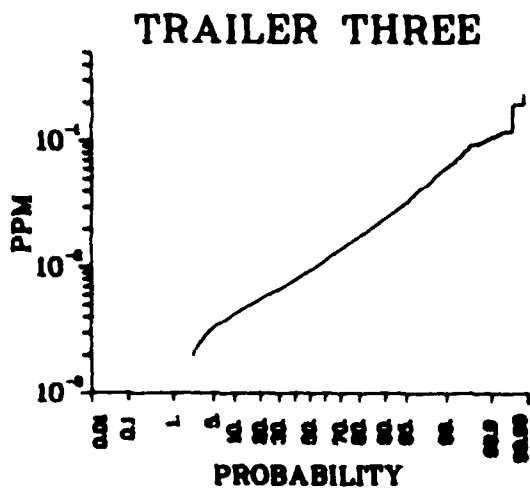
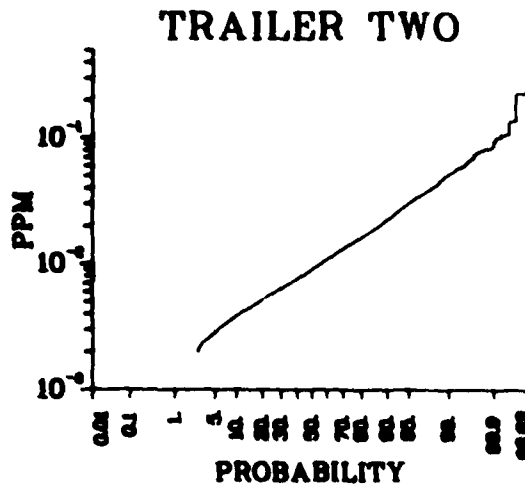
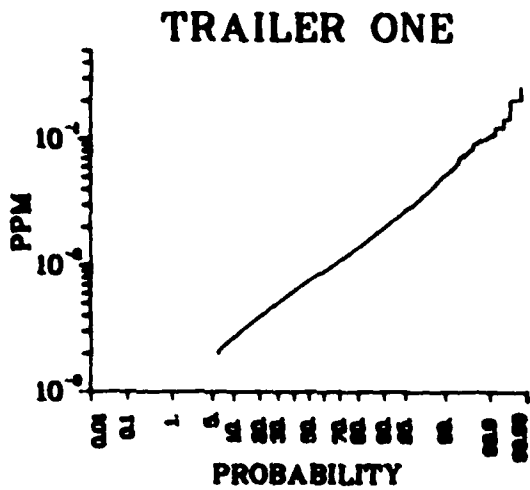
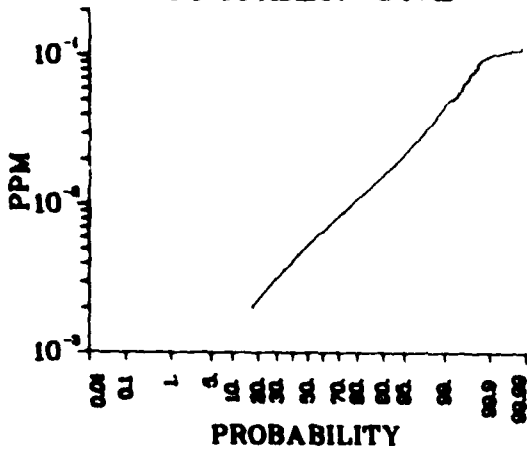


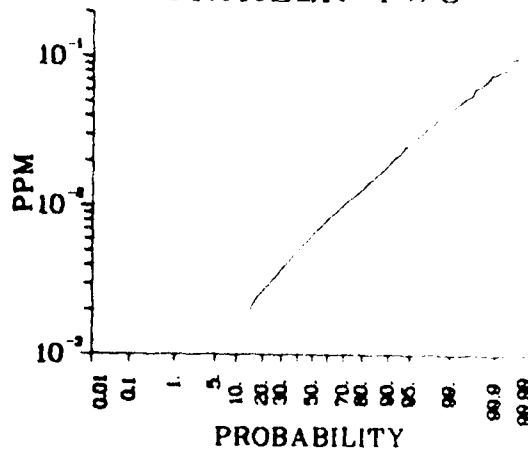
Fig. A-14

Cumulative Frequency Distributions of
Hourly Average NO_x Concentrations at
Williams AFB: June^x 1976 - June 1977

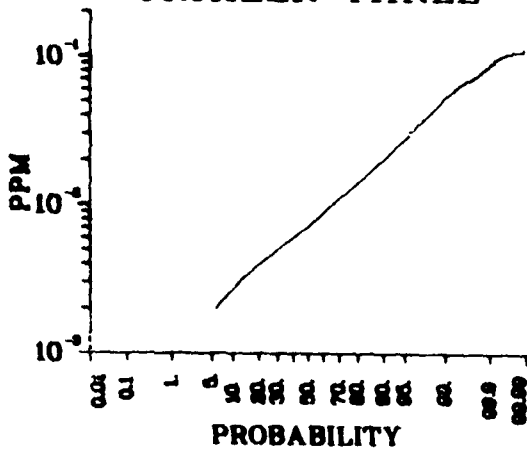
TRAILER ONE



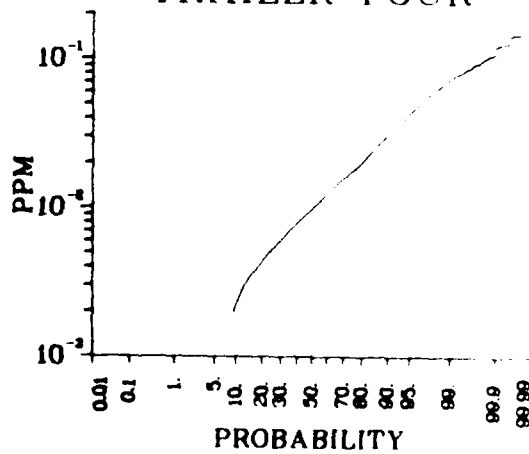
TRAILER TWO



TRAILER THREE



TRAILER FOUR



TRAILER FIVE

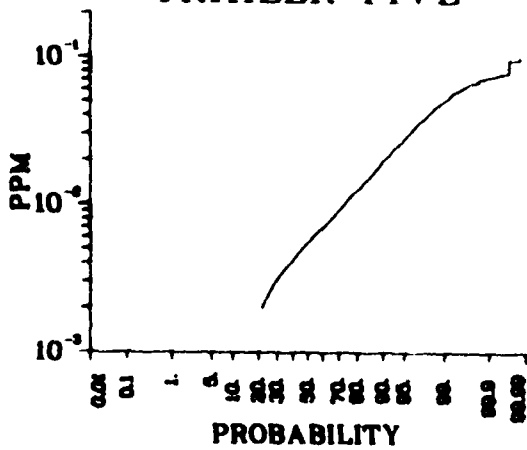


FIG. A-13

Cumulative Frequency Distributions of
Hourly Average NO_2 Concentrations at
Williams AFB: June 1976-June 1977

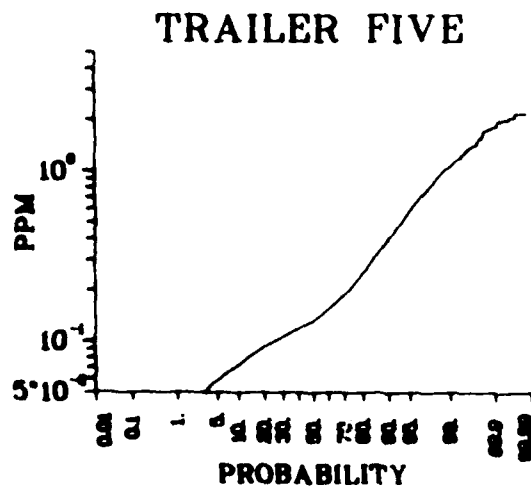
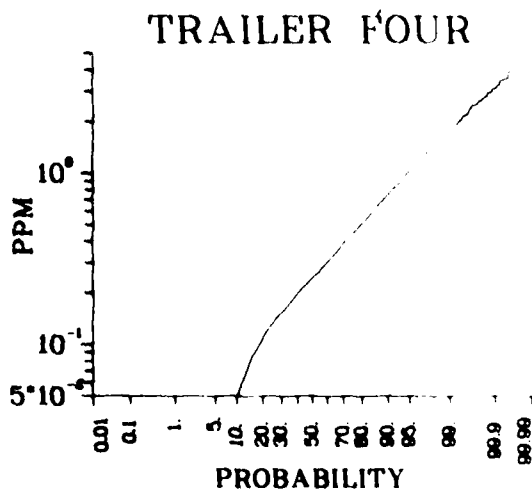
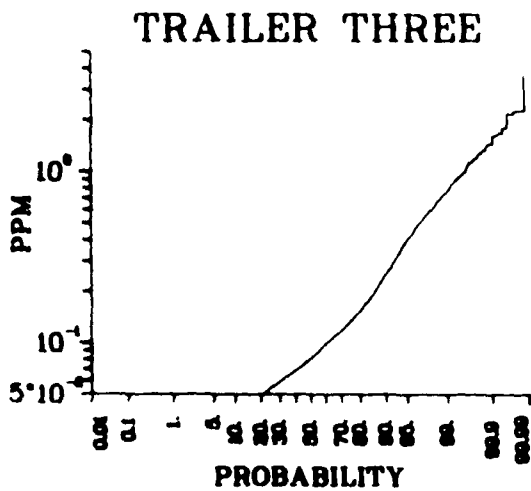
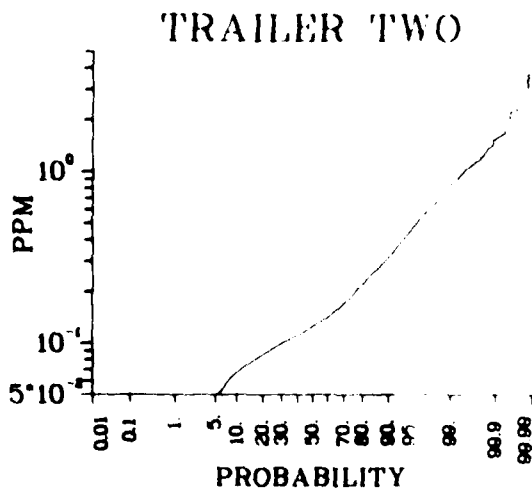
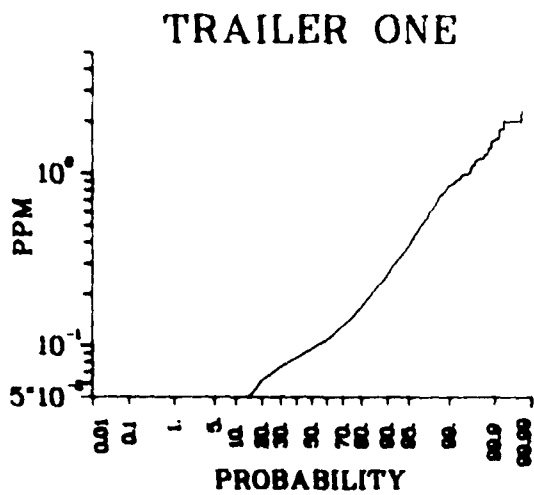


Fig. A-16

Cumulative Frequency Distributions of
Hourly Average CO Concentrations at
Williams AFB: June 1976-June 1977

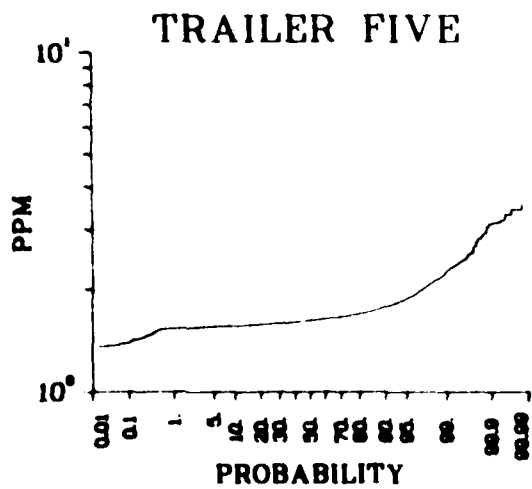
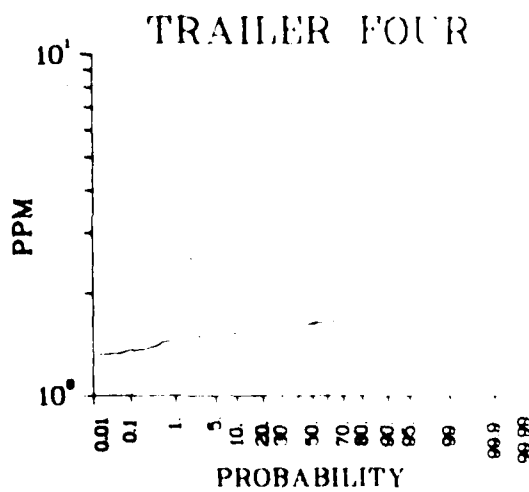
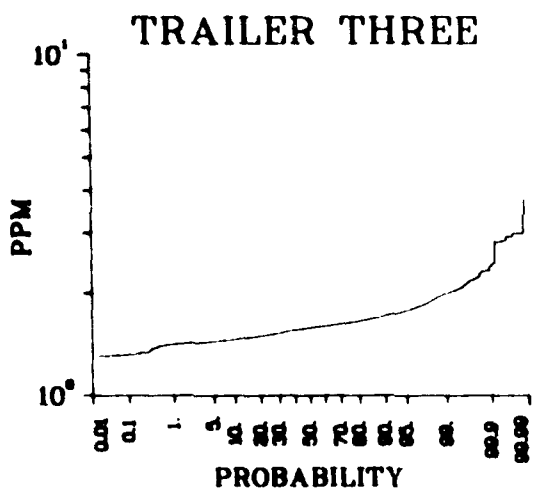
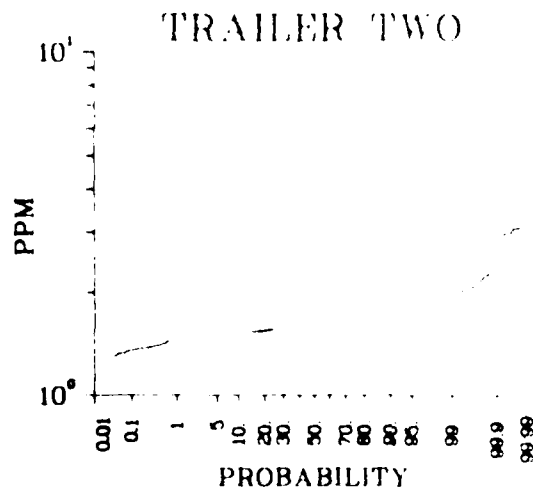
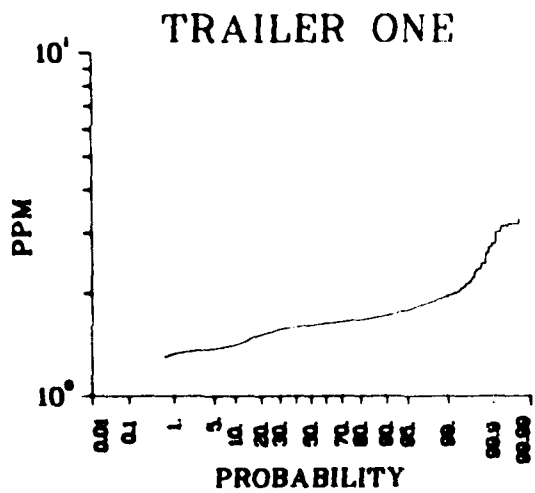


Fig. A-17

Cumulative Frequency Distributions of
Hourly Average CH_4 Concentrations at
Williams AFB: June 1976-June 1977

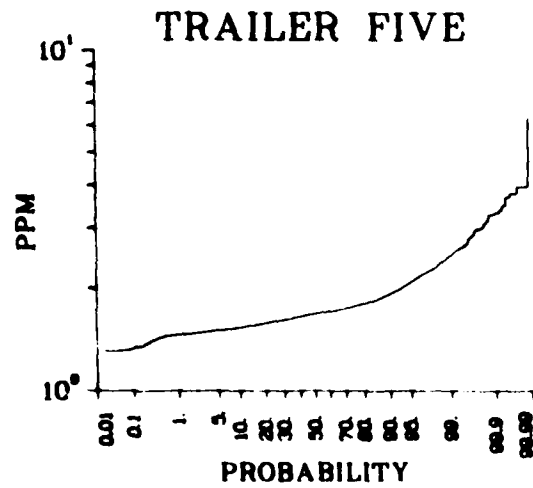
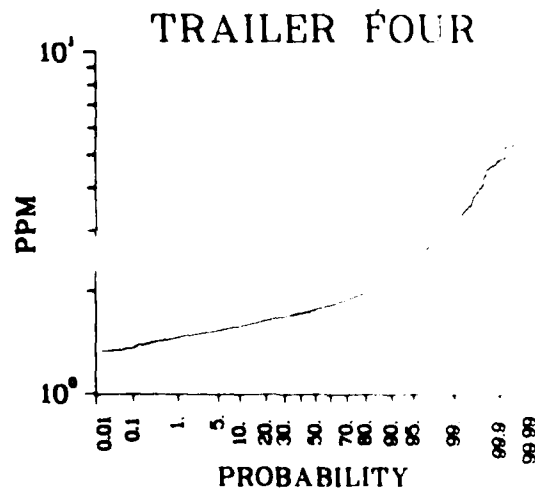
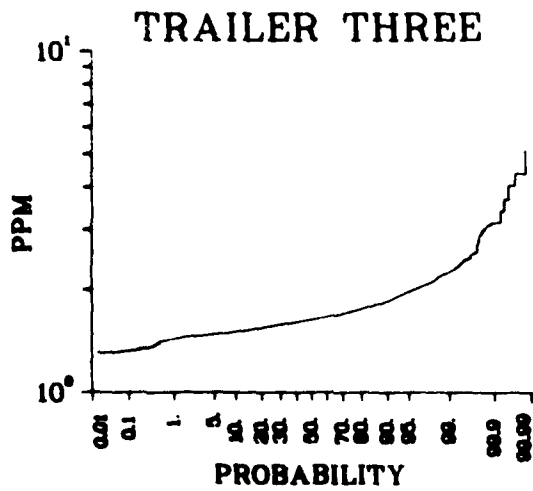
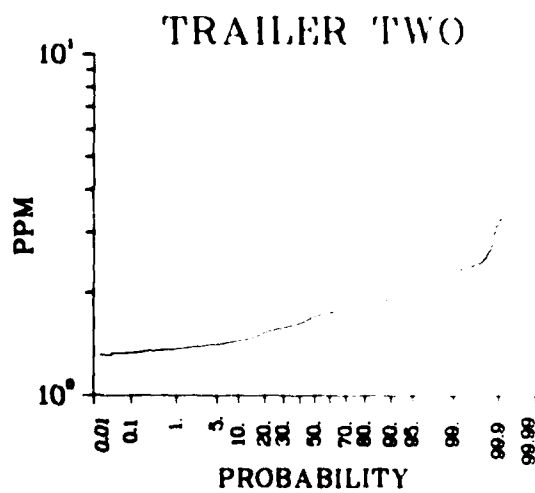
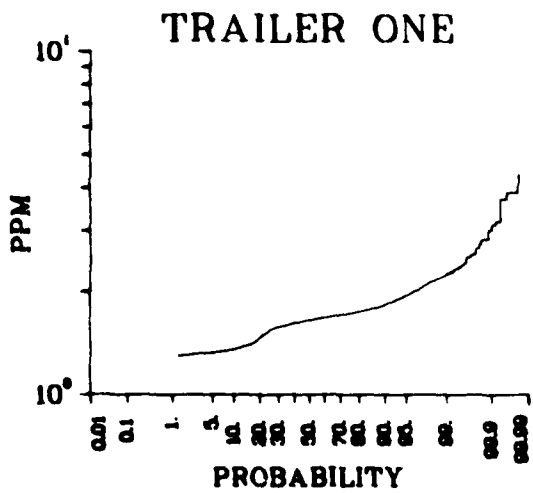
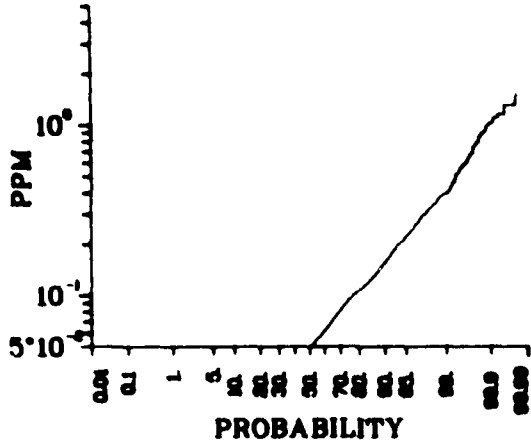


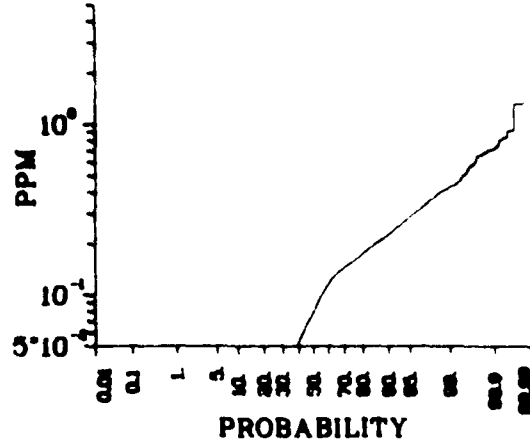
Fig. A-18

Cumulative Frequency Distributions of
Hourly Average THC Concentrations at
Williams AFB: June 1976-June 1977

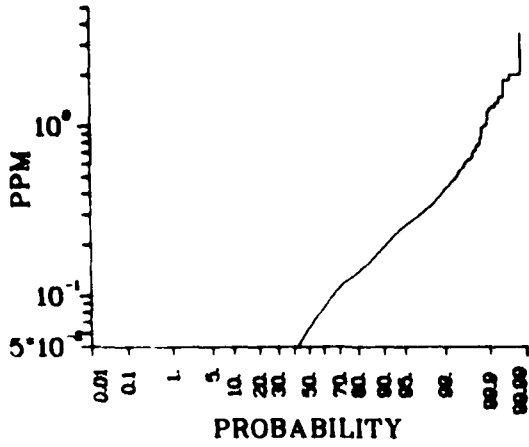
TRAILER ONE



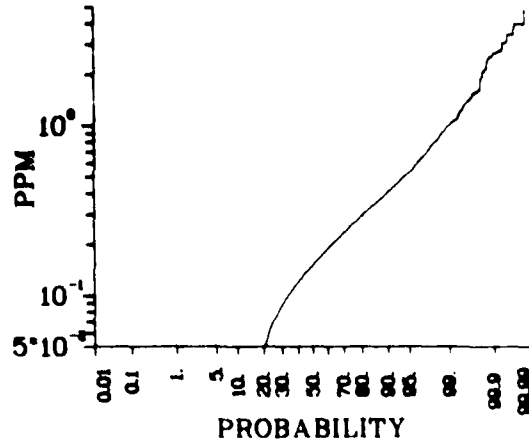
TRAILER TWO



TRAILER THREE



TRAILER FOUR



TRAILER FIVE

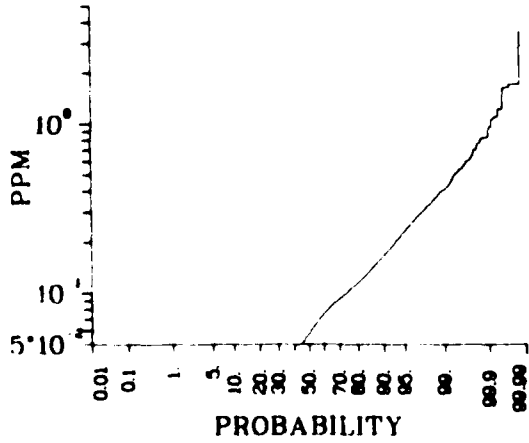


Fig. A-14

Cumulative Frequency Distributions of
Hourly Average NMHC Concentrations at
Williams AFB: June 1976 - June 1977

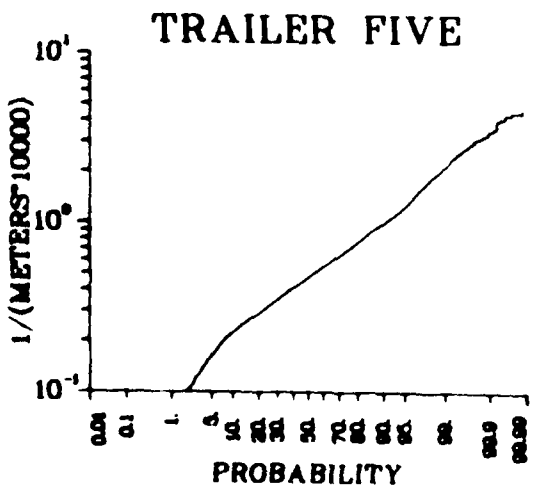
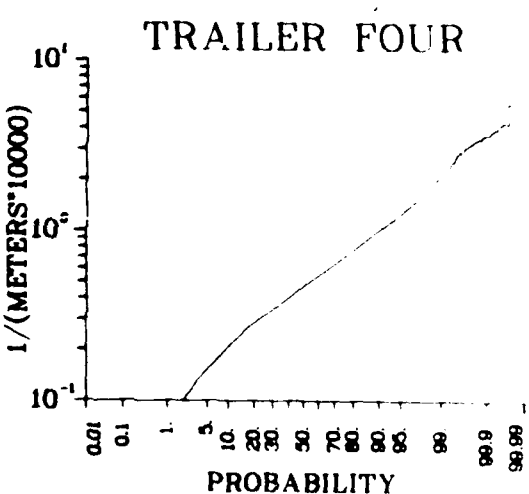
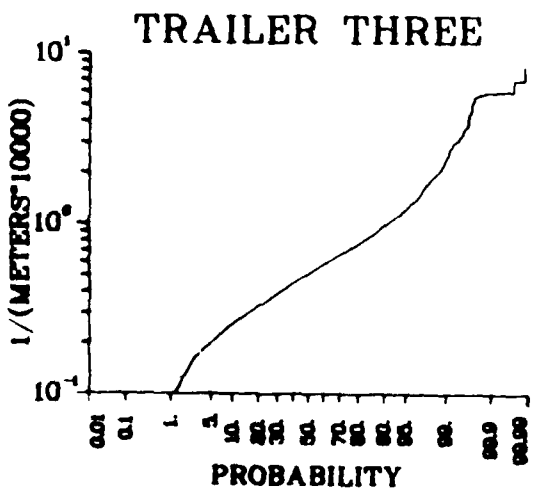
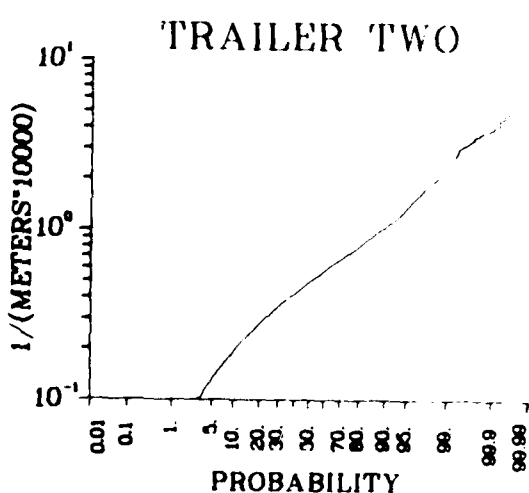
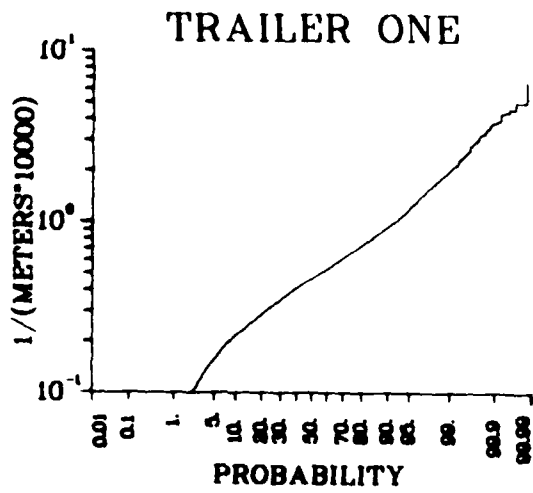


Fig. A-20

Cumulative Frequency Distributions of
Hourly Average Scattering Coefficients
at Williams AFB: June 1976-June 1977

Table A-1. *Siting Rationale*

Site No.	Rationale
1	<ul style="list-style-type: none"> a. Continuity with April 1973 feasibility study b. Upwind during early and late morning periods c. Power already installed for April 1973 study
2	<ul style="list-style-type: none"> a. Downwind of T-38 takeoff and touchdown location during the morning period (98% of all takeoffs and landings at Williams AFB are SE to NW) b. Downwind of T-37 and F5 takeoffs and touchdowns and taxi route for all aircraft during afternoon
3	<ul style="list-style-type: none"> a. Downwind of T-37 queuing and takeoff area during the morning period b. Downwind of taxi segment for all aircraft during the afternoon
4	<ul style="list-style-type: none"> a. Downwind of T-38 apron area during the morning periods b. Background to airfield operations during the afternoon periods
5	<ul style="list-style-type: none"> a. Downwind of all airport activities during the morning period b. Downwind of taxi to shutdown for T-38s c. Background location for later afternoon and early evening

Table A-2. Aircraft Activity Data Format

Header Card - One Per Day

①②③④⑤⑥⑦⑧⑨⑩⑪⑫⑬⑭⑮⑯⑰⑱⑲⑳㉑㉒㉓㉔㉕㉖㉗㉘㉙㉚㉛㉜㉝㉞㉟㊱㊲㊳㊴㊵㊶㊷㊸㊹㊺

751225C 275 327 129 14 5 9

Col. Content

1-6 YYMMDD = Year, month, day
 7 C => Total aircraft counts
 8-11 30L
 12-15 30C
 16-19 30R Full traffic count on these runways
 20-23 12R Right justify integers
 24-27 12C
 28-31 12L

Aircraft Activity Cards

①②③④⑤⑥⑦⑧⑨⑩⑪⑫⑬⑭⑮⑯⑰⑱⑲⑳㉑㉒㉓㉔㉕㉖㉗㉘㉙㉚㉛㉜㉝㉞㉟㊱㊲㊳㊴㊵㊶㊷㊸㊹㊺

751225N30LF-5 0753,0804/0800,0843/0810,0905/0812,0837/0845,0906/0915,1017
 751225I30CC-130 1530,1535,1610
 751225O30CC-130 1655,1702,1730
 751225V30LT-37 0824,0834/0838,0855/0805,0859/0845,0902/0850,0903/1250,1310
 751225A30LT-37 0620,0620,1410,1600

Col. Content

1-6 YYMMDD
 7 N => Normal operations - times are local takeoff and landing times.
 Slashes separate sorties.
 I => Transient inbound } Times are in GMT (i.e., Zulu)
 O => Transient outbound }
 V => Deviation - times are local engine start and takeoff times.
 Slashes separate sorties.
 A => Non-weather aborts - times are local engine start times
 8-10 Runway
 11-20 Aircraft type - left justified
 21-24)
 26-30 (Local 24-hour times separated by commas or slashes as
 : appropriate. (Zulu time for transient aircraft.)
 :
 76-79 .

Table A-3. Minimum, Maximum, and Threshold Concentration Values

Pollutant	Minimum ^a (C _{MIN})	Maximum ^d (C _{MAX})	Threshold ^a (C _T)
NO	-0.02	0.5	0.002
NO _x	-0.02	0.5	0.002
CH ₄	1.25	8.0	1.3
THC	1.25	8.0	1.3
CO	0.0	8.0	0.05
^b SCAT	0.0	9.9 ^b	0.1 ^b
NO ₂ = NO _x - NO	-0.2	0.5	0.002
	plus C _{MIN} and C _{MAX} cuts on NO ₂ and NO		
NMHC = THC - CH ₄	-0.2	8.0	0.05
	plus C _{MIN} and C _{MAX} cuts on THC and CH ₄		

^aValues given in ppm unless otherwise indicated.

^bValues given in units of 10⁴ m⁻¹.

Table A-4. HILLINGS AIR FORCE BASE DATA FOR THE PERIOD JUNE 1, 1976 TO JUNE 30, 1977

STATION NUMBER ...	NO. VALUES	ARITHMETIC MEAN	STD. APITH. DEVIATION	GEOMETRIC MEAN	STD. GEOM. DEVIATION	HIRSHCH VALUE	MEDIAN VALUE	MAXIMUM VALUE	NETTISEN CODE (NO)	DIGITS OF PRECISION (NO)	PERFORME (GHE)	TOTAL PERFORME (GHE)	NO. AIRBORNE REPAIRS (NO)	COMMON MODE (NO)	MEMORANDUM PAGE (GHE)
STATION NUMBER ... 1	6197	2.550E-03	3.311E-03	1.021E-03	6378	4523	1.600E+00	1.632E+00	6125	1.015E-02	1.600E+00	1.632E+00	6437	6055	6022
NO. VALUES	6197	2.550E-03	3.311E-03	1.021E-03	6378	4523	1.600E+00	1.632E+00	6125	1.015E-02	1.600E+00	1.632E+00	6437	6055	6022
ARITHMETIC MEAN	2.550E-03	3.311E-03	1.021E-03	6378	4523	1.600E+00	1.632E+00	1.632E+00	6125	1.015E-02	1.600E+00	1.632E+00	6437	6055	6022
STD. APITH. DEVIATION	3.311E-03	1.021E-03	6378	4523	1.600E+00	1.632E+00	1.632E+00	1.632E+00	6125	1.015E-02	1.600E+00	1.632E+00	6437	6055	6022
GEOMETRIC MEAN	1.021E-03	6378	4523	1.600E+00	1.632E+00	1.632E+00	1.632E+00	1.632E+00	6125	1.015E-02	1.600E+00	1.632E+00	6437	6055	6022
STD. GEOM. DEVIATION	2.537E+00	2.000E+00	2.000E+00	2.000E+00	2.000E+00	2.000E+00	2.000E+00	2.000E+00	6125	1.015E-02	1.600E+00	1.632E+00	6437	6055	6022
HIRSHCH VALUE	-1.010E-02	2.000E+00	2.000E+00	2.000E+00	2.000E+00	2.000E+00	2.000E+00	2.000E+00	6125	1.015E-02	1.600E+00	1.632E+00	6437	6055	6022
MEDIAN VALUE	1.900E-03	5.500E-03	2.600E-03	1.610E+00	1.630E+00	1.630E+00	1.630E+00	1.630E+00	6125	1.015E-02	1.600E+00	1.632E+00	6437	6055	6022
MAXIMUM VALUE	6.010E-02	9.550E-02	2.650E-01	3.550E+00	4.500E+00	4.500E+00	4.500E+00	4.500E+00	6125	1.015E-02	1.600E+00	1.632E+00	6437	6055	6022
STATION NUMBER ... 2	7371	2.855E-03	3.305E-03	1.173E-02	7411	7003	1.623E+00	1.623E+00	7324	1.173E-02	1.623E+00	1.623E+00	6018	6094	7421
NO. VALUES	7371	2.855E-03	3.305E-03	1.173E-02	7411	7003	1.623E+00	1.623E+00	7324	1.173E-02	1.623E+00	1.623E+00	6018	6094	7421
ARITHMETIC MEAN	2.855E-03	3.305E-03	1.173E-02	7411	7003	1.623E+00	1.623E+00	1.623E+00	7324	1.173E-02	1.623E+00	1.623E+00	6018	6094	7421
STD. APITH. DEVIATION	3.305E-03	1.173E-02	7411	7003	1.623E+00	1.623E+00	1.623E+00	1.623E+00	7324	1.173E-02	1.623E+00	1.623E+00	6018	6094	7421
GEOMETRIC MEAN	1.021E-03	6378	4523	1.600E+00	1.632E+00	1.632E+00	1.632E+00	1.632E+00	6125	1.015E-02	1.600E+00	1.632E+00	6437	6055	6022
STD. GEOM. DEVIATION	2.056E+00	2.000E+00	2.000E+00	2.000E+00	2.000E+00	2.000E+00	2.000E+00	2.000E+00	6125	1.015E-02	1.600E+00	1.632E+00	6437	6055	6022
HIRSHCH VALUE	-1.053E-02	2.000E+00	2.000E+00	2.000E+00	2.000E+00	2.000E+00	2.000E+00	2.000E+00	6125	1.015E-02	1.600E+00	1.632E+00	6437	6055	6022
MEDIAN VALUE	2.600E-03	6.200E-03	9.000E-03	1.630E+00	1.630E+00	1.630E+00	1.630E+00	1.630E+00	6125	1.015E-02	1.600E+00	1.632E+00	6437	6055	6022
MAXIMUM VALUE	6.560E-02	9.770E-02	2.910E-01	3.120E+00	4.500E+00	4.500E+00	4.500E+00	4.500E+00	6125	1.015E-02	1.600E+00	1.632E+00	6437	6055	6022
STATION NUMBER ... 3	7292	2.445E-03	2.935E-03	1.255E-02	7256	7212	1.507E+00	1.507E+00	7243	1.255E-02	1.507E+00	1.507E+00	7005	5614	7315
NO. VALUES	7292	2.445E-03	2.935E-03	1.255E-02	7256	7212	1.507E+00	1.507E+00	7243	1.255E-02	1.507E+00	1.507E+00	7005	5614	7315
ARITHMETIC MEAN	2.445E-03	2.935E-03	1.255E-02	7256	7212	1.507E+00	1.507E+00	1.507E+00	7243	1.255E-02	1.507E+00	1.507E+00	7005	5614	7315
STD. APITH. DEVIATION	2.935E-03	1.255E-02	7256	7212	1.507E+00	1.507E+00	1.507E+00	1.507E+00	7243	1.255E-02	1.507E+00	1.507E+00	7005	5614	7315
GEOMETRIC MEAN	1.021E-03	6378	4523	1.600E+00	1.632E+00	1.632E+00	1.632E+00	1.632E+00	6125	1.015E-02	1.600E+00	1.632E+00	6437	6055	6022
STD. GEOM. DEVIATION	2.022E+00	2.000E+00	2.000E+00	2.000E+00	2.000E+00	2.000E+00	2.000E+00	2.000E+00	6125	1.015E-02	1.600E+00	1.632E+00	6437	6055	6022
HIRSHCH VALUE	-6.200E-03	2.000E+00	2.000E+00	2.000E+00	2.000E+00	2.000E+00	2.000E+00	2.000E+00	6125	1.015E-02	1.600E+00	1.632E+00	6437	6055	6022
MEDIAN VALUE	2.000E-03	7.200E-03	9.500E-03	1.500E+00	1.500E+00	1.500E+00	1.500E+00	1.500E+00	6125	1.015E-02	1.600E+00	1.632E+00	6437	6055	6022
MAXIMUM VALUE	5.300E-02	1.150E-01	2.410E-01	3.770E+00	5.170E+00	5.170E+00	5.170E+00	5.170E+00	6125	1.015E-02	1.600E+00	1.632E+00	6437	6055	6022
STATION NUMBER ... 4	6762	5.255E-03	7.445E-03	1.255E-02	6731	6722	1.671E+00	1.671E+00	6812	1.255E-02	1.671E+00	1.671E+00	6897	6022	6018
NO. VALUES	6762	5.255E-03	7.445E-03	1.255E-02	6731	6722	1.671E+00	1.671E+00	6812	1.255E-02	1.671E+00	1.671E+00	6897	6022	6018
ARITHMETIC MEAN	5.255E-03	7.445E-03	1.255E-02	6731	6722	1.671E+00	1.671E+00	1.671E+00	6812	1.255E-02	1.671E+00	1.671E+00	6897	6022	6018
STD. APITH. DEVIATION	7.445E-03	1.255E-02	6731	6722	1.671E+00	1.671E+00	1.671E+00	1.671E+00	6812	1.255E-02	1.671E+00	1.671E+00	6897	6022	6018
GEOMETRIC MEAN	1.021E-03	6378	4523	1.600E+00	1.632E+00	1.632E+00	1.632E+00	1.632E+00	6125	1.015E-02	1.600E+00	1.632E+00	6437	6055	6022
STD. GEOM. DEVIATION	2.377E+00	2.000E+00	2.000E+00	2.000E+00	2.000E+00	2.000E+00	2.000E+00	2.000E+00	6125	1.015E-02	1.600E+00	1.632E+00	6437	6055	6022
HIRSHCH VALUE	-9.200E-03	2.000E+00	2.000E+00	2.000E+00	2.000E+00	2.000E+00	2.000E+00	2.000E+00	6125	1.015E-02	1.600E+00	1.632E+00	6437	6055	6022
MEDIAN VALUE	3.500E-03	7.200E-03	9.500E-03	1.500E+00	1.500E+00	1.500E+00	1.500E+00	1.500E+00	6125	1.015E-02	1.600E+00	1.632E+00	6437	6055	6022
MAXIMUM VALUE	9.600E-02	1.500E-01	1.500E-01	4.100E+00	7.100E+00	7.100E+00	7.100E+00	7.100E+00	6125	1.015E-02	1.600E+00	1.632E+00	6437	6055	6022
STATION NUMBER ... 5	6415	3.000E-03	3.910E-03	1.100E-02	6370	6321	1.400E+00	1.400E+00	6423	1.100E-02	1.400E+00	1.400E+00	6797	7000	7215
NO. VALUES	6415	3.000E-03	3.910E-03	1.100E-02	6370	6321	1.400E+00	1.400E+00	6423	1.100E-02	1.400E+00	1.400E+00	6797	7000	7215
ARITHMETIC MEAN	3.000E-03	3.910E-03	1.100E-02	6370	6321	1.400E+00	1.400E+00	1.400E+00	6423	1.100E-02	1.400E+00	1.400E+00	6797	7000	7215
STD. APITH. DEVIATION	3.910E-03	1.100E-02	6370	6321	1.400E+00	1.400E+00	1.400E+00	1.400E+00	6423	1.100E-02	1.400E+00	1.400E+00	6797	7000	7215
GEOMETRIC MEAN	1.021E-03	6378	4523	1.600E+00	1.632E+00	1.632E+00	1.632E+00	1.632E+00	6125	1.015E-02	1.600E+00	1.632E+00	6437	6055	6022
STD. GEOM. DEVIATION	2.000E+00	2.000E+00	2.000E+00	2.000E+00	2.000E+00	2.000E+00	2.000E+00	2.000E+00	6125	1.015E-02	1.600E+00	1.632E+00	6437	6055	6022
HIRSHCH VALUE	-1.000E-02	2.000E+00	2.000E+00	2.000E+00	2.000E+00	2.000E+00	2.000E+00	2.000E+00	6125	1.015E-02	1.600E+00	1.632E+00	6437	6055	6022
MEDIAN VALUE	2.400E-03	5.200E-03	6.000E-03	1.400E+00	1.400E+00	1.400E+00	1.400E+00	1.400E+00	6125	1.015E-02	1.600E+00	1.632E+00	6437	6055	6022
MAXIMUM VALUE	6.400E-02	1.000E-01	1.100E-01	3.100E+00	6.000E+00	6.000E+00	6.000E+00	6.000E+00	6125	1.015E-02	1.600E+00	1.632E+00	6437	6055	6022

Table A-6. HULLMAN RESEARCH CENTER, STATION 1, 2, 3, 4, 5

STATION NUMBER	NO. VALUES	ARITHMETIC MEAN	STD. DEVIATION	GEOMETRIC MEAN	STD. DEVIATION	MINIMUM VALUE	MAXIMUM VALUE
STATION NUMBER ... 1							
NO. VALUES	709	709	709	709	709	709	709
ARITHMETIC MEAN	8.90E+01	5.07E+03	6.70E+01	1.95E+00	1.61E+00	1.61E+00	1.61E+00
STD. DEVIATION	2.43E+01	4.31E+03	5.47E+01	1.47E+01	1.47E+01	1.47E+01	1.47E+01
GEOMETRIC MEAN	7.21E+01	4.27E+03	5.67E+01	1.64E+00	1.64E+00	1.64E+00	1.64E+00
STD. DEVIATION	1.20E+01	2.49E+03	1.99E+01	1.77E+00	1.77E+00	1.77E+00	1.77E+00
MINIMUM VALUE	-2.00E+01	-7.00E+03	-4.00E+01	1.00E+00	1.00E+00	1.00E+00	1.00E+00
MAXIMUM VALUE	8.00E+01	4.00E+03	5.00E+01	2.00E+00	2.00E+00	2.00E+00	2.00E+00
STATION NUMBER ... 2							
NO. VALUES	602	602	602	602	602	602	602
ARITHMETIC MEAN	5.07E+03	4.87E+03	1.00E+02	1.61E+00	1.61E+00	1.61E+00	1.61E+00
STD. DEVIATION	5.47E+03	3.70E+03	5.47E+01	1.47E+01	1.47E+01	1.47E+01	1.47E+01
GEOMETRIC MEAN	1.00E+03	2.49E+03	1.99E+01	1.77E+00	1.77E+00	1.77E+00	1.77E+00
STD. DEVIATION	1.20E+01	2.49E+03	1.99E+01	1.77E+00	1.77E+00	1.77E+00	1.77E+00
MINIMUM VALUE	-5.00E+03	-1.00E+04	-2.00E+01	1.00E+00	1.00E+00	1.00E+00	1.00E+00
MAXIMUM VALUE	4.99E+03	2.00E+04	4.00E+01	2.00E+00	2.00E+00	2.00E+00	2.00E+00
STATION NUMBER ... 3							
NO. VALUES	659	659	659	659	659	659	659
ARITHMETIC MEAN	2.10E+03	7.25E+03	9.44E+03	1.93E+00	1.93E+00	1.93E+00	1.93E+00
STD. DEVIATION	1.82E+03	4.87E+03	5.07E+03	7.93E+02	7.93E+02	7.93E+02	7.93E+02
GEOMETRIC MEAN	1.82E+03	5.07E+03	2.00E+03	1.60E+00	1.60E+00	1.60E+00	1.60E+00
STD. DEVIATION	1.00E+03	2.49E+03	1.99E+01	1.77E+00	1.77E+00	1.77E+00	1.77E+00
MINIMUM VALUE	-5.00E+03	-1.00E+04	-2.00E+01	1.00E+00	1.00E+00	1.00E+00	1.00E+00
MAXIMUM VALUE	1.82E+03	4.99E+03	4.00E+01	2.00E+00	2.00E+00	2.00E+00	2.00E+00
STATION NUMBER ... 4							
NO. VALUES	507	507	507	507	507	507	507
ARITHMETIC MEAN	4.00E+03	2.60E+03	1.67E+02	1.50E+00	1.50E+00	1.50E+00	1.50E+00
STD. DEVIATION	3.00E+03	1.82E+03	6.00E+01	1.47E+01	1.47E+01	1.47E+01	1.47E+01
GEOMETRIC MEAN	3.00E+03	1.82E+03	2.00E+01	1.64E+00	1.64E+00	1.64E+00	1.64E+00
STD. DEVIATION	1.20E+01	2.49E+03	1.99E+01	1.77E+00	1.77E+00	1.77E+00	1.77E+00
MINIMUM VALUE	-2.00E+03	-1.00E+04	-4.00E+01	1.00E+00	1.00E+00	1.00E+00	1.00E+00
MAXIMUM VALUE	1.00E+03	3.50E+03	4.00E+01	2.00E+00	2.00E+00	2.00E+00	2.00E+00
STATION NUMBER ... 5							
NO. VALUES	709	709	709	709	709	709	709
ARITHMETIC MEAN	3.10E+03	2.10E+03	1.00E+02	1.61E+00	1.61E+00	1.61E+00	1.61E+00
STD. DEVIATION	1.47E+03	1.47E+03	5.47E+01	1.47E+01	1.47E+01	1.47E+01	1.47E+01
GEOMETRIC MEAN	2.10E+03	1.82E+03	2.00E+01	1.64E+00	1.64E+00	1.64E+00	1.64E+00
STD. DEVIATION	1.20E+01	2.49E+03	1.99E+01	1.77E+00	1.77E+00	1.77E+00	1.77E+00
MINIMUM VALUE	-2.00E+03	-1.00E+04	-4.00E+01	1.00E+00	1.00E+00	1.00E+00	1.00E+00
MAXIMUM VALUE	2.10E+03	3.50E+03	4.00E+01	2.00E+00	2.00E+00	2.00E+00	2.00E+00

Table A-7. WILLOW AIR FORCE BASE DATA CENTER FOR THE MONTH OF APRIL, 1975

STATION NUMBER	NETRIC CODE	STATION TYPE	STATION NAME	STATION ADDRESS	STATION CITY	STATION STATE	STATION ZIP	STATION ELEVATION	STATION COMMENTS
STATION NUMBER 1	414	414	414	414	414	414	414	414	414
STATION TYPE	414	414	414	414	414	414	414	414	414
STATION NAME	414	414	414	414	414	414	414	414	414
STATION ADDRESS	414	414	414	414	414	414	414	414	414
STATION CITY	414	414	414	414	414	414	414	414	414
STATION STATE	414	414	414	414	414	414	414	414	414
STATION ZIP	414	414	414	414	414	414	414	414	414
STATION ELEVATION	414	414	414	414	414	414	414	414	414
STATION COMMENTS	414	414	414	414	414	414	414	414	414
STATION NUMBER 2	415	415	415	415	415	415	415	415	415
STATION TYPE	415	415	415	415	415	415	415	415	415
STATION NAME	415	415	415	415	415	415	415	415	415
STATION ADDRESS	415	415	415	415	415	415	415	415	415
STATION CITY	415	415	415	415	415	415	415	415	415
STATION STATE	415	415	415	415	415	415	415	415	415
STATION ZIP	415	415	415	415	415	415	415	415	415
STATION ELEVATION	415	415	415	415	415	415	415	415	415
STATION COMMENTS	415	415	415	415	415	415	415	415	415
STATION NUMBER 3	416	416	416	416	416	416	416	416	416
STATION TYPE	416	416	416	416	416	416	416	416	416
STATION NAME	416	416	416	416	416	416	416	416	416
STATION ADDRESS	416	416	416	416	416	416	416	416	416
STATION CITY	416	416	416	416	416	416	416	416	416
STATION STATE	416	416	416	416	416	416	416	416	416
STATION ZIP	416	416	416	416	416	416	416	416	416
STATION ELEVATION	416	416	416	416	416	416	416	416	416
STATION COMMENTS	416	416	416	416	416	416	416	416	416
STATION NUMBER 4	417	417	417	417	417	417	417	417	417
STATION TYPE	417	417	417	417	417	417	417	417	417
STATION NAME	417	417	417	417	417	417	417	417	417
STATION ADDRESS	417	417	417	417	417	417	417	417	417
STATION CITY	417	417	417	417	417	417	417	417	417
STATION STATE	417	417	417	417	417	417	417	417	417
STATION ZIP	417	417	417	417	417	417	417	417	417
STATION ELEVATION	417	417	417	417	417	417	417	417	417
STATION COMMENTS	417	417	417	417	417	417	417	417	417
STATION NUMBER 5	418	418	418	418	418	418	418	418	418
STATION TYPE	418	418	418	418	418	418	418	418	418
STATION NAME	418	418	418	418	418	418	418	418	418
STATION ADDRESS	418	418	418	418	418	418	418	418	418
STATION CITY	418	418	418	418	418	418	418	418	418
STATION STATE	418	418	418	418	418	418	418	418	418
STATION ZIP	418	418	418	418	418	418	418	418	418
STATION ELEVATION	418	418	418	418	418	418	418	418	418
STATION COMMENTS	418	418	418	418	418	418	418	418	418

Table A-10. Statistical Summary of Data Collected for the 1967-68 Season

Station Number	Year	Mean	Standard Deviation	Minimum	Maximum	Number of Observations
STATION NUMBER ... 1						
1. VALUES						
5.650E-03	599	1.697E+00	1.297E-01	4.99	600	5.00E-01
1.600E-03	599	1.697E+00	1.297E-01	4.99	600	5.00E-01
3.737E-03	599	1.697E+00	1.297E-01	4.99	600	5.00E-01
2.637E+00	599	1.697E+00	1.297E-01	4.99	600	5.00E-01
-1.000E-02	599	1.697E+00	1.297E-01	4.99	600	5.00E-01
3.737E-03	599	1.697E+00	1.297E-01	4.99	600	5.00E-01
6.000E-02	599	1.697E+00	1.297E-01	4.99	600	5.00E-01
STATION NUMBER ... 2						
1. VALUES						
2.610E-03	593	1.671E+00	1.297E-01	4.99	600	6.20E-01
2.010E-03	593	1.671E+00	1.297E-01	4.99	600	6.20E-01
2.370E-03	593	1.671E+00	1.297E-01	4.99	600	6.20E-01
1.750E+00	593	1.671E+00	1.297E-01	4.99	600	6.20E-01
-4.000E-04	593	1.671E+00	1.297E-01	4.99	600	6.20E-01
2.000E-03	593	1.671E+00	1.297E-01	4.99	600	6.20E-01
2.350E-02	593	1.671E+00	1.297E-01	4.99	600	6.20E-01
STATION NUMBER ... 3						
1. VALUES						
2.300E-03	549	1.657E+00	1.297E-01	4.99	550	5.00E-01
1.000E-03	549	1.657E+00	1.297E-01	4.99	550	5.00E-01
1.000E-03	549	1.657E+00	1.297E-01	4.99	550	5.00E-01
9.000E-03	549	1.657E+00	1.297E-01	4.99	550	5.00E-01
2.000E-03	549	1.657E+00	1.297E-01	4.99	550	5.00E-01
-3.000E-03	549	1.657E+00	1.297E-01	4.99	550	5.00E-01
1.500E-03	549	1.657E+00	1.297E-01	4.99	550	5.00E-01
1.900E-02	549	1.657E+00	1.297E-01	4.99	550	5.00E-01
STATION NUMBER ... 4						
1. VALUES						
6.800E-03	594	1.700E+00	1.297E-01	4.99	595	7.00E-01
2.000E-03	594	1.700E+00	1.297E-01	4.99	595	7.00E-01
3.000E-03	594	1.700E+00	1.297E-01	4.99	595	7.00E-01
2.000E-03	594	1.700E+00	1.297E-01	4.99	595	7.00E-01
-1.000E-03	594	1.700E+00	1.297E-01	4.99	595	7.00E-01
4.500E-03	594	1.700E+00	1.297E-01	4.99	595	7.00E-01
6.200E-02	594	1.700E+00	1.297E-01	4.99	595	7.00E-01
STATION NUMBER ... 5						
1. VALUES						
2.700E-03	609	1.700E+00	1.297E-01	4.99	610	6.00E-01
1.000E-03	609	1.700E+00	1.297E-01	4.99	610	6.00E-01
1.000E-03	609	1.700E+00	1.297E-01	4.99	610	6.00E-01
2.000E-03	609	1.700E+00	1.297E-01	4.99	610	6.00E-01
2.000E-03	609	1.700E+00	1.297E-01	4.99	610	6.00E-01
2.000E-03	609	1.700E+00	1.297E-01	4.99	610	6.00E-01
2.000E-03	609	1.700E+00	1.297E-01	4.99	610	6.00E-01
2.000E-03	609	1.700E+00	1.297E-01	4.99	610	6.00E-01

Table A-12. WILLOWS AND OTHER DATA SUMMARY FOR THE 1960-1961 GROWING SEASON

STATION NUMBER	NO. VALUES	ARITHMETIC MEAN	STDEV. DEVIATION	GEOMETRIC MEAN	STDEV. DEVIATION	MINIMUM VALUE	MAXIMUM VALUE	STATION NUMBER	NO. VALUES	ARITHMETIC MEAN	STDEV. DEVIATION	GEOMETRIC MEAN	STDEV. DEVIATION	MINIMUM VALUE	MAXIMUM VALUE
457	424	1.260E-02	1.650E-02	1.630E-01	1.750E-01	6.60E-02	6.71	457	424	1.260E-02	1.650E-02	1.630E-01	1.750E-01	6.60E-02	6.71
3.937E-03	1.200E-02	1.400E-02	1.400E-01	1.400E-01	1.400E-01	1.400E-01	2.400E-01	3.937E-03	1.200E-02	1.400E-02	1.400E-01	1.400E-01	1.400E-01	1.400E-01	2.400E-01
3.301E-03	8.000E-03	1.200E-02	1.200E-01	1.200E-01	1.200E-01	1.200E-01	1.500E-01	3.301E-03	8.000E-03	1.200E-02	1.200E-01	1.200E-01	1.200E-01	1.200E-01	1.500E-01
1.697E+00	2.500E+00	1.697E+00	1.697E+00	1.697E+00	1.697E+00	1.697E+00	1.697E+00	1.697E+00	2.500E+00	1.697E+00	1.697E+00	1.697E+00	1.697E+00	1.697E+00	1.697E+00
1.400E-03	1.400E-03	1.400E-03	1.400E-03	1.400E-03	1.400E-03	1.400E-03	1.400E-03	1.400E-03	1.400E-03	1.400E-03	1.400E-03	1.400E-03	1.400E-03	1.400E-03	1.400E-03
3.800E-03	8.000E-03	1.200E-02	1.200E-01	1.200E-01	1.200E-01	1.200E-01	1.200E-01	3.800E-03	8.000E-03	1.200E-02	1.200E-01	1.200E-01	1.200E-01	1.200E-01	1.200E-01
4.500E-02	9.500E-02	1.000E-01	1.000E-01	1.000E-01	1.000E-01	1.000E-01	1.000E-01	4.500E-02	9.500E-02	1.000E-01	1.000E-01	1.000E-01	1.000E-01	1.000E-01	1.000E-01
293	306	1.000E-02	1.200E-02	1.670E+00	1.870E+00	6.01	6.01	293	306	1.000E-02	1.200E-02	1.670E+00	1.870E+00	6.01	6.01
3.569E-03	1.000E-02	1.000E-02	1.000E-01	1.000E-01	1.000E-01	1.000E-01	1.000E-01	3.569E-03	1.000E-02	1.000E-02	1.000E-01	1.000E-01	1.000E-01	1.000E-01	1.000E-01
4.310E-03	1.000E-02	1.000E-02	1.000E-01	1.000E-01	1.000E-01	1.000E-01	1.000E-01	4.310E-03	1.000E-02	1.000E-02	1.000E-01	1.000E-01	1.000E-01	1.000E-01	1.000E-01
2.501E-03	6.750E-03	8.000E-03	8.000E-03	8.000E-03	8.000E-03	8.000E-03	8.000E-03	2.501E-03	6.750E-03	8.000E-03	8.000E-03	8.000E-03	8.000E-03	8.000E-03	8.000E-03
2.650E+00	2.650E+00	2.650E+00	2.650E+00	2.650E+00	2.650E+00	2.650E+00	2.650E+00	2.650E+00	2.650E+00	2.650E+00	2.650E+00	2.650E+00	2.650E+00	2.650E+00	2.650E+00
-5.000E-03	-9.400E-03	-8.000E-03	-8.000E-03	-8.000E-03	-8.000E-03	-8.000E-03	-8.000E-03	-5.000E-03	-9.400E-03	-8.000E-03	-8.000E-03	-8.000E-03	-8.000E-03	-8.000E-03	-8.000E-03
2.800E-03	7.500E-03	9.000E-03	9.000E-03	9.000E-03	9.000E-03	9.000E-03	9.000E-03	2.800E-03	7.500E-03	9.000E-03	9.000E-03	9.000E-03	9.000E-03	9.000E-03	9.000E-03
4.700E-02	7.500E-02	8.000E-02	8.000E-02	8.000E-02	8.000E-02	8.000E-02	8.000E-02	4.700E-02	7.500E-02	8.000E-02	8.000E-02	8.000E-02	8.000E-02	8.000E-02	8.000E-02
449	449	1.400E-02	1.500E-02	1.590E+00	1.750E+00	6.19	6.19	449	449	1.400E-02	1.500E-02	1.590E+00	1.750E+00	6.19	6.19
4.476E-03	1.400E-02	1.400E-02	1.400E-01	1.400E-01	1.400E-01	1.400E-01	1.400E-01	4.476E-03	1.400E-02	1.400E-02	1.400E-01	1.400E-01	1.400E-01	1.400E-01	1.400E-01
4.695E-03	1.600E-02	1.600E-02	1.600E-01	1.600E-01	1.600E-01	1.600E-01	1.600E-01	4.695E-03	1.600E-02	1.600E-02	1.600E-01	1.600E-01	1.600E-01	1.600E-01	1.600E-01
3.675E-03	9.750E-03	1.400E-02	1.400E-01	1.400E-01	1.400E-01	1.400E-01	1.400E-01	3.675E-03	9.750E-03	1.400E-02	1.400E-01	1.400E-01	1.400E-01	1.400E-01	1.400E-01
1.940E+00	2.500E+00	2.000E+00	2.000E+00	2.000E+00	2.000E+00	2.000E+00	2.000E+00	1.940E+00	2.500E+00	2.000E+00	2.000E+00	2.000E+00	2.000E+00	2.000E+00	2.000E+00
-3.600E-03	0.0	-6.000E-03	-6.000E-03	-6.000E-03	-6.000E-03	-6.000E-03	-6.000E-03	-3.600E-03	0.0	-6.000E-03	-6.000E-03	-6.000E-03	-6.000E-03	-6.000E-03	-6.000E-03
3.400E-03	1.000E-02	1.000E-02	1.000E-01	1.000E-01	1.000E-01	1.000E-01	1.000E-01	3.400E-03	1.000E-02	1.000E-02	1.000E-01	1.000E-01	1.000E-01	1.000E-01	1.000E-01
5.300E-02	1.100E-01	1.100E-01	1.100E-01	1.100E-01	1.100E-01	1.100E-01	1.100E-01	5.300E-02	1.100E-01	1.100E-01	1.100E-01	1.100E-01	1.100E-01	1.100E-01	1.100E-01
424	300	1.900E-02	3.000E-02	1.700E+00	2.000E+00	6.66	6.66	424	300	1.900E-02	3.000E-02	1.700E+00	2.000E+00	6.66	6.66
1.300E-02	2.600E-02	2.600E-02	2.600E-01	2.600E-01	2.600E-01	2.600E-01	2.600E-01	1.300E-02	2.600E-02	2.600E-02	2.600E-01	2.600E-01	2.600E-01	2.600E-01	2.600E-01
9.000E-03	1.000E-02	1.000E-02	1.000E-01	1.000E-01	1.000E-01	1.000E-01	1.000E-01	9.000E-03	1.000E-02	1.000E-02	1.000E-01	1.000E-01	1.000E-01	1.000E-01	1.000E-01
2.410E+00	2.410E+00	2.410E+00	2.410E+00	2.410E+00	2.410E+00	2.410E+00	2.410E+00	2.410E+00	2.410E+00	2.410E+00	2.410E+00	2.410E+00	2.410E+00	2.410E+00	2.410E+00
-1.500E-03	-1.500E-03	-1.500E-03	-1.500E-03	-1.500E-03	-1.500E-03	-1.500E-03	-1.500E-03	-1.500E-03	-1.500E-03	-1.500E-03	-1.500E-03	-1.500E-03	-1.500E-03	-1.500E-03	-1.500E-03
1.000E-02	1.000E-02	1.000E-02	1.000E-01	1.000E-01	1.000E-01	1.000E-01	1.000E-01	1.000E-02	1.000E-02	1.000E-02	1.000E-01	1.000E-01	1.000E-01	1.000E-01	1.000E-01
9.600E-02	1.500E-01	1.500E-01	1.500E-01	1.500E-01	1.500E-01	1.500E-01	1.500E-01	9.600E-02	1.500E-01	1.500E-01	1.500E-01	1.500E-01	1.500E-01	1.500E-01	1.500E-01
306	306	1.000E-02	1.600E-02	1.700E+00	1.800E+00	6.66	6.66	306	306	1.000E-02	1.600E-02	1.700E+00	1.800E+00	6.66	6.66
3.900E-03	1.000E-02	1.000E-02	1.000E-01	1.000E-01	1.000E-01	1.000E-01	1.000E-01	3.900E-03	1.000E-02	1.000E-02	1.000E-01	1.000E-01	1.000E-01	1.000E-01	1.000E-01
6.900E-03	1.400E-02	1.400E-02	1.400E-01	1.400E-01	1.400E-01	1.400E-01	1.400E-01	6.900E-03	1.400E-02	1.400E-02	1.400E-01	1.400E-01	1.400E-01	1.400E-01	1.400E-01
2.500E-03	8.000E-03	1.000E-02	1.000E-01	1.000E-01	1.000E-01	1.000E-01	1.000E-01	2.500E-03	8.000E-03	1.000E-02	1.000E-01	1.000E-01	1.000E-01	1.000E-01	1.000E-01
2.000E+00	2.000E+00	2.000E+00	2.000E+00	2.000E+00	2.000E+00	2.000E+00	2.000E+00	2.000E+00	2.000E+00	2.000E+00	2.000E+00	2.000E+00	2.000E+00	2.000E+00	2.000E+00
-1.000E-03	-9.000E-03	-6.000E-03	-6.000E-03	-6.000E-03	-6.000E-03	-6.000E-03	-6.000E-03	-1.000E-03	-9.000E-03	-6.000E-03	-6.000E-03	-6.000E-03	-6.000E-03	-6.000E-03	-6.000E-03
1.700E-03	6.000E-03	6.000E-03	6.000E-03	6.000E-03	6.000E-03	6.000E-03	6.000E-03	1.700E-03	6.000E-03	6.000E-03	6.000E-03	6.000E-03	6.000E-03	6.000E-03	6.000E-03
6.000E-02	1.000E-01	1.000E-01	1.000E-01	1.000E-01	1.000E-01	1.000E-01	1.000E-01	6.000E-02	1.000E-01	1.000E-01	1.000E-01	1.000E-01	1.000E-01	1.000E-01	1.000E-01

Table A-14. WILLIAMS AIR FORCE BASE DATA SUMMARY FOR THE 1960S - PERIOD 1977

STATION NUMBER	NO. VALUES	ARITHMETIC MEAN	STD. ARITH. DEVIATION	GEOMETRIC MEAN	STD. GEOM. DEVIATION	MINIMUM VALUE	MEDIAN VALUE	MAXIMUM VALUE	MEASURE (CM)	TOTAL MEASUREMENTS (NO.)	RECORDING INSTRUMENTS (TYPE)	
STATION NUMBER ... 1												
246	246	6.170E-03	1.071E-02	1.660E+00	237	1.660E+00	1.700E+00	236	237	1.700E+00	4.137E-02	240
4.064E-03	6.170E-03	1.071E-02	1.660E+00	237	1.660E+00	1.700E+00	236	237	1.700E+00	4.137E-02	240	4.260E-01
2.095E-03	6.170E-03	1.071E-02	1.660E+00	237	1.660E+00	1.700E+00	236	237	1.700E+00	4.137E-02	240	2.300E-01
3.747E-03	6.170E-03	1.071E-02	1.660E+00	237	1.660E+00	1.700E+00	236	237	1.700E+00	4.137E-02	240	3.000E-01
1.670E+00	6.170E-03	1.071E-02	1.660E+00	237	1.660E+00	1.700E+00	236	237	1.700E+00	4.137E-02	240	1.570E+03
0.0	6.170E-03	1.071E-02	1.660E+00	237	1.660E+00	1.700E+00	236	237	1.700E+00	4.137E-02	240	0.0
3.200E-03	6.170E-03	1.071E-02	1.660E+00	237	1.660E+00	1.700E+00	236	237	1.700E+00	4.137E-02	240	5.815E-01
2.090E-02	6.170E-03	1.071E-02	1.660E+00	237	1.660E+00	1.700E+00	236	237	1.700E+00	4.137E-02	240	1.850E+00
STATION NUMBER ... 2												
422	422	9.200E-03	1.640E-02	1.640E+00	335	1.640E+00	1.700E+00	413	335	1.700E+00	1.310E-01	405
3.150E-03	9.200E-03	1.640E-02	1.640E+00	335	1.640E+00	1.700E+00	413	335	1.700E+00	1.310E-01	405	5.780E-01
2.470E-03	9.200E-03	1.640E-02	1.640E+00	335	1.640E+00	1.700E+00	413	335	1.700E+00	1.310E-01	405	6.700E-01
2.600E-03	9.200E-03	1.640E-02	1.640E+00	335	1.640E+00	1.700E+00	413	335	1.700E+00	1.310E-01	405	2.950E-01
1.910E+00	9.200E-03	1.640E-02	1.640E+00	335	1.640E+00	1.700E+00	413	335	1.700E+00	1.310E-01	405	2.400E+00
-4.000E-03	9.200E-03	1.640E-02	1.640E+00	335	1.640E+00	1.700E+00	413	335	1.700E+00	1.310E-01	405	0.0
2.600E-03	9.200E-03	1.640E-02	1.640E+00	335	1.640E+00	1.700E+00	413	335	1.700E+00	1.310E-01	405	4.200E-01
2.390E-02	9.200E-03	1.640E-02	1.640E+00	335	1.640E+00	1.700E+00	413	335	1.700E+00	1.310E-01	405	4.130E+00
STATION NUMBER ... 3												
376	376	9.500E-03	1.200E-02	1.630E+00	403	1.630E+00	1.650E+00	459	403	1.650E+00	2.100E-02	402
2.580E-03	9.500E-03	1.200E-02	1.630E+00	403	1.630E+00	1.650E+00	459	403	1.650E+00	2.100E-02	402	5.510E-01
1.970E-03	9.500E-03	1.200E-02	1.630E+00	403	1.630E+00	1.650E+00	459	403	1.650E+00	2.100E-02	402	5.170E-01
2.040E-03	9.500E-03	1.200E-02	1.630E+00	403	1.630E+00	1.650E+00	459	403	1.650E+00	2.100E-02	402	4.300E-01
2.000E+00	9.500E-03	1.200E-02	1.630E+00	403	1.630E+00	1.650E+00	459	403	1.650E+00	2.100E-02	402	1.630E+00
-1.000E-03	9.500E-03	1.200E-02	1.630E+00	403	1.630E+00	1.650E+00	459	403	1.650E+00	2.100E-02	402	2.300E-02
2.100E-03	9.500E-03	1.200E-02	1.630E+00	403	1.630E+00	1.650E+00	459	403	1.650E+00	2.100E-02	402	4.170E-01
1.390E-02	9.500E-03	1.200E-02	1.630E+00	403	1.630E+00	1.650E+00	459	403	1.650E+00	2.100E-02	402	3.600E+00
STATION NUMBER ... 4												
211	211	1.600E-02	2.000E-02	1.700E+00	245	1.700E+00	1.810E+00	245	245	1.810E+00	1.450E-01	240
7.150E-03	1.600E-02	2.000E-02	1.700E+00	245	1.700E+00	1.810E+00	245	245	1.810E+00	1.450E-01	240	4.350E-01
7.150E-03	1.600E-02	2.000E-02	1.700E+00	245	1.700E+00	1.810E+00	245	245	1.810E+00	1.450E-01	240	2.000E-01
6.700E-03	1.600E-02	2.000E-02	1.700E+00	245	1.700E+00	1.810E+00	245	245	1.810E+00	1.450E-01	240	5.250E-01
2.570E+00	1.600E-02	2.000E-02	1.700E+00	245	1.700E+00	1.810E+00	245	245	1.810E+00	1.450E-01	240	1.000E+00
-4.000E-03	1.600E-02	2.000E-02	1.700E+00	245	1.700E+00	1.810E+00	245	245	1.810E+00	1.450E-01	240	0.0
5.000E-03	1.600E-02	2.000E-02	1.700E+00	245	1.700E+00	1.810E+00	245	245	1.810E+00	1.450E-01	240	3.500E-01
5.360E-02	1.600E-02	2.000E-02	1.700E+00	245	1.700E+00	1.810E+00	245	245	1.810E+00	1.450E-01	240	4.170E-01
STATION NUMBER ... 5												
376	376	8.670E-03	1.140E-02	1.670E+00	341	1.670E+00	1.700E+00	377	341	1.700E+00	7.810E-02	374
3.040E-03	8.670E-03	1.140E-02	1.670E+00	341	1.670E+00	1.700E+00	377	341	1.700E+00	7.810E-02	374	1.500E-01
2.000E-03	8.670E-03	1.140E-02	1.670E+00	341	1.670E+00	1.700E+00	377	341	1.700E+00	7.810E-02	374	3.000E-01
3.700E-03	8.670E-03	1.140E-02	1.670E+00	341	1.670E+00	1.700E+00	377	341	1.700E+00	7.810E-02	374	4.170E-01
0.0	8.670E-03	1.140E-02	1.670E+00	341	1.670E+00	1.700E+00	377	341	1.700E+00	7.810E-02	374	0.0
3.000E-03	8.670E-03	1.140E-02	1.670E+00	341	1.670E+00	1.700E+00	377	341	1.700E+00	7.810E-02	374	5.810E-01
2.070E-02	8.670E-03	1.140E-02	1.670E+00	341	1.670E+00	1.700E+00	377	341	1.700E+00	7.810E-02	374	1.850E+00

Table A-15. WILLIAMS AIR FORCE BASE DATA SUMMARY FOR THE MONTH OF APRIL, 1957

STATION NUMBER ...	NO. VALUES	ARITHMETIC MEAN	STD. DEVIATION	GEOMETRIC MEAN	STD. GEOM. DEVIATION	MINIMUM VALUE	MAXIMUM VALUE	WINDSPEED (MPH)	WIND DIRECTION (DEG)	TEMPERATURE (DEG F)	RELATIVE HUMIDITY (%)	WINDSPEED (MPH)	WIND DIRECTION (DEG)	TEMPERATURE (DEG F)	RELATIVE HUMIDITY (%)
STATION NUMBER ... 1	606	3.153E-03	7.019E-03	1.600E-02	1.600E-02	1.600E-02	1.600E-02	604	1.600E-02	1.600E-02	1.600E-02	606	1.600E-02	1.600E-02	606
STATION NUMBER ... 2	640	1.840E-03	1.400E-02	1.400E-02	1.400E-02	1.400E-02	1.400E-02	641	1.400E-02	1.400E-02	1.400E-02	641	1.400E-02	1.400E-02	641
STATION NUMBER ... 3	645	2.350E-03	1.000E-02	1.000E-02	1.000E-02	1.000E-02	1.000E-02	645	1.000E-02	1.000E-02	1.000E-02	645	1.000E-02	1.000E-02	645
STATION NUMBER ... 4	616	2.570E-03	1.700E-02	1.700E-02	1.700E-02	1.700E-02	1.700E-02	616	1.700E-02	1.700E-02	1.700E-02	616	1.700E-02	1.700E-02	616
STATION NUMBER ... 5	634	1.700E-03	9.000E-03	1.000E-02	1.000E-02	1.000E-02	1.000E-02	634	1.000E-02	1.000E-02	1.000E-02	634	1.000E-02	1.000E-02	634

Table A-16. WILLIAMS AIR FORCE BASE DATA SUMMARY FOR 1974 MONTHLY MEASUREMENTS

STATION NUMBER	NO. VALUES	ARITHMETIC MEAN	STD. ARITH. DEVIATION	GEO-METRIC MEAN	STD. GEO-M. DEVIATION	MINIMUM VALUE	MAXIMUM VALUE	WIND DIRECTION (DEG)	WIND SPEED (MPH)	REL. HUMIDITY (%)	TEMPERATURE (°C)	PRECIPITATION (MM)	REL. HUMIDITY (%)	PRECIPITATION (MM)
STATION NUMBER ... 1														
NO. VALUES	367	367	367	367	367	367	367	365	365	366	366	366	366	366
ARITHMETIC MEAN	9.700E-04	7.820E-03	8.330E-03	1.670E+00	1.670E+00	1.670E+00	1.670E+00	1.670E+00	1.670E+00	1.670E+00	1.670E+00	1.670E+00	1.670E+00	1.670E+00
STD. ARITH. DEVIATION	1.449E-03	6.700E-03	6.820E-03	6.771E-02	6.771E-02	6.771E-02	6.771E-02	6.771E-02	6.771E-02	6.771E-02	6.771E-02	6.771E-02	6.771E-02	6.771E-02
GEO-METRIC MEAN	1.565E-03	5.000E-03	6.000E-03	1.670E+00	1.670E+00	1.670E+00	1.670E+00	1.670E+00	1.670E+00	1.670E+00	1.670E+00	1.670E+00	1.670E+00	1.670E+00
STD. GEO-M. DEVIATION	2.000E-03	2.000E-03	1.800E-03	1.000E+00	1.000E+00	1.000E+00	1.000E+00	1.000E+00	1.000E+00	1.000E+00	1.000E+00	1.000E+00	1.000E+00	1.000E+00
MINIMUM VALUE	-1.600E-03	2.000E-03	0.0	1.000E+00	1.000E+00	1.000E+00	1.000E+00	1.000E+00	1.000E+00	1.000E+00	1.000E+00	1.000E+00	1.000E+00	1.000E+00
MAXIMUM VALUE	9.000E-04	5.700E-03	6.100E-03	1.670E+00	1.670E+00	1.670E+00	1.670E+00	1.670E+00	1.670E+00	1.670E+00	1.670E+00	1.670E+00	1.670E+00	1.670E+00
STATION NUMBER ... 2														
NO. VALUES	593	593	593	593	593	593	593	593	593	593	593	593	593	593
ARITHMETIC MEAN	-4.457E-04	1.453E-02	1.602E-02	1.500E+00	1.500E+00	1.500E+00	1.500E+00	1.500E+00	1.500E+00	1.500E+00	1.500E+00	1.500E+00	1.500E+00	1.500E+00
STD. ARITH. DEVIATION	3.750E-03	1.000E-02	1.100E-02	1.100E-02	1.100E-02	1.100E-02	1.100E-02	1.100E-02	1.100E-02	1.100E-02	1.100E-02	1.100E-02	1.100E-02	1.100E-02
GEO-METRIC MEAN	1.745E-03	1.150E-02	1.150E-02	1.570E+00	1.570E+00	1.570E+00	1.570E+00	1.570E+00	1.570E+00	1.570E+00	1.570E+00	1.570E+00	1.570E+00	1.570E+00
STD. GEO-M. DEVIATION	1.730E-03	2.000E-03	1.000E-03	1.000E+00	1.000E+00	1.000E+00	1.000E+00	1.000E+00	1.000E+00	1.000E+00	1.000E+00	1.000E+00	1.000E+00	1.000E+00
MINIMUM VALUE	-5.400E-03	1.200E-03	2.700E-03	1.000E+00	1.000E+00	1.000E+00	1.000E+00	1.000E+00	1.000E+00	1.000E+00	1.000E+00	1.000E+00	1.000E+00	1.000E+00
MAXIMUM VALUE	-1.150E-03	1.100E-02	1.000E-02	1.570E+00	1.570E+00	1.570E+00	1.570E+00	1.570E+00	1.570E+00	1.570E+00	1.570E+00	1.570E+00	1.570E+00	1.570E+00
STATION NUMBER ... 3														
NO. VALUES	594	594	594	594	594	594	594	594	594	594	594	594	594	594
ARITHMETIC MEAN	1.916E-03	9.820E-03	1.121E-02	1.647E+00	1.647E+00	1.647E+00	1.647E+00	1.647E+00	1.647E+00	1.647E+00	1.647E+00	1.647E+00	1.647E+00	1.647E+00
STD. ARITH. DEVIATION	1.597E-03	8.420E-03	8.600E-03	1.000E-03	1.000E-03	1.000E-03	1.000E-03	1.000E-03	1.000E-03	1.000E-03	1.000E-03	1.000E-03	1.000E-03	1.000E-03
GEO-METRIC MEAN	1.593E-03	6.630E-03	8.800E-03	1.647E+00	1.647E+00	1.647E+00	1.647E+00	1.647E+00	1.647E+00	1.647E+00	1.647E+00	1.647E+00	1.647E+00	1.647E+00
STD. GEO-M. DEVIATION	2.000E-03	2.000E-03	1.900E-03	1.000E+00	1.000E+00	1.000E+00	1.000E+00	1.000E+00	1.000E+00	1.000E+00	1.000E+00	1.000E+00	1.000E+00	1.000E+00
MINIMUM VALUE	-6.000E-04	2.000E-03	1.000E-03	1.000E+00	1.000E+00	1.000E+00	1.000E+00	1.000E+00	1.000E+00	1.000E+00	1.000E+00	1.000E+00	1.000E+00	1.000E+00
MAXIMUM VALUE	1.600E-03	6.500E-03	8.000E-03	1.570E+00	1.570E+00	1.570E+00	1.570E+00	1.570E+00	1.570E+00	1.570E+00	1.570E+00	1.570E+00	1.570E+00	1.570E+00
STATION NUMBER ... 4														
NO. VALUES	590	590	590	590	590	590	590	590	590	590	590	590	590	590
ARITHMETIC MEAN	2.240E-03	9.800E-03	1.212E-02	1.650E+00	1.650E+00	1.650E+00	1.650E+00	1.650E+00	1.650E+00	1.650E+00	1.650E+00	1.650E+00	1.650E+00	1.650E+00
STD. ARITH. DEVIATION	2.000E-03	1.000E-02	1.000E-02	1.000E-03	1.000E-03	1.000E-03	1.000E-03	1.000E-03	1.000E-03	1.000E-03	1.000E-03	1.000E-03	1.000E-03	1.000E-03
GEO-METRIC MEAN	1.800E-03	6.430E-03	8.400E-03	1.650E+00	1.650E+00	1.650E+00	1.650E+00	1.650E+00	1.650E+00	1.650E+00	1.650E+00	1.650E+00	1.650E+00	1.650E+00
STD. GEO-M. DEVIATION	2.600E-03	2.600E-03	2.500E-03	1.000E+00	1.000E+00	1.000E+00	1.000E+00	1.000E+00	1.000E+00	1.000E+00	1.000E+00	1.000E+00	1.000E+00	1.000E+00
MINIMUM VALUE	-1.600E-03	2.000E-03	3.000E-03	1.000E+00	1.000E+00	1.000E+00	1.000E+00	1.000E+00	1.000E+00	1.000E+00	1.000E+00	1.000E+00	1.000E+00	1.000E+00
MAXIMUM VALUE	1.500E-03	7.000E-03	9.100E-03	1.610E+00	1.610E+00	1.610E+00	1.610E+00	1.610E+00	1.610E+00	1.610E+00	1.610E+00	1.610E+00	1.610E+00	1.610E+00
STATION NUMBER ... 5														
NO. VALUES	595	595	595	595	595	595	595	595	595	595	595	595	595	595
ARITHMETIC MEAN	4.500E-03	4.500E-03	9.100E-03	1.641E+00	1.641E+00	1.641E+00	1.641E+00	1.641E+00	1.641E+00	1.641E+00	1.641E+00	1.641E+00	1.641E+00	1.641E+00
STD. ARITH. DEVIATION	3.600E-03	1.000E-02	1.000E-02	1.000E-03	1.000E-03	1.000E-03	1.000E-03	1.000E-03	1.000E-03	1.000E-03	1.000E-03	1.000E-03	1.000E-03	1.000E-03
GEO-METRIC MEAN	3.200E-03	3.200E-03	5.000E-03	1.600E+00	1.600E+00	1.600E+00	1.600E+00	1.600E+00	1.600E+00	1.600E+00	1.600E+00	1.600E+00	1.600E+00	1.600E+00
STD. GEO-M. DEVIATION	2.000E-03	2.000E-03	2.000E-03	1.000E+00	1.000E+00	1.000E+00	1.000E+00	1.000E+00	1.000E+00	1.000E+00	1.000E+00	1.000E+00	1.000E+00	1.000E+00
MINIMUM VALUE	-9.000E-04	2.000E-03	3.000E-03	1.000E+00	1.000E+00	1.000E+00	1.000E+00	1.000E+00	1.000E+00	1.000E+00	1.000E+00	1.000E+00	1.000E+00	1.000E+00
MAXIMUM VALUE	6.000E-03	3.000E-03	6.000E-03	1.600E+00	1.600E+00	1.600E+00	1.600E+00	1.600E+00	1.600E+00	1.600E+00	1.600E+00	1.600E+00	1.600E+00	1.600E+00

Table A-18. Cumulative Frequency Percentile Concentrations
(PPM) for Williams AFB Hourly NO Data:
June 1976-June 1977

Percentile	Station No.				
	1	2	3	4	5
50.	0.002	0.003	0.002	0.003	0.002
80.	0.004	0.004	0.004	0.008	0.005
90.	0.006	0.006	0.005	0.012	0.008
95.	0.008	0.007	0.007	0.018	0.010
98.	0.012	0.011	0.011	0.028	0.013
99.	0.016	0.016	0.015	0.038	0.016
99.5	0.023	0.021	0.020	0.048	0.022
99.9	0.052	0.045	0.037	0.075	0.036
99.95	0.060	0.050	0.045	0.096	0.045
99.99	0.106	0.115	0.094	0.131	0.059

Table A-19. Cumulative Frequency Percentile Concentrations
(PPM) for Williams AFB Hourly NO_x Data:
June 1976-June 1977

Percentile	Station No.				
	1	2	3	4	5
50.	0.008	0.009	0.009	0.014	0.008
80.	0.014	0.016	0.017	0.027	0.015
90.	0.020	0.022	0.024	0.040	0.023
95.	0.028	0.030	0.033	0.055	0.032
98.	0.039	0.041	0.048	0.080	0.047
99.	0.053	0.052	0.061	0.100	0.061
99.5	0.071	0.060	0.076	0.120	0.073
99.9	0.106	0.094	0.106	0.158	0.096
99.95	0.125	0.107	0.114	0.170	0.102
99.99	0.206	0.228	0.198	0.259	0.108

Table A-20. Cumulative Frequency Percentile Concentrations
(PPM) for Williams AFB Hourly NO₂ Data:
June 1976-June 1977

Percentile	Station No.				
	1	2	3	4	5
50.	0.005	0.006	0.007	0.010	0.006
80.	0.011	0.013	0.014	0.020	0.012
90.	0.016	0.019	0.020	0.031	0.020
95.	0.022	0.026	0.028	0.044	0.028
98.	0.034	0.036	0.041	0.061	0.041
99.	0.047	0.045	0.053	0.074	0.051
99.5	0.058	0.052	0.065	0.084	0.060
99.9	0.099	0.077	0.088	0.108	0.074
99.95	0.103	0.082	0.099	0.128	0.077
99.99	0.108	0.113	0.108	0.147	0.097

Table A-21. Cumulative Frequency Percentile Concentrations
(PPM) for Williams AFB Hourly CO Data:
June 1976-June 1977

Percentile	Station No.				
	1	2	3	4	5
50.	0.096	0.124	0.081	0.243	0.133
80.	0.168	0.221	0.154	0.514	0.249
90.	0.262	0.318	0.252	0.758	0.397
95.	0.386	0.444	0.400	1.027	0.582
98.	0.637	0.646	0.500	1.304	0.844
99.	0.856	0.832	0.765	1.775	1.050
99.5	0.988	1.029	0.968	2.182	1.261
99.9	1.553	1.548	1.454	3.140	1.810
99.95	1.810	1.667	1.684	3.567	1.972
99.99	2.026	2.471	2.261	3.962	2.172

Table A-22. Cumulative Frequency Percentile Concentrations
(PPM) for Williams AFB Hourly CH₄ Data:
June 1976-June 1977

Percentile	Station No.				
	1	2	3	4	5
50.	1.615	1.603	1.581	1.623	1.624
80.	1.675	1.686	1.654	1.735	1.697
90.	1.722	1.743	1.712	1.861	1.779
95.	1.792	1.800	1.780	2.010	1.882
98.	1.891	1.893	1.890	2.246	2.082
99.	1.966	1.966	1.966	2.420	2.237
99.5	2.071	2.043	2.069	2.655	2.415
99.9	2.735	2.422	2.392	3.446	3.120
99.95	3.135	2.995	2.825	3.689	3.199
99.99	3.339	3.100	2.987	3.980	3.440

Table A-23. Cumulative Frequency Percentile Concentrations
(PPM) for Williams AFB Hourly THC Data:
June 1976-June 1977

Percentile	Station No.				
	1	2	3	4	5
50.	1.651	1.704	1.637	1.775	1.685
80.	1.749	1.839	1.760	1.993	1.811
90.	1.829	1.917	1.856	2.218	1.938
95.	1.951	2.028	1.974	2.495	2.097
98.	2.131	2.161	2.119	2.866	2.309
99.	2.244	2.290	2.253	3.175	2.522
99.5	2.364	2.369	2.424	3.550	2.693
99.9	3.027	3.265	3.152	4.836	3.343
99.95	3.203	3.390	3.406	5.355	3.516
99.99	3.898	4.328	4.384	6.238	4.006

Table A-24. Cumulative Frequency Percentile Concentrations (PPM) for Williams AFB Hourly NMHC Data: June 1976-June 1977

Percentile	Station No.				
	1	2	3	4	5
50.	0.048	0.079	0.064	0.151	0.058
80.	0.107	0.176	0.137	0.295	0.116
90.	0.155	0.229	0.194	0.405	0.168
95.	0.224	0.288	0.257	0.527	0.234
98.	0.322	0.378	0.331	0.778	0.330
99.	0.397	0.435	0.417	1.007	0.412
99.5	0.559	0.515	0.516	1.297	0.530
99.9	0.990	0.727	1.222	2.541	0.842
99.95	1.152	0.842	1.372	3.075	1.233
99.99	1.554	1.330	2.002	3.983	1.734

Table A-25. Cumulative Frequency Percentile Scattering Coefficients ($\times 10^{-4} \text{ m}^{-1}$) for Williams AFB Hourly b_{SCAT} Data: June 1976-June 1977

Percentile	Station No.				
	1	2	3	4	5
50.	0.469	0.495	0.513	0.476	0.479
80.	0.737	0.809	0.771	0.781	0.772
90.	0.945	1.051	0.982	1.025	0.998
95.	1.207	1.352	1.243	1.286	1.249
98.	1.669	1.894	1.800	1.714	1.784
99.	2.030	2.333	2.453	2.117	2.133
99.5	2.499	3.136	3.254	2.696	2.606
99.9	3.861	3.974	5.896	3.701	3.466
99.95	4.408	4.550	5.962	4.197	4.021
99.99	5.067	5.828	7.000	5.686	4.468

APPENDIX B

METEOROLOGICAL DATA: PROCESSING AND ASSUMPTIONS

1. INTRODUCTION

The prime objectives of this research effort were to evaluate and assess the accuracy of AQAM, using only the meteorological input data that is routinely collected at U.S. Air Force bases. Initial time constraints dictated that the EPA collect and process this meteorological data in a manner similar to ETAC; however, the standard ETAC hourly meteorological data base for Williams AFB ultimately was used. These data, in the DATSAV-SURFACE format, were then merged together with the EPA provided acoustic sounder data. Additional EPA/NOAA acquired data on u, v, w wind velocities, solar radiation, and vertical temperature gradient exists for several months of this study but has yet to be integrated with the hourly average meteorological data base.

The method for determining Turner stability class from the USAF/ETAC data is discussed in this appendix. In addition, the acoustic sounder data coding is interpreted in the context of determination of an hourly mixing depth. The mixing depth is a key AQAM model input provided neither directly by ETAC or indirectly by a Short-Term AQAM calculation. Finally, a model for mixing depths is presented, based on ETAC-measured, surface-level meteorological parameters.

2. METEOROLOGICAL DATA

Meteorological parameters used to determine stability class by the Turner^{B-1} method are wind speed, cloud ceiling height, and amount of sky cover. All parameters were supplied by USAF/ETAC but only wind speed values could be used directly. A comprehensive table of codes for ceiling heights provided easy interpretation of this data field but the sky cover data field, also presented in code, was interpretable only with the aid of ETAC personnel (Capt. J. Clark, private communication, February 1979).

Sky cover denotes the amount (to the nearest tenth) of sky covered by clouds or hidden by surface-based obscuring phenomena. In order to completely resolve the sky cover data field, three steps were taken: (1) a description of the coded field was examined; (2) it was then compared to the Turner requirement (see Table B-1); and (3) an estimated sky cover (tenths) within bounds of the requirement was assigned. For example, the ETAC given code for sky cover is -8, indicating "broken" conditions having a sky cover of 0.6-0.9, inclusive; but the Turner method requires the range 0.5-1.0, inclusive, to define the same broken condition; therefore, wherever a code -8 is supplied, the value 0.6 is assigned as the sky cover. In the case of "partly obscured" conditions, we indicate only that the amount of cover is less than complete though the possibilities span the interval 0.1-0.9. Table B-2 gives the frequency of observed sky cover codes for the 13-month study period. The following table is used to illustrate the assignment procedure for the six different sky cover codes supplied among 13 months of hourly data.

<u>ETAC Code (NS)</u>	<u>Description</u>	<u>Turner Requirement</u>	<u>Sky cover</u>
0	CLEAR. The state of the sky when it is either cloudless or the sky cover is less than 0.1.	$COV < 0.4$	0.1
-3	SCATTERED. A sky cover of 0.1 through 0.5 at and between the level of a layer aloft.	$COV < 0.5$ (day) $COV < 0.4$ (night)	0.4
-8	BROKEN. A sky cover of 0.6 through 0.9 at and below the level of a layer aloft.	$0.5 < COV < 1.0$	0.6
9	OVERCAST. A sky cover of 1.0 (ten tenths) at and below the level of a layer aloft.	$COV = 1.0$	1.0
8	OBSCURED. The condition when sky is completely hidden by surface-based obscuring phenomena; e.g., fog, smoke, precipitation forms, etc.	$COV = 1.0$	1.0
10	PARTLY OBSCURED. The condition when 0.1 or more but not all of the sky is hidden by surface-based obscuring phenomena.	$COV < 1.0$.9

3. STABILITY CLASS INDEX AS DETERMINED BY EPA METHOD

An examination of the Single Source (CRSTER) Model^{B-2} revealed that one of seven stability classes is determined from meteorological data for each hour by its preprocessor. The first six of these categories (1-6) correspond to Pasquill's classifications (A-F).^{B-3} The seventh category corresponds to the "dashes" in Pasquill's original classification and represents the existence of a strong, ground-based nocturnal temperature inversion and nondefinable wind flow conditions. The CRSTER model preprocessor restricts changes in stability to one class per hour as shown in Fig. B-1. This type of restriction allows undesirable daytime stability classes such as 5, 6, and 7. Figure B-2 shows the result of unrestricted hourly class changes.

Initially, the preprocessor determines the hour angle of the sun and the times of sunrise and sunset from the day number, longitude, and time zone to permit differentiation of daytime and nighttime cases by the Woolf^{B-4} method. For daytime cases, the appropriate insolation class is selected by means of the Turner objective method using cloud cover, ceiling height, and solar elevation as indicators. This method assigns net radiation indices, using the criteria shown in Table B-3, for cases where the total cloud cover $\leq 5/10$. If the cloud cover $> 5/10$, but less than 10/10 (overcast), the insolation class is reduced by one category when the ceiling height is greater than 16,000 ft

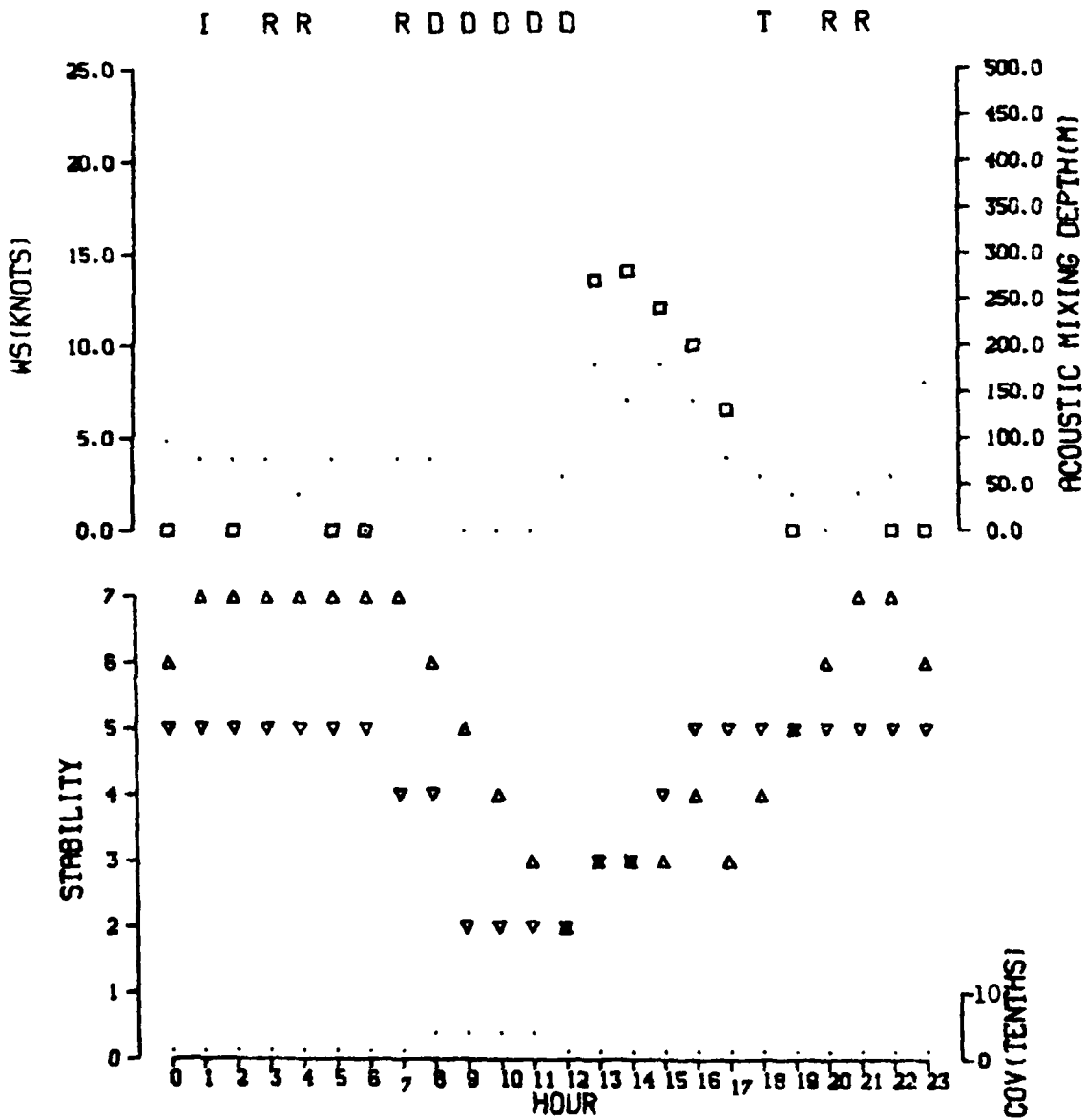


Fig. B-1. The Behavior of EPA Stability Index (Δ) When Restricted to Changes of One Class per Hour, December 10, 1976

(See legend following.)

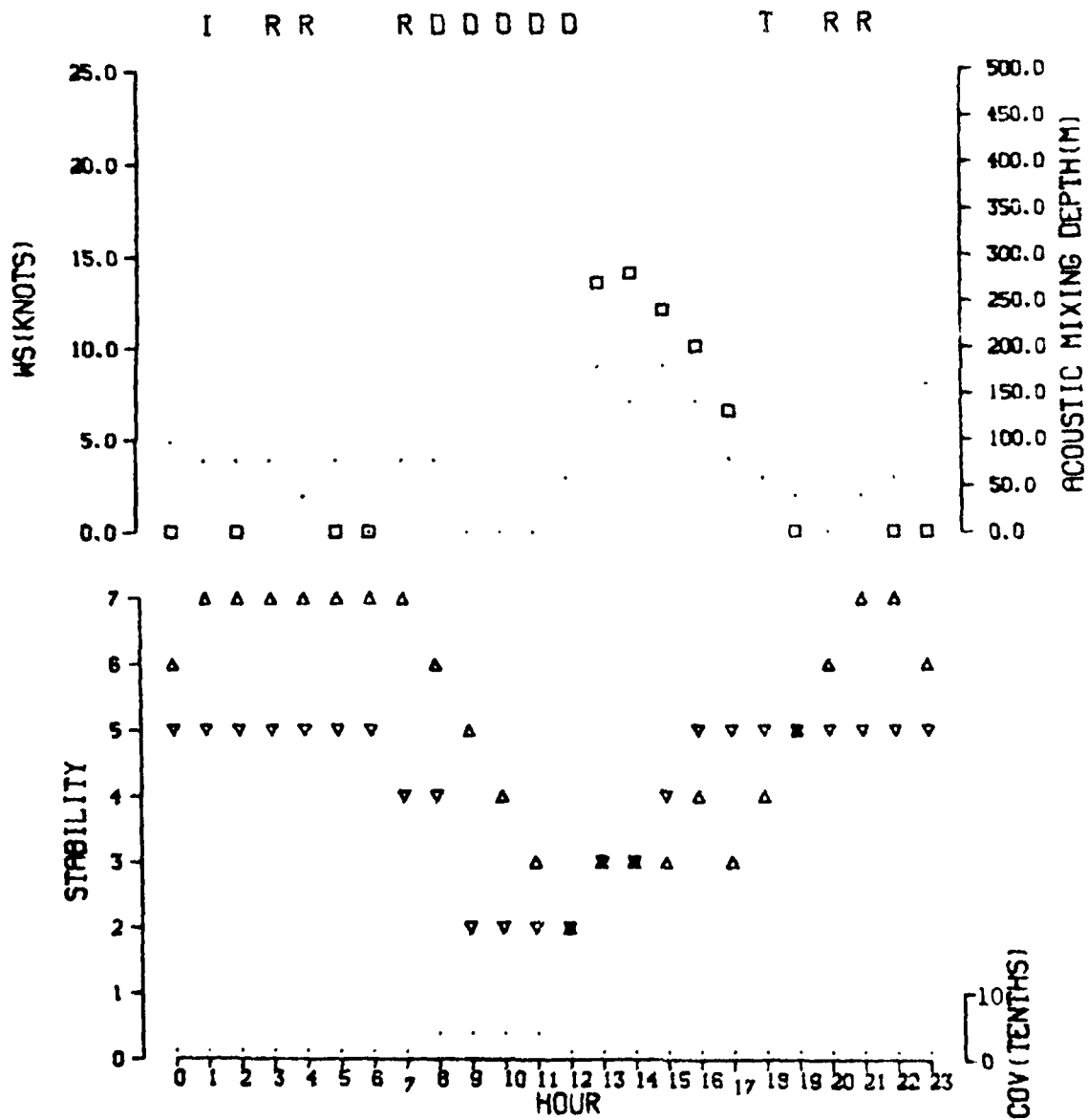


Fig. B-2. The Behavior of EPA Stability Index (Δ) for Unrestricted Hourly Class Changes, December 10, 1976

(See legend following.)

LEGEND FOR THE STABILITY CLASS INDEX ANALYSIS

TOP GRAPH

- Acoustic Sounder determined mixing layer height (meters).
- U Undefined layers.
- R Return due to noise, possible turbulence, rain, etc.
- D Daytime noise due to airbase activity.
- T Transition period.
- M Mechanical turbulence superimposed.
- X An expected height value was not supplied.
- I Inoperative equipment.
- Windspeed (knots)

BOTTOM GRAPH

- Δ Stability class index determined by EPA method.
- ∇ Stability class index determined by ANL method.
- Cloud amount in tenths of total cloud cover.

HORIZONTAL AXIS

The computed times of sunrise and sunset are indicated by lowered numerals.

and by two categories for ceilings between 7,000 and 16,000 ft. For ceilings below 7000 ft and 10/10 cloud cover (i.e., overcast), a net radiation of 0 is defined and neutral stability is specified. With the exception of the 10/10 low cloud cases, the net radiation index during daytime hours is never reduced below 1, or "weak." The final stability category is selected from Table B-1 and Turner's insolation classes.

Table B-1. Turner Requirement Related to Sky Cover^a

The net radiation index used with wind speed to obtain stability class is determined by the following procedure:

- 1) If the total cloud cover is 10/10 and the ceiling is less than 7000 ft, use net radiation index equal to 0 (whether day or night).
 - 2) For nighttime (between sunset and sunrise):
 - a) If total cloud cover $\leq 4/10$, use net radiation index equal to -2.
 - b) If total cloud cover $> 4/10$, use net radiation index equal to -1.
 - 3) For daytime:
 - a) Determine the insolation class number as a function of solar altitude from Table A-2.
 - b) If total cloud cover $\leq 5/10$, use the net radiation index in Table A-1 corresponding to the insolation class number.
 - c) If cloud cover $> 5/10$, modify the insolation class number by following six steps.
 - 1) Ceiling < 7000 ft, subtract 2.
 - 2) Ceiling ≥ 7000 ft but $< 16,000$ ft, subtract 1.
 - 3) Total cloud cover equal 10/10, subtract 1. (This will only apply to ceilings ≥ 7000 ft since cases with 10/10 coverage below 7000 ft are considered in item 1 above.)
 - 4) If insolation class number has not been modified by steps (1), (2), or (3) above, assume modified class number equal to insolation class number.
 - 5) If modified insolation class number is less than 1, let it equal 1.
 - 6) Use the net radiation index in Table A-1 corresponding to the modified insolation class number.
-

^aTaken from Ref. B-1.

Table B-2. Frequency Table of Sky Cover Codes

	0	-3	-8	8	9	10
1976 June	545	138	28	9		
July	54	594	87	9		
August	191	512	29	8	1	3
September	122	494	78	22		4
October	300	341	85	17		1
November	464	195	35	26		
December	391	232	70	51		
1977 January	127	267	80	28		2
February	256	300	92	18		6
March	330	281	82	44		7
April	273	359	64	23		1
May	258	387	84	15		
June	<u>130</u>	<u>457</u>	<u>82</u>	<u>24</u>		<u>3</u>
Total	3441	4557	896	294	1	27
% of Total (9216) ^a	37.3	49.4	9.7	3.2	.01	.29

^aExcludes 11 days for which pollutant observations are missing, 1977 January 2, 12, 15, 19, 20, 21, 22, 27, 28, 29, and 1977 June 30.

Table B-3. Insolation Classes as a Function of Solar Altitude for Cloud Cover $\leq 5/10^a$

Solar Elevation Angle (a)	Insolation Class	Net Radiation Index
$0^\circ < a < 15^\circ$	Weak	1
$15^\circ < a < 35^\circ$	Slight	2
$35^\circ < a < 60^\circ$	Moderate	3
$60^\circ < a$	Strong	4

^aFor $> 5/10$ cloud cover, see Section 3.

4. STABILITY CLASS INDEX AS DETERMINED BY ANL METHOD

This section is included mainly to document the method used to determine stability class indices during the initial phase of the Air Quality Assessment Model validation effort.

In the initial phase of the validation effort, pollutant concentrations were estimated at nine receptor locations. Subsequent data analysis on the acoustic sounder codes revealed that certain discrepancies existed at and around the time of sunset. One obvious discrepancy was the measurement of a finite lid-height occurring several hours after the presumed sunset time; thus a possible unstable condition was indicated as a stable condition.

Table B-4. Stability Classification Criteria

Surface wind speed (knots)	Daytime Insolation					Nighttime	
	Strong	Moderate	Slight	Weak	Overcast	≥ 5/10 Cloud	≤ 5/10 Cloud
< 1	1	1	2	3	4	6	7
2	1	2	2	3	4	6	7
3	1	2	2	3	4	6	7
4	1	2	3	4	4	5	6
5	1	2	3	4	4	5	6
6	2	2	3	4	4	5	6
7	2	2	3	4	4	4	5
8	2	3	3	4	4	4	5
9	2	3	3	4	4	4	5
10	3	3	4	4	4	4	5
11	3	3	4	4	4	4	4
> 12	3	4	4	4	4	4	4

A comparison of the ANL method to the EPA method showed that both are the same in every essential except that the ANL method assumed the following:

1. Designed for urban conditions, only the first five stability categories were allowed.
2. The times of sunrise and sunset were estimated from charts presented in the Smithsonian Meteorological Tables.
3. Fractional wind speeds were rounded when applied to Turner's Stability-Net Radiation table.

Of the two methods, EPA's method was selected for use in AQAM because of its more accurate determination of sunrise and sunset times; the need for which can be seen in Fig. B-2 where the lid height as seen by the acoustic sounder is approximately 130 m at the hour of sunset, 1700 hr, and a slightly unstable atmospheric condition (class 3) is correctly determined by the EPA method. On the other hand, a slightly stable atmospheric condition (class 5) is incorrectly determined by the ANL method.

5. MIXING DEPTH, DIRECT MEASUREMENT BY ACOUSTIC SOUNDER

The Acoustic Sounder information is presented in code as a six-digit number of the form ABmDEn, where AB and DE are average height values (tens of meters) from which echoes were received, "m" is a code used to explain a special local effect, and "n" is a code used to designate a specific atmospheric phenomena. In all cases of inoperative equipment the code is 999999.

The average height values, AB and DE, fall within the 20-500 m vertical range of the recording chart paper.

The special effects, m, cause graying of the sound pulse as indicated by the following four values:

1. Superimposed return due to noise, turbulence, or precipitation.
2. Background acoustical noise due to airbase activity.
3. Uncertain acoustical return due to unstable-stable atmospheric transition.
4. Apparent mechanical turbulence due to high wind speed.

The specific atmospheric phenomena, n, are conditions applied to the Williams Air Force Base study. The values of "n" (1-10) are described in Table B-5, which gives the AFB Acoustic Sounder Classification Codes.

The table below shows the assignment of mixing depth values based on these codes. They are used only in the development of a mixing depth algorithm (Section 6).

<u>Acoustic Sounder Class</u>	<u>Mixing Depth (meters)</u>
1 Top of radiation inversion	0.0
2 Drainage winds	0.0
3 Layered return	
a. Top of radiation inversion	0.0
b. Top of stratified echoes	0.0
c. Surface based	0.0
d. Undefined layers	9990.
e. Transition period	9993.
f. Mechanical turbulence	ABO. or 9994 if missing
4 Inversion base forced aloft	ABO. or 9998 if missing
5 Subsidence inversion	ABO. or 9998 if missing
6 Frontal inversion	ABO. or 9998 if missing
7 Daytime noise	9992.
8 Return due to noise	9991.
9 Top of mixing layer	
a. Top known	DEO. or 9998 if missing
b. Top unknown	9998.
c. Transition period	9993.
d. Mechanical turbulence	DEO. or 9998 if missing
10 Instrument inoperative	9999.

Figures B-3 and B-4 present frequency distributions of acoustic sounder measurements based on the hour of occurrence and the month of occurrence, respectively. These two figures supply the bases for the amount of present data deemed valid using the above interpretation of the Classification Codes.

6. DEVELOPMENT OF A MIXING DEPTH ALGORITHM

For daytime hours, the acoustic sounder provided mixing depths for 996 hours of the 13-month experiment. The paucity of data is due to the rapid daytime development of the mixed layer and the limited ranging capabilities (i.e., ≤ 500 m) of the acoustic sounder. These data are compared in Fig. B-5

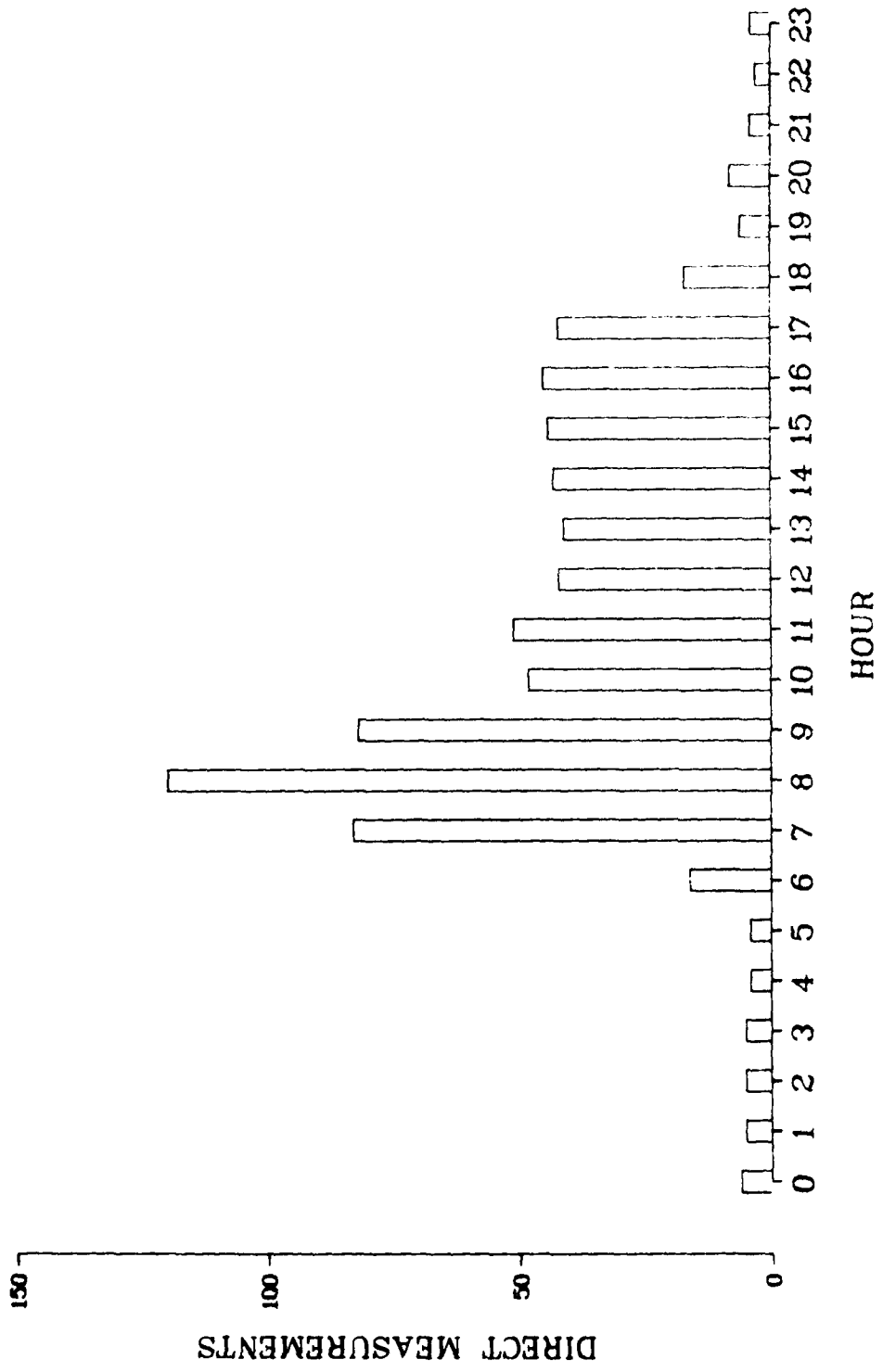


Fig. B-3. Frequency Distribution of Acoustic Sounder Measurements by Hour

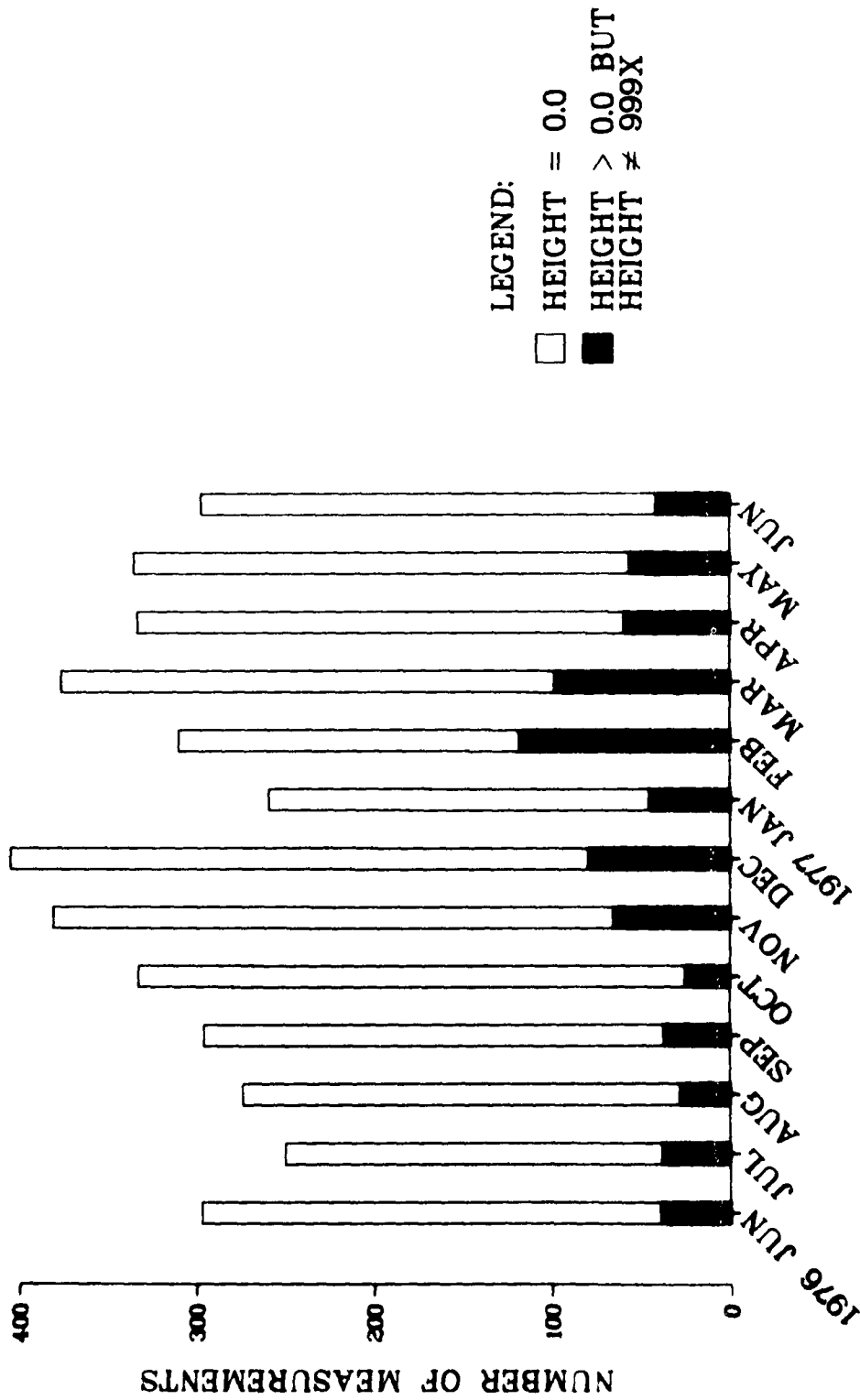


Fig. B-4. Frequency Distribution of Acoustic Sounder Measurements by Month

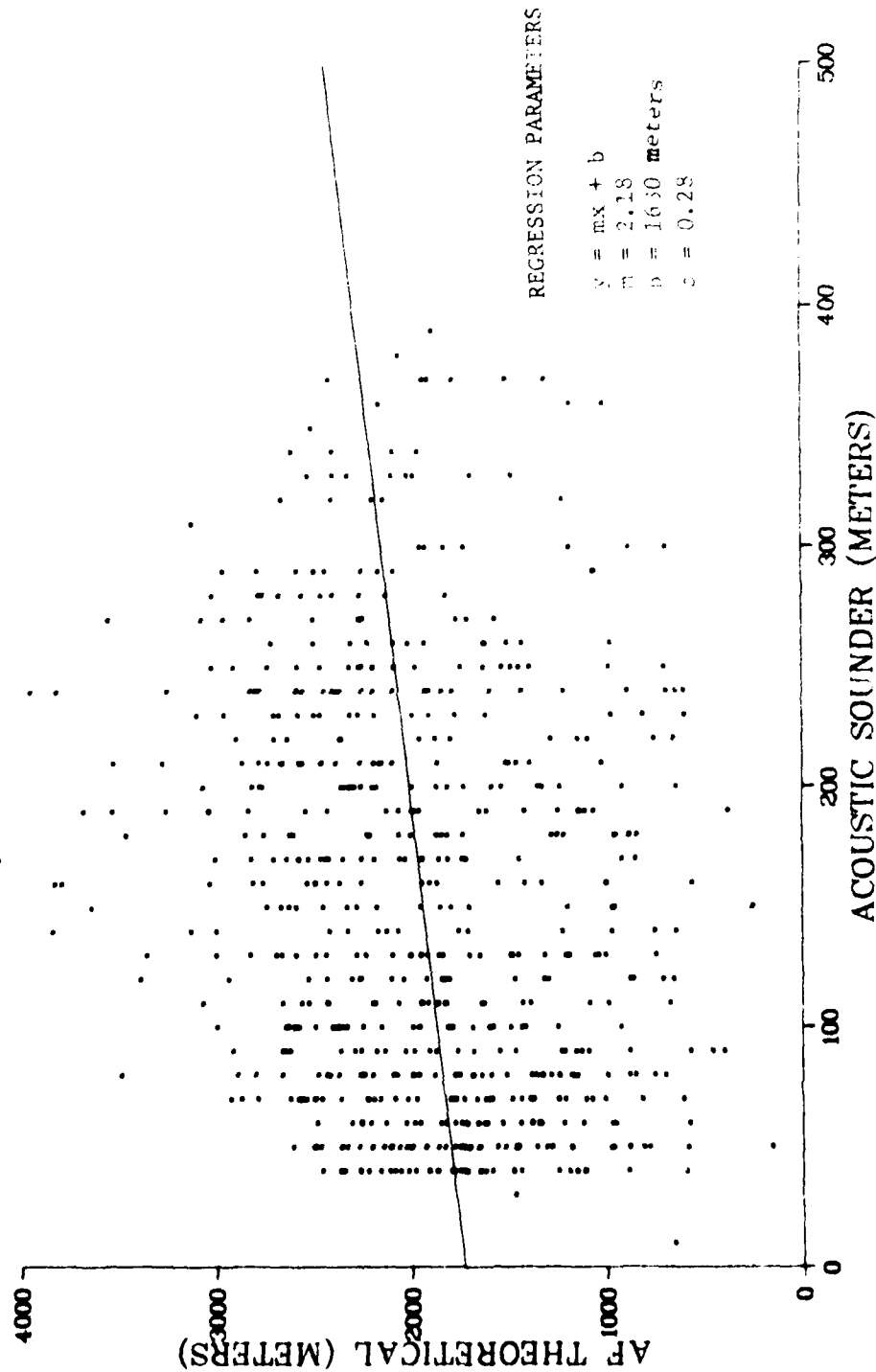


Fig. B-5. Scatter Plot of Acoustic Sounder Measured Lid Height vs. Nezak's Theoretical Model Predictions for Daytime Hours

Table B-5. Acoustic Sounder Classification Codes
for Williams AFB Study

1. Top of radiation inversion: ABO 001

AB is top in 10s of meters

This type of inversion is typical of night time desert locations. It is ground based around sunrise hours but aloft during late evening hours; stable to very stable atmospheric conditions. Much of the turbulent mixing occurs only in a shallow layer near the ground. The thickness of this shallow layer varies over a very wide range, from meters to hundreds of meters making it impracticable to define the layer height from this code.

2. Drainage winds: with or without stratified layers above: ABO DE2

AB is top of Drainage in 10s of meters

DE is top of stratified layers in 10s of meters

- | | | |
|-------------------------------------|------------|------------|
| a. AB: top of drainage | <u>ABO</u> | 002 |
| b. DE: top of stratified echoes | ABO | <u>DE2</u> |
| c. top of stratified echoes unknown | ABO | <u>002</u> |

Drainage winds are defined for the dense air that flows downhill in mountain-valley terrain. They were observed, specifically during winter months, to change directionally during their westward onset at approximately 2100 hr, to calm winds, and then eastward after 2200 hr. (*) There may or may not be stratified layers above the winds but the layer below the winds is assumed to be stable. The mixed layer as a whole may span several hundred meters in height making it impracticable to define the layer height from this code.

3. Layered return: use when there are layers in addition to radiation inversion: ABO DE3

- | | | |
|--|------------|---|
| a. AB: top of radiation inversion | <u>ABO</u> | 003 |
| b. DE: top of stratified echoes | ABO | <u>DE3</u> |
| c. surface based -- no radiation inversion | <u>000</u> | <u>DE3</u> |
| d. undefined layers | <u>000</u> | <u>003</u> or |
| | <u>ABO</u> | <u>003</u> if radiation inversion is determinable |
| e. transition (unstable to stable) | | |
| AB is top of transition layer | <u>AB3</u> | 003 |
| f. Mechanical turbulence superimposed | | |
| AB is top of echoes | <u>AB4</u> | 003 |

A layered return is produced when sounding echoes are stratified indicating the presence of multiple layers. In addition to the radiation inversion as defined in 1 above, the formation of multiple layers is strongly influenced by the onset of drainage winds. (*) The mixed layer, during these nighttime turbulence episodes, is defined by category (f) and will extend to the top of the echoes.

Table B-5. (Cont'd)

-
4. Inversion base forced aloft by surface heating: ABO DE4
- | | | |
|-------------------------------------|------------|------------|
| a. AB: base of echo | <u>ABO</u> | <u>DE4</u> |
| b. DE: top of stratified echoes | <u>ABO</u> | <u>DE4</u> |
| c. top of stratified echoes unknown | <u>ABO</u> | <u>004</u> |

This type of inversion is due to morning solar heating and is limited to one or two hours at Williams Air Force Base. The mixed layer in this case will extend to the base of the echo.

5. Subsidence inversion: ABO DE5
- | | | |
|-------------------------------------|------------|------------|
| a. AB: base of echo | <u>ABO</u> | <u>005</u> |
| b. DE: top of stratified echoes | <u>ABO</u> | <u>DE5</u> |
| c. top of stratified echoes unknown | <u>ABO</u> | <u>005</u> |

A subsidence inversion is usually caused by synoptic scale high pressure over the region. Since this condition did not occur throughout 13 months of records, the assignment of mixing depths posed no problem. However, mixing depths would have been treated in 4 above.

6. Frontal inversion: ABO DE6
- | | | |
|-------------------------------------|------------|------------|
| a. AB: base of echo | <u>ABO</u> | <u>DE6</u> |
| b. DE: top of stratified echoes | <u>ABO</u> | <u>DE6</u> |
| c. top of stratified echoes unknown | <u>ABO</u> | <u>006</u> |

Frontal inversion (same as 4 and 5 above except for cause).

7. Daytime noise: 002 000

Daytime noise is an undetermined graying of the return (background acoustical noise) due to air base activity.

8. Return due to noise, possible turbulence, rain, etc. 001 000

9. Top of mixing layer (thermal spikes), normal daytime situation ABO DE2
- | | | |
|----------------------|------------|------------|
| a. DE: top known | 000 | <u>DE9</u> |
| b. top unknown | 000 | <u>009</u> |
| c. transition period | <u>003</u> | <u>DE9</u> |

DE is top of transition layer return (NOTE: this is similar to case 3d above; however, thermal spikes are more prominent.)

- d. apparent mechanical turbulence due to higher
wind speed 004 DE9
DE is top of echoes

During normal daytime situations, the mixing depth is unobtainable only if the top is unknown (9b) or if the sounding return record is uncertain (9c).

10. Instrument inoperative or unable to read chart 999 999
-

(*) Bowen, J., EPA Las Vegas, private communication, March 1979.

with the theory of Nozaki,^{B-5} as corrected by ETAC, (J.B. Hooten, private communication, October, 1978), which gives the mixing depth L in meters as;

$$L = \frac{121 (6-J) (DPT)}{6} + \frac{J(0.087) (U_z + 0.5)}{6 f \ln (Z/Z_0)} .$$

where:

- J = the stability class index,
- DPT = the dew point depression (°C) i.e., the difference between surface temperature and dew point temperature,
- U_z = the wind speed in knots at anemometer height (Z = 373.4 cm),
- Z₀ = 5.0 cm is the roughness length characteristic of the anemometer exposure, and
- f = 0.0001 is the Coriolis parameter.

The comparison shows that the theory overpredicts the observed mixing depth substantially. In addition, comparison of Figs. B-6 and B-7 show the inability of this model to duplicate the observed lid height time dependence. One is cautioned, however, that the average height of the lid during afternoon hours is certainly underpredicted by these acoustic sounder data as the instrumental sensitivity cuts off at 500 m.

A substantially better fit to the acoustic sounder data has been obtained by chisquared optimization of the equation and choosing for lid height the maximum of the two expressions as follows:

$$H = C_1 + C_2 (T_G - T_{MIN}) e^{-\frac{t-t_{max}}{C_5}} + C_3 \theta + C_4 \frac{dT}{dt}$$

or

$$H = C_6 \cdot WSS$$

where:

- C₁ = 66.452 meters
- C₂ = 6.9644
- C₃ = 1.4402
- C₄ = -14.941
- C₅ = 6.1866
- C₆ = 8.4085
- t = hour of day (0-23)
- T = temperature (K) at hour t,
- WSS = wind speed (knots) at hour t,
- θ = the angle of altitude of the sun at hour t,

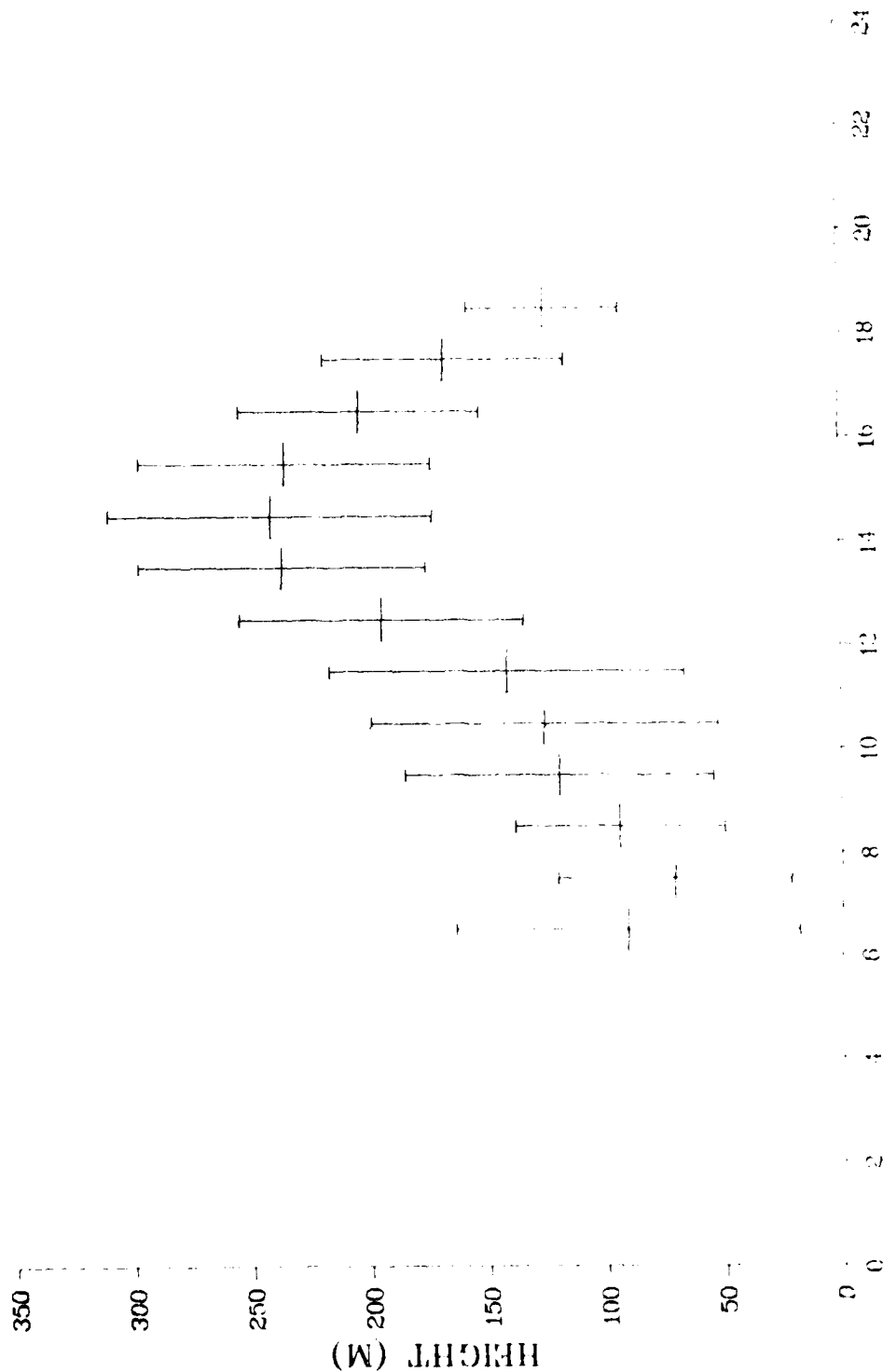


Fig. B-6. Average Daytime Depth of Mixed Layer by Acoustic Sounder

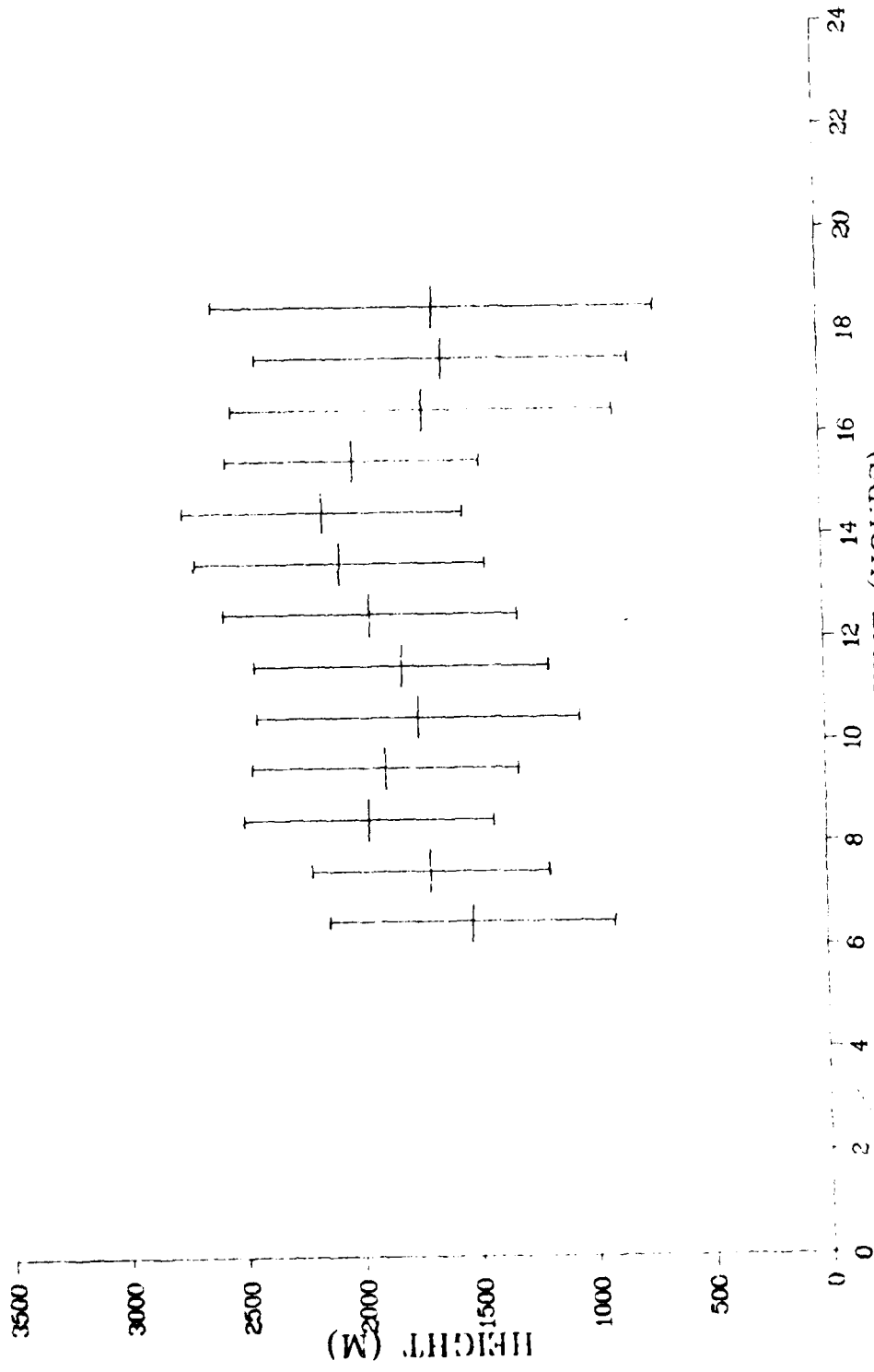


Fig. B-7. Average Daytime Depth of Mixed Layer by Nozaki

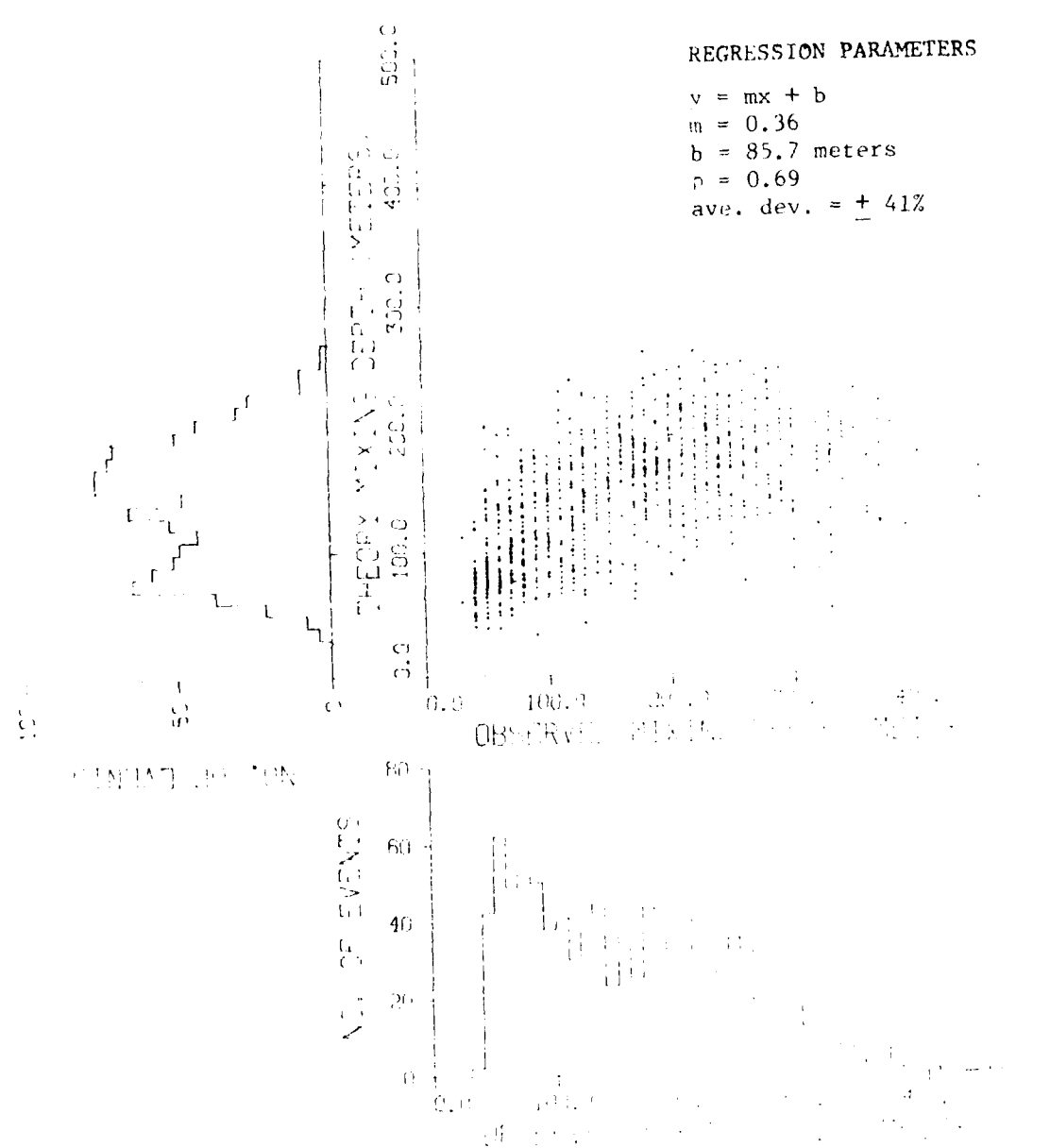


Fig. B-8. Mixing Depth: A Comparison of Observations versus a Theoretical Model

- T_G = the highest temperature attained up to hour t ,
 T_{MIN} = the lowest temperature attained up to hour t ,
 t_{MAX} = the hour at which T_G occurred.

Results of this comparison are presented in Fig. B-8. Although based entirely on surface observations, one obtains a correlation coefficient of 0.69, which is comparable to results obtained using vertical temperature soundings.^{B-6} This expression for mixing depth was then used for both AQAM I and II predictions throughout the 13-month period.

REFERENCES

- B-1. Turner, D.B., *A Diffusion Model for an Urban Area*, J. of Applied Meteorology, 3:83-91 (Feb. 1964).
- B-2. *User's Manual for Single-Source (CRSTER) Model*, EPA Publication No. EPA-450/2-77-013, Environmental Protection Agency, Research Triangle Park, N.C. (July 1977).
- B-3. Pasquill, F., *Atmospheric Diffusion*, D. Van Nostrand Co., Ltd., London, 2nd Ed. (1974).
- B-4. Woolf, H.M., *On the Computation of Solar Elevation Angles and the Determination of Sunrise and Sunset Times*, NASA Technical Memorandum NASA TM X-1646, Washington (Sept. 1968).
- B-5. Nozaki, K.Y., *Mixing Depth Model Using Hourly Surface Observations*, Part I, USAF/ETAC report 7053 (Nov. 1973).
- B-6. Benkley, C.W., and L.L. Schulman, *Estimating Hourly Mixing Depths from Historical Meteorological Data*, J. of Applied Meteorology, 18:722-780 (June 1979).

APPENDIX C

SOURCE EMISSIONS INVENTORY PROGRAM: INPUT MODIFICATIONS

1. INTRODUCTION

The Source Inventory Program^{C-1} computes the total annual pollutant emission for several source categories at a given airbase, thus it must be run successfully before the Short-Term Dispersion Code^{C-2} can be used.

The required input to the Source Inventory Program was prepared at Williams Airforce Base, Ariz., by the Stanford Research Institute (SRI).^{C-3} The input consists of operational information related to aircraft and nonaircraft source activity (see Figs. C-1 to C-7),* as well as information about the airbase environ sources (Fig. C-8), such as the Phoenix area. Modifications to some of the airbase operational information were requested by the U.S. Air Force and involved the addition of aircraft names, engine names, engine identification numbers, engine fuel rates, and engine-pollutant-emission rates. These items were modified as were the number of airbase aircraft parking areas and their center coordinates, the number of taxiway segments and their end point coordinates, and the annual account of each aircraft type and runway usage. In addition, data related to aerospace ground equipment and aircraft refueling operations were extended to include three additional aircraft types. Finally, all training-fire point sources were deleted from the input, though times of actual training fires were noted.

The requested modifications are detailed in this appendix.

2. NAMELIST DATA, REASSIGNED PROGRAMMED DATA

The Williams Air Force Base (WAFB) AQAM Source Inventory Program input as supplied by Stanford Research Institute (SRI) has undergone several additions and updates per Air Force requests.

The namelist input to the Source Inventory Program consists of three namelist group names: (1) EGDATA, engine data; (2) ACDATA, cycle data; and (3) DSDATA, temporal distribution data.

These data are considered to be good overall averages of aircraft engine emission factors, aircraft landing and takeoff parameters, and the temporal distribution of aircraft and airbase activities; thus they are automatically used by the program when the user has not input other data.

EGDATA is the only group name considered in the update process for which the reassignments involve the addition of aircraft names, engine names, engine ID numbers, fuel rates, and engine pollutant emission data.

Two tables, Tables C-1 and C-2,* are presented to record the change from the SRI supplied input to the updated input. Note that the extended list

*Figures and tables appear consecutively at the end of this appendix.

of aircraft types results from actual observations at WAFB and from guidelines submitted by the Air Force dated 12 October 1978.

3. DATA SET 4, AIRBASE AIRCRAFT AND RUNWAY TOTALS

The information coded in this data set defines the total number of aircraft types, runways, parking areas, a special-case wind condition, and taxiway segments. The following table shows the value of these parameters for the SRI and updated inventories.

	<u>SRI</u>	<u>Update</u>
Aircraft Types	4	6
Runways	6	6
Parking Areas	4	3
Special-Case Wind	1	1
Taxiway Segments	16	24

4. DATA SET 5, AIRCRAFT ACTIVITY

Activity for aircraft is defined as the total annual number of arrivals, departures, and touch-and-go operations. Each arrival and each departure of an aircraft is considered as an operation in the landing and takeoff cycle. A touch-and-go, however, is a complete cycle and occurs during a training flight when an aircraft approaches and lands on a runway, travels down the runway for several seconds, accelerates, and lifts off.

Estimates of activity for aircraft were made from actual counts at WAFB taken during the period 1 June 1976 to 30 June 1977. A review of counts of June and July 1976 shows that the information needed to determine touch-and-go operations is presented as "daily estimated averages of total runway activity." These daily estimated averages could not be used realistically in the summation methods required for an annual number of operations. Therefore, the activity for aircraft is redefined to reflect twice the activity information presented for the 6 month period August 1976-January 1977.

Tables C-3 and C-4 are presented to record the change from the SRI supplied activity to the updated activity, respectively. Note the new TRANSIENT aircraft category consists of the F4, C130H, and C140 aircraft types. In regard to touch-and-go cycles, an account is made for both normal and transient operations by F5, T37, and T38 aircraft.

5. DATA SET 6, AIRCRAFT PARKING AREAS

Information in this data set must describe the geometries of the aircraft parking areas. The center coordinate of each square in a series of squares making up the parking area is defined along with the length of a side of each square. The model assumes the square is situated so that a line drawn parallel with its right or left side will be directed north-south.

Tables C-5 and C-6 record the change from the SRI supplied geometries to the updated geometries. Figure C-9 shows the location of aircraft parking areas relative to taxiways, runways, and ambient air monitors.

6. DATA SET 7, AIRCRAFT TAXIWAY PATH SEGMENTS

Each taxiway path used by aircraft at WAFB is defined as a series of connected straight line segments. Information in this data set describes the geometries of these straight line segments and assigns to each an identifying line number. The line number is used for defining the particular segments that will be used to make up a complete taxiway path.

Tables C-7 and C-8 record the change from the SRI supplied geometries and the updated geometries. Figure C-10 shows the numbered taxiway segments relative to the airbase runway configuration.

7. DATA SET 8, AIRCRAFT RUNWAY INFORMATION

All information concerning airbase runways is defined in this data set. Annual arrivals and departures are defined for each runway (see Tables C-9 and C-10) as well as length and direction. Its length is the physical length of the runway pavement; its direction is determined by its orientation in relation to true north (see Tables C-11 and C-12).

Each individual aircraft type may use several different runways for landing and takeoff operations. Therefore, inbound and outbound taxiway paths are defined to/from each aircraft parking area to/from every airbase runway by a sequence of taxiway segment numbers.

Table C-13 records the update of aircraft movement over the taxiway segment configuration (see Fig. C-10).

8. AEROSPACE GROUND EQUIPMENT EMISSIONS

Aerospace Ground Equipment (AGE) consists of all motorized equipment except refueling tanks used to support incoming and outgoing aircraft. These support vehicles generally consist of coolers, power generators, heaters, and hydraulic test stands. The emissions for this equipment must be determined and input directly into the model. The model assumes that all AGE activities occur in the aircraft parking areas, but the emissions are calculated separately from those emissions resulting from aircraft parking activities. Since the update of this data set involved only the replacement of the single C-141 aircraft type with F4, C130H, and C141 aircraft types, Table C-14 is provided to record the updated input.

APPENDIX C, TABLE C-14: FUEL, SPILLAGE, AND VENTING TOTALS

The total amount of fuel used for refueling and venting aircraft is calculated as the sum of the fuel used for refueling and the amount of surplus

fuel drained from the aircraft fuel lines. Since the update of this data set involved only the replacement of the single TRANSIENT category with F4, C130H, and C141 aircraft types, Table C-15 is presented to record the updated input.

10. DATA SET 13, TRAINING FIRE POINT SOURCES

Training fire point sources are defined as shallow ground level sites on the airbase that are filled with fuel and ignited for the purpose of training airbase personnel in the art of fire fighting.

The update to this data set involved the deletion of all sites (a total of 4), designated by SRI, from the inventory. Thus, training fire point sources are not considered in the WAFB modeling effort.

REFERENCES

- C-1. Menicucci, D., *AQAM Data Reduction and Operations Guide*, Air Force Weapons Laboratory Report No. AFWL-TR-75-307 (Oct. 1976).
- C-2. Bingaman, D.J., *Air Quality Assessment Model for Air Force Operations -- Short Term Emission/Dispersion Computer Code Documentation*, Air Force Civil Engineering Center Report No. AFCEC-TR-76-34 (Apr. 1977).
- C-3. Viezee, M., *Source Emission Inventory Data Collection for Williams Air Force Base*, Final Technical Report, Stanford Research Institute, Menlo Park, Calif. (Sept. 1976).

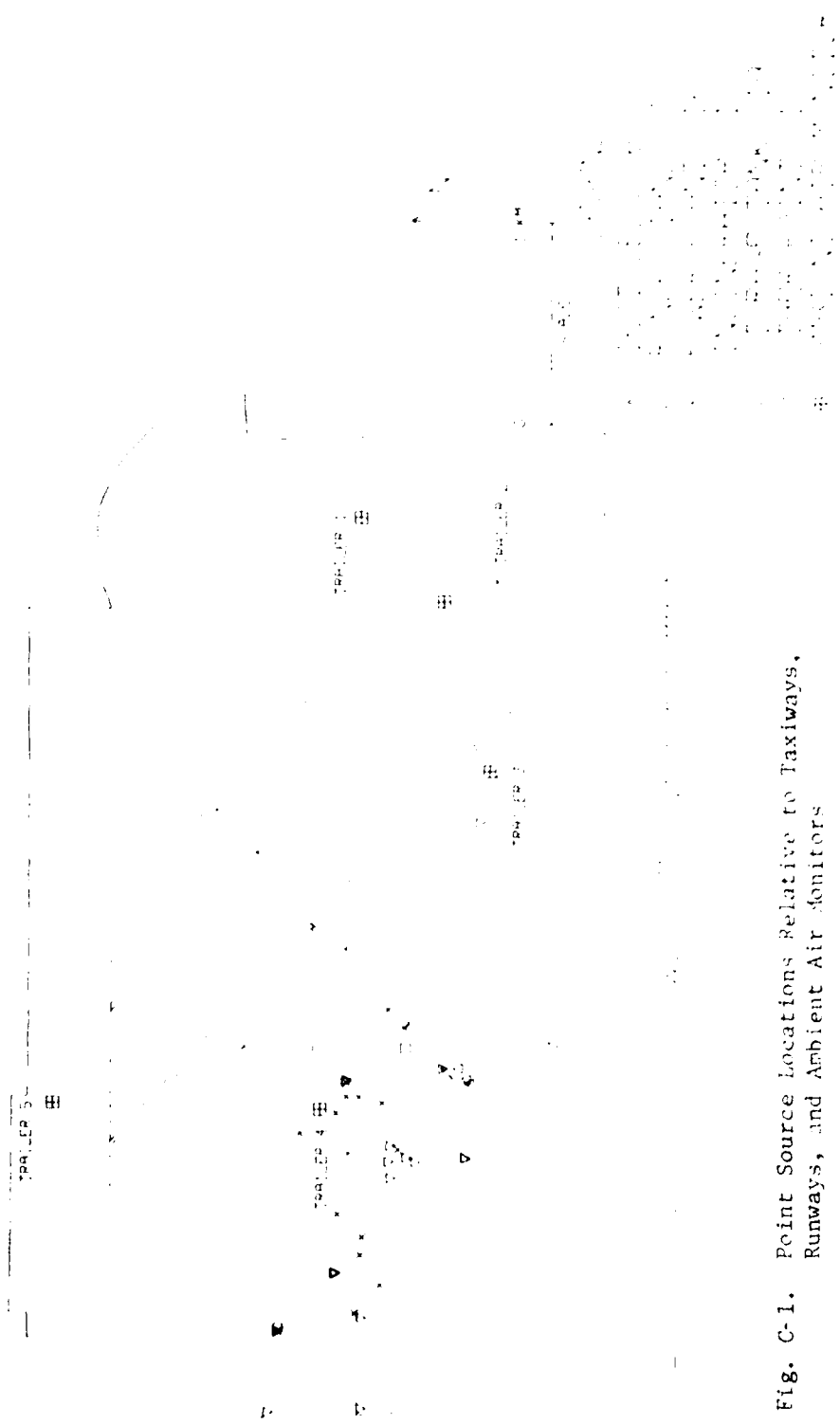


Fig. C-1. Point Source Locations Relative to Taxiways, Runways, and Ambient Air Monitors

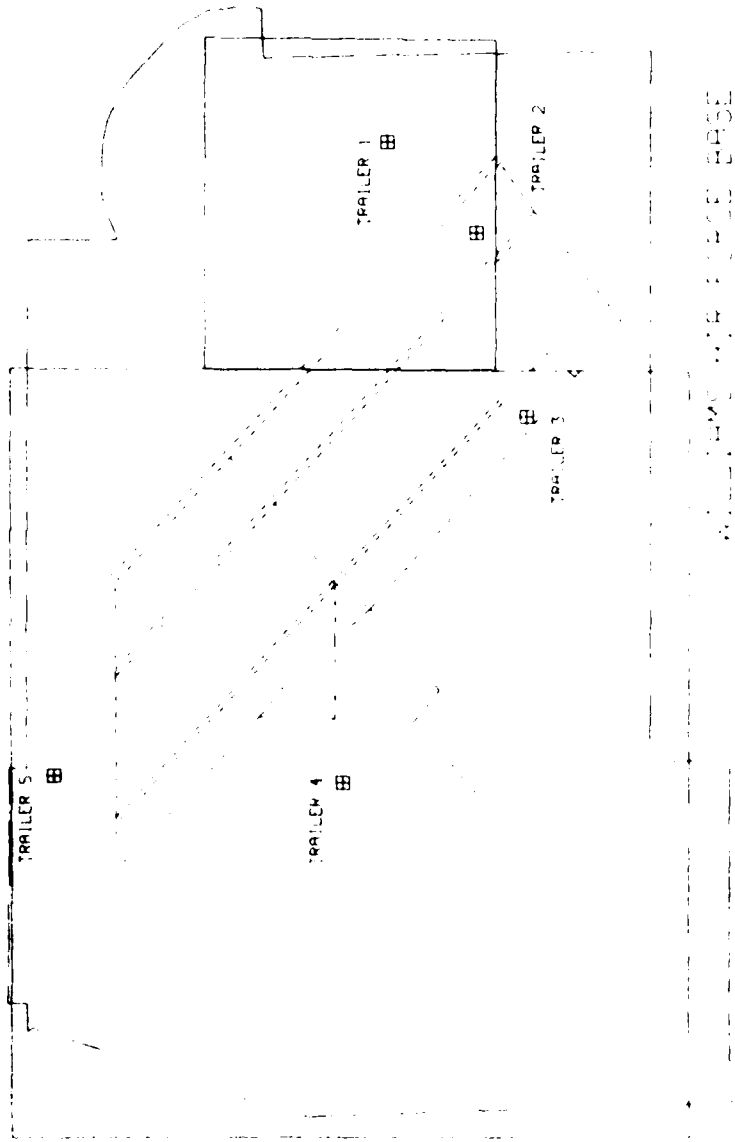


Fig. C-2. Petroleum Storage Tank Locations Relative to Taxiways, Runways, and Ambient Air Monitors

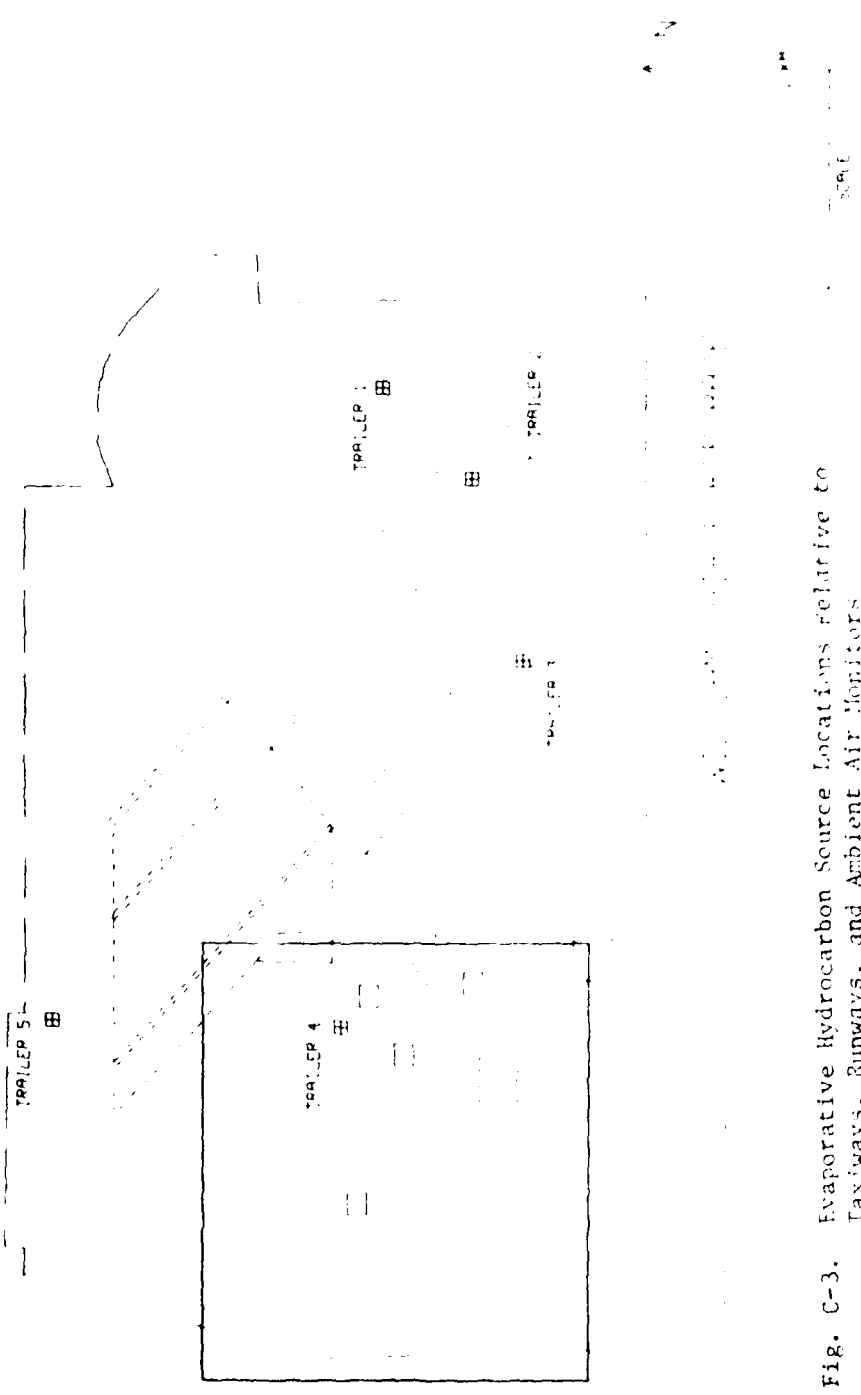


Fig. C-3. Evaporative Hydrocarbon Source Locations Relative to Taxiways, Runways, and Ambient Air Monitors

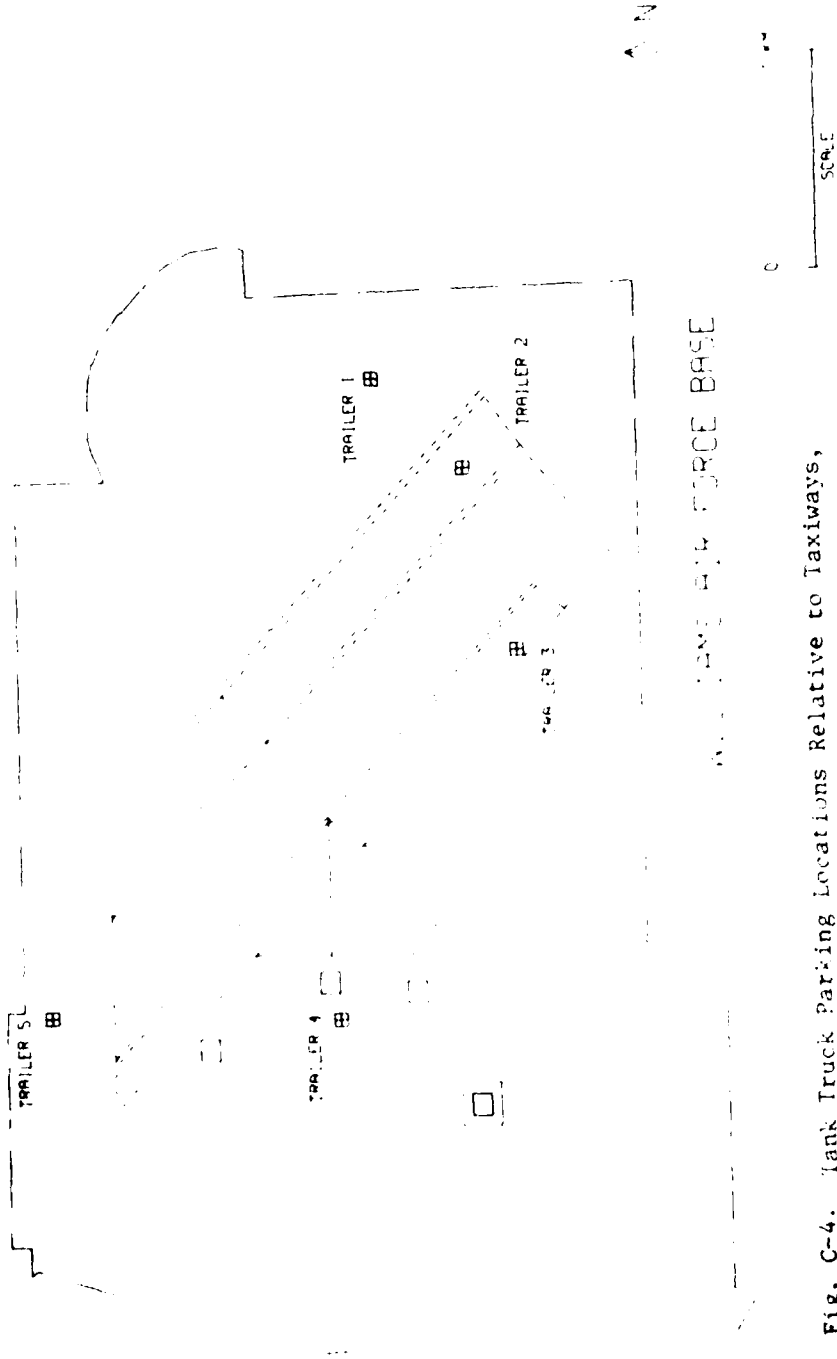


Fig. C-4. Tank Truck Parking Locations Relative to Taxiways, Runways, and Ambient Air Monitors

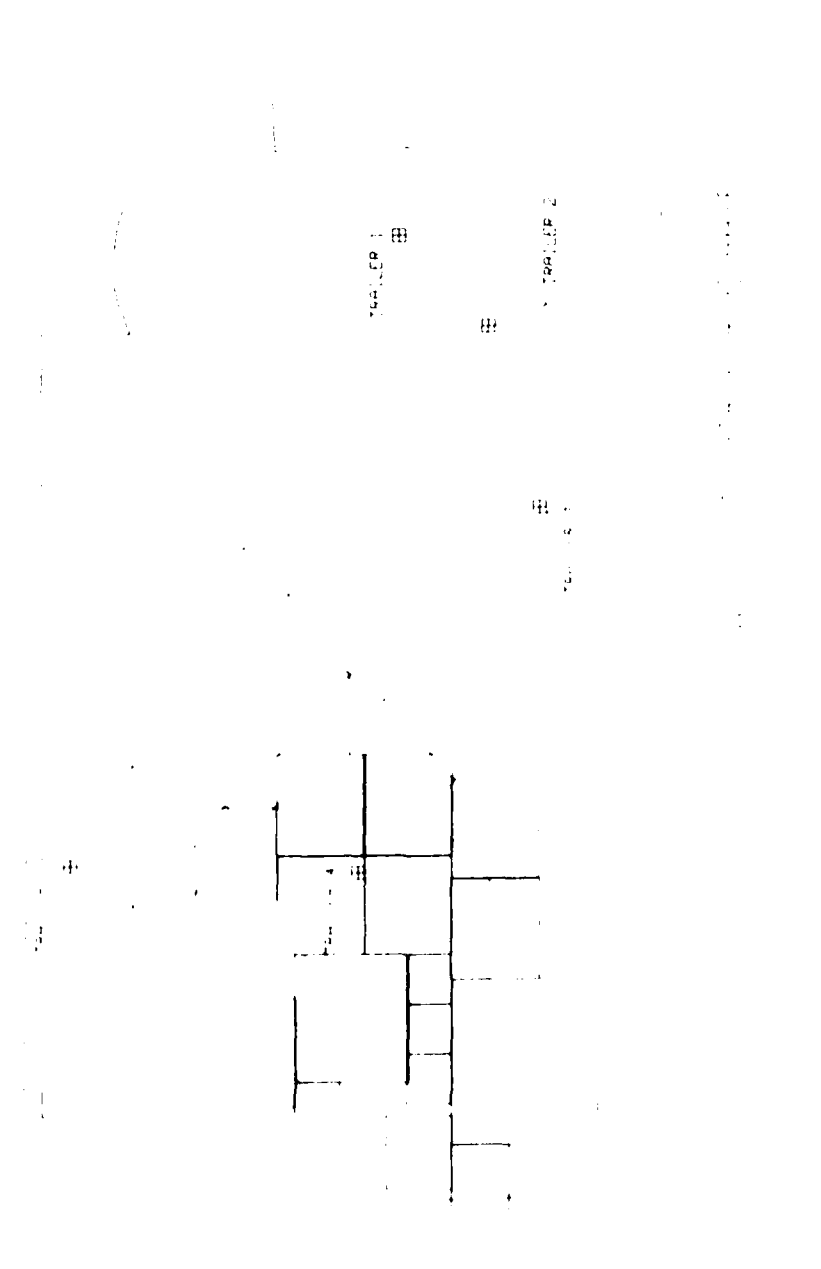


Fig. C-5. Vehicle Parking Locations Relative to Runways, Runways, and Ambient Air Monitors

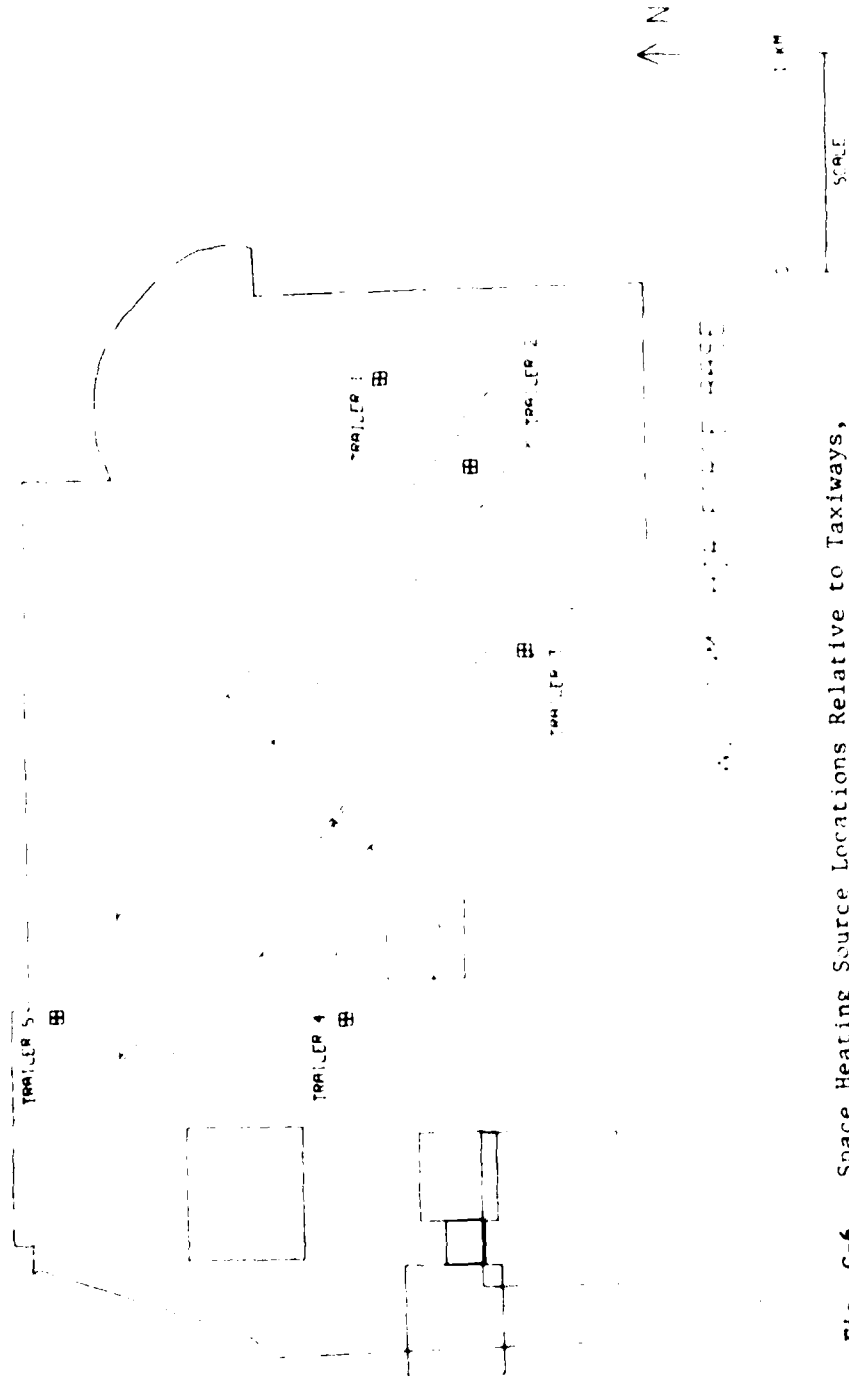


Fig. C-6. Space Heating Source Locations Relative to Taxiways, Runways, and Ambient Air Monitors

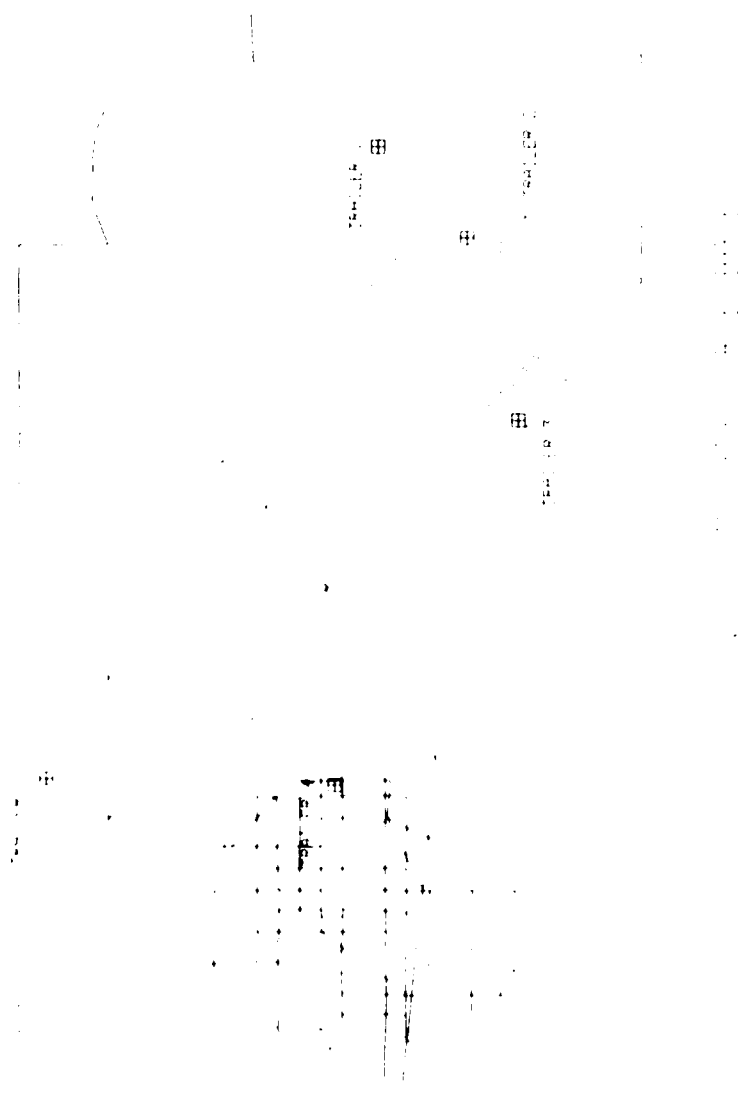


Fig. C-7. Non-Aircraft Line Source Locations Relative to Taxiways, Runways, and Ambient Air Monitors

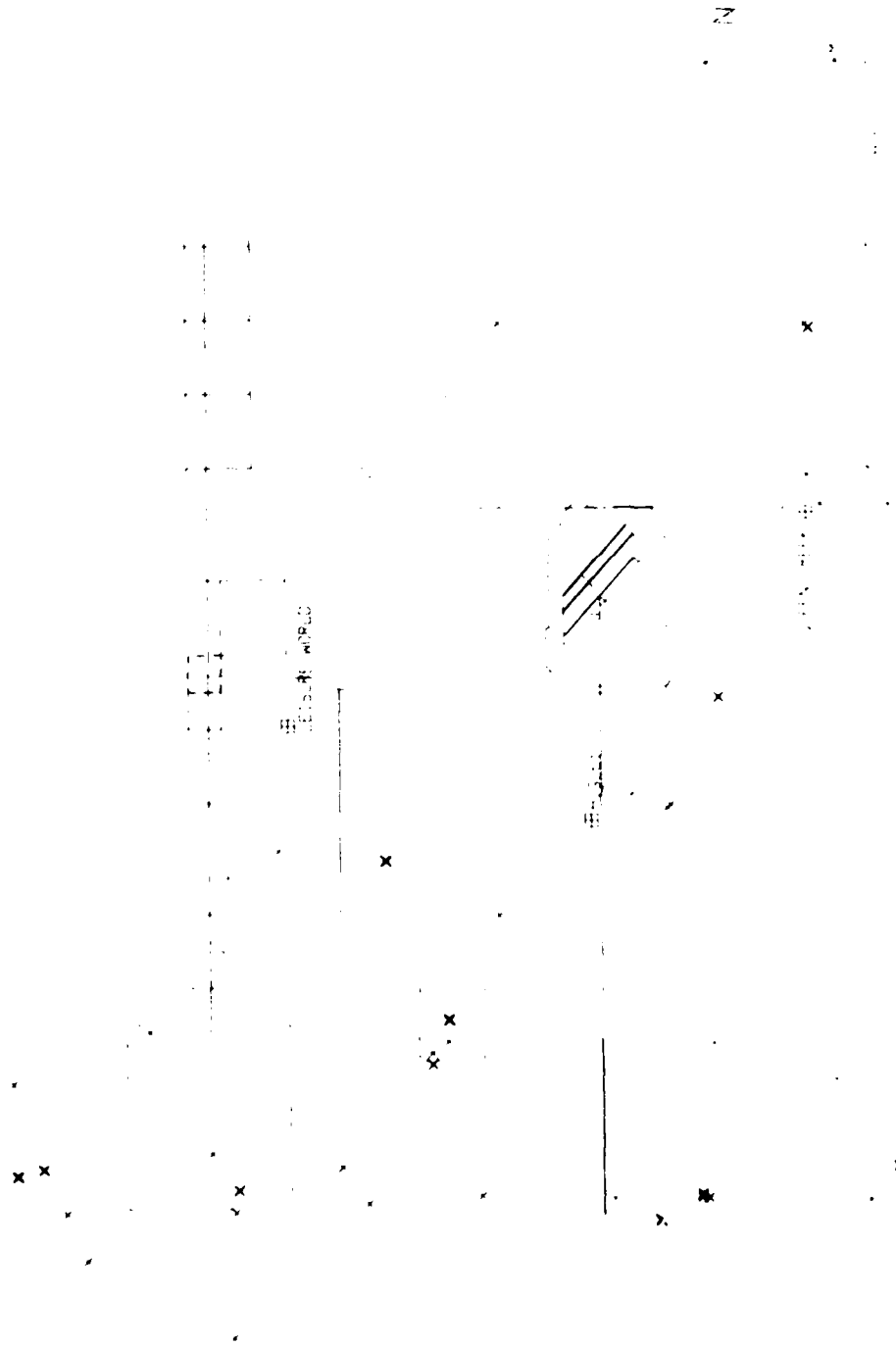


Fig. C-8. Environ (Area, Point, Line) Source Locations Relative to Williams Air Force Base, AZ

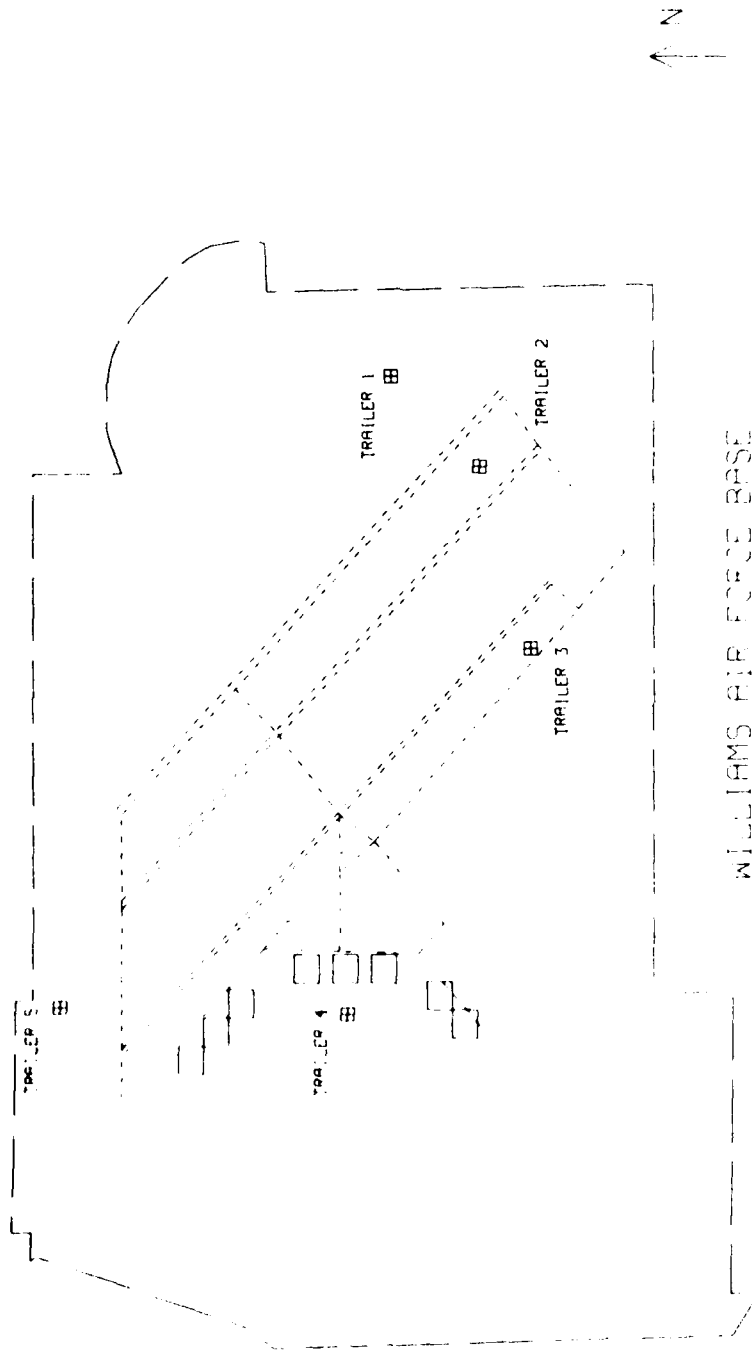
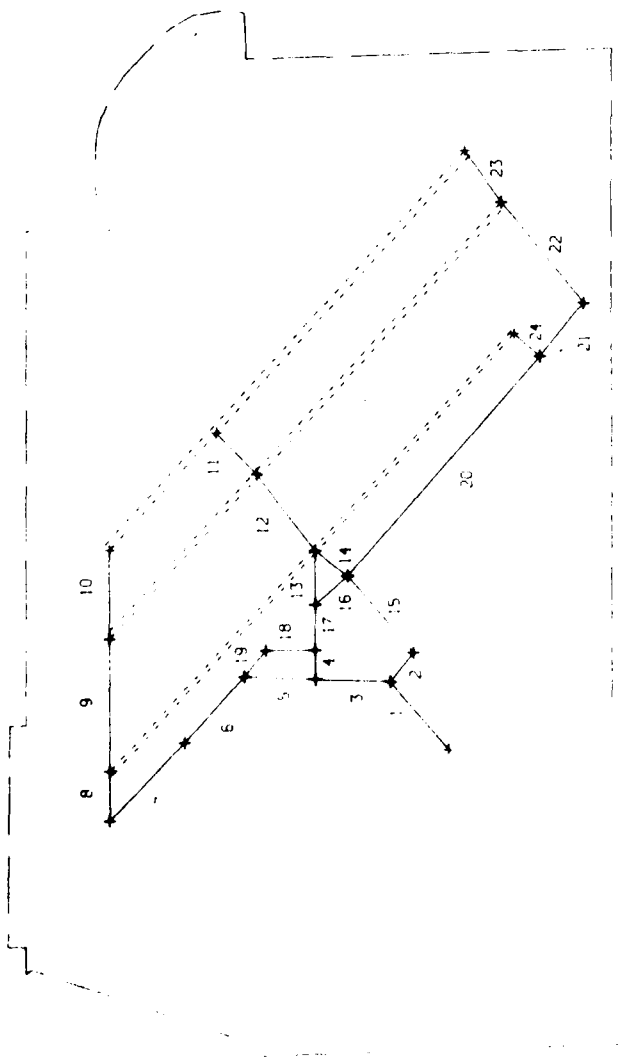


Fig. C-9. Aircraft Parking Areas Relative to Taxiways, Runways, and Ambient Air Monitors



WILLIAMS AIR FORCE BASE

Fig. C-10. Airbase Taxiway Segments (Aircraft Line Sources) Relative to Airbase Runway Configuration

Table C-1. Engine Data (SRI)

(ACNAME) AIRCRAFT NAME	AIRCRAFT ID	(EGNAME) ENGINE NAME	(IDACEF) ENGINE ID	THRUST SETTING	(EGFF) FUEL RATE 1000 LB /HR	Pollutant Emission Data in Pounds per 1000 lbs of Fuel (EGEMEC)			
						CO	HC	NOX	PM
Transient	50	J79-G15	1	Idle	1.131	56.70	16.70	2.47	0.50
				Normal	2.720	11.40	1.33	4.25	2.22
				Military	8.921	2.28	0.22	8.94	2.36
				After Br	32.240	4.00	0.01	3.11	0.15
F5	13	J85	6	Idle	0.453	180.00	29.90	1.26	0.013
T38	32			Normal	1.462	43.30	3.37	2.32	0.017
				Military	2.630	29.30	0.84	2.68	0.018
				After Br	8.323	26.00	0.07	1.99	0.008
T37	31	J69	14	Idle	0.231	127.00	19.50	1.53	0.729
				Normal	0.698	49.10	1.29	2.67	0.017
				Military	1.095	31.30	0.50	3.60	0.020

Table C-2. Engine Data (Update)

(ACNAME) AIRCRAFT NAME	AIRCRAFT ID	(EGNAME) ENGINE NAME	(IDACEF) ENGINE ID	THRUST SETTING	(EGFF) FUEL RATE 1000 LB /HR	Pollutant Emission Data in Pounds per 1000 lbs of Fuel (EGEMEC)			
						CO	HC	NOX	PM
F4	12	J79-G15	1	Idle	1.130	57.00	12.00	2.50	0.50
				Normal	3.500	9.40	1.10	4.80	1.80
				Military	8.929	2.20	0.20	8.90	2.20
				After Br	32.240	4.00	0.01	3.11	0.15
C141	14	TF33-P3	4	Idle	0.900	84.00	107.0	1.8	0.23
				Normal	3.797	6.30	2.6	5.8	0.99
				Military	7.436	1.70	0.6	10.0	1.73
F5	13	J85	6	Idle	0.469	178.0	30.0	1.30	0.003
T38	32			Normal	1.000	73.6	6.40	1.80	0.007
				Military	2.527	29.0	0.80	2.60	0.018
				After Br	8.323	26.0	0.07	1.99	0.008
T37	31	J69	14	Idle	0.231	129.0	19.0	1.5	0.55
				Normal	0.288	107.0	11.1	1.7	0.28
				Military	1.095	32.0	0.5	3.6	0.02
C130H	44	T56-A15	21	Idle	0.493	18.1	15.1	2.4	0.38
				Normal	0.827	8.5	3.4	3.7	0.47
				Military	2.392	1.6	0.2	11.7	0.71

Table C-3. Aircraft Activity (SRI)

Aircraft Name	Annual Number of		
	Arrivals	Departures	T/G Cycles
1. F5	8391	8391	1682
2. T37	39662	39662	63357
3. T38	77281	77281	55963
4. TRAN	8112	8112	0

Table C-4. Aircraft Activity (Update)

Aircraft Name	Annual Number of		
	Arrivals	Departures	T/G Cycles
1. F5	6566	6666	15493
2. T37	25394	25904	34614
3. T38	27180	27686	64125
4. F4	1310	1320	0
5. C130H	66	62	0
6. C140	20	22	0

Table C-5. Aircraft Parking Area Geometries (SRI)

Area	Square	Center Coordinate (UTM)		Length (km)
		X	Y	
1	1	438.10	3685.57	0.10
2	1	437.70	3686.10	0.20
	2	437.90	3685.90	0.20
	3	438.00	3685.70	0.20
3	1	437.95	3684.70	0.20
	2	438.10	3684.90	0.20
	3	438.11	3685.05	0.14
4	1	438.15	3685.25	0.10
	2	438.15	3685.35	0.10

Table C-6. Aircraft Parking Area Geometries (Update)

Area	Square	Center Coordinate (UTM)		Length (km)
		X	Y	
1	1	437.41	3686.10	0.13
	2	437.54	3685.97	0.13
	3	437.67	3685.84	0.13
2	1	437.83	3685.50	0.13
	2	437.83	3685.30	0.13
	3	437.83	3685.10	0.13
3	1	437.71	3684.81	0.13
	2	437.58	3684.68	0.13

Table C-7. Taxiway Segment Geometries (SRI)

Line No.	Ground Level Coordinates of One End of Line		Ground Level Coordinates at Opposite End of Line		Segment Length (km)
	X (1)	Y (1)	X (2)	Y (2)	
1	440.800	3684.430	440.560	3684.180	0.347
2	440.560	3684.180	440.050	3683.750	0.667
3	439.760	3683.980	440.050	3683.750	0.370
4	439.760	3683.980	439.940	3684.140	0.241
5	439.760	3683.980	438.530	3685.230	1.754
6	438.530	3685.230	438.230	3685.580	0.461
7	438.530	3685.230	438.130	3685.250	0.400
8	438.130	3685.250	438.080	3684.820	0.433
9	438.130	3685.250	438.130	3685.500	0.250
10	438.130	3685.500	438.230	3685.580	0.128
11	438.230	3685.580	437.870	3685.900	0.482
12	438.230	3685.580	437.520	3686.380	1.070
13	437.870	3685.900	437.520	3686.380	0.594
14	437.520	3686.380	437.730	3686.380	0.210
15	437.730	3686.380	438.400	3686.380	0.670
16	438.400	3686.380	438.830	3686.380	0.430

Table C-8. Taxiway Segment Geometries (Update)

Line No.	Ground Level Coordinates of One End of Line		Ground Level Coordinates at Opposite End of Line		Segment Length (km)
	X (1)	Y (1)	X (2)	Y (2)	
1	437.570	3684.600	437.900	3684.920	0.460
2	437.900	3684.920	438.040	3684.790	0.191
3	437.900	3684.920	437.910	3685.330	0.410
4	437.910	3685.330	438.050	3685.330	0.140
5	437.910	3685.330	437.920	3685.720	0.390
6	437.920	3685.720	437.600	3686.050	0.460
7	437.600	3686.050	437.220	3686.460	0.559
8	437.220	3686.460	437.460	3686.460	0.240
9	437.460	3686.460	438.100	3686.460	0.640
10	438.100	3686.460	438.530	3686.460	0.430
11	439.100	3685.870	438.900	3685.650	0.297
12	438.900	3685.650	438.530	3685.330	0.489
13	438.530	3685.330	438.270	3685.330	0.260
14	438.530	3685.330	438.410	3685.150	0.216
15	438.410	3685.150	438.040	3684.790	0.516
16	438.410	3685.150	438.270	3685.330	0.228
17	438.270	3685.330	438.050	3685.330	0.220
18	438.050	3685.600	438.050	3685.330	0.270
19	437.920	3685.720	438.050	3685.600	0.177
20	438.410	3685.150	439.470	3684.090	1.499
21	439.470	3684.090	439.730	3683.850	0.354
22	439.730	3683.850	440.220	3684.300	0.665
23	440.220	3684.300	440.470	3684.500	0.320
24	439.470	3684.090	439.580	3684.230	0.178

Table C-9. Annual Aircraft Arrivals and Departures (SRI)

Runway		F5	T37	T38	TRAN
30L	Arrivals	0	34515	0	0
	Departures	0	34515	0	0
30C	Arrivals	2960	4353	24917	7950
	Departures	2960	4353	24917	7950
30R	Arrivals	5263	0	50818	0
	Departures	5263	0	50818	0
12R	Arrivals	0	704	0	0
	Departures	0	704	0	0
12C	Arrivals	60	704	508	324
	Departures	60	704	508	324
12L	Arrivals	107	0	1037	0
	Departures	107	0	1037	0

Table C-10. Annual Aircraft Arrivals and Departures (Update)

Runway		F5	T37	T38	F4	C130H	C141
30L	Arrivals	0	24608	0	0	66	18
	Departures	0	25140	0	0	60	18
30C	Arrivals	5084	0	21962	1270	0	0
	Departures	6356	0	26884	1286	0	0
30R	Arrivals	1180	0	4396	0	0	0
	Departures	0	0	0	0	0	0
12R	Arrivals	0	786	0	0	0	2
	Departures	0	764	0	0	2	4
12C	Arrivals	260	0	654	40	0	0
	Departures	310	0	802	34	0	0
12L	Arrivals	42	0	168	0	0	0
	Departures	0	0	0	0	0	0

Table C-11. WAFB Runway Geometries (SRI)

Runway	Coordinate (UTM)		Angle (Deg)	Length (km)
	X	Y		
30L	439.94	3684.14	315	3.17
30C	440.56	3684.18	315	3.12
30R	440.80	3684.43	315	2.85
12R	437.73	3686.38	135	3.17
12C	438.40	3686.38	135	3.12
12L	438.83	3686.38	135	2.85

Table C-12. WAFB Runway Geometries (Update)

Runway	Coordinate (UTM)		Angle (Deg)	Length (km)
	X	Y		
30L	439.58	3684.23	316	3.08
30C	440.22	3684.30	316	3.03
30R	440.47	3684.50	316	2.76
12R	437.46	3686.46	136	3.08
12C	438.10	3686.46	136	3.03
12L	438.53	3686.46	136	2.76

Table C-13. Aircraft Movement over Taxiway Segments

Runway	Aircraft Name	Annual Arrivals	Inbound Taxi Segments	Parking Area	Annual Departures	Outbound Taxi Segments
30L	T37	24608	8,7	1	25140	6,19,18,17,16,20,24
	C130H	66	8,7,6,5	2	60	4,17,16,20,24
	C140	18	8,7,6,5	2	18	4,17,16,20,24
30C	F5	5084	9,8,7,6,5	2	6356	4,17,16,20,21,22
	T38	10981	9,8,7,6,5,3	2	13442	3,4,17,16,20,21,22
	T38	10981	9,8,7,6,5,3,1	3	13442	1,3,4,17,16,20,21,22
	F4	1270	9,8,7,6,5	2	1286	4,16,16,20,21,22
30R	F5	1180	10,9,8,7,6,5	2	0	
	T38	2198	10,9,8,7,6,5,3	2	0	
	T38	2198	10,9,8,7,6,5,3,1	3	0	
12R	T37	786	24,20,16,17,18,19,6	1	764	7,8
	C130H	0		2	2	5,6,7,8
	C141	2	24,20,16,17,4	2	4	5,6,7,8
12C	F5	260	22,21,20,16,17,4	2	310	5,6,7,8,9
	T38	318	22,21,20,16,17,4,3	2	401	3,5,6,7,8,9
	T38	318	22,21,20,16,17,4,3,1	3	401	1,3,5,6,7,8,9
	F4	40	22,21,20,16,17,4	2	34	5,6,7,8,9
12L	F5	42	23,22,21,20,16,17,4	2	0	
	T38	84	23,22,21,20,16,17,4,3	2	0	
	T38	84	23,22,21,20,16,17,4,3,1	3	0	

Table C-14. Service Vehicle Emissions in
Kilograms per Operation
(Arrival or Departure)

	CO	THC	NOX	PM	SOX
Gasoline:					
F5	0.674	0.040	0.002	0.005	0.001
T37	0.133	0.008	0.001	0.001	0.001
T38	0.674	0.040	0.002	0.005	0.001
F4	0.674	0.040	0.002	0.005	0.001
C130H	0.674	0.040	0.002	0.005	0.001
C140	0.674	0.040	0.002	0.005	0.001
JP4:					
F5	0.072	0.007	0.014	0.007	0.002
T37	0.003	0.001	0.001	0.0001	0.001
T38	0.072	0.007	0.014	0.007	0.002
F4	0.072	0.007	0.014	0.007	0.002
C130H	0.072	0.007	0.014	0.007	0.002
C141	0.072	0.007	0.014	0.007	0.002

Table C-15. Refueling Information
(JP4-Jet Fuel)

	F5	T37	T38	F4	C130H	C141
Refueling Value (liters per fillup)	2146	587	1105	1893	1893	1893
Fuel Spillage (Liters per fillup)	4	10	4	4	4	4
Fuel Venting (Liters per arrival)	2	0	2	2	2	2
Fuel Venting (Liters per departure)	0	2	0	2	2	2

APPENDIX D
AIRCRAFT OPERATIONS DATA

1. OBJECTIVE

The objectives of this appendix are: first, to develop plans and procedures for the acquisition and reduction of aircraft time-in-mode and aircraft activity data; second, to present a summary of an aircraft time-in-mode study performed at Williams AFB; and third, to present a summary of aircraft activity at Williams for the 13-month period of the EPA air quality monitoring experiment.^{D-1}

2. BASE OPERATIONS

Williams Air Force Base is a relatively remote, air-training command base near Phoenix, Arizona. The main mission of the base is the training of jet fighter pilots. There are three squadrons at this airbase, each with its own type of aircraft (Fig. D-1), and these aircraft account for most of the air traffic: approximately 2100 T-37 flights, 2300 T-38 flights, and 550 F-5 flights per month, depending on the number of students in training at a particular time.

The layout of runways and parking areas for squadron aircraft is illustrated in Fig. D-2. Only three runways are used at any given time. Runways prefixed by a 12 are used only when the northwesterly wind exceeds 10 knots. The suffixes L, C, and R denote left, center, and right, respectively. Runway 30L is used almost exclusively by T-37 aircraft. Runways 30C and 30R are used jointly by T-38 and F-5 aircraft. Transient aircraft operations are normally performed on runway 30C. A schedule of aircraft operations by aircraft type and runway is provided in Table D-1.

3. DATA ACQUISITION AND REDUCTION OF AIRCRAFT TIME-IN-MODE

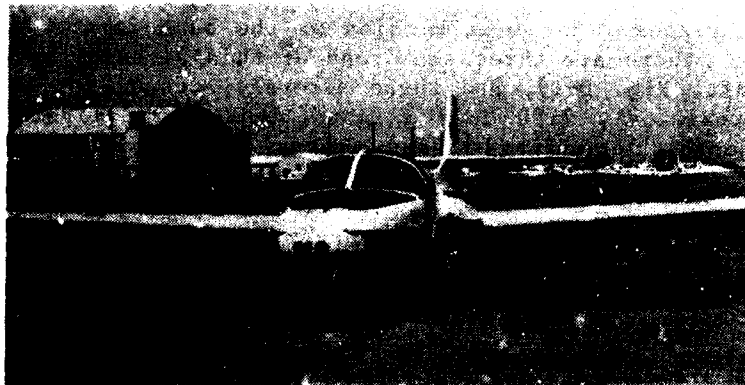
Time-in-mode is the time spent in modes of ground operations. A mode is simply a subdivision of an aircraft ground (or air) operation. These times can be characterized statistically as an average for each group of time-in-mode observations. Naugle^{D-2} has collected aircraft time-in-mode data and has given estimates of time-in-mode for several aircraft types at five Air Force bases. This present effort was made because of the need for accuracy in source inventory data to be used for Williams.

The results of a six-day study of aircraft time-in-mode at Williams Air Force Base are presented in Table D-2. Only time-in-mode observations for squadron aircraft ground operations were made. Observations of idle at start-up times were made from the parking areas; all other time-in-mode observations were made from the control tower. Approximately 1200 separate aircraft mode observations were made during the study.

The time-in-mode observations were stratified according to aircraft, runway, taxiway segment, pad area, and aircraft mode. A diagnostic investigation



T-37 Aircraft



T-38 Aircraft



F-5 Aircraft

Fig. D-1. Aircraft Squadrons at Williams Air Force Base

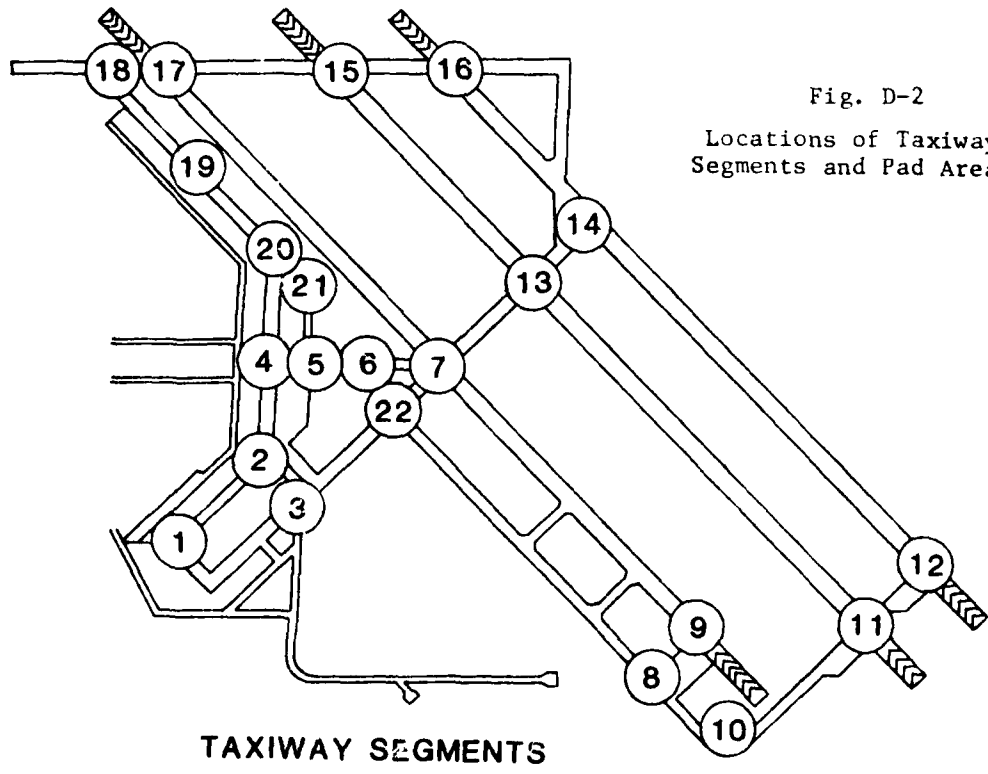
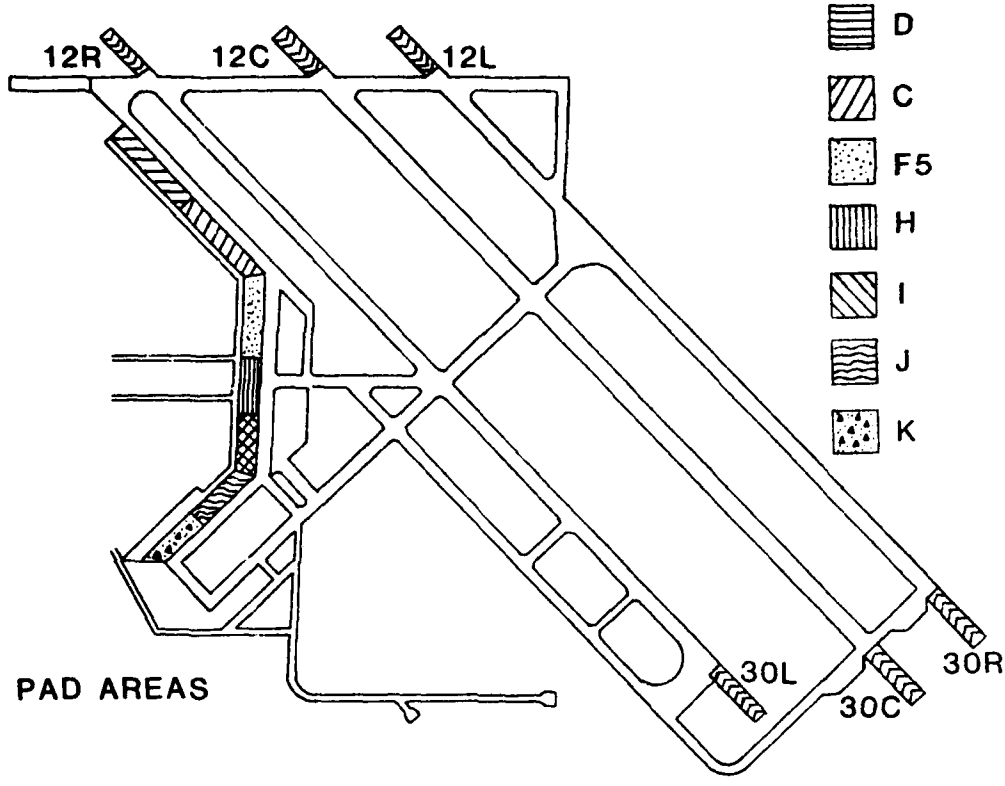


Fig. D-2
Locations of Taxiway
Segments and Pad Areas

Table D-1. Schedule of Aircraft Operations

Schedule	Runway	Aircraft	Operation
1	30L	T-37	Takeoff
2	30L	T-37	Landing
3	30L	T-37	Touch-and-Go
4	12R	T-37	Takeoff
5	12R	T-37	Landing
6	12R	T-37	Touch-and-Go
7	30R	T-38	Takeoff
8	30R	T-38	Landing
9	30R	T-38	Touch-and-Go
10	30C	T-38	Takeoff
11	30C	T-38	Landing
12	30C	T-38	Touch-and-Go
13	12L	T-38	Takeoff
14	12L	T-38	Landing
15	12L	T-38	Touch-and-Go
16	12C	T-38	Takeoff
17	12C	T-38	Landing
18	12C	T-38	Touch-and-Go
19	30R	F-5	Takeoff
20	30R	F-5	Landing
21	30R	F-5	Touch-and-Go
22	30C	F-5	Takeoff
23	30C	F-5	Landing
24	30C	F-5	Touch-and-Go
25	12L	F-5	Takeoff
26	12L	F-5	Landing
27	12L	F-5	Touch-and-Go
28	12C	F-5	Takeoff
29	12C	F-5	Landing
30	12C	F-5	Touch-and-Go
31	30C	Transient	Takeoff
32	30C	Transient	Landing
33	12C	Transient	Takeoff
34	12C	Transient	Landing

of the observations for each aircraft mode was performed to provide insight into the distributional characteristics. The median, mean, standard deviation, and the number of observations were computed. Observations of time-in-mode were contaminated by queuing situations, aborted operations, and emergency situations.

An examination of the size of the standard deviation relative to the mean reveals that the inbound modes immediately preceding takeoff and the outbound modes immediately following landings, with the exception of taxiing

Table D-2. Time-in-Mode Data

Operation	Aircraft Mode	Throttle Setting	Number of		Standard Deviation	Explanation	
			Observations	Median			
<u>T-37 Aircraft</u>							
Outbound	Idle at Startup	46	24	263.00	266.50	49.67	
	Taxi	55	13	391.00	373.61	39.96	General Taxi to Last Chance
	Taxi	55	36	152.00	160.89	37.52	General Taxi to Segment 5
	Taxi	55	14	189.00	190.93	36.43	Taxi to Point 5 from Pad B
	Taxi	55	17	130.00	134.40	16.12	Taxi to Point 5 from Pad C
	Taxi	55	41	215.00	216.19	21.95	Taxi from Pt. 5-Last Chance
	Taxi	55	5	--	166.80	22.96	Taxi from Pad D to Point 21
	Last Chance	40	10	89.00	106.03	61.22	
	Preflight Check	45	32	99.50	101.30	12.44	
	Taxi	44	44	21.00	22.48	5.56	Taxi onto Runway
	Engine Check	100	43	30.00	34.14	12.05	Military
	Runway Roll	100	49	21.00	20.58	1.99	Military
	Inflight	Climbout	100	--	--	--	
		Approach	80	--	--	--	
Inbound	Landing Roll	60	55	124.00	121.34	12.48	
	Taxi	55	50	24.50	25.00	1.26	Taxi to Postflight
	Postflight	40	57	64.60	72.49	36.52	
	Taxi	55	43	119.50	129.15	39.64	Taxi Inbound (General)
	Taxi	55	9	164.00	164.67	38.47	Taxi to Pad Area (General)
	Taxi	55	29	104.00	104.02	21.87	Taxi to Pad D
	Taxi	55	14	155.50	158.36	32.37	Taxi to Pad C
	Shutdown	40	8	31.50	31.00	5.93	
<u>T-38 Aircraft</u>							
Outbound	Idle at Startup	46	28	270.00	282.06	62.95	
	Taxi	60	40	120.00	131.45	42.26	General Taxi to Point 5
	Taxi	60	15	434.00	421.80	71.82	Taxi to Last Chance (General)
	Taxi	60	4	--	79.00	18.17	Taxi to Point 5 from Pad B
	Taxi	60	14	102.56	105.79	25.57	Taxi to Point 5 from Pad C
	Taxi	60	15	137.00	144.27	32.27	Taxi to Point 5 from Pad D
	Taxi	60	7	--	185.29	26.71	Taxi to Point 5 from Pad E
	Taxi	60	22	265.00	260.77	28.75	Taxi from Pt. 5-Last Chance
	Last Chance	50	49	73.00	74.13	12.21	
	Taxi	60	39	30.00	34.03	16.51	Taxi to Preflight
	Preflight	50	29	96.60	108.16	73.40	
	Taxi	60	46	24.00	24.50	6.63	Taxi onto Runway
	Engine Check	100	46	27.00	32.53	16.54	Military
	Runway Roll	100+Afterburner	38	19.00	19.74	2.72	Military and Afterburner
Inflight	Climbout	100+Afterburner	--	--	--	Military and Afterburner	
	Approach	88	--	--	--		
Inbound	Landing Roll	55	32	89.00	87.50	16.76	
	Taxi (30R)	60	11	90.00	89.91	19.39	Taxi to Postflight
	Taxi (30C)	60	23	51.00	51.74	12.30	Taxi to Postflight
	Postflight	50	40	45.00	48.60	21.61	
	Taxi	50	46	402.50	393.03	79.61	Taxi Inbound (General)
	Taxi	50	19	410.00	386.79	78.03	Taxi to Pad G
	Taxi	50	7	--	347.00	112.61	Taxi to Pad H
	Taxi	50	4	--	361.50	23.53	Taxi to Pad I
	Taxi	50	--	413.00	413.47	52.60	Taxi to Pad J
	Taxi	50	--	446.50	443.62	58.96	Taxi to Pad K
<u>F-5 Aircraft</u>							
Outbound	Idle at Startup	50	16	257.60	265.19	59.93	
	Taxi	65	30	314.00	336.87	--	Taxi Outbound (General)
	Taxi	65	21	79.00	95.09	21.36	Taxi from Pad to Segment 6
	Taxi	65	9	235.00	251.78	36.45	Segment 6 to Weapons Area
	Weapons Area/						
	Last Chance	50	11	107.00	161.54	165.42	
	Taxi	65	13	43.00	40.77	13.81	Taxi to Runway Clearance
	Runway Clearance/						
	Preflight	50	3	--	92.00	37.27	
	Taxi	65	2	--	--	--	Taxi onto Runway
Engine Check	100	10	32.50	41.80	18.33		
Runway Roll	100+Afterburner	12	16.50	17.50	2.47		
Inflight	Climbout	100	--	--	--		
	Approach	80	--	--	--		
Inbound	Landing Roll	60	18	75.00	73.56	5.29	
	Taxi	50	18	77.00	69.61	22.82	Taxi to Runway
	Postflight/Dearming	50	15	108.00	165.00	135.50	
	Taxi	50	14	221.00	230.79	45.96	Taxi to Pad Area

operations, are the most highly contaminated distributions. Such contaminated distributions create problems in choosing a spatial distribution or most typical value to associate with the time-in-mode.

Preflight and postflight modes for the F-5 aircraft exhibited the largest standard deviations. The extent of contamination of the observations of time-in-mode depends on the number of aircraft in a flight, the ground service crew, pilot proficiency, and whether arming or dearming is to be performed. This range illustrates the fact that there may be more than one independent mechanism functioning in an aircraft operational mode.

4. DETAILED AIRCRAFT ACTIVITY AT WILLIAMS AIR FORCE BASE FOR THE PERIOD 1 JUNE 1976-30 JUNE 1977

The aircraft activity information transcribed from flight forms AIG 355, ATC 90, and TW124 consists primarily of the dates and times of actual takeoffs and landings of all aircraft making use of the Williams Air Force Base (WAFB) facilities. Form ATC 355, the Runway Supervisory Unit (RSU) Log, pertains to operations involving successful takeoff or landing of local aircraft; Form AIG 90, the Aircraft Traffic Log, pertains to the activities of transient aircraft; and Form TW124, the Flight Deviation Report, pertains to operations which involve deviations from scheduled takeoff. These Air Force flight forms, used during the air pollution monitoring program, were the most reliable source on which to base hourly emissions activity data needed for the Air Quality Assessment Model (AQAM) evaluation effort.

The completed transcription process provided the aircraft activity data base, which consists of the daily records described in Table D-3 where each day's activity begins with one Header Card giving the year, month, day, and full traffic count on each airbase runway. Any number of Activity Cards may follow the Header but each one must restate the date, specify only one of five possible operations, denote the runway in use, give the aircraft type involved, and list the military times of the operation.

a. Aircraft Mix at Williams Air Force Base

A review of the activity data base for the period 1 June 1976-30 June 1977 shows that aircraft at WAFB involves scheduled and nonscheduled flight operations of approximately 50 different aircraft types. While most aircraft are small twin-engine trainer types, others are helicopter types and larger cargo types equipped with either turboprop engines or jet engines.

Table D-4 provides a monthly summary of aircraft types using WAFB during the study period. This information also appears later as part of the Monthly Activity Summary found in Attachment B.

b. Classification of Aircraft Types at Williams Air Force Base

For summary report purposes, seven aircraft classes will emerge when similar aircraft are grouped to their engine-emission characteristics.

Table D-3. Aircraft Activity Data Format

Header Card - One Per Day

<u>Col.</u>	<u>Content</u>						
1-6	YYMMDD = Year, month, day						
7	C => Total aircraft counts						
8-11	<table border="0"> <tr> <td>30L</td> <td rowspan="5">Full traffic count on these Right justify integers</td> </tr> <tr> <td>30C</td> </tr> <tr> <td>30R</td> </tr> <tr> <td>12R</td> </tr> <tr> <td>12C</td> </tr> </table>	30L	Full traffic count on these Right justify integers	30C	30R	12R	12C
30L		Full traffic count on these Right justify integers					
30C							
30R							
12R							
12C							
12-15							
16-19							
20-23							
24-27							
28-31	12L						

Aircraft Activity Cards

<u>Col.</u>	<u>Content</u>			
1-6	YYMMDD			
7	<p>N => Normal operations - times are local takeoff and landing times. Slashes separate sorties.</p> <table border="0"> <tr> <td>I => Transient inbound</td> <td rowspan="2">} Times are in GMT (i.e., Zulu)</td> </tr> <tr> <td>O => Transient outbound</td> </tr> </table> <p>V => Deviation - times are local engine start and takeoff times. Slashes separate sorties.</p> <p>A => Non-weather aborts - times are local engine start times</p>	I => Transient inbound	} Times are in GMT (i.e., Zulu)	O => Transient outbound
I => Transient inbound	} Times are in GMT (i.e., Zulu)			
O => Transient outbound				
8-10	Runway			
11-20	Aircraft type - left justified			
21-24	<table border="0"> <tr> <td rowspan="5">} Local 24-hour times separated by commas or slashes as appropriate. (Zulu time for transient aircraft.)</td> </tr> <tr> </tr> <tr> </tr> <tr> </tr> <tr> </tr> </table>	} Local 24-hour times separated by commas or slashes as appropriate. (Zulu time for transient aircraft.)		
} Local 24-hour times separated by commas or slashes as appropriate. (Zulu time for transient aircraft.)				
26-30				
.				
.				
76-79				

Table D-4. Monthly Summary of Aircraft Mix at WAFB

Month	Aircraft Type					
June 1976	F5	F4	T37	T38	RF4P	C140
	A4	A7	T39	A6P	F100	C135
	A6	H1	AH1	SH5	OH58	
	H3		UH1	HH1		
July	F5	F4	T37	T38	C130	C130A
	A4	H1	UH1	H46	F101	VC130
	A6	T2	T39	T33	C135	KC135
	C4		H3P	TA4	CH46	
		TC4	F14			
August	F5	F4	T37	T38	C130	F100P
	A4	A3	A37	T33	F105	
	T2	E2	UH1	T39	C135	
	C9					
September	F5	F4	T37	T38	C130	A21P
	A4	T2	T33	T39	F101	F100
	C9	H1	UH1	H53	CH46	CH53
	A7		H46	T28	OH58	
October	F5	F4	T37	T38	T39	C130
	C9	A7	UH1	TA4	RF4	C140
	H2	A4	A37	T33	T28	VC140
	H1	T2	A6	A48		
November	F5	T37	T38	TRANHEL	TRANTRN	TRANRCP
December	F5	F4	T37	T38	300C	BEECH55
	A7	A4	1A1	TA4	C135	BARON
	H3	H1	T39	CH3	OV10	F101
	A6		T33	AV8	OU10	F100
		F14	UH1	OH58		
January 1977	F5	T37	T38	TRANHEL	TRANTRN	TRANRCP
	A4	T39				
February	T37	T38	T39	C130	F5	
	A4	F100	H1	F4	UH1	
	T33	A3	OV10	A7	T43	
	C140	1357	T28	T2	H53	
	AV8	CF5				
March	T37	T38	F5	T39	A4	F4
	F106	A7	T33	T2	UH1	OV10
	F100	C130	C4	TC4		
April	T37	T38	F5	A4	AV8	
	F4	H58	T39	OH58	H3	
	A37	H1	A6	C130	T2	
	UH1	H46	C135	BEECH 55	F101	
	OV10	T33	C140			

Table D-4. (Cont'd)

Month	Aircraft Type				
May 1977	T37	T38	F5	C130	U21
	T33	OV10	F101	A4	H1
	UH1	F4	F100	C9	T41
	VC140	H53	T39	A7	C135
	H46				
June	T37	T38	F5	H46	A4
	T39	H1	CESSNA1	T33	F4
	C130	C140	H3	OV10	A6

Classes 1, 2, and 3 will be used to designate aircraft types F5, T37, and T38, respectively. Classes 4, 5, and 6 will be used to designate three classes of transient aircraft, comprising aircraft types that are similar to F4, C130, and C141, respectively, where F4 represents a fighter type class, C130 a turboprop engine class, and C141 a multiengine jet class. Class 7 will be reserved for transient aircraft of the helicopter type.

For AQAM evaluation purposes, only the first six classes of aircraft will be considered; class 7, the helicopter types, will be omitted.

Table D-5 shows a listing of transient aircraft types and their respective classification. Note that all aircraft-type notations are as given after the information transcription process.

c. Definitions for Aircraft Activity Operations at WAFB

Aircraft activity data compiled for WAFB during the period 1 June 1976-30 June 1977 provides an accounting for aircraft operations that were normal, transient, and aborted or otherwise deviated from takeoff.

(1) Normal Operations

Normal operations are defined for aircraft types F5, T37, and T38 only. Local military time was recorded at the moment of liftoff (during takeoff mode) and again at the moment of touchdown (during the landing mode). For landing operations involving touch-and-go maneuvers, the military time recorded was the moment of last touchdown. Whether some Air Force flights did or did not originate at WAFB, their takeoff or landing time was reported in this normal group.

(2) Transient Operations

Transient operations are defined for all aircraft. Greenwich Mean Time (Zulu) was recorded for each inbound and each outbound transient

Table D-5. Classification of Transient Aircraft at WAFB

Class 4	Class 5	Class 6	Class 7
A4	A3	C4	AH7
A6	Beech 55	C9	CH3
A7	Beech Baron	C135	CH46
A37	C130	C140	CH56
AV8	C130A	C141	H1
B57	Cessna 1	CF5	H2
F4	Cessna 300	KC135	H3
F14	E-2	T2	H46
F100	OV-10	TC4	H53
F101	T-28	VC140	H58
F105	T-41		HH1
F106	T-43		OH58
RF4	TA-1		SH5
Tee	TRANRCP		U10
T39	300C*		U21
TA4			UH7
TRANTRN			TRANHEL
A48*			H3P*
A6P*			
A21P*			
F100P*			
RF4P*			

*This aircraft type is questionable: possible data recording error.

operation. These operations at WAFB account for nonscheduled aircraft arrivals and departures.

(3) Abort Operations

Abort operations are defined for aircraft types F5, T37, and T38 only. Local time was recorded at the moment of aircraft engine-start. This is the only recorded information in regard to nonweather abort operations.

(4) Deviation Operations

Deviation from scheduled takeoff is an operation defined for aircraft types F5, T37, and T38 only. Local time was recorded if the time at engine-start deviated more than 5 minutes from scheduled start time and again if the time at takeoff deviated more than 10 minutes from scheduled takeoff. Upon completion of the takeoff procedure, the deviation operation becomes identical to a normal operation; only exceeding it in duration by several minutes of ground-time. The total ground-time being the full time interval between engine-start and final liftoff.

d. Edits to the Aircraft Activity Data Base

Some of the entries resulting from the transcription process were found to be erroneous and were resolved by making a best-guess estimate of actual time values. For example, some normal operation time entries (sorties) would extend beyond the hour of midnight, while other takeoff/landing times for sorties seemed transposed.

In the cases where time entries would extend beyond the midnight hour, the sortie was assumed to begin and then end on consecutive days. This was achieved by substituting the time -1 (i.e., unspecified) as the landing time, then adding, for the next day, a sortie whose takeoff time was -1 and landing time was used from the previous record.

In the cases where sortie times seemed to be transposed, the time entries were interchanged.

(1) Edits to Normal Operations Data

Table D-6 provides the list of edits made to the normal operations portion of aircraft activity data for WAFB. The date, runway, and aircraft type are given in columns 1, 2, and 3 respectively. Uncorrected takeoff and landing times are shown in columns 4 and 5 beside the corrected times shown in columns 6 and 7. The indicator, -1, shows a nonoperation so these are not included when the operations are tallied.

(2) Edits to Deviation Operations Data

Table D-7 provides the list of edits made to the deviation operations portion of aircraft activity data. The date, runway, and aircraft type are given in columns 1, 2, and 3, respectively. Uncorrected aircraft engine-start and takeoff times are shown in columns 4 and 5 and their corrected times appear in columns 6 and 7.

e. Full Traffic Count on Airbase Runways

The layout of airbase runways is shown in Fig. D-2. Runways prefixed by a 12 are used only when the northwesterly wind exceeds 10 knots. The letters

Table D-6. Edits to Normal Operations Data at WAFB

Date	Rnwy	Aircraft Type	Uncorrected		Corrected	
			T ^a	L ^b	T	L
760630	30C	F5	1600	1554	1600	1654
760702	30C	T38			-1	0043
760702	30C	T38			-1	0058
760702	30C	T38			0005	0057
760701	30C	T38	2343	0043	2343	-1
760701	30C	T38	2350	0058	2350	-1
760701	30C	T38	0005	0057		
760702	30C	T38			-1	0008
760702	30C	T38			-1	0018
760702	30C	T38			-1	0030
760702	30C	T38			-1	0024
760701	30C	T38	2308	0008	2308	-1
760701	30C	T38	2318	0018	2318	-1
760701	30C	T38	2327	0030	2327	-1
760701	30C	T38	2330	0024	2330	-1
760720	30C	T38	2311	0007	2311	-1
760721	30C	T38			-1	0007
760720	30C	T38	2306	0005	2306	-1
760720	30C	T38	2308	0007	2308	-1
760721	30C	T38			-1	0005
760721	30C	T38			-1	0007
760712	30C	T38	2322	0019	2322	-1
760713	30C	T38			-1	0019
760712	30C	T38	2311	0006	2311	-1
760713	30C	T38			-1	0006
760712	30C	T38	2308	0004	2308	01
760713	30C	T38			-1	0004
760712	30C	T38	2342	0032	2342	-1
760713	30C	T38			-1	0032
760712	30C	T38	2314	0001	2314	-1
760713	30C	T38			-1	0001
760712	30C	T38	2335	0036	2335	-1
760713	30C	T38			-1	0036
760819	30C	T38	2312	0006	2312	-1
760819	30C	T38	2314	0005	2314	-1
760820	30C	T38			-1	0006
760820	30C	T38			-1	0005
760818	30C	T38	2322	0004	2322	-1
760818	30C	T38	2330	0013	2330	-1
760818	30C	T38	2330	0013	2330	-1
760819	30C	T38			-1	0004
760819	30C	T38			-1	0013
760819	30C	T38			-1	0013

Table D-6. (Cont'd)

Date	Rnwy	Aircraft Type	Uncorrected		Corrected	
			T ^a	L ^b	T	L
760812	30C	T38	2317	0024	2317	-1
760812	30C	T38	2329	0026	2329	-1
760812	30C	T38	2334	0026	2334	-1
760813	30C	T38			-1	0024
760813	30C	T38			-1	0026
760813	30C	T38			-1	0026
760811	30C	T38	1909	1621	1509	1621
760802	30C	T38	2304	0004	2304	-1
760803	30C	T38			-1	0004
761108	30R	T38	1311	1252	1211	1252
761108	30L	T37	1120	0247	1120	1247
761201	30L	T37	1836	1728	1836	1928
761203	30L	T37	1640	1451	1340	1451
761210	30C	T38	1509	1410	1309	1410
770112	30C	T38	1617	1533	1617	1733
770120	30C	F5	1513	1317	1153	1317
770222	30C	T38	2224	1907	2224	-1
770301	30C	F5	1303	0901	1303	1401
770301	30C	F5	1750	0849	1750	1849
770307	30C	T38	1403	1237	1203	1237
770308	30C	T38	1329	0442	1329	1442
770308	30C	T38	1249	0620	1249	1620
770314	30C	F5	1620	1408	1620	1708
770331	30C	T38	1805	1351	1805	1851
770408	30C	T38	1233	1125	1033	1125
770408	30C	T38	1233	1125	1033	1125
770415	30L	T37	1939	1058	0939	1058
770504	30C	T38	1744	1003	0844	1003
770523	30C	F5	1132	1013	1132	1213
770607	30C	T38	1259	1042	1259	1402
770614	30C	F5	0822	0600	0822	-1
770620	30C	T38	2343	0047	2343	-1
770620	30C	T38	2343	0026	2343	-1
770620	30C	T38	0003	0049		
770620	30C	T38	0003	0036		
770621	30C	T38			-1	0047
770621	30C	T38			-1	0026
770621	30C	T38			0003	0049
770621	30C	T38			0003	0036
770629	30C	T38	2228	0000	2228	-1

^aT = Takeoff Time^bL = Landing Time

Table D-7. Edits to Deviation Operations Data at WAFB

Date	Rnwy	Aircraft Type	Uncorrected		Corrected	
			ES ^a	T ^b	ES	T
760621	30C	T38	0654	0619	0604	0619
760818	30C	T38	1658	1620	1658	1720
760804	30C	T38	1723	1540	1723	1740
760901	30C	T38	1439	1352	1339	1352
760902	30C	T38	1545	1401	1545	1601
760929	30C	T38	1656	1620	1606	1620
761027	30C	T38	1630	1605	1605	1630
761027	30C	T38	1334	1251	1251	1334
761103	30R	T38	1555	1514	1455	1514
761109	30R	T38	1510	1447	1410	1447
761122	30R	T38	1545	1403	1345	1403
761123	30L	T37	1558	1402	1558	1602
761215	30C	T38	1156	1116	1056	1116
770201	30C	T38	1147	1101	1107	1121
770519	30L	T37	1717	1628	1617	1628
770523	30C	T38	0750	0728	0728	0750
770601	30C	T38	--	1332	1312	1322
770614	30L	T37	--	1556	1546	1556
770620	30C	T38	2130	1249	2130	2149
770624	30L	T37	1327	0357	1327	1357
770628	30C	T38	1630	1045	1630	1645

^aES = Takeoff Time

^bL = Landing Time

L, C, and R denote left, center, and right, respectively. Runway 30L is used almost exclusively by T37 aircraft; runways 30C and 30R are used jointly by T38 and F5 aircraft.

The full traffic count on a runway is determined as the sum of landing plus takeoff operations, plus twice the number of touch-and-go operations on that runway. It is unfortunate that these daily runway traffic counts, gathered during the WAFB experimental period, were inaccurate because of the several methods used to record aircraft operations. Specifically, three methods exist by which runway traffic counts were recorded, thus the data base, in effect, is partitioned into three subsets, in regard to daily traffic counts: (1) the actual count or the daily average based on estimated monthly activity, depending on the runway, (2) the actual count on each runway, and (3) the actual count or the daily average based on actual monthly activity, depending on the runway.

(1) Full Traffic Count for June and July 1976

The methods used to record June and July 1976 full traffic counts are runway dependent. For runway 30L (and 12R), which are used almost exclusively by T37 aircraft, the actual daily activity count is recorded. Traffic counts for runways 30C (and 12C) and 30R (and 12L), used jointly by T38 and F5 aircraft, are average daily traffic counts derived from estimated monthly activity.

(2) Full Traffic Count for August 1976-January 1977

For the 6-month period, August 1976-January 1977, the traffic count for each runway is given as the actual daily activity count.

(3) Full Traffic Count for February-June 1977

The methods used to record February-June 1977 full traffic counts are runway dependent. For runways 30L and 12R, used almost exclusively by T37 aircraft, the counts were supplied by the Flight Records Branch, WAFB, and represent, for most days, the actual daily activity count. However, there are several days for which the traffic count is an estimated value.

The traffic counts for runway 30C, used jointly by T38 and F5 aircraft, were recorded on AFCS Form 5a (Control Tower and GCA logs). The use of the Tower and GCA logs provided an estimate of daily traffic counts since the Tower, in addition to controlling the center runway (30C), always assumes control of other runways whenever shutdowns of respective RSUs occur. During shutdown periods, no distinction is made between runway use by aircraft.

The traffic counts for runway 30R, used jointly by T38 and F5 aircraft, were supplied by the Air Traffic Control Superintendent at WAFB. Daily traffic counts were derived by equally distributing the supplied monthly totals of RSU station name GASSER among the weekdays of the month, i.e., both weekends and holidays were excluded.

f. Touch-and-go Training Flights

Touch-and-go training flights are carried out by student pilots using T37, T38, and F5 aircraft. In performing these maneuvers, an aircraft approaches and lands on a runway, travels down the runway for several seconds, accelerates, and lifts off. The runway in use depends on the aircraft involved. Runway 30L is used exclusively by T37 aircraft and runways 30C and 30R are shared by T38 and F5 aircraft.

Unlike the hour of landing and hour of takeoff described for normal operations, we define an hourly, discrete time history of touch-and-go operations specific to runway and aircraft type as a function of the total number of operations (landing and takeoff) on that runway by the relation:

$$TG_{ij} = \frac{1}{2} \left(\frac{HA_{ij}}{\sum_{j=1}^N \sum_{i=1}^{24} HA_{ij}} \right) \cdot \left(\text{Full Traffic Count} - \sum_{j=1}^N \sum_{i=1}^{24} (HA_{ij} + HT_{ij}) \right)$$

where:

HA_{ij} = the number of landing operations on the runway by aircraft type j during hour i ,

HT_{ij} = the number of takeoff operations on the runway by aircraft type j during hour i , and

FTC = the daily total of landings, takeoffs, plus twice the touch-and-go operations on the runway.

In consideration of the Full Traffic Count as derived by the several methods stated above, it is realized that the imbedded touch-and-go operations specific to runway 30C or runway 30R do not distinguish between the aircraft types F5 or T38. Thus, all or none of these operations could be performed by either aircraft type. Therefore, we note that both F5 and T38 aircraft are equipped with two J85 aircraft engines and that all significant operational parameters, such as their altitude at final phase of approach; their speed at point of touchdown, etc., are much the same. It can be concluded that the above relationship is sufficient for this application of the AQAM, though it may not suffice for more detailed studies, such as air quality impact analysis of individual aircraft types.

g. Summary Report of Aircraft Activity at WAFB for the Period
1 June 1976-30 June 1977

In order to demonstrate the type of activity data available for input to the Air Quality Assessment Model, a computerized program was developed that summarizes the Aircraft Activity Information collected at WAFB, Arizona. The input data to the program is formatted as shown in Table D-3; resulting summaries, formatted with different headings but identical bodies, are produced for the following:

- (i) Hourly Aircraft Activity (A one day example summary is presented in Attachment A),
- (ii) Daily Aircraft Activity (not presented here),
- (iii) Monthly Aircraft Activity (Attachment B),
- (iv) Grand Totals of Aircraft Activity (Attachment C).

Summaries (i) and (ii) are headed by each date having a day-label such as, *weekday* (for Monday through Friday), *weekend day* (for Saturday or Sunday), *weekday-holiday*, or *weekend-holiday*. It is instructive to note that a holiday pattern is realized when very low aircraft activity periods are examined. The following table illustrates the observed pattern for the dates that reported no aircraft activity at all.

<u>Dates</u>	<u>Holiday</u>	<u>Day of Week</u>
3 July 1976		
4 July 1976	Independence Day	Sunday
5 July 1976		
6 Sept. 1976	Labor Day	Monday
11 Oct. 1976	Columbus Day	Monday
25 Oct. 1976	Veterans Day	Monday
24 Dec. 1976		
25 Dec. 1976	Christmas Day	Saturday
26 Dec. 1976		
31 Dec. 1976		
1 Jan. 1977	New Year's Day	Saturday
2 Jan. 1977		
29 May 1977		
30 May 1977	Memorial Day	Monday

Thanksgiving Day, Thursday, 25 November 1976, although a holiday, was found to have one outbound transient fighter operation.

In the body of each summary we see that the column "Full Traffic Count" is an aggregate of all aircraft types, but that each of the other columns have aircraft type indicators with the corresponding meaning as follows:

F5	Class 1
T37	Class 2
T38	Class 3
F	Class 4 (F4 - Fighter Class)
T	Class 5 (C130 - Turboprop engine class)
M	Class 6 (C141 - Multiengine jet class)
H	Class 7 (Helicopter class)

The repeated indicators are then grouped by the mode of the operation (landing-inbound, takeoff-outbound, ground time, touch-and-go), and then, where appropriate, by the previously defined activity operations Normal, Deviation, Abort, or Transient.

The frequency of occurrence of each of the activity operations, in mode of the aircraft type, is given for each airbase runway. The ground time of deviation operations, however, is given in minutes on the runway.

Six runways are identified from which all airbase aircraft operations are performed. The computer program is coded so as to assure that the following assumptions, regarding runway use, are preserved:

- (1) All T37 operations (landing, takeoff, and touch-and-go) are performed on the inside runway (30L or 12R).
- (2) All C130 and all C141 operations (transient) are performed on 30L (n.b., only 30L can handle the heavy aircraft).
- (3) All T38 and F5 operations are performed on either the center runway (30C or 12C) or the outside runway (30R or 12L) with the shared pattern as follows:

- (i) All takeoffs (T38 and F5) occur from the center runway (30C or 12C).
- (ii) 88% of T38 landings occur on the outside runway (30R or 12L), the remainder occur on the center runway (30C or 12C).
- (iii) 80% of F5 landings occur on the outside runway (30R or 12L), the remainder occur on the center runway (30C or 12C).

Just as was stated above about the holiday pattern of aircraft activity, we note here a weekend pattern of aircraft activity. In general, there are cases of weekend airbase aircraft activity, but these events are not recorded as are the weekday events. Some specially requested weekend data were supplied covering the weekends of December 1976 and January 1977 and these data, though limited, served to define the weekend pattern of events at WAFB.

REFERENCES

- D-1. Zeller, K.F., and R.B. Evans, *Airport quality and Its Control*, J. of the Air Pollution Control Association, 15:12 (Dec. 1965).
- D-2. Naugle, D.F., and S.R. Nelson, *USAF Aircraft Pollution Emission Factors and Landing and Takeoff (LTO) Cycles*, AFWL-TR-74-303, Air Force Weapons Laboratory, Kirkland Air Force Base, N.M. (1975).

ATTACHMENT A: HOURLY AIRCRAFT ACTIVITY SUMMARY; A ONE-DAY EXAMPLE, 6 AUGUST 1976

		AIRCRAFT ACTIVITY HOURLY SUMMARY 76006											
		---NORMAL OPERATIONS---				---DEVIATIONS---				---GROUND TIME/MTG---			
		---TAXI/F---		---L/D/MS---		---TAXI/OSF---		---GROUND TIME/MTG---		---AR/OTS---			
		F5	T38	F5	T38	F5	T38	F5	T38	F5	T38	F5	T38
HP 1*		0.0	0.0	0.0	0.0	0.0	0.0	0.0	0.0	0.0	0.0	0.0	0.0
HP 2*		0.0	0.0	0.0	0.0	0.0	0.0	0.0	0.0	0.0	0.0	0.0	0.0
HP 3*		0.0	0.0	0.0	0.0	0.0	0.0	0.0	0.0	0.0	0.0	0.0	0.0
HP 4*		0.0	0.0	0.0	0.0	0.0	0.0	0.0	0.0	0.0	0.0	0.0	0.0
HP 5*		0.0	0.0	0.0	0.0	0.0	0.0	0.0	0.0	0.0	0.0	0.0	0.0
HP 6*		0.0	0.0	0.0	0.0	0.0	0.0	0.0	0.0	0.0	0.0	0.0	0.0
HP 7		0.0	0.0	0.0	0.0	0.0	0.0	0.0	0.0	0.0	0.0	0.0	0.0
TOTAL		0.0	0.0	0.0	0.0	0.0	0.0	0.0	0.0	0.0	0.0	0.0	0.0
HP 8		0.0	0.0	0.0	0.0	0.0	0.0	0.0	0.0	0.0	0.0	0.0	0.0
TOL		0.0	0.0	0.0	0.0	0.0	0.0	0.0	0.0	0.0	0.0	0.0	0.0
TOC		0.0	0.0	0.0	0.0	0.0	0.0	0.0	0.0	0.0	0.0	0.0	0.0
TOE		0.0	0.0	0.0	0.0	0.0	0.0	0.0	0.0	0.0	0.0	0.0	0.0
TOF		0.0	0.0	0.0	0.0	0.0	0.0	0.0	0.0	0.0	0.0	0.0	0.0
TOG		0.0	0.0	0.0	0.0	0.0	0.0	0.0	0.0	0.0	0.0	0.0	0.0
TOH		0.0	0.0	0.0	0.0	0.0	0.0	0.0	0.0	0.0	0.0	0.0	0.0
TOTAL		0.0	0.0	0.0	0.0	0.0	0.0	0.0	0.0	0.0	0.0	0.0	0.0
HP 9		0.0	0.0	0.0	0.0	0.0	0.0	0.0	0.0	0.0	0.0	0.0	0.0
TOL		0.0	0.0	0.0	0.0	0.0	0.0	0.0	0.0	0.0	0.0	0.0	0.0
TOC		0.0	0.0	0.0	0.0	0.0	0.0	0.0	0.0	0.0	0.0	0.0	0.0
TOE		0.0	0.0	0.0	0.0	0.0	0.0	0.0	0.0	0.0	0.0	0.0	0.0
TOF		0.0	0.0	0.0	0.0	0.0	0.0	0.0	0.0	0.0	0.0	0.0	0.0
TOG		0.0	0.0	0.0	0.0	0.0	0.0	0.0	0.0	0.0	0.0	0.0	0.0
TOH		0.0	0.0	0.0	0.0	0.0	0.0	0.0	0.0	0.0	0.0	0.0	0.0
TOTAL		0.0	0.0	0.0	0.0	0.0	0.0	0.0	0.0	0.0	0.0	0.0	0.0
HP 10		0.0	0.0	0.0	0.0	0.0	0.0	0.0	0.0	0.0	0.0	0.0	0.0
TOL		0.0	0.0	0.0	0.0	0.0	0.0	0.0	0.0	0.0	0.0	0.0	0.0
TOC		0.0	0.0	0.0	0.0	0.0	0.0	0.0	0.0	0.0	0.0	0.0	0.0
TOE		0.0	0.0	0.0	0.0	0.0	0.0	0.0	0.0	0.0	0.0	0.0	0.0
TOF		0.0	0.0	0.0	0.0	0.0	0.0	0.0	0.0	0.0	0.0	0.0	0.0
TOG		0.0	0.0	0.0	0.0	0.0	0.0	0.0	0.0	0.0	0.0	0.0	0.0
TOH		0.0	0.0	0.0	0.0	0.0	0.0	0.0	0.0	0.0	0.0	0.0	0.0
TOTAL		0.0	0.0	0.0	0.0	0.0	0.0	0.0	0.0	0.0	0.0	0.0	0.0

AIRCRAFT ACTIVITY HOURLY SUMMARY 760006

	---NORMAL OPERATIONS---				---DEVIATIONS---				---GROUND TIME(MIN)---							
	F5	T37	T38	F5	T37	T38	F5	T37	T38	F5	T37	T38	F5	T37	T38	
HR 16																
301	0.0	11.0	0.0	0.0	2.0	0.0	0.0	1.0	0.0	0.0	0.0	0.0	0.0	0.0	0.0	0.0
302	0.0	0.0	15.0	0.0	0.0	1.0	0.0	0.0	2.0	0.0	0.0	0.0	0.0	0.0	0.0	0.0
303	0.0	0.0	0.0	0.0	0.0	4.0	0.0	0.0	0.0	0.0	0.0	0.0	0.0	0.0	0.0	0.0
304	0.0	0.0	0.0	0.0	0.0	0.0	0.0	0.0	0.0	0.0	0.0	0.0	0.0	0.0	0.0	0.0
305	0.0	0.0	0.0	0.0	0.0	0.0	0.0	0.0	0.0	0.0	0.0	0.0	0.0	0.0	0.0	0.0
306	0.0	0.0	0.0	0.0	0.0	0.0	0.0	0.0	0.0	0.0	0.0	0.0	0.0	0.0	0.0	0.0
TOTAL	0.0	11.0	15.0	0.0	2.0	6.0	0.0	1.0	2.0	0.0	2.0	0.0	0.0	0.0	0.0	0.0
HR 17																
301	0.0	0.0	7.0	0.0	0.0	0.0	0.0	0.0	0.0	0.0	0.0	0.0	0.0	0.0	0.0	0.0
302	0.0	0.0	0.0	0.0	0.0	0.0	0.0	0.0	0.0	0.0	0.0	0.0	0.0	0.0	0.0	0.0
303	0.0	0.0	0.0	0.0	0.0	0.0	0.0	0.0	0.0	0.0	0.0	0.0	0.0	0.0	0.0	0.0
304	0.0	0.0	0.0	0.0	0.0	0.0	0.0	0.0	0.0	0.0	0.0	0.0	0.0	0.0	0.0	0.0
305	0.0	0.0	0.0	0.0	0.0	0.0	0.0	0.0	0.0	0.0	0.0	0.0	0.0	0.0	0.0	0.0
306	0.0	0.0	0.0	0.0	0.0	0.0	0.0	0.0	0.0	0.0	0.0	0.0	0.0	0.0	0.0	0.0
TOTAL	0.0	0.0	7.0	0.0	0.0	0.0	0.0	0.0	0.0	0.0	0.0	0.0	0.0	0.0	0.0	0.0
HR 18																
301	0.0	0.0	0.0	0.0	0.0	0.0	0.0	0.0	0.0	0.0	0.0	0.0	0.0	0.0	0.0	0.0
302	0.0	0.0	0.0	0.0	0.0	0.0	0.0	0.0	0.0	0.0	0.0	0.0	0.0	0.0	0.0	0.0
303	0.0	0.0	0.0	0.0	0.0	0.0	0.0	0.0	0.0	0.0	0.0	0.0	0.0	0.0	0.0	0.0
304	0.0	0.0	0.0	0.0	0.0	0.0	0.0	0.0	0.0	0.0	0.0	0.0	0.0	0.0	0.0	0.0
305	0.0	0.0	0.0	0.0	0.0	0.0	0.0	0.0	0.0	0.0	0.0	0.0	0.0	0.0	0.0	0.0
306	0.0	0.0	0.0	0.0	0.0	0.0	0.0	0.0	0.0	0.0	0.0	0.0	0.0	0.0	0.0	0.0
TOTAL	0.0	0.0	0.0	0.0	0.0	0.0	0.0	0.0	0.0	0.0	0.0	0.0	0.0	0.0	0.0	0.0
HR 19																
301	0.0	0.0	0.0	0.0	0.0	0.0	0.0	0.0	0.0	0.0	0.0	0.0	0.0	0.0	0.0	0.0
302	0.0	0.0	0.0	0.0	0.0	0.0	0.0	0.0	0.0	0.0	0.0	0.0	0.0	0.0	0.0	0.0
303	0.0	0.0	0.0	0.0	0.0	0.0	0.0	0.0	0.0	0.0	0.0	0.0	0.0	0.0	0.0	0.0
304	0.0	0.0	0.0	0.0	0.0	0.0	0.0	0.0	0.0	0.0	0.0	0.0	0.0	0.0	0.0	0.0
305	0.0	0.0	0.0	0.0	0.0	0.0	0.0	0.0	0.0	0.0	0.0	0.0	0.0	0.0	0.0	0.0
306	0.0	0.0	0.0	0.0	0.0	0.0	0.0	0.0	0.0	0.0	0.0	0.0	0.0	0.0	0.0	0.0
TOTAL	0.0	0.0	0.0	0.0	0.0	0.0	0.0	0.0	0.0	0.0	0.0	0.0	0.0	0.0	0.0	0.0
HR 20																
301	0.0	0.0	0.0	0.0	0.0	0.0	0.0	0.0	0.0	0.0	0.0	0.0	0.0	0.0	0.0	0.0
302	0.0	0.0	0.0	0.0	0.0	0.0	0.0	0.0	0.0	0.0	0.0	0.0	0.0	0.0	0.0	0.0
303	0.0	0.0	0.0	0.0	0.0	0.0	0.0	0.0	0.0	0.0	0.0	0.0	0.0	0.0	0.0	0.0
304	0.0	0.0	0.0	0.0	0.0	0.0	0.0	0.0	0.0	0.0	0.0	0.0	0.0	0.0	0.0	0.0
305	0.0	0.0	0.0	0.0	0.0	0.0	0.0	0.0	0.0	0.0	0.0	0.0	0.0	0.0	0.0	0.0
306	0.0	0.0	0.0	0.0	0.0	0.0	0.0	0.0	0.0	0.0	0.0	0.0	0.0	0.0	0.0	0.0
TOTAL	0.0	0.0	0.0	0.0	0.0	0.0	0.0	0.0	0.0	0.0	0.0	0.0	0.0	0.0	0.0	0.0

AIROPORT ACTIVITY SUPPLY SUMMARY 760005

	INCOMING OPERATIONS										OUTBOUND				TOUCH-AND-GO OPERATIONS		
	F5	137	133	F	T	H	H	F5	137	133	F	T	H	F5	137	133	
HR 12	0.	0.	0.	0.	0.	0.	0.	0.	0.	0.	0.	0.	0.	0.	0.	0.	
30L	0.	0.	0.	0.	0.	0.	0.	0.	0.	0.	0.	0.	0.	0.	11.9	0.0	
30C	0.	0.	0.	0.	0.	0.	0.	0.	0.	0.	0.	0.	0.	0.0	0.0	0.0	
30R	0.	0.	0.	0.	0.	0.	0.	0.	0.	0.	0.	0.	0.	0.0	0.0	0.0	
102	0.	0.	0.	0.	0.	0.	0.	0.	0.	0.	0.	0.	0.	0.0	0.0	0.0	
103	0.	0.	0.	0.	0.	0.	0.	0.	0.	0.	0.	0.	0.	0.0	0.0	0.0	
104	0.	0.	0.	0.	0.	0.	0.	0.	0.	0.	0.	0.	0.	0.0	0.0	0.0	
TOTAL	0.	0.	0.	0.	0.	0.	0.	0.	0.	0.	0.	0.	0.	0.0	11.9	33.4	
HR 13	0.	0.	0.	0.	0.	0.	0.	0.	0.	0.	0.	0.	0.	0.0	0.0	0.0	
30L	0.	0.	0.	0.	0.	0.	0.	0.	0.	0.	0.	0.	0.	0.0	7.7	0.0	
30C	0.	0.	0.	0.	0.	0.	0.	0.	0.	0.	0.	0.	0.	2.5	0.0	0.0	
30R	0.	0.	0.	0.	0.	0.	0.	0.	0.	0.	0.	0.	0.	14.3	0.0	15.5	
102	0.	0.	0.	0.	0.	0.	0.	0.	0.	0.	0.	0.	0.	0.0	0.0	0.0	
103	0.	0.	0.	0.	0.	0.	0.	0.	0.	0.	0.	0.	0.	0.0	0.0	0.0	
104	0.	0.	0.	0.	0.	0.	0.	0.	0.	0.	0.	0.	0.	0.0	0.0	0.0	
TOTAL	0.	0.	0.	0.	0.	0.	0.	0.	0.	0.	0.	0.	0.	17.4	7.7	21.6	
HR 14	0.	0.	0.	0.	0.	0.	0.	0.	0.	0.	0.	0.	0.	0.0	0.0	0.0	
30L	0.	0.	0.	0.	0.	0.	0.	0.	0.	0.	0.	0.	0.	0.0	0.0	0.0	
30C	0.	0.	0.	0.	0.	0.	0.	0.	0.	0.	0.	0.	0.	0.0	0.0	0.0	
30R	0.	0.	0.	0.	0.	0.	0.	0.	0.	0.	0.	0.	0.	0.0	0.0	0.0	
102	0.	0.	0.	0.	0.	0.	0.	0.	0.	0.	0.	0.	0.	0.0	0.0	0.0	
103	0.	0.	0.	0.	0.	0.	0.	0.	0.	0.	0.	0.	0.	0.0	0.0	0.0	
104	0.	0.	0.	0.	0.	0.	0.	0.	0.	0.	0.	0.	0.	0.0	0.0	0.0	
TOTAL	0.	0.	0.	0.	0.	0.	0.	0.	0.	0.	0.	0.	0.	0.0	0.0	0.0	
HR 15	0.	0.	0.	0.	0.	0.	0.	0.	0.	0.	0.	0.	0.	0.0	0.0	0.0	
30L	0.	0.	0.	0.	0.	0.	0.	0.	0.	0.	0.	0.	0.	0.0	0.0	0.0	
30C	0.	0.	0.	0.	0.	0.	0.	0.	0.	0.	0.	0.	0.	0.0	0.0	0.0	
30R	0.	0.	0.	0.	0.	0.	0.	0.	0.	0.	0.	0.	0.	0.0	0.0	0.0	
102	0.	0.	0.	0.	0.	0.	0.	0.	0.	0.	0.	0.	0.	0.0	0.0	0.0	
103	0.	0.	0.	0.	0.	0.	0.	0.	0.	0.	0.	0.	0.	0.0	0.0	0.0	
104	0.	0.	0.	0.	0.	0.	0.	0.	0.	0.	0.	0.	0.	0.0	0.0	0.0	
TOTAL	0.	0.	0.	0.	0.	0.	0.	0.	0.	0.	0.	0.	0.	0.0	0.0	0.0	
HR 16	0.	0.	0.	0.	0.	0.	0.	0.	0.	0.	0.	0.	0.	0.0	0.0	0.0	
30L	0.	0.	0.	0.	0.	0.	0.	0.	0.	0.	0.	0.	0.	0.0	0.0	0.0	
30C	0.	0.	0.	0.	0.	0.	0.	0.	0.	0.	0.	0.	0.	0.0	0.0	0.0	
30R	0.	0.	0.	0.	0.	0.	0.	0.	0.	0.	0.	0.	0.	0.0	0.0	0.0	
102	0.	0.	0.	0.	0.	0.	0.	0.	0.	0.	0.	0.	0.	0.0	0.0	0.0	
103	0.	0.	0.	0.	0.	0.	0.	0.	0.	0.	0.	0.	0.	0.0	0.0	0.0	
104	0.	0.	0.	0.	0.	0.	0.	0.	0.	0.	0.	0.	0.	0.0	0.0	0.0	
TOTAL	0.	0.	0.	0.	0.	0.	0.	0.	0.	0.	0.	0.	0.	0.0	0.0	0.0	

----- AIRCRAFT ACTIVITY HOURLY SUMMARY 760826 -----

	----- INCOMING -----							----- TRANSIENT OPERATIONS -----							----- TOUCH AND GO OPERATIONS -----		
	F5	T37	T39	F	T	M	H	F5	T37	T39	F	T	M	H	F5	T37	T39
HR 17	0.	0.	0.	0.	0.	0.	0.	0.	1.	0.	0.	0.	0.	0.	0.0	6.8	0.0
30L	0.	0.	0.	0.	0.	0.	0.	0.	0.	0.	0.	0.	0.	0.	0.0	0.0	1.8
30C	0.	0.	0.	3.	0.	0.	0.	0.	0.	0.	0.	0.	0.	0.	0.0	0.0	0.0
30R	0.	0.	0.	0.	0.	0.	0.	0.	0.	0.	0.	0.	0.	0.	0.0	0.0	0.0
10P	0.	0.	0.	0.	0.	0.	0.	0.	0.	0.	0.	0.	0.	0.	0.0	0.0	0.0
10C	0.	0.	0.	0.	0.	0.	0.	0.	0.	0.	0.	0.	0.	0.	0.0	0.0	0.0
10L	0.	0.	0.	0.	0.	0.	0.	0.	0.	0.	0.	0.	0.	0.	0.0	0.0	0.0
TOTAL	0.	0.	0.	3.	0.	0.	0.	0.	1.	2.	0.	0.	0.	0.	0.0	6.8	7.9
HR 18	0.	1.	0.	0.	0.	0.	0.	0.	0.	0.	0.	1.	0.	0.	0.0	6.0	0.0
30L	0.	0.	0.	0.	0.	0.	0.	0.	0.	0.	0.	0.	0.	0.	0.0	0.0	0.0
30C	0.	0.	0.	5.	0.	0.	0.	0.	0.	0.	0.	0.	0.	0.	0.0	0.0	0.0
30R	0.	0.	0.	0.	0.	0.	0.	0.	0.	0.	0.	0.	0.	0.	0.0	0.0	0.0
10P	0.	0.	0.	0.	0.	0.	0.	0.	0.	0.	0.	0.	0.	0.	0.0	0.0	0.0
10C	0.	0.	0.	0.	0.	0.	0.	0.	0.	0.	0.	0.	0.	0.	0.0	0.0	0.0
10L	0.	0.	0.	0.	0.	0.	0.	0.	0.	0.	0.	0.	0.	0.	0.0	0.0	0.0
TOTAL	0.	1.	0.	5.	0.	0.	0.	0.	0.	0.	2.	1.	0.	0.	1.9	6.0	7.9
HR 19	0.	0.	0.	0.	0.	0.	0.	0.	1.	0.	0.	0.	0.	0.	0.0	0.0	0.0
30L	0.	0.	0.	0.	0.	0.	0.	0.	0.	0.	0.	0.	0.	0.	0.0	0.0	0.0
30C	0.	0.	0.	1.	0.	0.	0.	0.	0.	0.	4.	0.	0.	0.	0.0	0.0	0.0
30R	0.	0.	0.	0.	0.	0.	0.	0.	0.	0.	0.	0.	0.	0.	0.0	0.0	0.0
10P	0.	0.	0.	0.	0.	0.	0.	0.	0.	0.	0.	0.	0.	0.	0.0	0.0	0.0
10C	0.	0.	0.	0.	0.	0.	0.	0.	0.	0.	0.	0.	0.	0.	0.0	0.0	0.0
10L	0.	0.	0.	0.	0.	0.	0.	0.	0.	0.	0.	0.	0.	0.	0.0	0.0	0.0
TOTAL	0.	0.	0.	1.	0.	0.	0.	0.	1.	0.	4.	0.	0.	0.	0.0	0.0	17.7
HR 20	0.	0.	0.	0.	0.	0.	0.	0.	0.	0.	0.	0.	0.	0.	0.0	0.0	0.0
30L	0.	0.	0.	0.	0.	0.	0.	0.	0.	0.	0.	0.	0.	0.	0.0	0.0	0.0
30C	0.	0.	0.	0.	0.	0.	0.	0.	0.	0.	0.	0.	0.	0.	0.0	0.0	0.0
30R	0.	0.	0.	0.	0.	0.	0.	0.	0.	0.	0.	0.	0.	0.	0.0	0.0	0.0
10P	0.	0.	0.	0.	0.	0.	0.	0.	0.	0.	0.	0.	0.	0.	0.0	0.0	0.0
10C	0.	0.	0.	0.	0.	0.	0.	0.	0.	0.	0.	0.	0.	0.	0.0	0.0	0.0
10L	0.	0.	0.	0.	0.	0.	0.	0.	0.	0.	0.	0.	0.	0.	0.0	0.0	0.0
TOTAL	0.	0.	0.	0.	0.	0.	0.	0.	0.	0.	0.	0.	0.	0.	0.0	0.0	0.0
HR 21*	0.	0.	0.	0.	0.	0.	0.	0.	0.	0.	0.	0.	0.	0.	0.0	0.0	0.0
HR 22*	0.	0.	0.	0.	0.	0.	0.	0.	0.	0.	0.	0.	0.	0.	0.0	0.0	0.0
HR 23*	0.	0.	0.	0.	0.	0.	0.	0.	0.	0.	0.	0.	0.	0.	0.0	0.0	0.0
HR 24*	0.	0.	0.	0.	0.	0.	0.	0.	0.	0.	0.	0.	0.	0.	0.0	0.0	0.0

AIRCRAFT ACTIVITY MONTHLY SUMMARY JULY 1976

	---NORMAL OPERATIONS---				---DEVIATIONS---				---ASSETS---				FULL TRAFFIC COUNT
	---TAKEOFF---		---LANDING---		---TIME OFF---		---GROUND TIME (MIN)---		F5		T33		
30L	0	0	0	0	0	0	0	0	0	0	0	0	9739
30C	0	2031	0	0	0	174	0	4912	0	0	0	0	7720
30D	0	0	2449	69	0	0	407	0	0	0	0	0	14270
30E	0	0	0	505	0	0	1535	0	0	0	0	0	73
30F	0	23	0	0	0	0	0	0	0	0	0	0	50
30G	0	0	45	1	0	0	9	0	0	0	0	0	75
30H	0	0	0	0	0	0	37	0	0	0	0	0	0
TOTAL	596	2019	2494	503	2025	194	2455	0	4912	11367	0	12	18

	---INBOUND---				---OUTBOUND---				TOUCH-AND-GO OPERATIONS---				
	F5	T37	T33	T38	F5	T37	T33	T38	F5	T37	T33	T38	
30L	0	0	0	0	0	0	0	0	0	0	0	0	0.0
30C	12	0	86	54	0	7	0	93	57	0	0	0	2073.5
30D	0	0	0	0	0	0	0	0	0	0	0	0	0.0
30E	0	0	0	0	0	0	0	0	0	0	0	0	0.0
30F	0	0	0	0	0	0	0	0	0	0	0	0	0.0
30G	0	0	0	0	0	0	0	0	0	0	0	0	0.0
30H	0	0	0	0	0	0	0	0	0	0	0	0	0.0
TOTAL	12	0	86	54	0	7	0	93	57	0	0	0	2073.5

AIRCRAFT TYPES USING HAFO	---INBOUND---				---OUTBOUND---				TOUCH-AND-GO OPERATIONS---				
	T37	T33	T38	T39	F4	F9	T33	T38	F4	F9	T33	T38	
30L	0	0	0	0	0	0	0	0	0	0	0	0	0.0
30C	12	0	86	54	0	7	0	93	57	0	0	0	2073.5
30D	0	0	0	0	0	0	0	0	0	0	0	0	0.0
30E	0	0	0	0	0	0	0	0	0	0	0	0	0.0
30F	0	0	0	0	0	0	0	0	0	0	0	0	0.0
30G	0	0	0	0	0	0	0	0	0	0	0	0	0.0
30H	0	0	0	0	0	0	0	0	0	0	0	0	0.0
TOTAL	12	0	86	54	0	7	0	93	57	0	0	0	2073.5

ACCOUNT ACTIVITY MONTHLY SUMMARY - AUGUST 1976

ACCOUNT TYPE	ACCOUNT ACTIVITY												TOTAL	
	1	2	3	4	5	6	7	8	9	10	11	12		
1000	0	0	0	0	0	0	0	0	0	0	0	0	0	0
2000	0	0	0	0	0	0	0	0	0	0	0	0	0	0
3000	0	0	0	0	0	0	0	0	0	0	0	0	0	0
4000	0	0	0	0	0	0	0	0	0	0	0	0	0	0
5000	0	0	0	0	0	0	0	0	0	0	0	0	0	0
6000	0	0	0	0	0	0	0	0	0	0	0	0	0	0
7000	0	0	0	0	0	0	0	0	0	0	0	0	0	0
8000	0	0	0	0	0	0	0	0	0	0	0	0	0	0
9000	0	0	0	0	0	0	0	0	0	0	0	0	0	0
TOTAL	0	0	0	0	0	0	0	0	0	0	0	0	0	0

ACCOUNT TYPE	ACCOUNT ACTIVITY												TOTAL	
	1	2	3	4	5	6	7	8	9	10	11	12		
1000	0	0	0	0	0	0	0	0	0	0	0	0	0	0
2000	0	0	0	0	0	0	0	0	0	0	0	0	0	0
3000	0	0	0	0	0	0	0	0	0	0	0	0	0	0
4000	0	0	0	0	0	0	0	0	0	0	0	0	0	0
5000	0	0	0	0	0	0	0	0	0	0	0	0	0	0
6000	0	0	0	0	0	0	0	0	0	0	0	0	0	0
7000	0	0	0	0	0	0	0	0	0	0	0	0	0	0
8000	0	0	0	0	0	0	0	0	0	0	0	0	0	0
9000	0	0	0	0	0	0	0	0	0	0	0	0	0	0
TOTAL	0	0	0	0	0	0	0	0	0	0	0	0	0	0

AIRCRAFT ACTIVITY MONTHLY SUMMARY SEPT. 1976

	NORMAL OPERATIONS			DEVIATIONS			ADVERTS			TOTAL					
	F5	T37	T38	F5	T37	T38	F5	T37	T38						
304	0	1824	0	0	200	0	0	4	0	9761					
30C	441	0	2392	0	0	523	0	0	14	7337					
30R	0	0	0	0	0	0	0	0	0	12923					
309	0	0	0	0	0	0	0	0	0	0					
300	0	47	0	0	1	0	0	0	0	13					
30C	15	0	55	2	0	12	0	0	0	42					
30L	0	0	0	0	0	0	0	0	0	0					
30B	0	0	0	0	0	0	0	0	0	0					
TOTAL	455	1931	2447	457	1875	2401	0	201	525	0	4223	12970	0	4	14

	TRANSIENT OPERATIONS			OUTBOUND			TOUCH-AND-GO OPERATIONS										
	F5	T37	T38	F5	T37	T38	F5	T37	T38								
304	0	19	0	0	19	0	0	18	0	0.0	2553.0	0.0					
30C	4	0	25	39	0	0	14	0	0	187.5	0.0	1920.0					
30R	0	0	0	0	0	0	0	0	0	192.5	0.0	1920.0					
309	0	0	0	0	0	0	0	0	0	0.0	0.0	0.0					
300	0	0	0	0	0	0	0	0	0	0.0	122.5	0.0					
30C	0	0	2	11	0	0	2	0	0	6.1	0.0	20.0					
30L	0	0	0	0	0	0	0	0	0	49.5	0.0	0.0					
TOTAL	4	19	27	50	3	2	14	6	19	26	51	3	2	13	1011.6	2630.5	6039.4

AIRCRAFT TYPES USING BASE	T37	T38	F5	ARAP	A4	T3	533	534
CP	0	0	0	0	0	0	0	0
CP53	0	0	0	0	0	0	0	0
T37	0	0	0	0	0	0	0	0
T38	0	0	0	0	0	0	0	0
F5	0	0	0	0	0	0	0	0
UAT	0	0	0	0	0	0	0	0
F101	0	0	0	0	0	0	0	0
F102	0	0	0	0	0	0	0	0
F103	0	0	0	0	0	0	0	0
F104	0	0	0	0	0	0	0	0
F105	0	0	0	0	0	0	0	0
F106	0	0	0	0	0	0	0	0
F107	0	0	0	0	0	0	0	0
F108	0	0	0	0	0	0	0	0
F109	0	0	0	0	0	0	0	0
F110	0	0	0	0	0	0	0	0
F111	0	0	0	0	0	0	0	0
F112	0	0	0	0	0	0	0	0
F113	0	0	0	0	0	0	0	0
F114	0	0	0	0	0	0	0	0
F115	0	0	0	0	0	0	0	0
F116	0	0	0	0	0	0	0	0
F117	0	0	0	0	0	0	0	0
F118	0	0	0	0	0	0	0	0
F119	0	0	0	0	0	0	0	0
F120	0	0	0	0	0	0	0	0
F121	0	0	0	0	0	0	0	0
F122	0	0	0	0	0	0	0	0
F123	0	0	0	0	0	0	0	0
F124	0	0	0	0	0	0	0	0
F125	0	0	0	0	0	0	0	0
F126	0	0	0	0	0	0	0	0
F127	0	0	0	0	0	0	0	0
F128	0	0	0	0	0	0	0	0
F129	0	0	0	0	0	0	0	0
F130	0	0	0	0	0	0	0	0
F131	0	0	0	0	0	0	0	0
F132	0	0	0	0	0	0	0	0
F133	0	0	0	0	0	0	0	0
F134	0	0	0	0	0	0	0	0
F135	0	0	0	0	0	0	0	0
F136	0	0	0	0	0	0	0	0
F137	0	0	0	0	0	0	0	0
F138	0	0	0	0	0	0	0	0
F139	0	0	0	0	0	0	0	0
F140	0	0	0	0	0	0	0	0
F141	0	0	0	0	0	0	0	0
F142	0	0	0	0	0	0	0	0
F143	0	0	0	0	0	0	0	0
F144	0	0	0	0	0	0	0	0
F145	0	0	0	0	0	0	0	0
F146	0	0	0	0	0	0	0	0
F147	0	0	0	0	0	0	0	0
F148	0	0	0	0	0	0	0	0
F149	0	0	0	0	0	0	0	0
F150	0	0	0	0	0	0	0	0
F151	0	0	0	0	0	0	0	0
F152	0	0	0	0	0	0	0	0
F153	0	0	0	0	0	0	0	0
F154	0	0	0	0	0	0	0	0
F155	0	0	0	0	0	0	0	0
F156	0	0	0	0	0	0	0	0
F157	0	0	0	0	0	0	0	0
F158	0	0	0	0	0	0	0	0
F159	0	0	0	0	0	0	0	0
F160	0	0	0	0	0	0	0	0
F161	0	0	0	0	0	0	0	0
F162	0	0	0	0	0	0	0	0
F163	0	0	0	0	0	0	0	0
F164	0	0	0	0	0	0	0	0
F165	0	0	0	0	0	0	0	0
F166	0	0	0	0	0	0	0	0
F167	0	0	0	0	0	0	0	0
F168	0	0	0	0	0	0	0	0
F169	0	0	0	0	0	0	0	0
F170	0	0	0	0	0	0	0	0
F171	0	0	0	0	0	0	0	0
F172	0	0	0	0	0	0	0	0
F173	0	0	0	0	0	0	0	0
F174	0	0	0	0	0	0	0	0
F175	0	0	0	0	0	0	0	0
F176	0	0	0	0	0	0	0	0
F177	0	0	0	0	0	0	0	0
F178	0	0	0	0	0	0	0	0
F179	0	0	0	0	0	0	0	0
F180	0	0	0	0	0	0	0	0
F181	0	0	0	0	0	0	0	0
F182	0	0	0	0	0	0	0	0
F183	0	0	0	0	0	0	0	0
F184	0	0	0	0	0	0	0	0
F185	0	0	0	0	0	0	0	0
F186	0	0	0	0	0	0	0	0
F187	0	0	0	0	0	0	0	0
F188	0	0	0	0	0	0	0	0
F189	0	0	0	0	0	0	0	0
F190	0	0	0	0	0	0	0	0
F191	0	0	0	0	0	0	0	0
F192	0	0	0	0	0	0	0	0
F193	0	0	0	0	0	0	0	0
F194	0	0	0	0	0	0	0	0
F195	0	0	0	0	0	0	0	0
F196	0	0	0	0	0	0	0	0
F197	0	0	0	0	0	0	0	0
F198	0	0	0	0	0	0	0	0
F199	0	0	0	0	0	0	0	0
F200	0	0	0	0	0	0	0	0

REPORT ACTIVITY MONTHLY COUNTRY NOVEMBER 1975

TOTAL	PERSONAL OPERATIONS		DEVIATIONS		TOTAL	TOTAL	TOTAL	TOTAL	TOTAL
	F5	T38	F5	T38					
602	0	225	0	140	0	365	0	0	0
171	0	0	0	0	0	0	0	0	0
101	0	63	0	0	0	0	0	0	0
21	0	79	0	17	0	0	0	0	0
0	0	0	0	0	0	0	0	0	0
TOTAL	603	2731	2345	611	2730	2002	0	3059	1995

TOTAL	PERSONAL OPERATIONS		DEVIATIONS		TOTAL	TOTAL	TOTAL	TOTAL	TOTAL
	F5	T38	F5	T38					
0	0	0	0	0	0	0	0	0	0
0	0	0	0	0	0	0	0	0	0
0	0	0	0	0	0	0	0	0	0
0	0	0	0	0	0	0	0	0	0
0	0	0	0	0	0	0	0	0	0
TOTAL	0	0	169	15	0	0	0	100	15

REPORT TYPES USING WFO T38 F5 T38 T38 T38 T38 T38 T38 T38 T38

----- AIRCRAFT ACTIVITY MONTHLY SUMMARY ----- SEPTEMBER 1976

AIRCRAFT TYPE	OPERATIONS				MILES				TOTAL	TOTAL	TOTAL	TOTAL	TOTAL
	FLY	LAND	TOTAL	PERCENT	FLY	LAND	TOTAL	PERCENT					
500	100	100	200	100	100	100	200	100	100	100	100	100	100
502	150	150	300	150	150	150	300	150	150	150	150	150	150
504	0	0	0	0	0	0	0	0	0	0	0	0	0
506	0	0	0	0	0	0	0	0	0	0	0	0	0
508	0	0	0	0	0	0	0	0	0	0	0	0	0
510	0	0	0	0	0	0	0	0	0	0	0	0	0
512	0	0	0	0	0	0	0	0	0	0	0	0	0
TOTAL	534	527	1452	503	1475	1478	0	1478	3035	0	0	0	23

AIRCRAFT TYPE	OPERATIONS				MILES				TOTAL	TOTAL	TOTAL	TOTAL	TOTAL
	FLY	LAND	TOTAL	PERCENT	FLY	LAND	TOTAL	PERCENT					
500	100	100	200	100	100	100	200	100	100	100	100	100	100
502	150	150	300	150	150	150	300	150	150	150	150	150	150
504	0	0	0	0	0	0	0	0	0	0	0	0	0
506	0	0	0	0	0	0	0	0	0	0	0	0	0
508	0	0	0	0	0	0	0	0	0	0	0	0	0
510	0	0	0	0	0	0	0	0	0	0	0	0	0
512	0	0	0	0	0	0	0	0	0	0	0	0	0
TOTAL	534	527	1452	503	1475	1478	0	1478	3035	0	0	0	23

AIRCRAFT TYPE	OPERATIONS				MILES				TOTAL	TOTAL	TOTAL	TOTAL	TOTAL
	FLY	LAND	TOTAL	PERCENT	FLY	LAND	TOTAL	PERCENT					
500	100	100	200	100	100	100	200	100	100	100	100	100	100
502	150	150	300	150	150	150	300	150	150	150	150	150	150
504	0	0	0	0	0	0	0	0	0	0	0	0	0
506	0	0	0	0	0	0	0	0	0	0	0	0	0
508	0	0	0	0	0	0	0	0	0	0	0	0	0
510	0	0	0	0	0	0	0	0	0	0	0	0	0
512	0	0	0	0	0	0	0	0	0	0	0	0	0
TOTAL	534	527	1452	503	1475	1478	0	1478	3035	0	0	0	23

AIRCRAFT TYPE	OPERATIONS				MILES				TOTAL	TOTAL	TOTAL	TOTAL	TOTAL
	FLY	LAND	TOTAL	PERCENT	FLY	LAND	TOTAL	PERCENT					
500	100	100	200	100	100	100	200	100	100	100	100	100	100
502	150	150	300	150	150	150	300	150	150	150	150	150	150
504	0	0	0	0	0	0	0	0	0	0	0	0	0
506	0	0	0	0	0	0	0	0	0	0	0	0	0
508	0	0	0	0	0	0	0	0	0	0	0	0	0
510	0	0	0	0	0	0	0	0	0	0	0	0	0
512	0	0	0	0	0	0	0	0	0	0	0	0	0
TOTAL	534	527	1452	503	1475	1478	0	1478	3035	0	0	0	23

ALPCRAFT ACTIVITY MONTHLY SUMMARY JANUARY 1977

	---NORMAL OPERATIONS---			---DEVIATIONS---			---ARRIS---			FULL TRAFFIC -COUNT-
	TAKEOFF	LANDING	GROUND TIME(MIN)	TAKEOFF	T38	T33	F5	T37	T33	
30L	0	0	0	0	0	0	0	0	0	0
30C	0	0	0	0	0	0	0	0	0	0
30D	654	0	2394	0	475	0	0	0	0	11771
30E	0	0	0	0	1879	0	0	0	0	7076
30F	0	0	0	0	0	0	0	0	0	15215
30G	0	25	0	0	0	0	0	0	0	100
30H	37	0	30	0	6	0	0	0	0	55
30I	0	0	0	0	24	0	0	0	0	144
TOTAL	691	2374	2424	677	2351	2424	0	715	3177	0

	---TRANSIENT OPERATIONS---			---TRANSIENT OPERATIONS---			---TOUCH-AND-GO---		
	INBOUND	OUTBOUND	TOUCH-AND-GO	INBOUND	OUTBOUND	TOUCH-AND-GO	INBOUND	OUTBOUND	TOUCH-AND-GO
30L	0	0	0	0	0	0	0	0	0
30C	0	0	0	0	0	0	0	0	0
30D	0	0	0	0	0	0	0	0	0
30E	0	0	0	0	0	0	0	0	0
30F	0	0	0	0	0	0	0	0	0
30G	0	0	0	0	0	0	0	0	0
30H	0	0	0	0	0	0	0	0	0
30I	0	0	0	0	0	0	0	0	0
TOTAL	0	0	0	0	0	0	0	0	0

ALPCRAFT TYPES USING RWYS F5 T33 T37 T38 T39 T40 T41 T42 T43 T44

AIRCRAFT ACTIVITY MONTHLY SUMMARY FEBRUARY 1977

	AIRCRAFT OPERATIONS		OPERATIONS		OPERATIONS		OPERATIONS		OPERATIONS		OPERATIONS		OPERATIONS		OPERATIONS		OPERATIONS	
	F5	T37	F5	T37	F5	T37	F5	T37	F5	T37	F5	T37	F5	T37	F5	T37	F5	T37
301	0	0	0	0	0	0	0	0	0	0	0	0	0	0	0	0	0	0
302	0	0	0	0	0	0	0	0	0	0	0	0	0	0	0	0	0	0
303	0	0	0	0	0	0	0	0	0	0	0	0	0	0	0	0	0	0
304	0	0	0	0	0	0	0	0	0	0	0	0	0	0	0	0	0	0
305	0	0	0	0	0	0	0	0	0	0	0	0	0	0	0	0	0	0
306	0	0	0	0	0	0	0	0	0	0	0	0	0	0	0	0	0	0
307	0	0	0	0	0	0	0	0	0	0	0	0	0	0	0	0	0	0
TOTAL	321	908	1314	300	260	1252	0	167	534	0	3165	10050	0	2	16			

	AIRCRAFT OPERATIONS		OPERATIONS															
	F5	T37	F5	T37	F5	T37	F5	T37	F5	T37	F5	T37	F5	T37	F5	T37	F5	T37
301	0	0	0	0	0	0	0	0	0	0	0	0	0	0	0	0	0	0
302	0	0	0	0	0	0	0	0	0	0	0	0	0	0	0	0	0	0
303	0	0	0	0	0	0	0	0	0	0	0	0	0	0	0	0	0	0
304	0	0	0	0	0	0	0	0	0	0	0	0	0	0	0	0	0	0
305	0	0	0	0	0	0	0	0	0	0	0	0	0	0	0	0	0	0
306	0	0	0	0	0	0	0	0	0	0	0	0	0	0	0	0	0	0
307	0	0	0	0	0	0	0	0	0	0	0	0	0	0	0	0	0	0
TOTAL	8	20	115	95	6	2	40	7	20	101	30	6	3	40	100	200	0	0

	AIRCRAFT OPERATIONS		OPERATIONS															
	F5	T37	F5	T37	F5	T37	F5	T37	F5	T37	F5	T37	F5	T37	F5	T37	F5	T37
301	0	0	0	0	0	0	0	0	0	0	0	0	0	0	0	0	0	0
302	0	0	0	0	0	0	0	0	0	0	0	0	0	0	0	0	0	0
303	0	0	0	0	0	0	0	0	0	0	0	0	0	0	0	0	0	0
304	0	0	0	0	0	0	0	0	0	0	0	0	0	0	0	0	0	0
305	0	0	0	0	0	0	0	0	0	0	0	0	0	0	0	0	0	0
306	0	0	0	0	0	0	0	0	0	0	0	0	0	0	0	0	0	0
307	0	0	0	0	0	0	0	0	0	0	0	0	0	0	0	0	0	0
TOTAL	0	0	0	0	0	0	0	0	0	0	0	0	0	0	0	0	0	0

AIRCRAFT ACTIVITY MONTHLY SUMMARY MAY 1977

	NORMAL OPERATIONS				DEVIATIONS				TRAFFIC				TOTAL
	F5	T37	T38	T39	F5	T37	T38	T39	F5	T37	T38	T39	
TOL	0	1792	0	0	0	143	0	0	0	0	1	0	8764
SLC	617	0	2910	0	0	585	0	12891	0	0	0	17	9333
SLB	0	0	0	0	0	0	0	0	0	0	0	0	19000
SLC	0	0	0	0	0	0	0	0	0	0	0	0	0
SLB	0	0	0	0	0	0	0	0	0	0	0	0	0
TOTAL	617	1792	2910	589	140	585	0	2074	12891	0	1	17	

	TRANSIENT OPERATIONS				OUTBOUND				TOUCH-AND-GO			
	F5	T37	T38	T39	F5	T37	T38	T39	F5	T37	T38	T39
SLC	0	59	0	0	0	0	0	0	0	0	0	0
SLB	21	0	200	65	0	199	0	0	0	0	0	0
SLC	0	0	0	0	0	0	0	0	0	0	0	0
SLB	0	0	0	0	0	0	0	0	0	0	0	0
TOL	1	0	0	0	0	0	0	0	0	0	0	0
SLB	0	0	0	0	0	0	0	0	0	0	0	0
TOTAL	22	59	202	65	0	199	0	0	0	0	0	0

AIRCRAFT TYPES USING WAFB	TRANSIENT OPERATIONS				OUTBOUND				TOUCH-AND-GO			
	F5	T37	T38	T39	F5	T37	T38	T39	F5	T37	T38	T39
SLC	0	59	0	0	0	0	0	0	0	0	0	0
SLB	21	0	200	65	0	199	0	0	0	0	0	0
SLC	0	0	0	0	0	0	0	0	0	0	0	0
SLB	0	0	0	0	0	0	0	0	0	0	0	0
TOL	1	0	0	0	0	0	0	0	0	0	0	0
SLB	0	0	0	0	0	0	0	0	0	0	0	0
TOTAL	22	59	202	65	0	199	0	0	0	0	0	0

APPENDIX E

ESSAY: VERIFICATION OF SHORT-TERM AIR QUALITY MODELS USING THE GAUSSIAN DISPERSION APPROACH

by Karl Zeller, EPA*

(January 1977)

1. INTRODUCTION

A need exists to define an acceptable approach for the verification of short-term Gaussian air quality simulation models for single and multiple source complexes. The demand for answers to air quality questions is so strong that some models have been formulated and applied extensively prior to proper evaluation. It is hoped that proposed models would be subjected to a verification procedure to enable the model developer either to defend a particular use of his model or to indicate possible situations in which his model produces invalid or questionable results.

Each complex Gaussian air quality model is comprised of submodels to describe source emissions, pollutant dispersion and transport, plume rise, source-receptor geometry, and meteorology. In the modeling of complex geometric situations, it is currently necessary to use empirical dispersion parameter values (standard deviations of plume spread as a function of down-wind distance or time and atmospheric stability) derived from continuous point sources. Sometimes these values are applied with subjective modifications. For example, models used for airports or highways use the same dispersion parameters as models used for elevated area or point sources.

One logical approach would involve the separate verification of each of the submodels based on specific experiments; however, expenses involved usually dictate that accuracy of the overall model be examined.

There are many opinions as to how a Gaussian model that uses subjective modifications to handle the various configurations encountered should be validated, verified, or calibrated. In this discussion, a specific approach for Gaussian models is suggested. The data requirements for model verification include meteorology and emission data (the necessary information for model concentration calculations), and measured air quality concentrations (including background information) with which to compare the calculations.

Previous verification programs comparing short-term (1-3 hours) calculations (Koch 1971; Rote, et al., 1973) with observations have demonstrated the difficulty in coming to specific conclusions using any one comparison technique or statistic. The scatter diagram approach prevalent in the literature has not been particularly useful for verification because of wide scatter and low correlation between measured and calculated concentrations. The reason direct comparison of calculations to observations does not provide good results is the statistical nature of the complex Gaussian model. For instance, the Gaussian approach assumes steady-state conditions over a specific period of time, usually one hour. In reality a continuous point

*Present address: Environmental Research and Technology, Inc.,
Fort Collins, CO

source plume is subjected to many variations of wind velocity during any given hour. When modeling intermittent or moving sources such as automobiles or aircraft, simplifying assumptions are necessarily made; for instance, taxiing aircraft are usually modeled as line sources considered to be continuous over periods relatively long compared to individual aircraft taxi time. In reality, there is not a continuous Gaussian plume stretched out downwind of such sources but intermittent ones which are locally distorted by variable wind speed and direction (turbulence). Data collection for such comparisons is presently accomplished by a network of monitors at fixed horizontal and vertical locations. The total number of monitors or stations in most studies is usually less than five due to monetary restraints. Considering these limitations, it is not surprising that short-term calculations and observations do not correlate well. The comparison of cumulative frequency distributions on the other hand has enabled some modelers to make general statements about the overall performance of their specific models.

2. RECOMMENDED VERIFICATION APPROACH

It is assumed that a large data base is taken over a period long enough (at least one year) to provide information under the varying conditions of meteorology and emission modes. Assuming such a data base is available, the following procedures for model verification are proposed.

a. Discussion of Data Base

A discussion of the data base should include efforts made to provide background information and quality assurance during the actual collection of data. A discussion of the adequacy of the numbers and locations of actual air quality monitoring sites should be included, together with specific geometry relating sources and receptors to the general meteorological conditions during the data collection period.

b. Comparisons for Analysis

A thorough verification requires that data and concentration calculations (model predictions) be compared under a number of different circumstances. Because of the conglomerate nature of the complex Gaussian model, certain meteorological conditions or receptor locations may give better or worse results compared to others in the same model application. Each monitoring location should therefore be evaluated separately in addition to overall evaluation of the model. Evaluating each monitoring location separately will give the modeler an indication of the performance of the dispersion submodel under different situations. This is important because at the present time the dispersion submodels of most Gaussian complex models have been altered and are subjective in nature and not based on applicable dispersion experiments. There is reason to believe that a great deal of the wide scatter in observed and predicted values already discussed is due to the dispersion submodel as well as faulty emission estimates. The pollution data should be stratified in at least the following categories:

- (1) High and low emission density periods.
- (2) Periods of the day (can include more than one hour) dependent upon emission operations and meteorology.
- (3) Seasons (this category is optional - depends on the nature of the data and problems).
- (4) Meteorological categories:
 - wind direction - increments depend on situation.
 - wind speed - increments depend on situation.
 - stability category - Pasquill categories or in some cases stable, neutral, and unstable will be sufficient.
 - mixing height - two or three categories based on a chosen mixing height dependent upon the scale of the model application. For instance, in the case of airport models: mixing height below 100 m; mixing height above 100 m; and unlimited mixing.

Note that the above categories are not meant to be mutually exclusive. Also, only data that are above the noise level of the particular pollutant-monitoring instruments used should be evaluated. Although there is a specific interest in pollutant levels approaching National Ambient Air Quality Standards, all levels should be evaluated.

c. Cumulative Frequency Distributions and Error Limits

The data should first be sorted according to the above scheme; for instance, all cases in a specific wind direction category, all cases during the morning hours, etc. (approximately 26 separate categories). The data should then be displayed on cumulative frequency distribution diagrams, similar to the one in Fig. E-1, if at least 30 observations within a given category are available. If there are less than 30 observations, a scatter diagram of observed versus calculated concentrations should be prepared. Longer term averages, for instance, monthly or yearly, will inherently have fewer data points for comparisons and therefore will require the scatter diagram approach for verification. The use of the scatter diagram will give a qualitative feel for the performance of the model even though in some cases resultant coefficients for calibration purposes may be lacking in significance.

It is desirable to have a number measure of model performance for specific cases. A cumulative frequency distribution of the calculation error should be constructed to allow the modeler to report the percentage of trials for which his estimate was within a specific range of the observation. A similar approach was used by Koch and Thayer (1971); frequency distribution plots of absolute value of overpredictions and underpredictions similar to

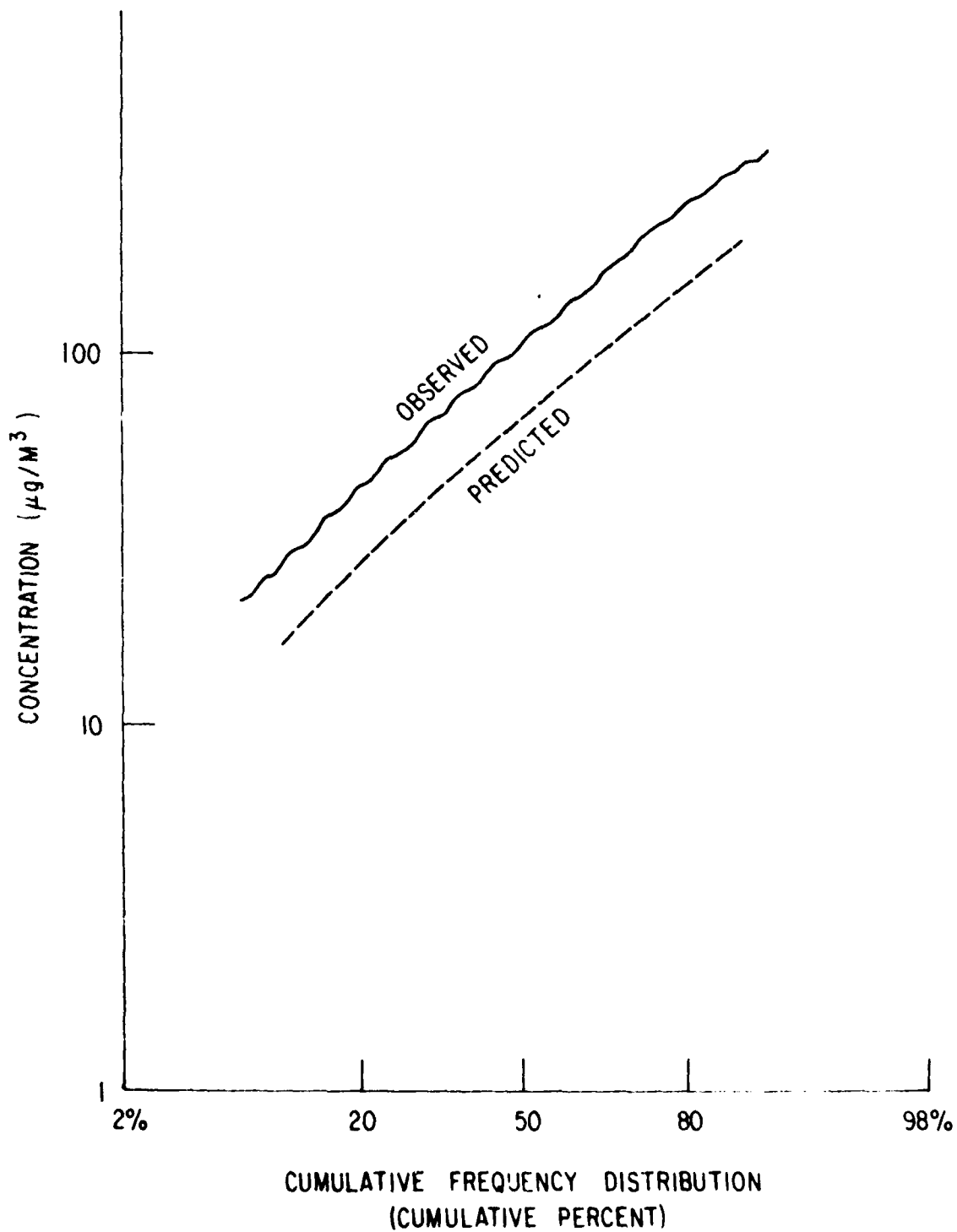


Fig. E-1. Cumulative Frequency Distribution for Site #X during Periods of E Wind Direction.

those in Fig. E-2 should be prepared. The approach suggested in this discussion is to subtract each observation from each corresponding model prediction. This will provide information on the distribution of overpredictions and underpredictions in addition to the overall tendency of the model to over- or under-predict in that specific category. Subtracting the cumulative percentage of overpredictions from the cumulative percentage of underprediction (see Fig. E-2) at a specific concentration difference will give the percent of comparisons that fall within that specific concentration error limit. The error limits and corresponding percentages can then be plotted on a frequency distribution diagram similar to Fig. E-3. The modeler will then be able to report that in the given situation his predictions were within x ($\mu\text{g}/\text{m}^3$) y percent of the time for that particular data category using the verification data set. It must be recognized that the percentage of error is not displayed in the above technique; i.e., the number difference between a predicted value of 2 and measured value of 4 is the same as between that of 100 and 102 but the percent error is quite different.

d. Percent Error Distribution

In order to evaluate the percentage error and make the verification results usable for all ranges of concentrations, the following procedure should be followed:

Using the same categories previously discussed, prepare frequency diagrams of the percent error, E_i , as shown in Fig. E-4:

$$E_i = \frac{x_c - (\bar{x}_o - \bar{x}_b)}{(\bar{x}_o - \bar{x}_b)} * 100,$$

where:

- E_i = percent error per case,
- \bar{x}_c = model calculation without background,
- \bar{x}_o = observed air quality, and
- \bar{x}_b = estimate of background air quality.

The display of Fig. E-4 will also enable the model evaluator to discuss model bias, \bar{E} , randomness, σ_E^2 , and overall variance, σ_T^2 , for each category:

where:

$$\bar{E} = \frac{1}{n} \sum_{i=1}^n E_i \text{ (bias),}$$

$$\sigma_E^2 = \frac{1}{n} \sum_{i=1}^n (E_i - \bar{E})^2 \text{ represents the randomness, and}$$

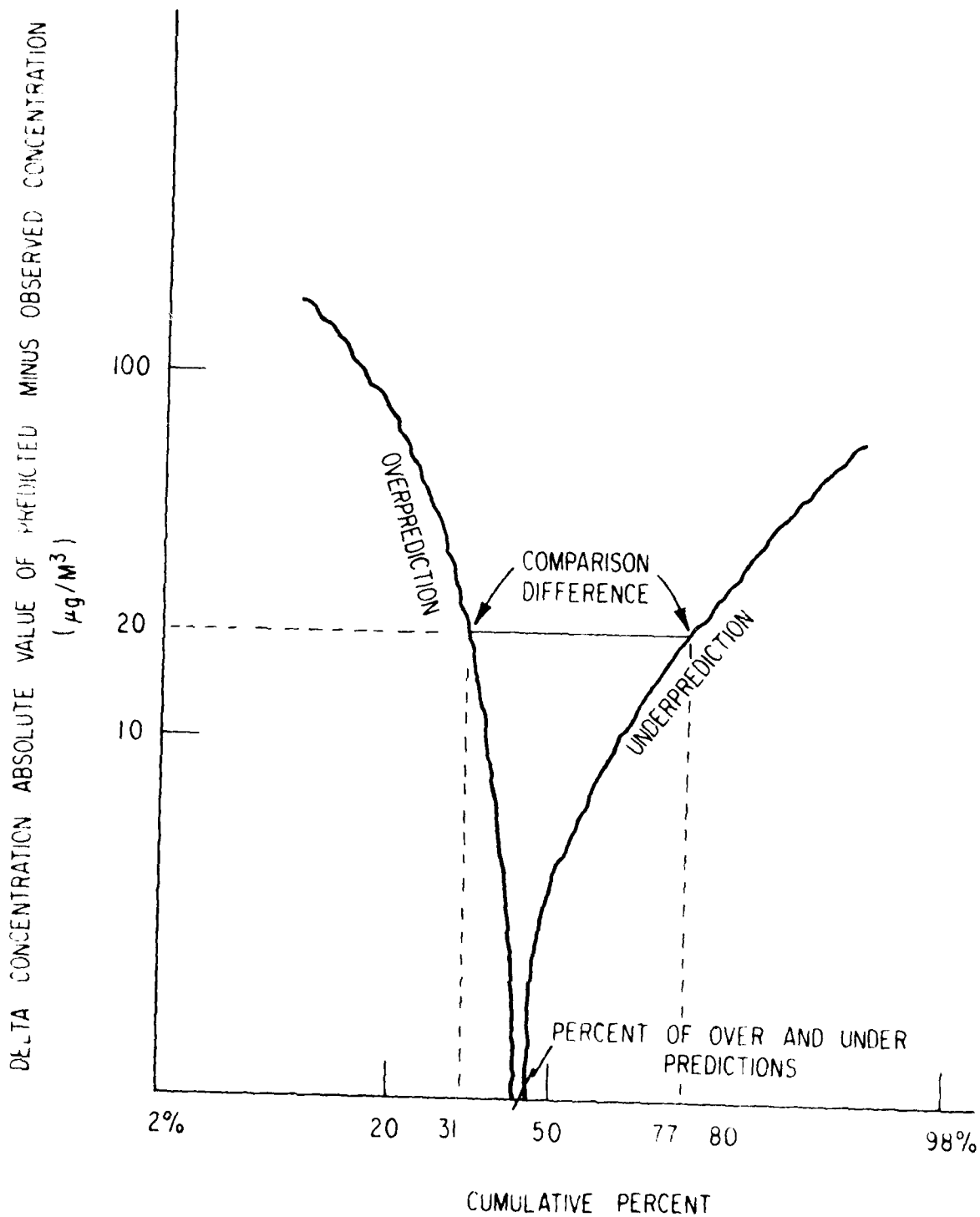


Fig. E-2. Delta Concentration: In This Example, 77-31, or 46 Percent of the Time, the Difference between Observed and Predicted was within $\pm 20 \mu\text{g}/\text{m}^3$

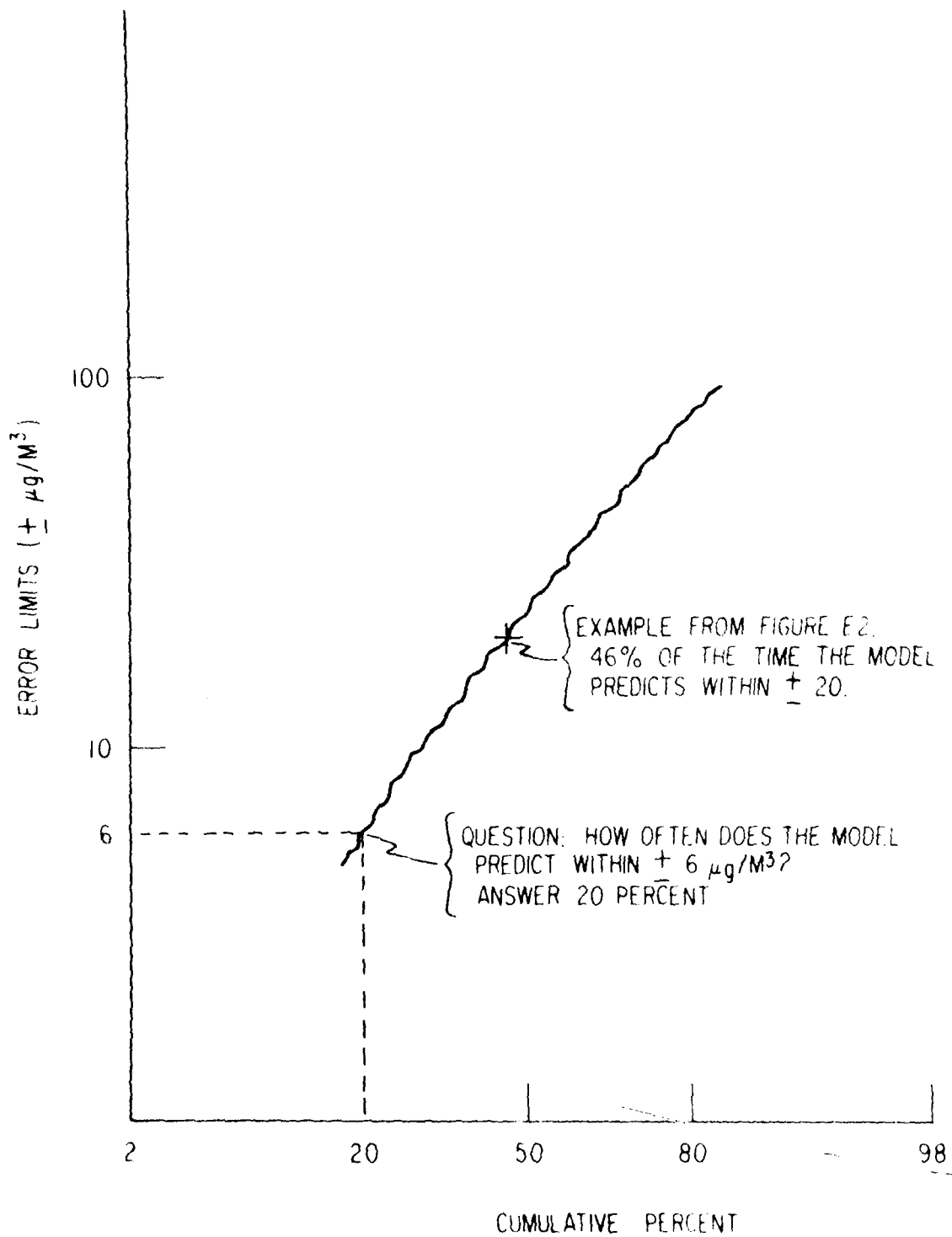


Fig. E-3. Error Limit Diagram

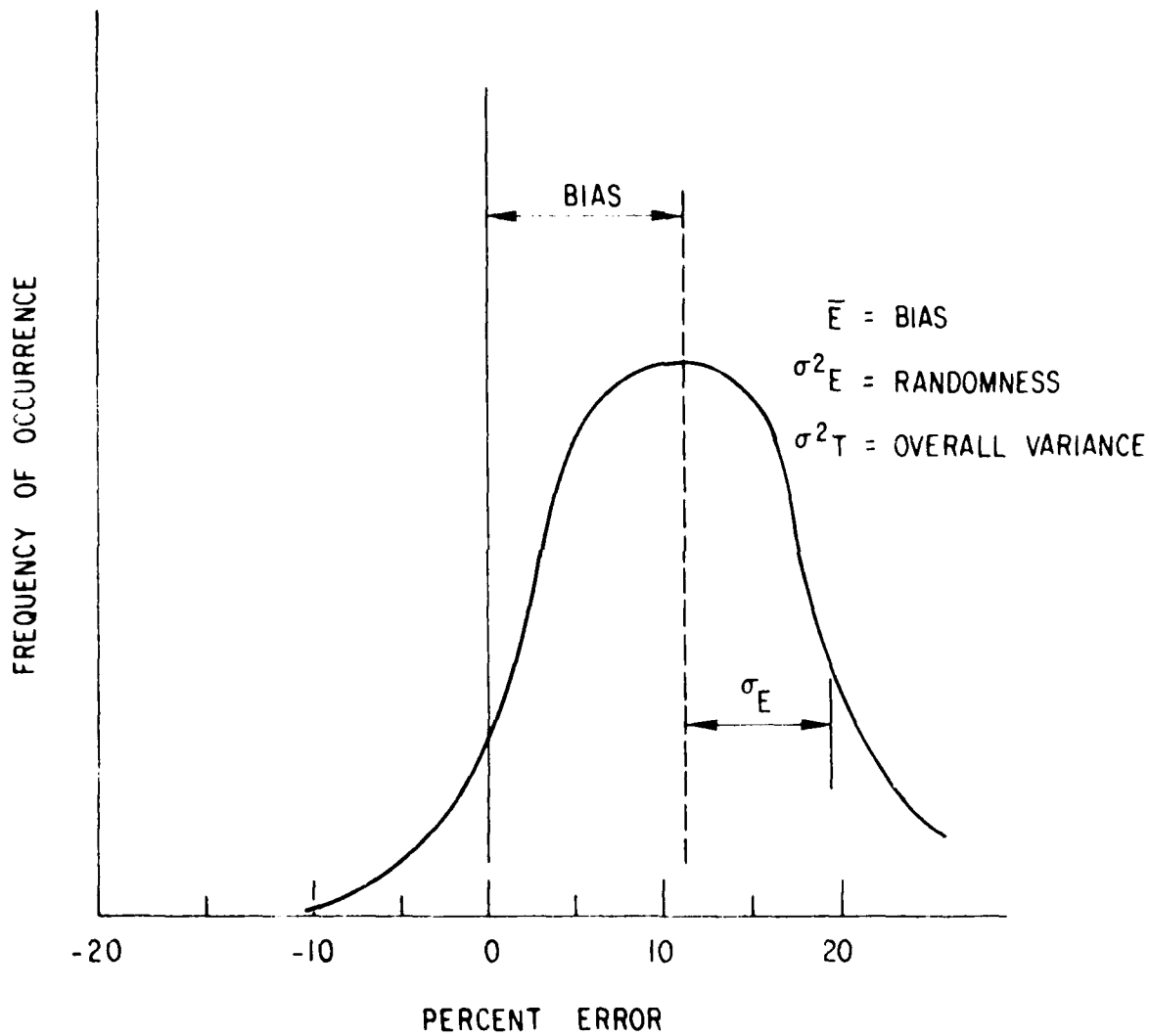


Fig. E-4. Percent Error Distribution

$$\sigma_T^2 = \frac{1}{n} \sum_{i=1}^n E_i^2 \text{ the overall variance.}$$

This information could also be displayed on a percent error -- cumulative frequency diagram similar to Fig. E-5. In this diagram the slope, curvature, and position from 50 percent frequency of the line would indicate randomness, normality, and bias, respectively.

In Fig. E-5 a horizontal line through zero percent error represents a perfect model. A very good model with no bias, allowing for the random nature of the model input parameters would possibly look like the distribution represented by the dashed line. An example application of this diagram would be as follows: suppose the modeler was trying to substantiate a specific model calculation of 8. He could say that in the category represented by Fig. E-5, solid line, 95 percent of the time his model has an error of 20 percent or less. Therefore, only in one out of twenty cases when 8 is predicted (by the model) will the actual value χ_0 be 10 (i.e. $-2=(8-\chi_0)/\chi_0$) or greater, or there is a 95% confidence in the value being 10 or less.

e. Emission Sub-model Adjustment

Because each of the inputs to the model have uncertainties expressed as a standard deviation (σ), the model output cannot be expected to match perfectly with the measured concentrations. However, if the actual variations of the input parameters are independent of each other, and the input parameters are the true mean values of their distributions, then the percentage error assuming $\chi_b = 0$, $E = (\chi_c \text{ model} - \chi_0 \text{ observation})$, should be normally distributed with mean zero and a total standard deviation, σ_T . If the mean \bar{E} is significantly different from zero, as determined by a statistical test, then the question, What is causing the error? should be asked. Assuming that adequate quality assurance is maintained for the measured pollution concentration and meteorological data, the largest uncertainties will probably be either in the emission inventory or within the model itself.

Although in theory, the measured product of the concentration, χ_0 , observation and the wind velocity, \bar{u} , is a flux (mass/area-time) and can be used with a model to compute the emissions Q (gm/sec), this inverse of the standard modeling technique is not practical. A possible technique to test the emission inventory would be to break the data sets into two significantly different meteorological conditions such as stable and unstable. If the emission inventory is in error and the model is consistent, \bar{E} should show similar bias from zero for both periods.

If the \bar{E} values are significantly different for both conditions the emission inventory and the model may both be in error.

Such an analysis can be used to justify modifying the emission inventory Q to set \bar{E} to zero for both data sets as a whole. If this adjustment of Q is valid, then a third data set, independent of the two used as above, can be used to determine \bar{E} . If \bar{E} is not significantly different from zero for this new data set, then the adjusted Q values would appear to be the valid ones to use for further study of the model.

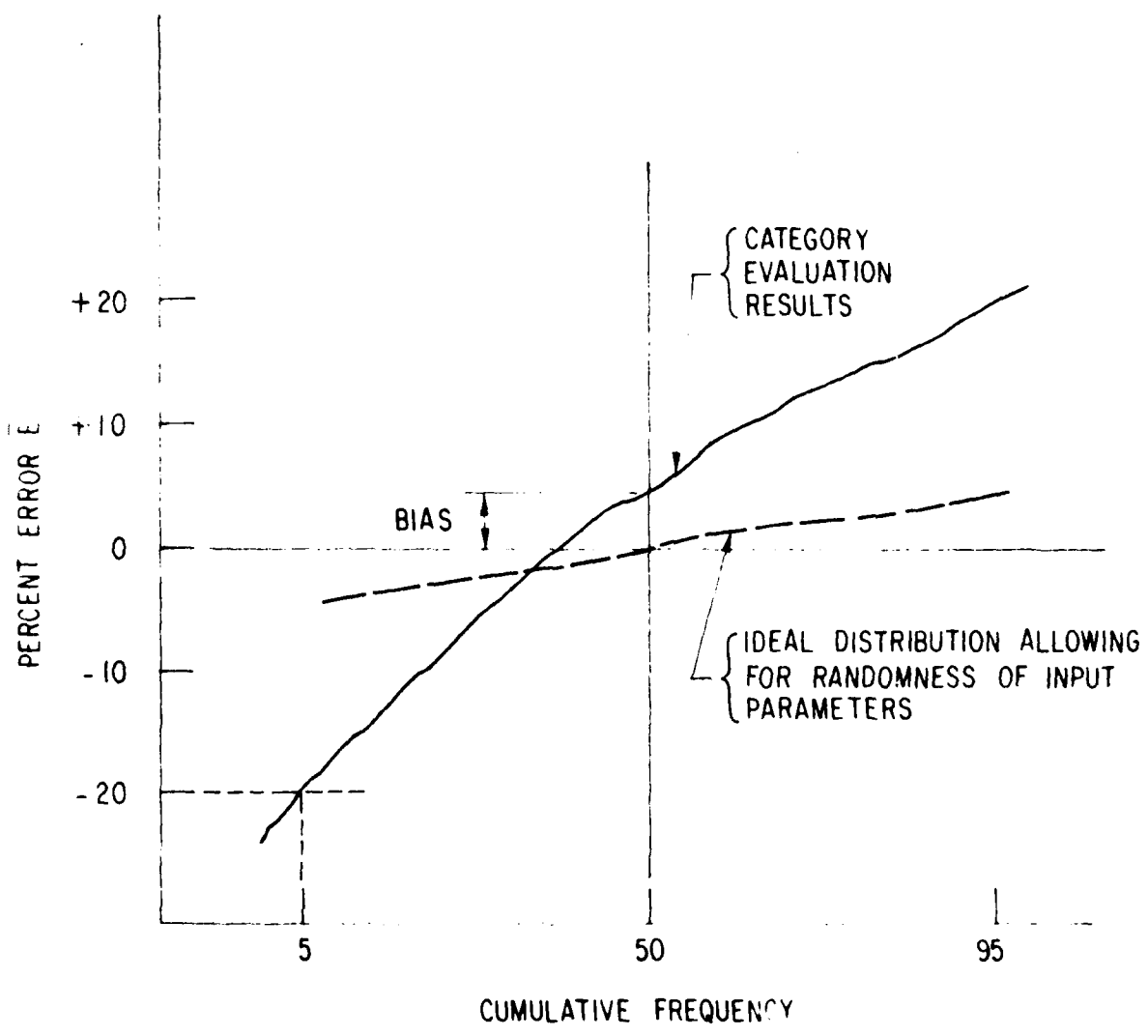


Fig. E-5. Percent Error - Cumulative Frequency Diagram

1. Model Verification Discussion

A subjective discussion should accompany each comparison, pointing out various aspects specific to the model and data base being used. The discussion will depend upon the interpretation of the investigator. Next, the data should be multistratified using the above single categories; for instance, one stratum may be all cases during winter morning periods with wind flow from a northerly direction, atmospheric conditions stable, and low wind speeds. In this case the categories would be mutually exclusive. This data comparison should also be presented in both frequency distribution and scatter diagrams of observed versus predicted if there are more than 30 examples; and scatter diagrams, only, if there are less than 30 examples. Each distribution and/or scatter diagram should be evaluated and subjectively discussed.

It is recognized that there is a great expense involved in extensive model calculations to fulfill the above requirements. Perhaps, in practice, models can be evaluated generally in the broad single category groups using a subset of the total data set to evaluate cumulative frequency distributions. A few of the multistratified categories should then be selected for specific model performance, preferably those with the most data. When the model is then used in a specific application and that application is in question and not previously verified, the data base would be reevaluated for the specific situation in question.

3. CONCLUSIONS

Upon completion of the above analysis, assuming a good air quality data base, the modeler would have a good idea of how valid his model really is. In addition, an independent model user or Environmental Impact Statement (EIS) reviewer, would be able to scan the verification report and obtain a quick feel of how the model performs compared to a real data set.

The recommended verification procedure discussed above does not require specific model correlation coefficients or any other number on which to determine a pass/fail grade for the model.

The final decision, therefore, as to whether the model is valid, will not depend upon any specific performance limitation; it will depend upon the user's ability to support the use of the model in any instance, based on the verification analysis.

ACKNOWLEDGMENT

Thanks are due Dr. David Mage, EPA, Research Triangle Park, N.C., for helpful suggestions used in the preparation of this discussion.

REFERENCES

Koch, Robert C., and Scott D. Thayer, *Validation and Sensitivity Analysis of the Gaussian Plume Multiple-Source Urban Diffusion Model*, Geomet Rep. No. EF-60 NTIS No. PB-206-951, EPA No. APTD-0935 (1971).

Rote, D.M., I.T. Wang, L.E. Wangen, R.W. Hecht, R.R. Cirillo, and J. Pratapas, *Airport Vicinity Air Pollution Study*, Argonne National Laboratory Report to Federal Aviation Administration, Report No. FAA-RD-73-113 (Dec. 1973).

APPENDIX F
STATISTICAL ANALYSIS OF AIR POLLUTION DATA
AND THE VALIDATION OF THE AQAM

1. INTRODUCTION

This section first discusses several past airport air pollution programs and previous attempts to validate air pollution models. Statistical methods for testing several hypotheses related to both the analysis of air pollution measurements and the problem of model validation are proposed. Included in the discussion are descriptive statistics and distributional considerations, time series analysis, and multiple linear regression analysis, all of which are proposed in the diagnostic investigation and analysis of observed and predicted air pollution concentrations for use in defining the limits of accuracy of the AQAM. Emphasis has been placed on the details of general interest and justification of these techniques rather than on the presentation of the rigorous mathematical formalism behind each one. The essential mathematical details and computational methods employed in these techniques are both lengthy and quite complicated, and should be described subsequent to their implementation in another report by Argonne National Laboratory. For the present, however, the reader should consult references to the literature that are provided for specific mathematical details of the techniques described here.

2. PAST AIRPORT AIR POLLUTION AND MODEL VALIDATION PROGRAMS

Past airport air quality monitoring studies including Thayer,^{F-1} Platt,^{F-2} Rote,^{F-3} and MacWalters et al.^{F-4} have failed to observe concentrations of air pollutants significantly above local background. In order to understand the complexity of validating or verifying or defining the limits of accuracy of airport air pollution models, one must appreciate the difficulties involved in monitoring ambient air quality levels at airports and in attempting to relate them to aircraft activity. An investigation of recent airport air pollution monitoring programs was therefore performed.

In the final report to the EPA-NERC,* "Air Quality Measured at Atlanta International Airport before and during Experimental Aircraft Taxiing Operations," MacWalters et al.^{F-4} have concluded that:

it is not possible to detect statistically significant reduction in air quality levels which could be attributed to the emissions control procedures... and the analysis of air quality measurements failed to show a statistically significant improvement as a result of the application of aircraft emissions control procedures... In view of the limited application of emissions controls and the resultant small change in emissions during any given hour, a substantially longer sampling period would be required to detect a statistically significant effect.

*Environmental Protection Agency, National Environmental Research Center, Las Vegas, Nevada

Plume rise effect and masking of aircraft aerometric signals by background were advanced as possible explanations for the results of the Atlanta study.

One of the earliest attempts to study the sensitivity and accuracy of an air quality computer model for airports was performed by Platt et al.^{F-2} on a model called "AIREC." Meteorological parameters were subjected to a sensitivity analysis using the average and maximum value (the maximum obtained as the average of the three highest values) as the two levels for each factor being considered. The resulting changes in the calculated concentrations were then evaluated as a percentage of the data values:

The results of the sensitivity analysis for the meteorological parameters have a direct bearing on the selection of short-term periods used to calculate maxima concentrations in the impact analysis. Hence, time periods that exhibit low wind speeds, stable atmospheric conditions, and high wind persistence in the prevailing direction should be selected.

The accuracy of the model was investigated indirectly in the analysis of various control techniques. Source parameters including strength and location of emissions sources with respect to a receptor were studied. These investigations reinforced the following limitations to the validity of the model:

- (1) the model is limited to time periods that are much longer than the characteristic times of individual aircraft activity; and
- (2) the model is limited to receptors that are not in proximity to the emission sources (closer than 100 meters).

Such limitations of spatial and temporal resolution of any air quality computer model need to be established in defining the accuracy of the model.

Under EPA contract, GEOMET has completed a program of air quality measurement, model development, and model validation at Washington National Airport.

Statistical analysis techniques for model validation of the NREC and modified NREC models^{F-5} are developed in the Geomet Task I Program Plan *Model Verification -- Aircraft Emissions Impact on Air Quality*. The validation of the model involves:

- (1) Comparison of versions of the NREC model -- performed by comparing frequency distributions for observations and predictions for specified pollutant-location-averaging time combinations. Other methods for analyzing the error of the predictions, such as the Wilcoxon test or the t-test for paired comparisons are suggested, based on an examination of the data.
- (2) In comparing predicted and observed annual means, the bias of predictions are proposed to be tested using the

binomial test to determine if there is a significant deviation from the expected value.

- (3) Comparison of the number of times the predicted and observed values exceed air quality standards. This required fitting lognormal distributions to the available values of predicted and observed data, and comparing these to the standard in order to calculate the number of times during the year that the standard is exceeded for each distribution.
- (4) Determination of the conditions under which the NREC model operated best and worst by stratification of the data into subsets of specific meteorological and/or emissions conditions and using the Kolomogorov-Smirnov test (referenced below) to compare frequency distributions of observed and predicted concentrations.

In the NREC and the modified NREL (GEOMET) model ...

The steady-state Gaussian plume model, which is the kernel of the concentration calculation and assumes steady conditions during the period of calculation (in this case one hour), is characteristically not expected to give good results when compared to observations on a paired-comparisons, hour-by-hour basis. Such a model, when performing well, will reproduce distributions and means to a reasonable degree, and this will be highly useful for most purposes, including those of making comparisons with standards, and studying the impact of various types of contributing sources ...

Several measures (descriptive statistics) and statistical tests, including the t-test for paired means (Graybill;^{F-6} Brownlee,^{F-7} simple linear regression (Rao),^{F-8} the Spearman rank correlation coefficient and matched pair sign rank test (Kendall),^{F-9} and the Kolomogorov-Smirnov goodness of fit test (Kolomogorov),^{F-10-12} were discussed. These techniques were proposed for the statistical treatment of the data, but are not related to the testing of specific hypotheses concerning the model validation. The discussion of each technique includes the statement of the null hypothesis and abbreviated discussion of the underlying assumptions and methodology, along with the format of the printout for each test. While it is recognized that such techniques are the subject of numerous textbooks on statistics, no references were provided for further examination of discussions of these methods.

The appropriateness of different measures and tests is not adequately developed and neither are the inferences made subsequent to the application of the tests. The fact that paired comparisons were "not generally bad," or that the t-tests were "good" tells the reader very little. The p-values, or level of statistical confidence at which the reversal of the null hypothesis takes place, were not even mentioned. The assumptions of normality and independence underlying the application of correlation and regression analysis in particular appeared no place to be supported by preliminary investigations.

At Washington National Airport the contributions of aircraft and airport-related sources make up only a very small fraction of the total air pollution burden in the airport vicinity. Since the aircraft and airport contributions, which are the most important elements in the model study, represent such small fractions of the measured concentrations and since no correlation between them was demonstrated, one cannot be sure that the model as it relates to these factors has been validated.

Only a few air quality computer models have been developed specifically for simulating the impact of the airport complex on ambient air quality (Thayer;^{F-1} Platt et al.;^{F-2} and Rote^{F-3,13,14}). A recent study, *A Survey of Computer Models for Predicting Air Pollution from Airports*, prepared for the FAA by Haber,^{F-15} concludes that no properly controlled verification of airport models has been performed to date:

Airport air pollution models, recognizing the uncertainties inherent in the transport and diffusion process, use the Gaussian type description. These have, however, not been properly validated... Adequate validation has been hampered by the difficulties in obtaining reliable data and by the complex nature of the problem.

Among the defects in airport air pollution computer programs, Haber^{F-15} notes the large volumes of complex input, the need for large computers for the comprehensive air quality computer programs, the lack of appropriate attention to the relative significance of different pollutants, and the program's failure to recognize large uncertainties in both the input data and the models implemented in the programs. He also concludes that:

Since meteorological variables can be observed but not controlled emissions data should be substantially under the control of the investigator.

By conducting a controlled experiment at a relatively remote, high volume military airport where accurate statistics on aircraft type mix and activity are available, Haber^{F-15} notes that:

The basic Gaussian transport and diffusion equations can be validated and any shortcomings identified...questions regarding the accuracy of sets of values for diffusion coefficients and their appropriateness for line sources (as has been suggested by ANL) should be validated empirically.

The problems of evaluation and validation of air pollution models are discussed by Brier^{F-16} in *Statistical Questions Relating to the Validation of Air Quality Simulation Models, a report to EPA-RTP*.^{*} (Haber^{F-15} has described model validation as "reproducibly generating adequate estimates.") Brier's discussion enlarges as well upon the appropriateness of statistical and analysis techniques such as the computation of the mean square error (MSE) and regression analysis (including robust linear regression). He fails to

^{*}Environmental Protection Agency, Research Triangle Park, North Carolina.

mention, however, that the MSE is a dispersion parameter whereas the median is a location parameter. In discussing the effect of outlier points on the results of regression and correlation techniques, he graphically illustrates the fact that a great deal of thought must go into the selection of a technique.

Briers' general guidelines and suggestions for a validation procedure include a sensitivity analysis to indicate any internal inconsistencies in the model and to understand parameters that dominate the process, followed by MSE and regression analyses supported by appropriate diagnostic investigations of input-output errors and of the assumptions concerning normality.

As Koopmans (personal communication) (see also Ref. F-36) points out:

The use of robust methods to fit regression lines here would conspire to make the model look much better than it really is. A scatter diagram may well be useful for displaying this data, but fitting a regression line, with all of the corresponding problems, appears a very poor choice of method, since much of the important information lies in the outliers. Possibly, a combination of regression lines with independent explanation of the outliers would be useful.

3. DESCRIPTIVE STATISTICS AND DISTRIBUTIONAL CONSIDERATIONS

A great deal of attention has been focused on the issue of determining the distributional characteristics of ambient air pollution concentrations. Most researchers will agree that air pollution data appear to have a skewed underlying distribution. There are several distributions that could be used for expressing this type of skewed data. The actual or empirical distribution of air pollution concentrations do not have negative values and are usually asymmetrical with the longer tails extending above the median concentration. The lognormal distribution has been proposed as accurately describing air pollutant concentrations by Zimmer and Larsen,^{F-17} Larsen,^{F-18,19} and Mage.^{F-20} During the EPA Symposium on Statistical Aspects of Air Quality Data (October 1974),* Benarie, Knox, Pollack, Turner, and Lynn all demonstrated the usefulness of the frequency distribution in the analysis of air pollutant concentrations. Standard statistical calculations may be applied if we first transform the concentrations to their logarithms base 10. The geometric mean is calculated as the antilogarithm of the mean logarithm. The standard geometric deviation is the antilogarithm of the standard deviation of the logarithms. If the data follow a lognormal distribution, then the cumulative percentages fall approximately on a straight line on log-probability paper. The 50 percentile point is given by the geometric mean and the slope of the line is given by the geometric standard deviation.

Larsen^{F-21} has concluded that "concentrations are approximately lognormally distributed for all pollutants in all cities for all averaging times," based on actual air quality data. Larsen contends that the lognormal distribution provides a simple means for prediction purposes especially useful in

*Environmental Protection Agency, Research Triangle Park, North Carolina.

air pollution control applications. Mage^{F-20} by treating diffusion as a stochastic process has obtained the censored three-parameter lognormal model, of which Larsen's standard two-parameter model is a special case. The new model has been compared with actual air pollutant concentration data and appears superior to the standard lognormal model, especially in its approximation for the upper percentile points of the cumulative distribution function. It is probable that this improvement results not just from addition of another parameter but from the fact that the new model is more appropriate for the underlying physical processes that generate atmospheric pollutant concentrations.

The method for estimating the parameters of the censored three-parameter lognormal model is rather complicated in comparison to that for the two-parameter model and involves numerical optimization for determining a best-fitting, cumulative distribution function, using a weighted least squares approach. The model is "censored", meaning that it will predict negative concentrations that are simply taken to be zero. The censored three-parameter model proposed by Mage appears to agree or fit the actual data in the upper tail of the distribution more satisfactorily than does Larsen's standard two-parameter model. While Larsen's model^{F-21} may be adequate for making assumptions about control strategies, the place for more complicated distributions like the one proposed by Mage,^{F-20} is in fitting large bodies of data so as to produce a better estimate of the behavior of the upper tail of the distribution.

An important aspect of any sampling program is to determine the fraction of time in which a certain concentration is exceeded. The empirical cumulative frequency distribution plot can be used to get the percent of the sample population exceeding any specified concentration. However, one must keep in mind the accuracy and resolution obtained in estimates associated with the tail of the distribution. A very few observations, sometimes referred to as extreme values, are usually available on which to base the extreme percentile points. Since the standards promulgated by the Environmental Protection Agency are stated in terms of exceedance, the frequency of occurrence of high concentrations are of major importance. For this reason, the straight line or more complex fitted cumulative frequency equations need to be critically examined and interpreted, and supported by diagnostic investigations of the basic assumptions concerning normality and independence. Aitchison and Brown^{F-22} provide a general discussion of the lognormal theory and distribution methods, and should be consulted for general discussions of lognormal distributions.

Another technique known as the boxplot has been suggested by J. W. Tukey^{F-23} for examining distributional characteristics. The boxplot technique consists of building a stem-and-leaf data structure, similar to a histogram, in which stems correspond to higher order digits and leaves to lower order digits in the observations. The structure is used to compute plotting positions for outlier points and extreme values, and a box indicating the interquartile range and the median. The boxplot produces a horizontal schematic display that indicates the distributional character of the observations. Under the assumption of normality, a certain percentage of the observations fall outside of the interquartile range. Outliers and extreme values are determined as a result of their being outside of the interquartile

range and the number of such data values exceeding the proportion of observations normally found in the tails of the normal distribution. The application of the boxplot technique to the original data and to the log 10 transform of the data will provide insight into the assumption that the data are intrinsically normal, that is to say, lognormal. This technique offers new perspectives on the distributional character of the data, identifies outliers, and provides estimates of several descriptive statistics.

Saltzman^{F-24} has suggested a nomographic representation for estimating confidence intervals for mean values and determination of confidence intervals for proportions of a population exceeding a specified concentration if the data follow a normal or lognormal distribution. Johnson and Leone^{F-25} provide a discussion of confidence-interval estimation of the population-cumulative-distribution function. Such methods may prove useful when comparing two or more cumulative frequency distributions for significant differences, and also should provide insight as to the accuracy of specific percentile points that are based on observed or predicted data being compared to air quality standards.

Most natural phenomena are observed as statistical distributions and can be represented by a frequency curve, the parameters of which can be estimated from the observations. As R. McCammon^{F-26} has suggested:

Natural events are the product of compound effects resulting from multiple causes and the observed distributions are not always representative of homogeneous populations, but rather a mixture of two or more subpopulations each of which possesses unique parameters. An observation therefore can represent a sample from one of several populations. ...The statistical problem that arises is the dissection of a mixed frequency distribution into its individual components...

Background concentrations for various pollutants superimposed on concentrations for which modeled emissions activity are known to occur can often cause the empirical frequency distribution to appear to be bimodal. This is normally reflected in the cumulative distribution function's departure from a straight line when plotted on log paper. The inability to relate pollution levels to emissions activity can usually be explained by the masking effect the background concentrations have on the pollution signal. A graphical-analytic technique for dissecting normal or lognormal distributions by graphical estimation of the parameters for the two distributions has been proposed by McCammon.^{F-26} Dissecting the distributions is accomplished through the use of graphical first estimates of the lognormal components followed by a regression analysis that provides final estimates. A chi-square test can be used to test the hypotheses that the data represent a mixture of two lognormal distributions. Such an approach could help to identify the distribution of background concentrations and at the same time would produce a better straight line fit for the higher percentiles of the cumulative frequency distribution that is of particular interest in defining the limits of accuracy of air pollution predictions. Having identified a background group using such a technique, descriptive statistics for background subtracted aerometric signals can be computed easily.

Robust techniques for the estimation of the mean, median, and confidence-interval estimates have been explored and developed by Dixon and Tukey,^{F-27} Tukey and McLaughlin,^{F-28} and Gross.^{F-29} The computation of descriptive statistics are often made under the assumption that the data follow a normal or intrinsically normal distribution. In practice this assumption is often false. A procedure called the wave-interval, proposed by Gross^{F-29} for the construction of a confidence interval that is not dependent on the normality assumption, has been found to perform very well and is recommended for general use in place of the t-interval for sample sizes of eight or more. It is assumed that the distribution of the data is unimodal and symmetric and is most likely long-tailed. This technique is recommended for the estimation of descriptive statistics such as the mean, median, and confidence limits for small sample sizes as a means of compensating for extreme points and outliers. Small sample sizes will undoubtedly arise in the stratification of available data on factors such as level of emissions activity, time of day, etc.

It is important to emphasize the role of graphics related to the previous discussions. Plots of actual and fitted cumulative frequency distributions, boxplots, and other descriptive statistics are essential aids in the analysis and interpretation of air pollution data. Graphics, as we shall see in the next section are also extremely important in time series analysis and in plotting the data itself.

4. TIME SERIES METHODS

This section describes time series analysis as it relates to the statistical analysis of air pollution and meteorological data. The time dependent nature of such data and the likelihood of serial correlation found in such measurements make obvious the need for analyzing such data in terms of its frequency composition. This section provides background on time series concepts, attempts to justify the use of time series analysis, and discusses specific analysis techniques, providing the reader with references for further reading.

Cleveland^{F-30} has proposed the use of the inverse autocorrelation of a time series in the analysis of air pollution data. Two different methods for estimating the inverse autocorrelation arise from two different methods of estimating the spectral density -- autoregressive and periodogram smoothing. The estimates of the inverse autocorrelations can be used to assist in identifying a parsimonious, moving average, autoregressive model for the series. The feasibility of the autoregressive-moving average models has been demonstrated by Lee.^{F-31} The use of time series in the analysis of air pollution monitoring data has also been suggested by Barlow and Singpurwalla,^{F-32} Saltzman,^{F-33} Marcus,^{F-34} and Tiao and Hamming.^{F-35}

The value of a time series at any given time is called the amplitude component at that time. A useful measure of the "activity" of the time series is its power. The amplitude is a positive number measured in the amplitude units of the problem at hand. The phase is a dimensionless parameter that measures the displacement of the sinusoid relative to the given time origin.

An extensive treatment of the spectral analysis of time series has been given by Koopmans.^{F-36} Among his views on time series are:

In the same sense that various colors of light are composed of a blend of monochromatic components and musical tones are formed by a superimposition of pure harmonics, time series can be constructed by composing a number of harmonic functions with varying frequencies, amplitudes and phases. Every time series has an explicit spectral representation in terms of frequency, amplitude and phase.

Time series data analysis and theory also is discussed extensively by Brillinger,^{F-37} and the Fourier analysis of time series by Bloomfield^{F-38} provides considerable detail on spectrum analysis and discussion of the general framework of time series analysis methods. Additionally, a bibliography of time series analysis papers has been given by Wold.^{F-39}

The principal goal of spectrum analysis is to decompose the power of the given time series into its harmonic components, that is, to estimate the power spectrum from the available data. The estimated spectrum can then be used to gain information about the mechanism that generated the data. The statistical theory of spectral analysis has been based on certain hypotheses, that the underlying process is stationary and Gaussian and that the process mean is zero and the spectrum is continuous. Some of the preprocessing operations performed on the data before a spectrum analysis is performed are intended to bring the data into reasonable conformity with these hypotheses. A non-zero mean and possible trend in the mean can be either an indication of non-stationarity or of a drift in the instrumentation systems. The estimation and removal of linear or quadratic trends that best fit the data in the least squares sense can be subtracted from the original data with the resulting residual conforming more closely to the stationary hypothesis.

Several important reasons for the use of time series analysis are outlined below:

- (1) As a diagnostic and exploratory tool in checking the assumptions of independence and normality needed for other statistical tests, particularly those related to significant testing, and frequency distribution construction techniques;
- (2) As a means of analyzing the serial correlations in the data;
- (3) As a method of examining frequency dependent correlations (called coherence between two time series); correlation methods in the time domain -- for example, examining correlation by using straight line methods -- can be very sensitive to the assumption of independence and invalidated by the presence of serial correlation;
- (4) As an exploratory tool in searching for periodicity and gross variation of power with frequency to provide insight into the mechanism behind the data; and

- (5) That it is frequently possible to describe complex physical mechanisms better in the frequency domain than in the time domain.

By examining periodicities in the data, we have another way of looking at some of the fundamental mechanisms that produce diurnal patterns and pollution episodes. The correspondence between aircraft emissions and pollution concentrations should be readily observable through an examination of the spectral parameters.

Two models of spectral analysis are now described -- the univariate spectral analysis and the bivariate spectral analysis of time series. Multivariate spectral analysis has not been considered for the present.

Univariate spectral analysis involves the computation of the power spectrum or, as it is also called, the estimated spectral density. The power spectrum is the Fourier transform of the autocorrelation function. The Fourier transform of a sequence of autocorrelations contains precisely the same information found in the original autocorrelations themselves.

Many statistical analysis methods that operate on the data in the time domain make no use of the time dependency in the data. For example, in the estimation of the frequency or cumulative frequency distributions, the data are sorted into non-decreasing order, and information in the time dependency of the data is no longer available. An important property of time series analysis is that much of the time dependence in the data is preserved. The accumulated spectrum is essentially the first integral of the spectrum and can be used to indicate a range of frequencies that contain a substantial proportion of the total power of the time series.

Univariate time series analysis is also an important tool in the design of digital filters. By examining the spectrum, the effect of filtering can be seen in terms of the frequency composition of the time series. In this fashion, digital filters can be developed that remove frequency components that might be regarded as noise prior to the analysis of trends. For example, if the original data are sampled every five minutes, but only hourly averages are required, then the frequency components in the data due to noise in the five-minute data can be removed or filtered out, resulting in a smoothed five-minute series that can be used to calculate the one-hour data. In a similar fashion, the effect of the intake-manifold, averaging bottles can be investigated by examining the spectrum of already smoothed pollution concentrations. Similarities between the spectra of two series, such as peaks at similar frequencies, may raise the possibility that the series are related. To investigate such possibilities, we compute estimates of the cross spectrum of the two series. This is an extension of the definition of the spectrum and is usually estimated by smoothing the cross-periodogram, and is performed in the bivariate spectral analysis of the two series.

Bivariate spectral analysis for the spectral decomposition of two series into various spectral parameters is equivalent to descriptive statistics. These include the estimated spectral density of each series, the phase function that indicates the relative shift of harmonic components of the two time series at the same frequency, the transfer function that indicates the linear relationship between the two series in the same way regression

coefficients relate the linear relationship between two data sets, and the coherence function that provides an estimate of the frequency-dependent correlation between the two series.

Because of the vast amounts of numerical information contained in the estimates of spectral parameters, graphs should be obtained for the spectral parameters of interest. For the univariate spectral analysis these include the estimated spectrum and the accumulated spectrum. In the bivariate spectral analysis are included the spectral densities for each series, as well as the phase, transfer and coherence functions. Plots of the original and corrected data traces should also be obtained.

A general outline of the application of time series is given below:

- (1) Collect all data for times series analysis, making efforts to ensure that the data are feasible and if necessary adjust the data for comparability.
- (2) Obtain a graph of the time series.
- (3) Perform trend analysis.
- (4) Accommodate and adjust for seasonal variations if required.
- (5) Adjust the data for trend.
- (6) Compute and graph all spectral parameters of interest.

It is proposed that spectral analysis be applied to the air pollution and meteorological data traces for each station. Missing data can be compensated for by simple linear interpolation, which does not affect the estimated spectral parameters. The purposes of these time series analysis techniques have been discussed in the section of this report dealing with statements of hypotheses.

5. MULTIPLE LINEAR REGRESSION ANALYSIS

There are two main uses of the multiple linear regression technique. The first provides an analysis technique for the evaluation of the relative effects and significance of factors affecting the dependent variable. In this case, the dependent variable is the response under study and the independent variables are the actual values of parameters related to the responses. The second usage provides an important framework for planning and analysis of sensitivity experiments. This technique is especially useful in situations in which each response or dependent variable may be expensive or difficult to obtain.

Consider the regression equation of the form:

$$Y = B_0 + B_1X_1 + B_2X_2 + \dots + E$$

where:

Y = the dependent variable, which is the response quantity under consideration,

X_i = independent variables,

β_j = regression coefficients (sometimes called partial coefficients), and

E = the random error term.

A discussion of the assumptions underlying the application of regression methods can be found in most statistics texts, such as *Fitting Equations to Data* by Daniel and Wood,^{F-40} which discuss the least squares method. These assumptions concern a knowledge of the correct form of the regression equation, use of typical data in the analysis, and assurance that the dependent variables are statistically uncorrelated (or, more generally, are said to be independent). Less important assumptions are: that the dependent variables have the same (though unknown) variance, that the values of the independent variables are known without error, and that the random error is normally distributed.

The use of regression methods and experimental designs in the context of performing sensitivity analysis is to estimate the effects of the independent variables of interest (and possibly their interactions) in a reasonable number of experimental runs or values of the dependent variable. Fractional factorial designs, discussed extensively by Cochran and Cox^{F-41} can be used for this purpose. These designs provide estimates of the main effects and, if desired, some low-order interactions with a minimal number of computer runs or values of the independent variable.

The model using two levels of the factors is called a first-order model and, hence, contains no higher order terms. If for some factor a quadratic component is to be estimated, the factorial designs must be replanned to take that factor at three or more levels. In practice, however, the quadratic effects are often neglected in the earlier stages of experimentation in order to make decisions about future experiments on the basis of the first-order model. Orthogonal polynomials are suggested when quadratic effects are to be estimated.

The fitted equation could fail to be statistically significant because (1) the assumed form of the equation is not the true or (2) the variation of observed points, though random, is so large that the fitted equation could have arisen by random sampling from a population with all partial regression coefficients equal to zero.

The hypothesis that all true partial regression coefficients, β_j 's, equal zero, can be tested by an F-test of the variance accounted for by regression relative to the error variance. The F-value calculated from the data can be compared with the tabulated F-value,^{F-42} and the hypothesis that all true partial regression coefficients equal zero can be rejected if the calculated F-value is larger.^{F-43} This same hypothesis, if rejected, also allows testing to determine whether the regression accounts for a significant amount of the variation observed in Y , the response quantity.

It is recommended that the modified Gram-Schmidt analysis of variance be used to perform the least squares solution in the factorization process in solving the regression equation. In the modified Gram-Schmidt procedure, all

columns of the design matrix are orthogonalized successively with respect to the previous orthogonal column in the overall process. The advantage gained is in dealing with ill-conditioned matrices. For such cases, the modified Gram-Schmidt method works adequately. P-44,45

6. RECOMMENDATIONS

It is recommended that the one-hour aircraft activity tape be reduced from the discrete flight time data and that explanations of assumptions underlying the estimation of such quantities as the number of touch-and-go operations per hour be provided.

Since the actual aircraft modes discussed here will very likely be different from the modes to be used in the AQAM, some explanation of the rationale behind the choice of AQAM modes should be developed.

Since a vast amount of numerical information will be involved in the observed and predicted data sets and will also be generated during the AQAM model validation, it is recommended that computer graphics capabilities be utilized extensively in all phases of the investigation. Graphic routines for general two-dimensional plotting (scatter diagrams, time histories, etc.), wind and pollution rose, effective source mapping, and two-dimensional contouring will be required. The importance of graphics capabilities cannot be overstressed. Any development costs will be substantially offset by the contributions these techniques will make in the analysis process.

It is recommended that all statistical analysis of data from the Williams AFB air pollution monitoring program, including the reduction of the raw data tapes and the computation of cumulative frequency distributions, be coordinated with the AQAM model validation program performed by Argonne National Laboratory.

Time series analysis is recommended for use in the investigation of assumptions and hypotheses, for the analysis of serial correlations in the data, and for the determination of frequency dependent correlations (coherence) between two time series.

Multiple regression analysis is recommended as a means of analyzing experimental designs in the determination of the relative significance and importance of emissions (including at least total on-base sources, aircraft, and background) and meteorology (including data stratified on wind direction, wind speed, atmospheric stability, and diurnal patterns) on the accuracy of AQAM predictions. The following considerations are recommended in the overall definition of accuracy of the AQAM:

- (1) *Identification of pollutant(s), time periods and conditions under which the model performs best and worst.*
- (2) *Comparison of predicted and observed exceedances of the air quality standards.*

- (3) General comparison of predictions and observations during worst case air pollution episodes. These episodes should include time periods of substantial aircraft activity and periods of persistent atmospheric stability by an analysis of data from the Williams AFB air pollution monitoring program.

REFERENCES

- F-1. Thayer, S.D., et al., *Model Verification - Aircraft Emissions Impact on Air Quality*, Geomet Report No. EF-262, EPA Contract No. 68-02-0665 (May 1974).
- F-2. Platt, M., et al., *The Potential Impact of Aircraft upon Air Quality*, Northern Research and Engineering Corp., Report No. 1167-1, NTIS No. PB208-950 (Dec. 1971).
- F-3. Rote, D.M., et al., *Airport Vicinity Air Pollution Study*, Argonne National Laboratory Report to Federal Aviation Administration, Report No. FAA-RD-73-113 (Dec. 1973).
- F-4. MacWalters, J.T., R.C. Koch, and S.D. Thayer, *Air Quality Measured at Atlanta International Airport before and during Experimental Aircraft Taxiing Operations*, Geomet Report No. EF-330, EPA Contract No. 68-03-0358, Geomet, Inc., Rockville, Md. (June 1974).
- F-5. Zimmerman, J., *Model Verification - Aircraft Emission Impact on Air Quality*, No. E-152, Environmental Protection Agency, Research Triangle Park, N.C. (Oct. 1972).
- F-6. Graybill, F.A., *Linear Statistical Models*, McGraw-Hill, N.Y. (1961).
- F-7. Brownlee, K.A., *Statistical Theory and Methodology in Science and Engineering*, John Wiley & Sons, Inc., N.Y. (1965).
- F-8. Rao, C.R., *Linear Statistical Inferences and Its Applications*, John Wiley & Sons, N.Y. (1965).
- F-9. Kendall, M.G., *Rank Correlation Method*, C. Griffin, London (1948).
- F-10. Kolomogorov, A.N., and S.V. Fomin, *Elements of the Theory of Functional Analysis*, translated from the 1st Russian Edition, by Leo F. Boron, Graylock Press, Rochester, N.Y. (1957).
- F-11. Kolomogorov, A.N., *Foundations of the Theory of Probability*, translation edited by Nathan Morrison, 2nd English Ed., Chelsea Publications Co., N.Y. (1965).
- F-12. Gnedenko, B.V., and A.N. Kolomogorov, *Limit Distributions for Sums of Independent Random Variables*, translated from Russian and annotated by K.L. Chung with appendix by J.L. Boob, Addison-Wesley Publication Co., Cambridge, Mass. (1954).

- F-13. Rote, D.M., and L.E. Wangen, *A Generalized Air Quality Assessment Model for Air Force Operations*, AFWL-TR-74-304, Argonne National Laboratory, Argonne, Ill. (Feb. 1975).
- F-14. Wangen, L.E., and D.M. Rote, *A Generalized Air Quality Assessment Model for Air Force Operations - An Operator's Guide*, AFWL-TR-74-54, Argonne National Laboratory, Argonne, Ill. (July 1974).
- F-15. Haber, J.M., *A Survey of Computer Models for Predicting Air Pollution from Airports*, TR-75-1231, J.H. Wiggins Co., Redondo Beach, Calif. (May 1975).
- F-16. Brier, G.W., *Statistical Questions Relating to the Validation of Air Quality Simulation Models*, NTIS-PB-241-886, Environmental Protection Agency, National Environmental Research Center Meteorology Laboratory, Research Triangle Park, N.C. (March 1975).
- F-17. Zimmer, C.E., and R.I. Larsen, *Calculating Air Quality and It's Control*, J. of the Air Pollution Control Assn., 18(12) (Dec. 1965).
- F-18. Larsen, R.I., et al., *Analyzing Air Pollutant Concentration and Usage Data*, J. of the Air Pollution Control Assn., 17(2) (1967).
- F-19. Larsen, R.I., *A Mathematical Model for Relating Air Quality Measurements to Air Quality Standards*, Air Programs Publications, No. AP-89, Environmental Protection Agency, Research Triangle Park, N.C. (Nov. 1971).
- F-20. Mage, D.T., *An Improved Statistical Model for Analyzing Air Pollution Concentration Data*, U.S. Environmental Protection Agency, Las Vegas, Nevada, for presentation at the 68th Annual Meeting of the Air Pollution Control Association, Boston, Mass., pp. 3-27 (June 15-20, 1975).
- F-21. Larsen, R.I., *A New Mathematical Model of Air Pollutant Concentration Averaging Time and Frequency*, J. of the Air Pollution Control Assn., 16(1):24-30 (Jan. 1969).
- F-22. Aitchison, J., and J.A.C. Brown, *The Lognormal Distribution*, Cambridge University Press, Cambridge (1957).
- F-23. Tukey, J.W., *Exploratory Data Analysis*, MIT Lecture Notes, Cambridge, Mass. (cir. 1971).
- F-24. Saltzman, B.E., *Simplified Methods for Statistical Interpretation of Monitoring Data*, J. of the Air Pollution Control Assn., 13(2) (1972).
- F-25. Johnson, N.L., and E.C. Leone, *Statistics and Experimental Design in Engineering and the Physical Sciences, Vol. II*, John Wiley & Sons, Inc., N.Y. (1964).
- F-26. McCammon, R.B., *An Interactive Computer Graphics Approach for Detecting a Mixture of Normal (or Lognormal) Distributions*, U.S. Geological Survey, National Center 952, Reston, Va. (1976); Computer Graphics, 1(2), Proc. of the Third Annual Conference on Computer Graphics, Interactive Techniques and Image Processing - Siggraph, University of Pennsylvania, Philadelphia (July 14-16, 1976).

- F-27. Dixon, W.J., and J.W. Tukey, *Approximate Behavior of the Distribution of Winsorized (Trimming/Winsorization 2)*, *Technometrics*, 10(1) (1968).
- F-28. Tukey, J.W., and D.H. McLaughlin, *Less Vulnerable Confidence and Significance Procedures for Location Based on a Single Sample: Trimming/Winsorization*, *The Indian Journal of Statistics, Series A*, 25(Pt. 4), Reprint, Sankhya, Statistical Publishing Society, Calcutta, India (Sept. 1963).
- F-29. Gross, A.M., *A Robust Confidence Interval for Location for Symmetric, Longtailed Distributions*, *Proc., National Academy of Science*, 70:1995-1997 (July 1973).
- F-30. Cleveland, W.S., *The Inverse Autocorrelations of a Time Series and Their Applications*, *Technometrics*, 14(2):277-293 (May 1972).
- F-31. Lee, T.S., *Feasibility Study of Arma (p, q) Models Applied to Natural Phenomena*, Symposium on Air Force Applications of Modern Control Theory at the Air Force Institute of Technology, Wright-Patterson Air Force Base, Ohio (1975).
- F-32. Barlow, R.E., and N.D. Singpurwalla, *Averaging Time and Maxima for Dependent Observations*, from *Proc. of the Symposium on Statistical Aspects of Air Quality Data*, EPA-650/4-74-038 (Oct. 1974).
- F-33. Saltzman, B.E., *Fourier Analysis of Air Monitoring Data*, from *Proc. of the Symposium on Statistical Aspects of Air Quality Data*, EPA-650/4-74-038 (Oct. 1974).
- F-34. Marcus, A.H., *A Stochastic Model for Estimating Pollutant Exposure by Means of Air Quality Data*, from *Proc. of the Symposium on Statistical Aspects of Air Quality Data*, EPA-650/4-74-038 (Oct. 1974).
- F-35. Tiao, G.C., and W.J. Hamming, *A Statistical Analysis of the Los Angeles Ambient Carbon Monoxide Data 1955-1972*, *J. of the Air Pollution Control Assn.*, 25(11) (Nov. 1975).
- F-36. Koopmans, L.H., *The Spectral Analysis of the Series*, Academic Press, N.Y. (1974).
- F-37. Brillinger, D.R., *Time Series Data Analysis and Theory*, Holt, Rinehart and Winston, Inc. (1975).
- F-38. Bloomfield, P., *Fourier Analysis of Time Series: An Introduction*, John Wiley & Sons, Inc., N.Y. (1976).
- F-39. Wold, H.O.A., *Bibliography on Time Series and Stochastic Processes*, Oliver and Boyd, London (1965).
- F-40. Daniel, C., and F.F. Wood, *Fitting Equations to Data*, Wiley-Interscience, John Wiley & Sons, Inc., N.Y. (1971).

- F-41. Cochran, W.G., and G.M. Cox, *Experimental Designs*, John Wiley & Sons, Inc., N.Y. (n.d.)
- F-42. Abramowitz, M., and I. Stegun, *Handbook of Mathematical Functions*, Dover Publications, Inc., N.Y. (1964).
- F-43. Crow, E., F. Davis, and M. Maxfield, *Statistics Manual*, Research Department, U.S. Naval Ordnance Test Station, Dover Publications, Inc., N.Y. (1960).
- F-44. Isaacson, E., and H.B. Keller, *Analysis of Numerical Methods*, John Wiley & Sons, Inc., N.Y. (1971).
- F-45. Parlett, B.N., *The LU and QR Algorithms*, in *Mathematic Methods for Digital Computers*, edited by Ralston and Wilf (July 1964).

BIBLIOGRAPHY

- Abramowitz, M., and I. Stegun, *Handbook of Mathematical Functions*, Dover Publications, Inc., N.Y. (1964).
- Air Pollution Control District, County of Los Angeles, *Jet Aircraft Exhaust and Air Quality in the Vicinity of the Los Angeles International Airport*, Air Pollution Control District, County of Los Angeles (1971).
- Bingaman, D.J., L.E. Wangen, and S.D. Zeller, *A Statistical Program for the Analysis of Air Quality Computations and Measurements*, Argonne National Laboratory, Argonne, Ill. (June 1975).
- Bendat, J.S., and A.G. Pierson, *Random Data: Analysis and Measurement Procedures*, Wiley-Interscience, John Wiley & Sons, Inc., N.Y. (1971).
- Beyer, W., ed., *The Handbook of Tables for Probability and Statistics*, Chemical Rubber Co., Cleveland (1974).
- Blackman, R.B., and J.W. Tukey, *The Measurement of Power Spectra*, Dover Publications, Inc., N.Y. (1958).
- Brehmer, R.A., et al., Linwood-Share Library (No. 360 D-13.6.008), COSMICS, University of Georgia, Athens, and Vim Library (No. G2-Cal-Linwood), Software Distribution Dept., CDC, Palo Alto, Calif. (n.d.).
- Brown, B., *Development of a Non-Storage Method Estimating Traffic at Non-Towered Airports*, FAA-RD-74-177, Systems Consultants, Inc. (1974).
- Brown, B., *Estimating Operations at Non-Towered Airports using the Non-Storage Method*, FAA-RD-74-178, Systems Consultants, Inc. (1974).
- Crawford, J.E., *An Analytical Model for Airfield Environment Analysis*, AFWL-TR-71-70, Kirtland Air Force Base, N.M. (May 1972).
- Daniel, G., F.S. Wood, and J.W. Gorman, *Fitting Equations to Data*, Wiley-Interscience, N.Y. (1971).

Beming, W.E., *Statistical Adjustment of Data*, John Wiley & Sons, Inc., N.Y. (1948).

Belanney, B.T., *Air Quality Assessment Model (AQAM) Field Data Collection Guide*, AFWL-TR-75-220, Kirtland Air Force Base, N.M. (Aug. 1975).

Environmental Studies Center, *Guidelines for Air Quality Maintenance Planning and Analysis*, Plan Preparation, Report No. PB-237-581, Vol. 2, Environmental Studies Center, Research Triangle Park, N.C. (July 1974).

Gifford, F.A., *Modeling Urban Air Pollution*, Atmospheric Environment, 7:131-136, Great Britain (1973).

Gold, B., and C.M. Rader, *Digital Processing of Signals*, McGraw-Hill Book Co., N.Y. (1969).

Goldberg, S., *Introduction to Difference Equations*, John Wiley & Sons, Inc., N.Y. (1967).

Grenander, U., and M. Roseblatt, *Statistical Analysis of Stationary Time Series*, John Wiley & Sons, Inc., N.Y. (1957).

Hahn, G.J., and S.S. Shapiro, *Statistical Models in Engineering*, John Wiley & Sons, Inc., N.Y. (1967).

Hillier, F.S., and G.J. Lieberman, *Introduction to Operations Research*, Holden-Day, Inc., San Francisco (1968).

Hocking, R.R., and W.B. Smith, *Optimum Incomplete Multinomial Samples*, Technometrics, 14(2) (1972).

Jon, P.W.M., *Statistical Design and Analysis of Experiments*, The MacMillan Co., N.Y. (n.d.).

Kahn, H.D., *Note on the Distribution of Air Pollutants*, J. of the Air Pollution Control Assn., 23(11):973 (Nov. 1973).

Kalpasanov, Y., and G. Kurchatova, *Investigation on the Statistical Form of Distribution of Certain Chemical Pollutants in Air*, submitted for publication to the J. of the Air Pollution Control Assn. (1974).

Kapteyn, J.C., *Skew Frequency Curves in Biology and Statistics*, published by Noordhoff, Astronomical Laboratory, Groningen, Netherlands (1903).

Kirkwood, J.G., *Statistical Mechanics of Transport Processes: General Theory*, J. of Chemical Physics, 14:180 (1946).

Kramer, C.Y., *On the Analysis of Variance of Two-Way Classification with Unequal Sub-Class Numbers*, Biometrics, 11:441-452 (Dec. 1955).

Land, C.E., *An Evaluation of Approximate Confidence Interval Estimation Methods for Lognormal Means*, Technometrics, 14(1) (1972).

Lange, R., *ADPIC - A Three Dimensional Transport-Diffusion Model for the Dispersal of Atmospheric Pollutants and its Validation Against Regional Tracer Studies*, USRL-76170, Preprint, Lawrence Livermore Laboratory, University of California, Livermore (1975).

Langan, L., *Remote Sensing Measurements of Regional Gaseous Pollution*, AIAA Paper No. 71-1060, Joint Conference on Sensing of Environmental Pollutants, Palo Alto, Calif. (Nov. 1971).

Libby, P.A., ed., *The Fluid Dynamics Aspects of Air Pollution Related to Aircraft Operations*, AGARD-AR-55, Technical Editing and Reproduction, Ltd., Harford House, London (1974).

Los Angeles County Air Pollution Control District, *Study of Jet Aircraft Emissions and Air Quality in the Vicinity of the Los Angeles International Airport*, NTIS No. PB-198-699 (April 1971).

Lucke, J.W., and G.W. Brown, *Fatigue Data Processing with a Small Digital Computer*, ISA Transactions, 11(2):128-134 (1971).

Marcus, A.H., *Air Pollutant Averaging Times: Notes on a Statistical Model*, Atmospheric Environment, 7:265-270, Pergamon Press, Great Britain (1973).

Mendenhall, W., *Introduction to Linear Models and the Design and Analysis of Experiments*, Wadsworth Publishing Co., Inc., Belmont, Calif. (1968).

Mendenhall, W., *The Design and Analysis of Experiments*, Duxburg Press, Wadsworth Publishing Co., Inc., Belmont, Calif. (1968).

Menicucci, D.F., *Air Quality Assessment Model (AQAM) Data Reduction and Operation Guide*, AFWL-TR-75-307, Air Force Weapons Laboratory, Kirtland Air Force Base, N.M. (Dec. 1975).

Naugle, D.F., *Pollution Emission Analysis of U.S. Air Force Aircraft and Airbases*, 75-93.1 for presentation at the 68th Annual Meeting of the Air Pollution Control Assn., Boston (June 15-20, 1975).

Naugle, D.F., and S.R. Nelson, *USAF Aircraft Pollution Emission Factors and Landing and Takeoff (LTO) Cycles*, AFWL-TR-74-303, Air Force Weapons Laboratory, Kirtland Air Force Base, N.M. (1975).

Ostle, B., *Statistics in Research*, the Iowa State University Press, Ames (1963).

Parzen, E., Discussion No. 2, *Discussion of The Inverse Autocorrelations of a Time Series and Their Applications*, by William S. Cleveland, Technometrics, 14(2) (1972).

Ralston, A., and H.S. Wilf, *Mathematical Methods for Digital Computers*, Vol. II, John Wiley & Sons, Inc., N.Y. (1967).

Rote, D.M., *Computation of Dispersion from Area Sources*, Argonne National Laboratory, Argonne, Ill. (April 1976).

Sclove, S.L., (Y vs X) or ($\log Y$ vs X)?, *Technometrics*, 14(2) (1972).

Sprunger, P.R., and L.E. Wangen, *Numerical Studies on the Sensitivity of the Air Quality Assessment Model to Potential Errors in Model Parameters*, Argonne National Laboratory, Argonne, Ill. (1975).

Soong, F.F., *Random Differential Equations in Science and Engineering*, Academic Press, N.Y. (1973).

Wyzga, R.E., *Method to Estimate Missing Air Pollution Data*, *J. of the Air Pollution Control Assn.*, 23(3) (March 1973).

APPENDIX G: STATION-BY-STATION COMPARISON OF MEASURED & COMPUTED CONCENTRATIONS

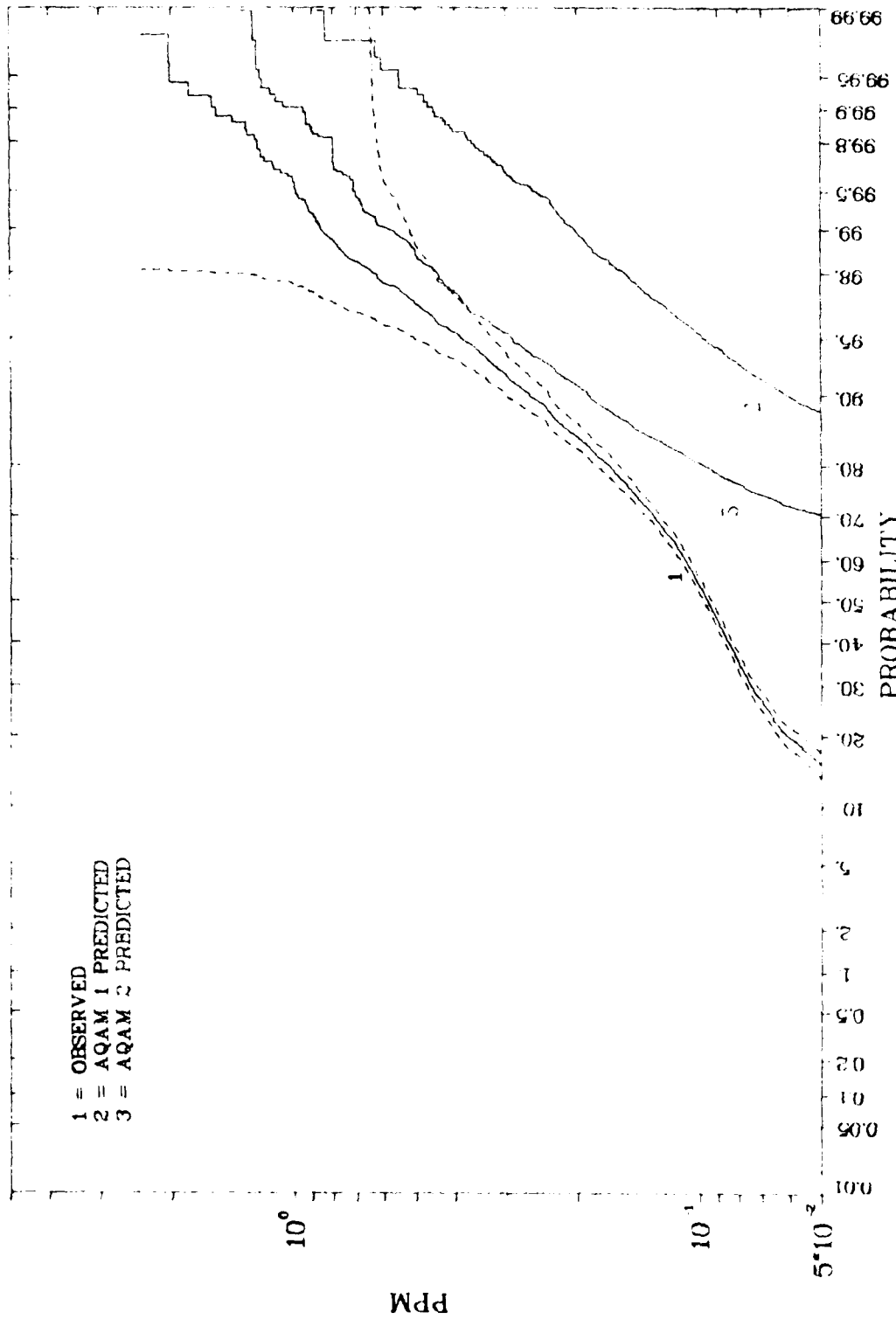


Fig. G-1a. Cumulative Frequency Distributions of CO at Station 1.

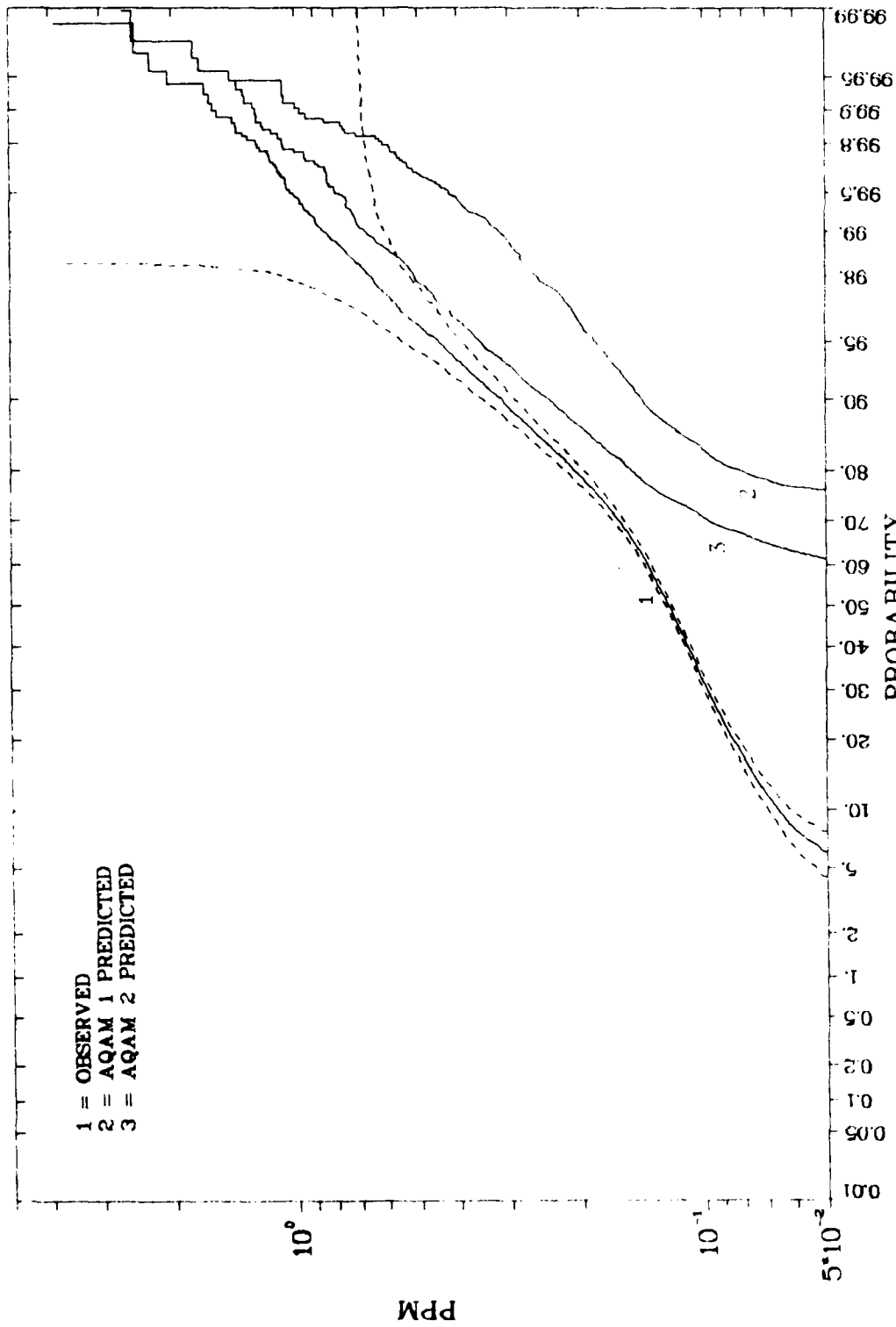


Fig. G-lb. Cumulative Frequency Distributions of CO at Station 2.

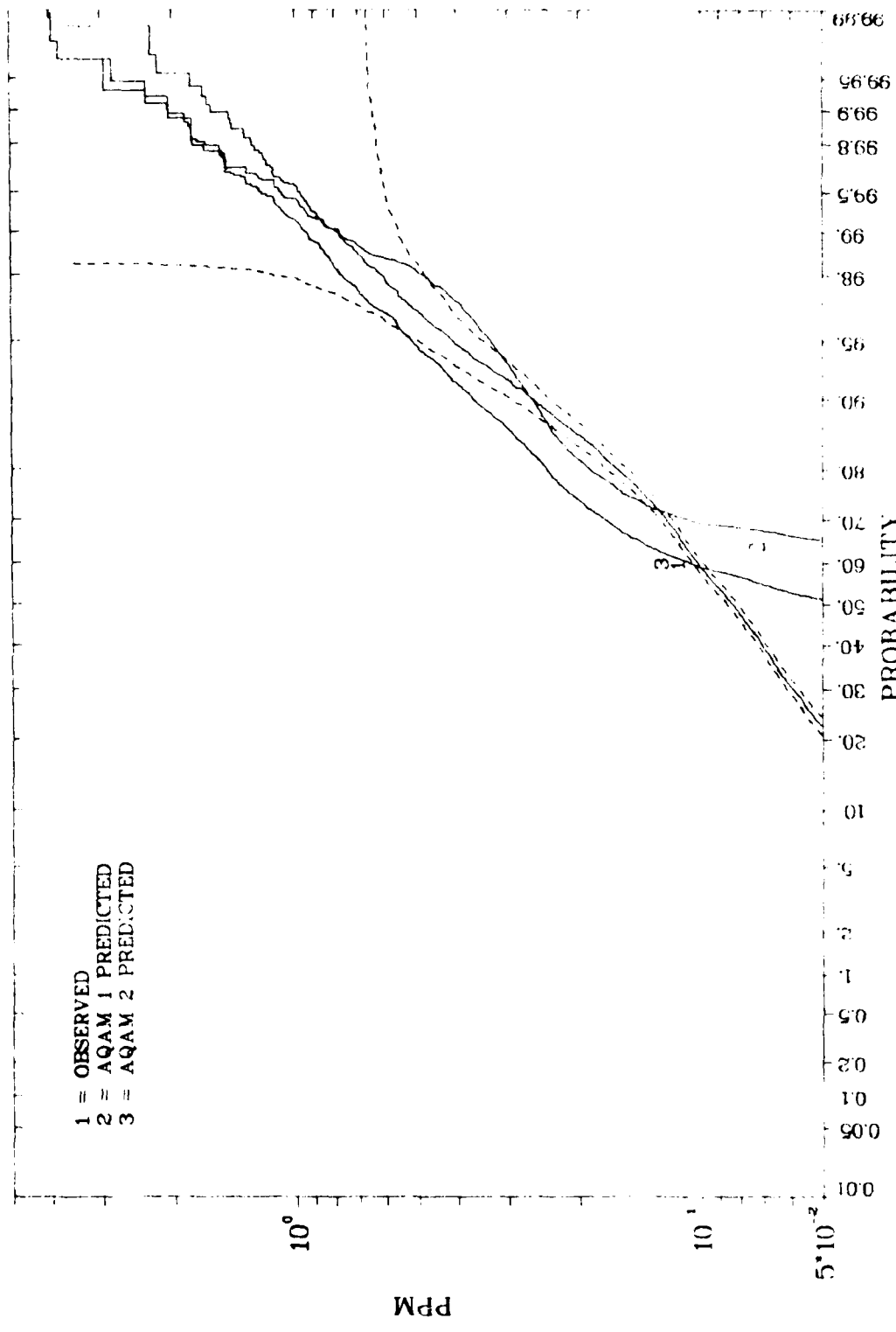


Fig. G-1c. Cumulative Frequency Distributions of CO at Station 3.

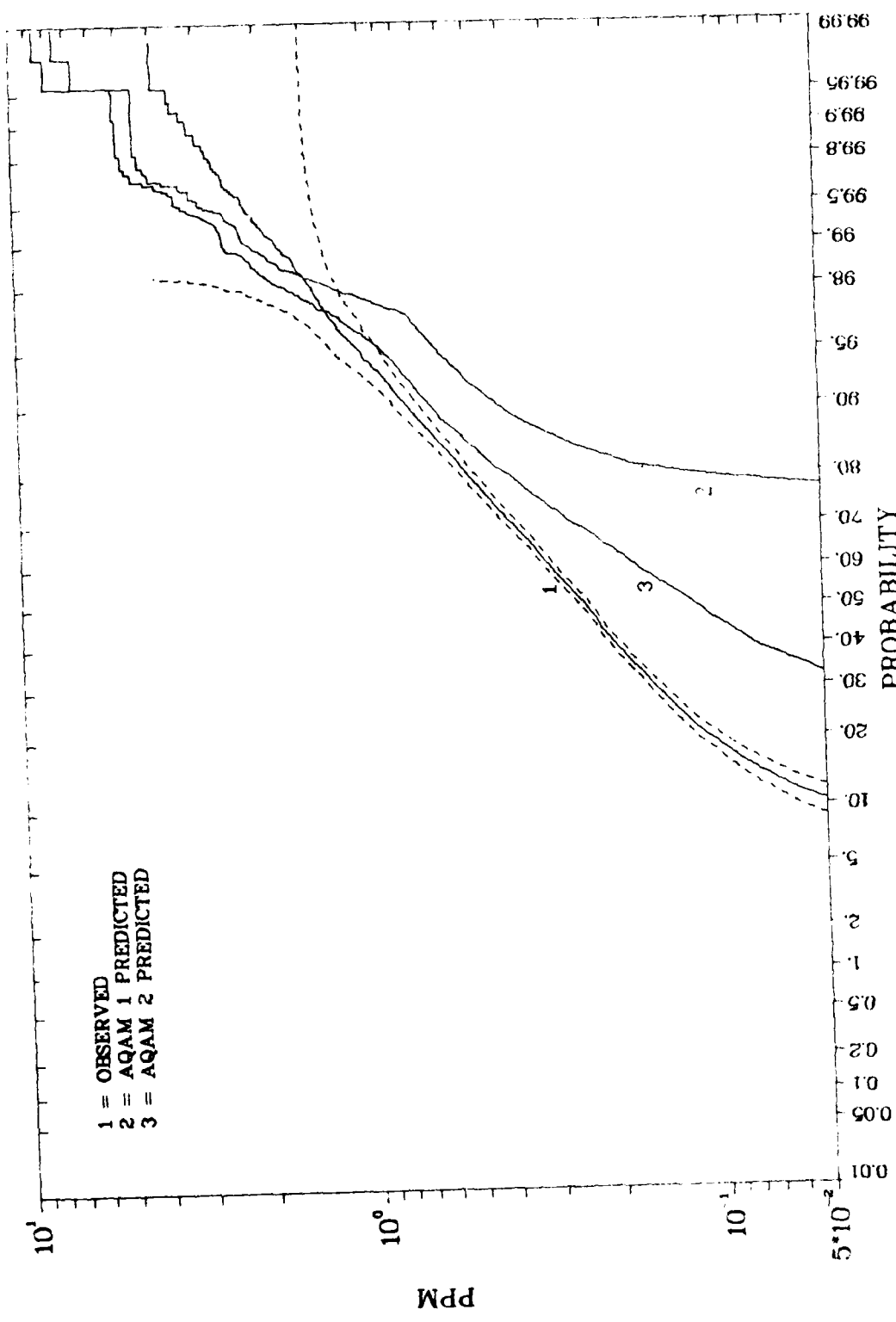


Fig. G-1d. Cumulative Frequency Distributions of CO at Station 4.

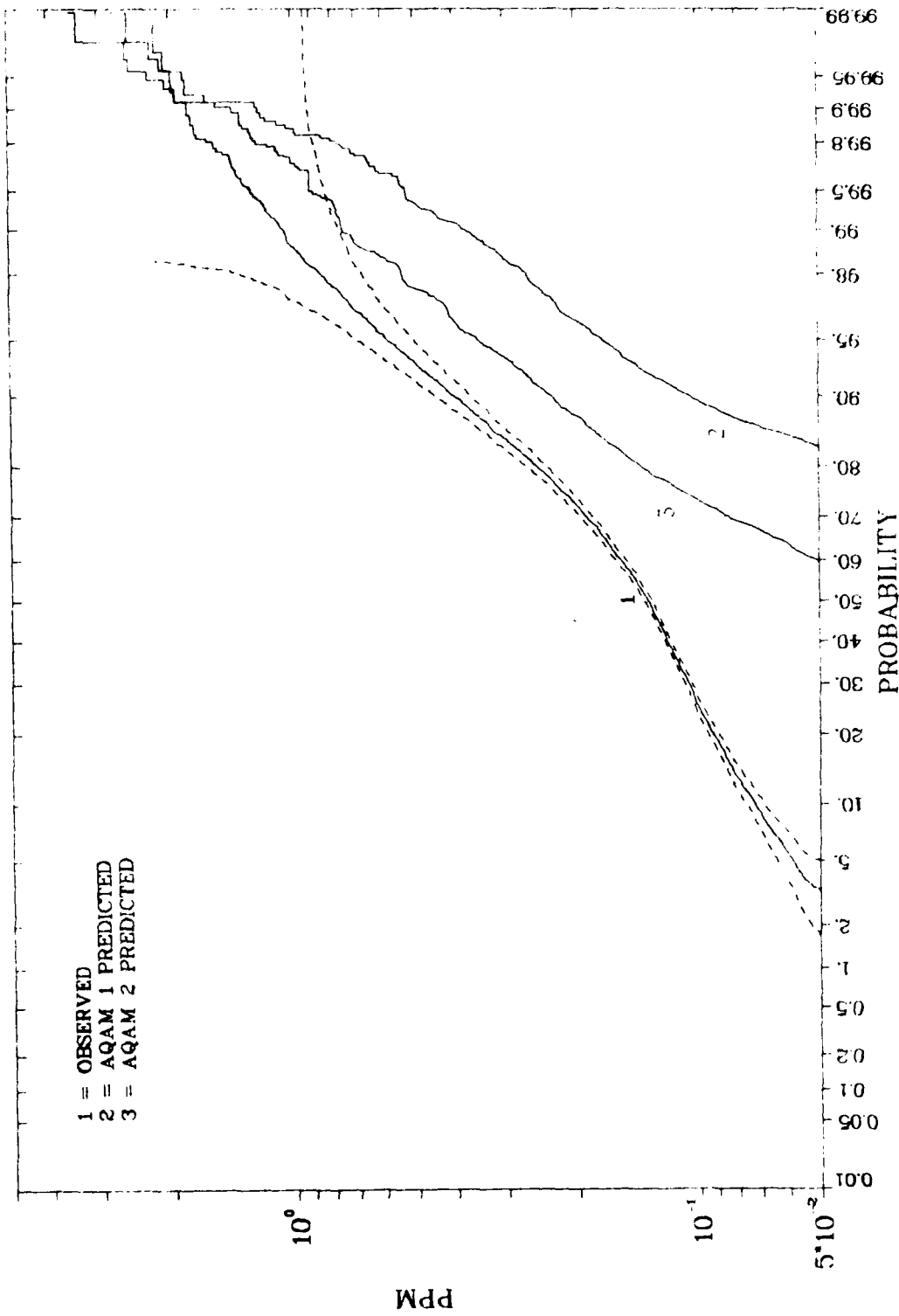


Fig. G-1e. Cumulative Frequency Distributions of CO at Station 5.

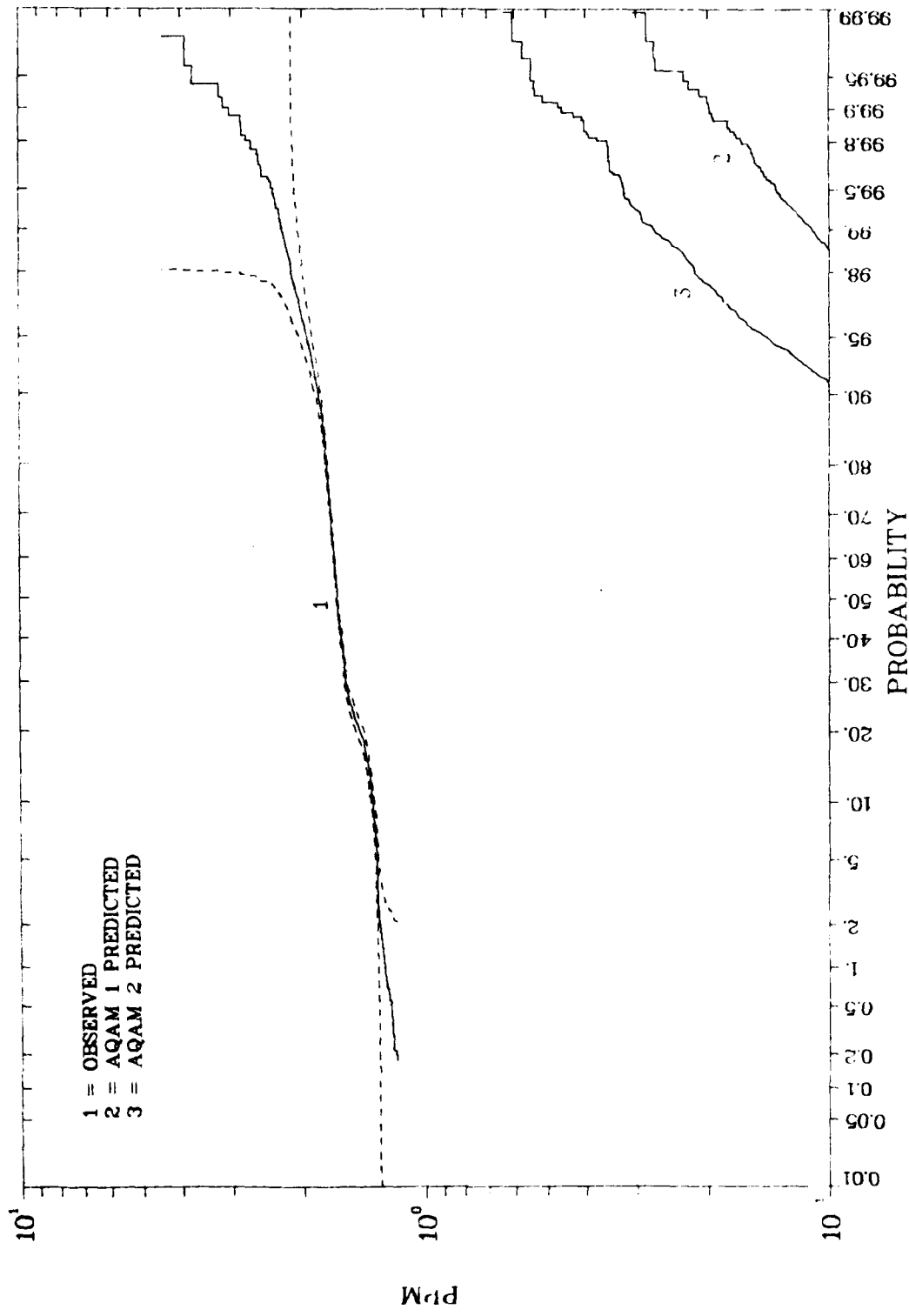


Fig. G-2a. Cumulative Frequency Distributions of THC at Station 1.

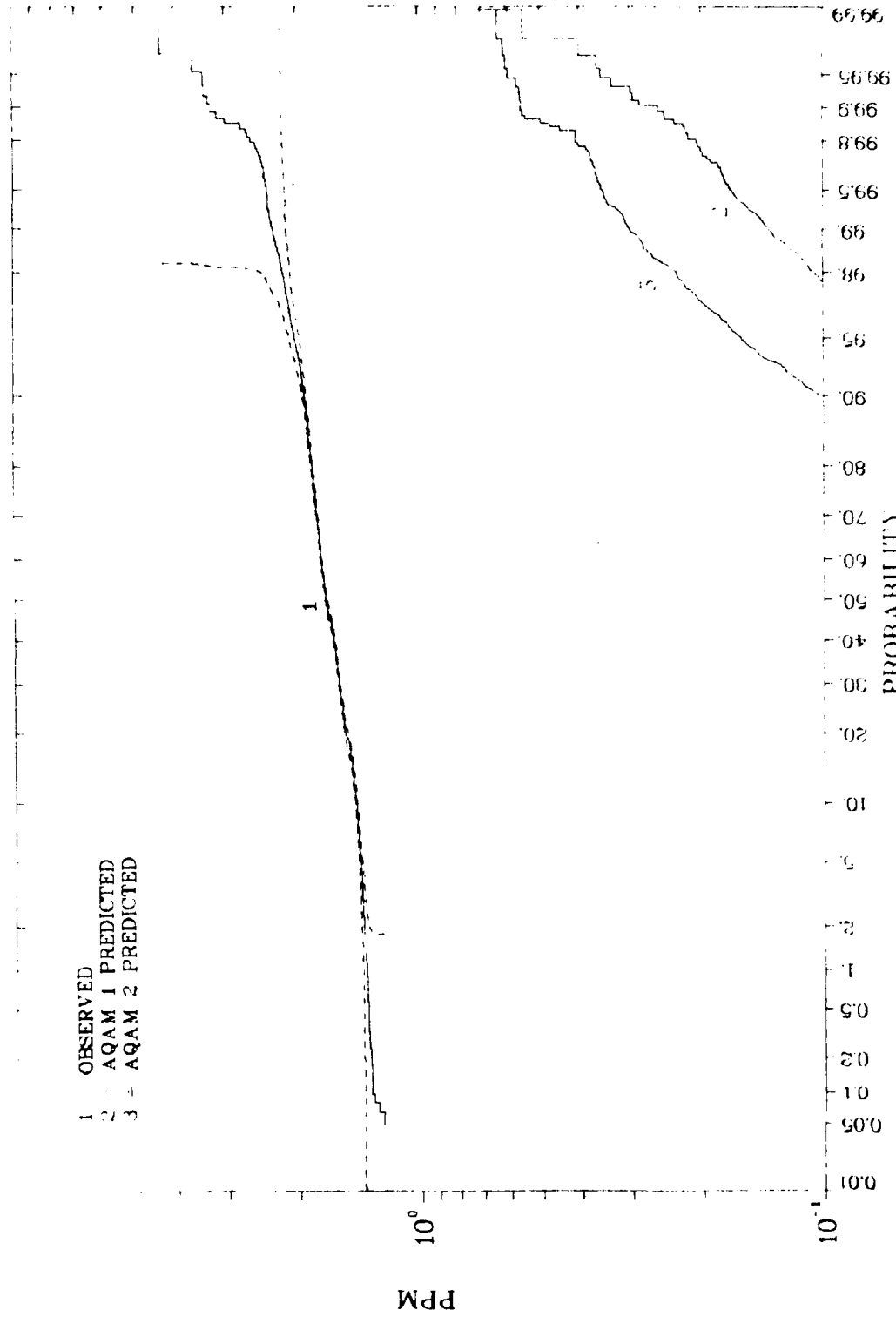


Fig. G-2b. Cumulative Frequency Distributions of THC at Station 2.

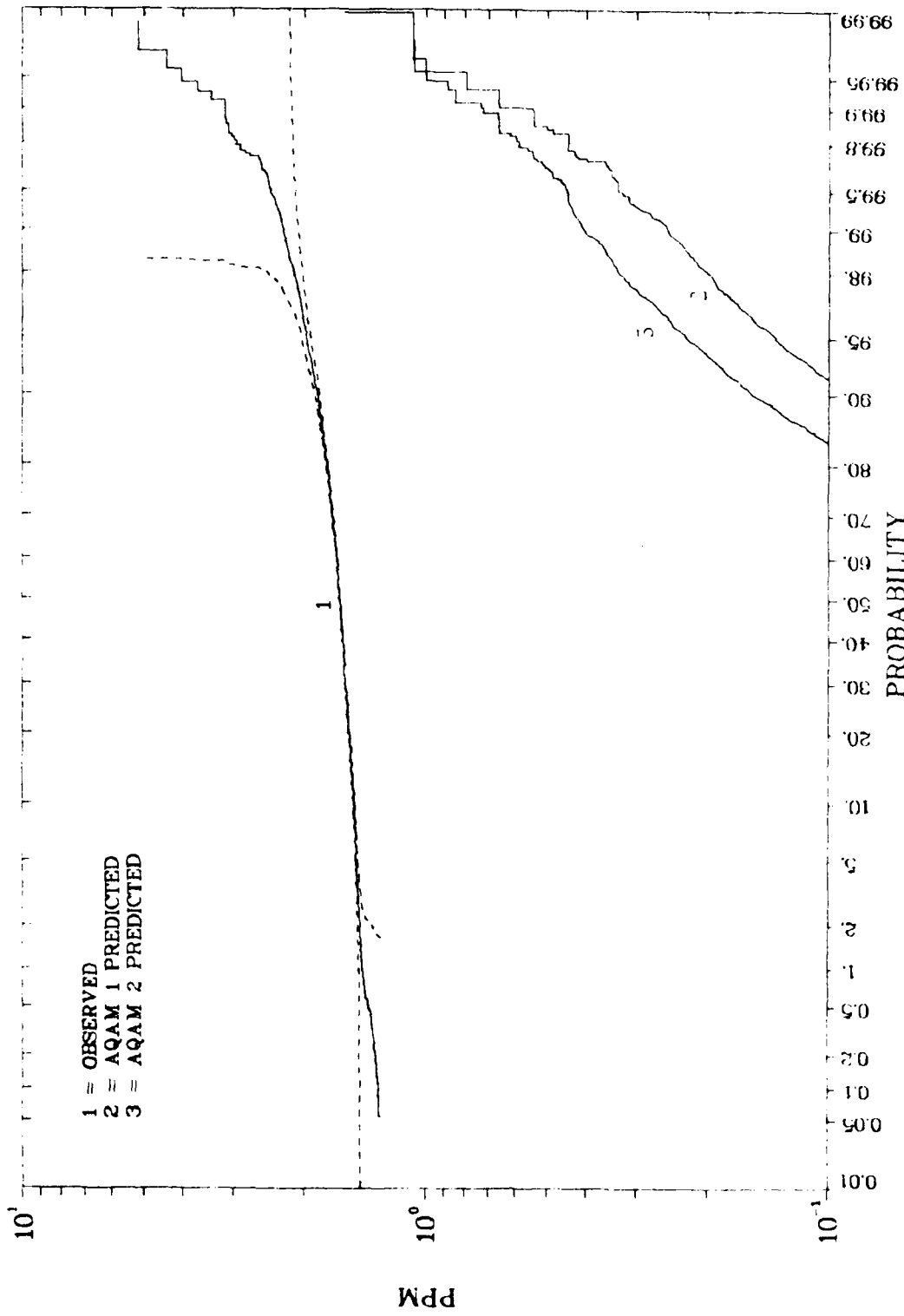


Fig. G-2c. Cumulative Frequency Distributions of THC at Station 3.

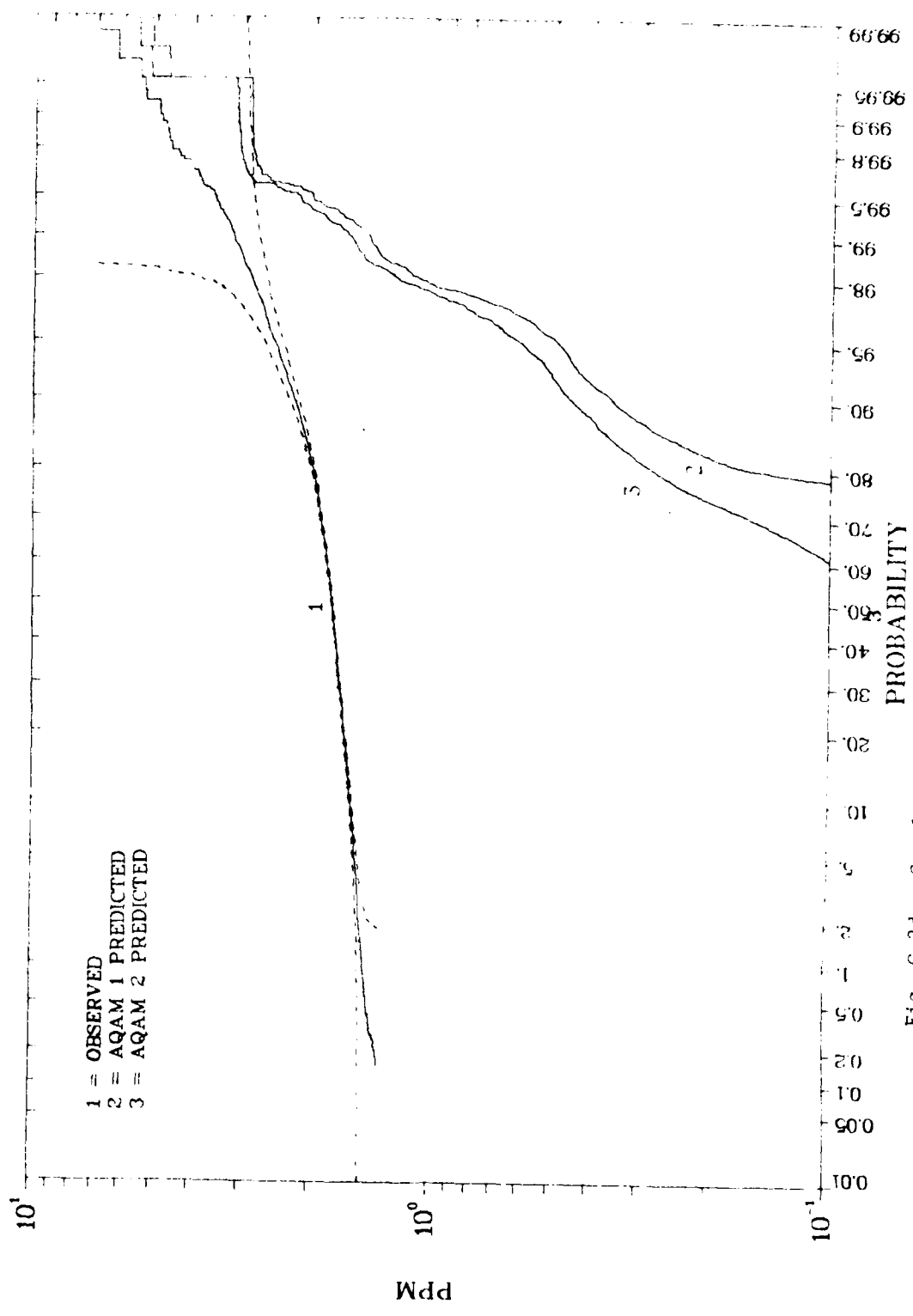


Fig. G-2d. Cumulative Frequency Distributions of THC at Station 4.

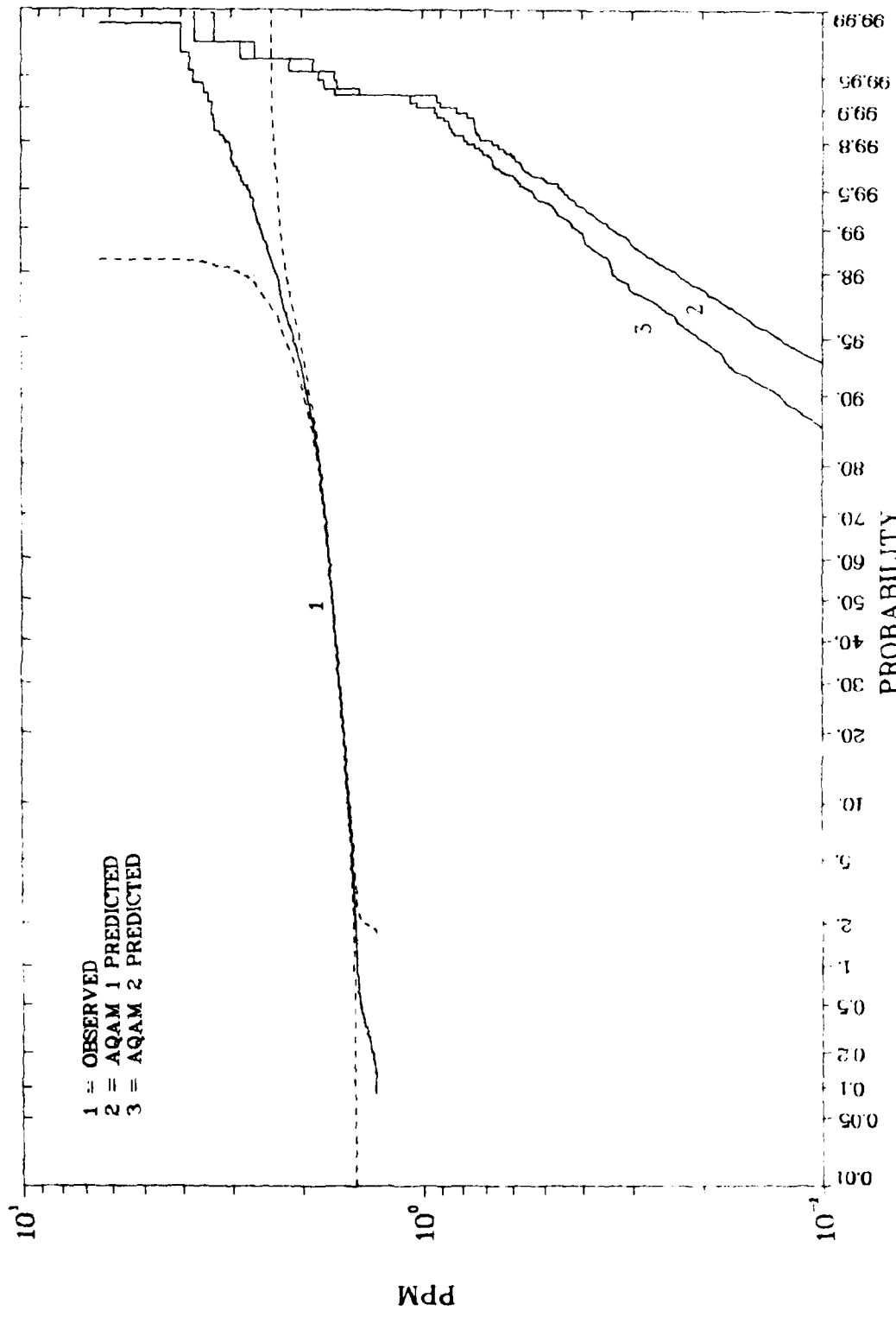


Fig. G-2e. Cumulative Frequency Distributions of THC at Station 5.

- 1 = OBSERVED (THC-CH4)
- 2 = AQAM 1 THC
- 3 = AQAM 2 THC

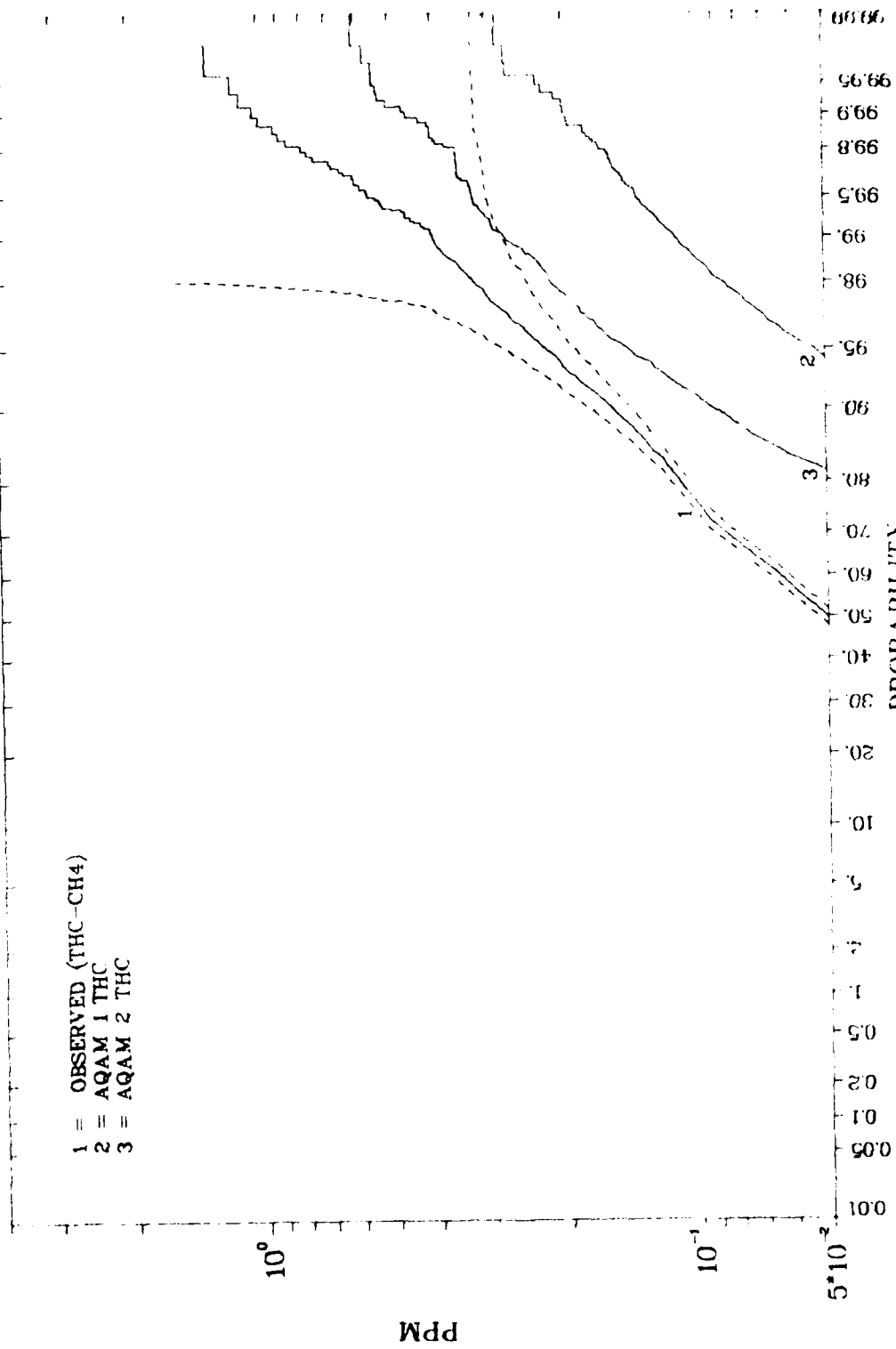


Fig. G-3a. Cumulative Frequency Distributions of NHC at Station 1.

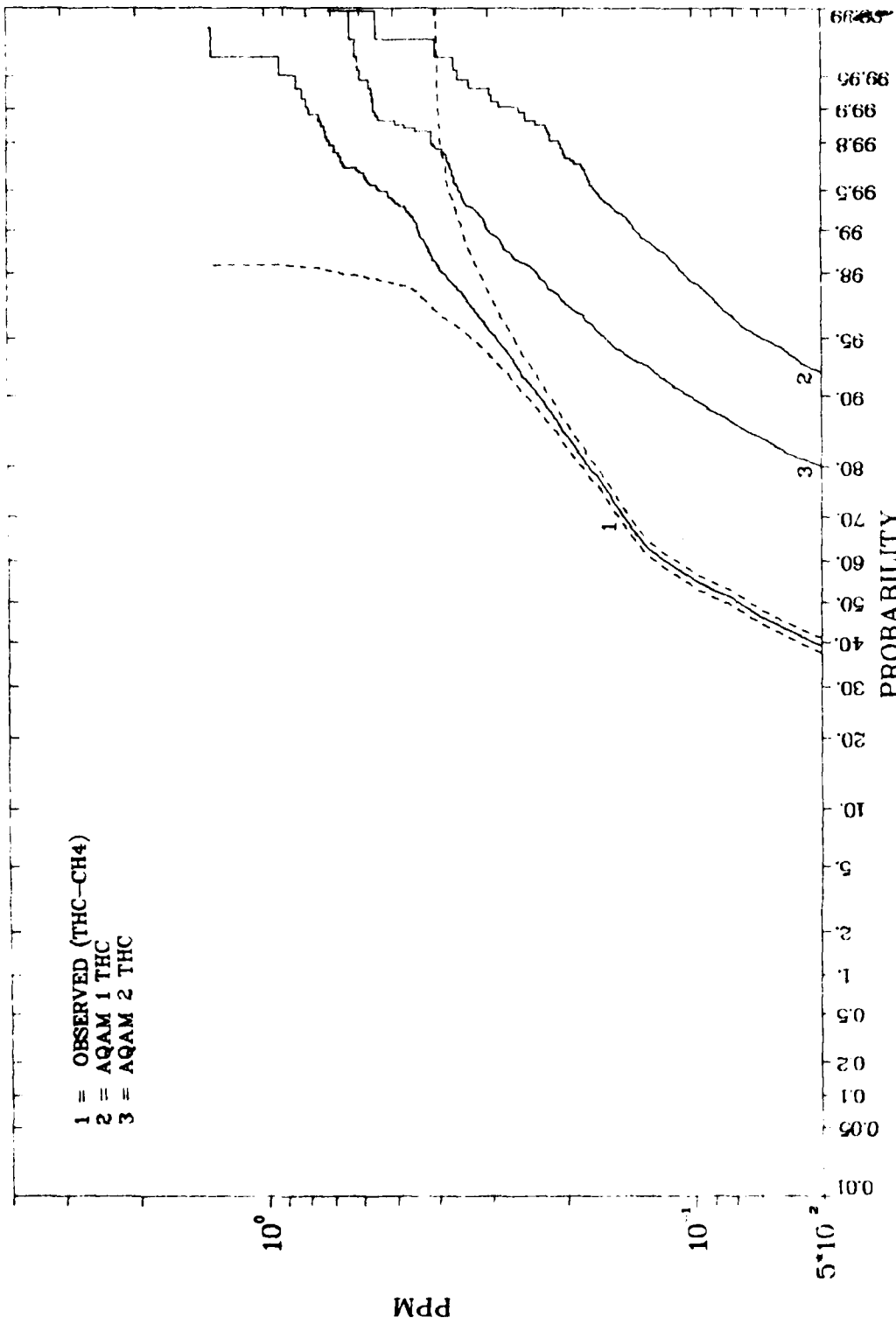


Fig. G-3b. Cumulative Frequency Distributions of NMHC at Station 2.

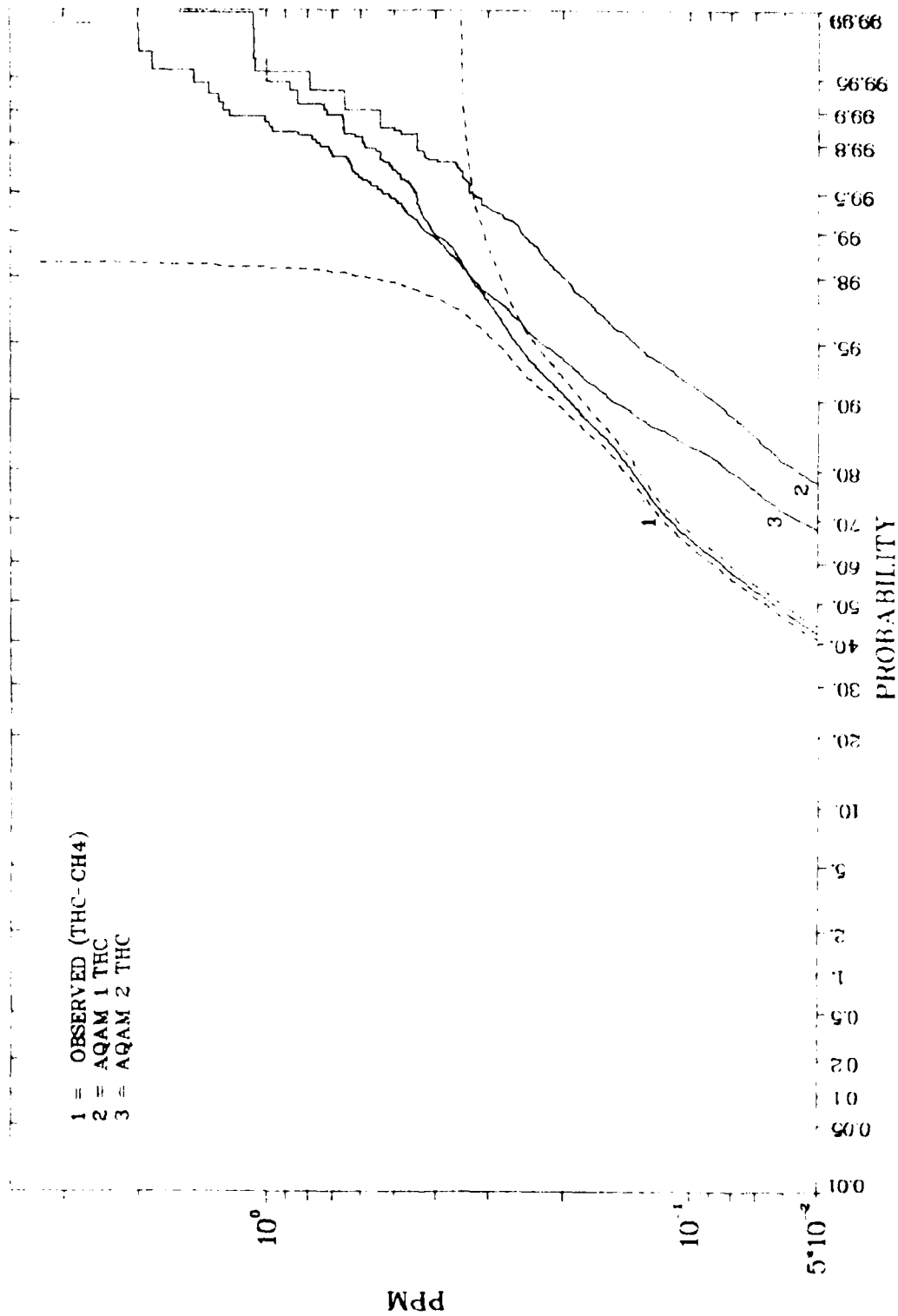


Fig. G-3c. Cumulative Frequency Distributions of NHC at Station 3.

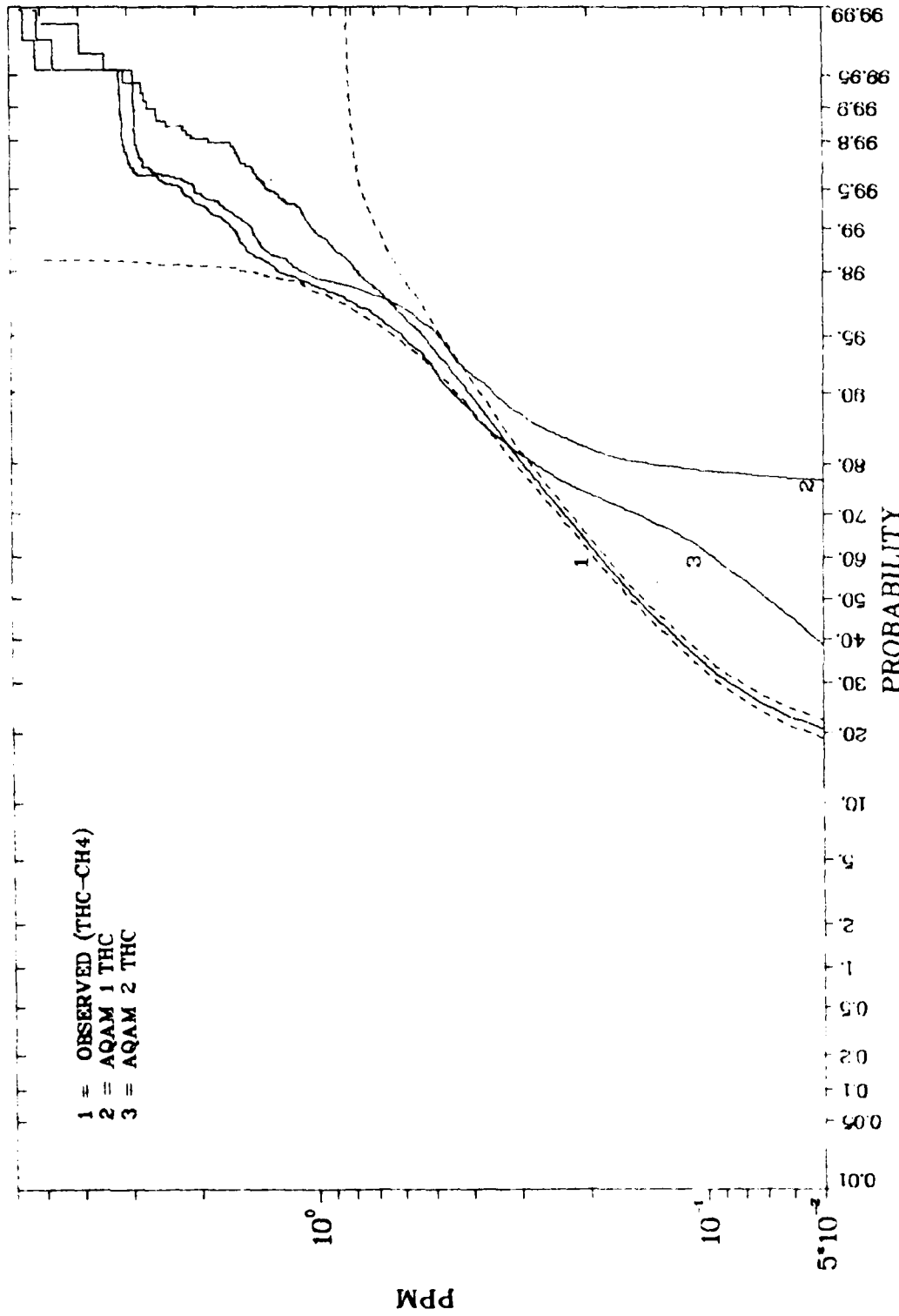


Fig. G-3d. Cumulative Frequency Distributions of NHC at Station 4.

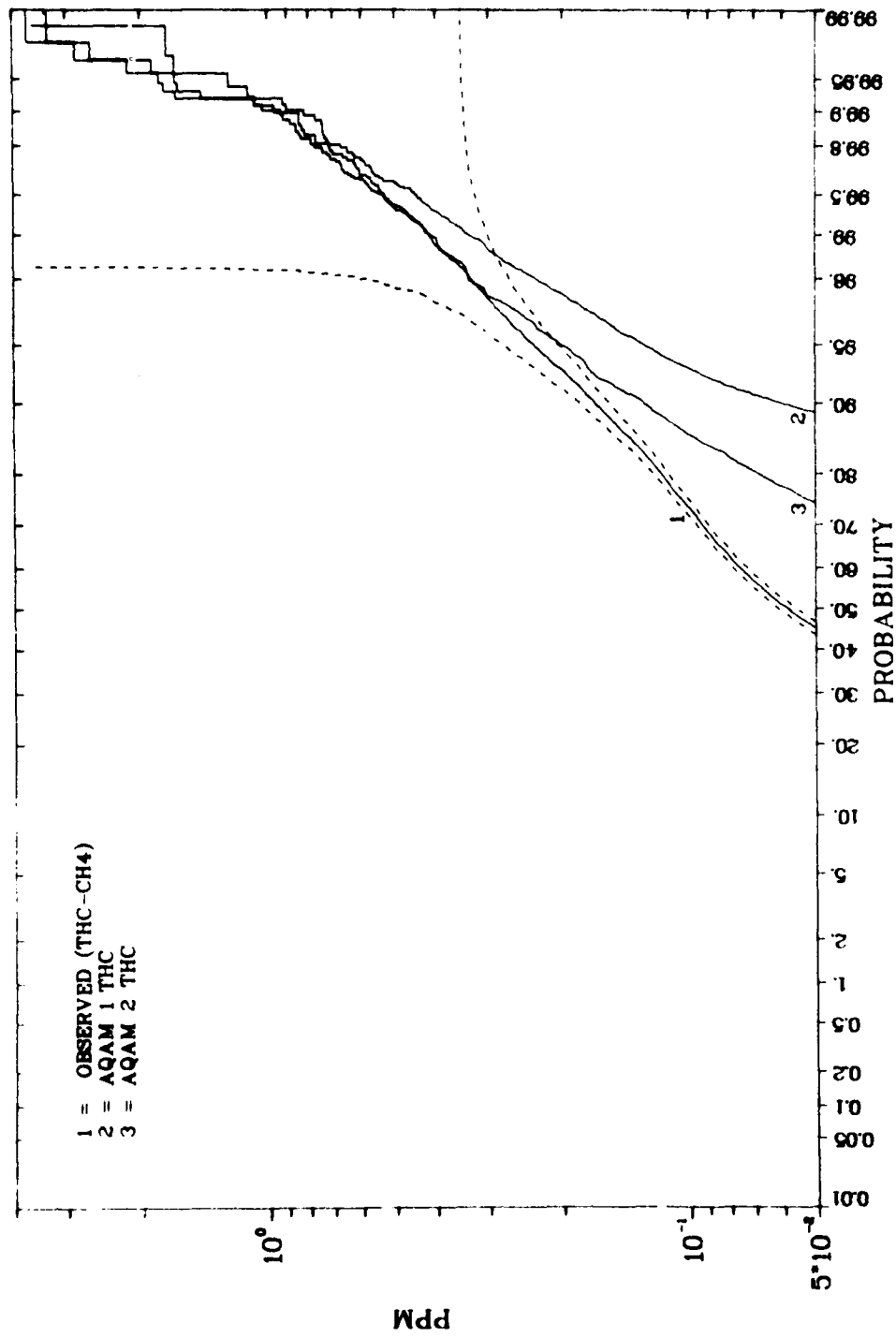


Fig. G-3e. Cumulative Frequency Distributions of NMIC at Station 5.

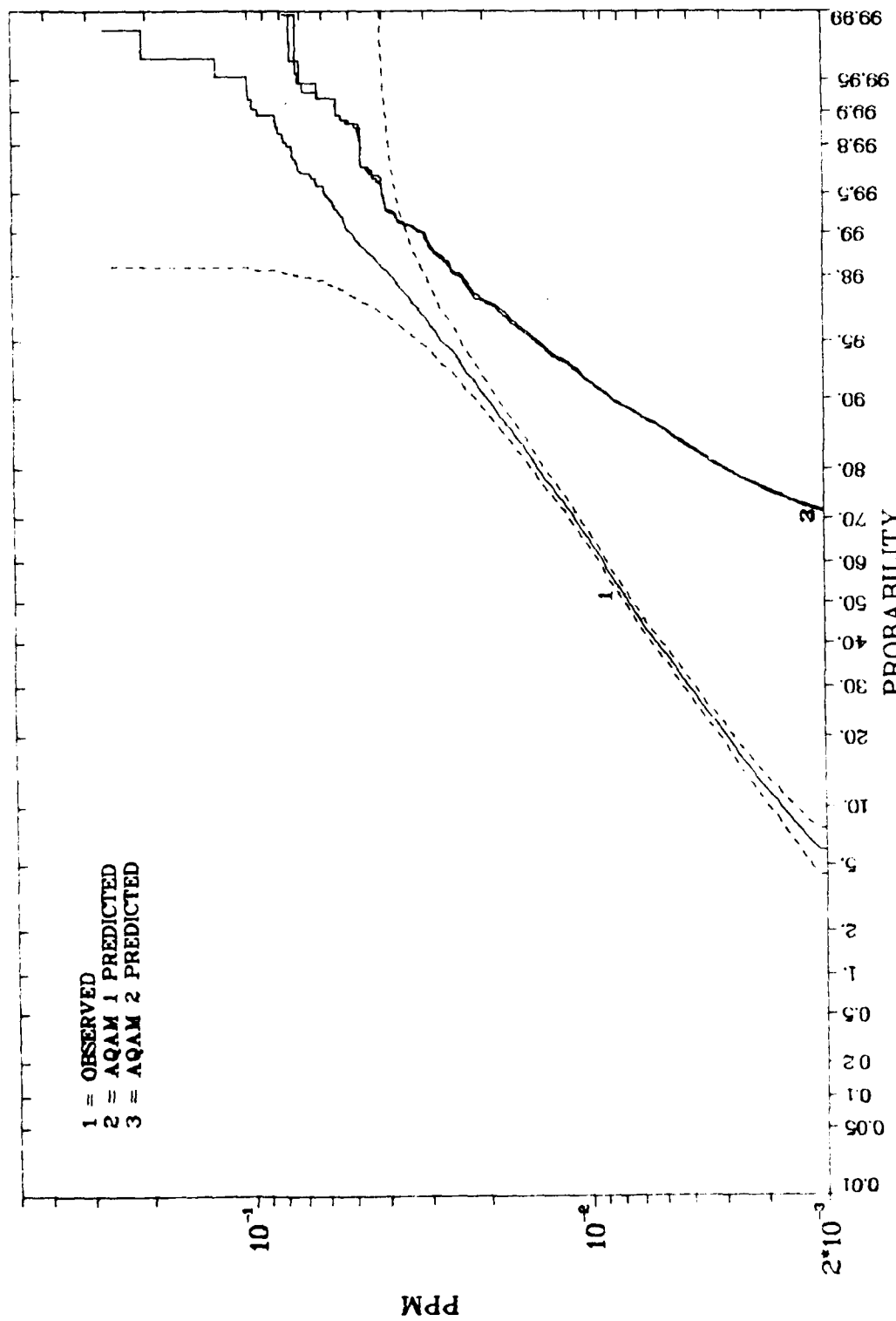


Fig. G-4a. Cumulative Frequency Distributions of NO_x at Station 1.

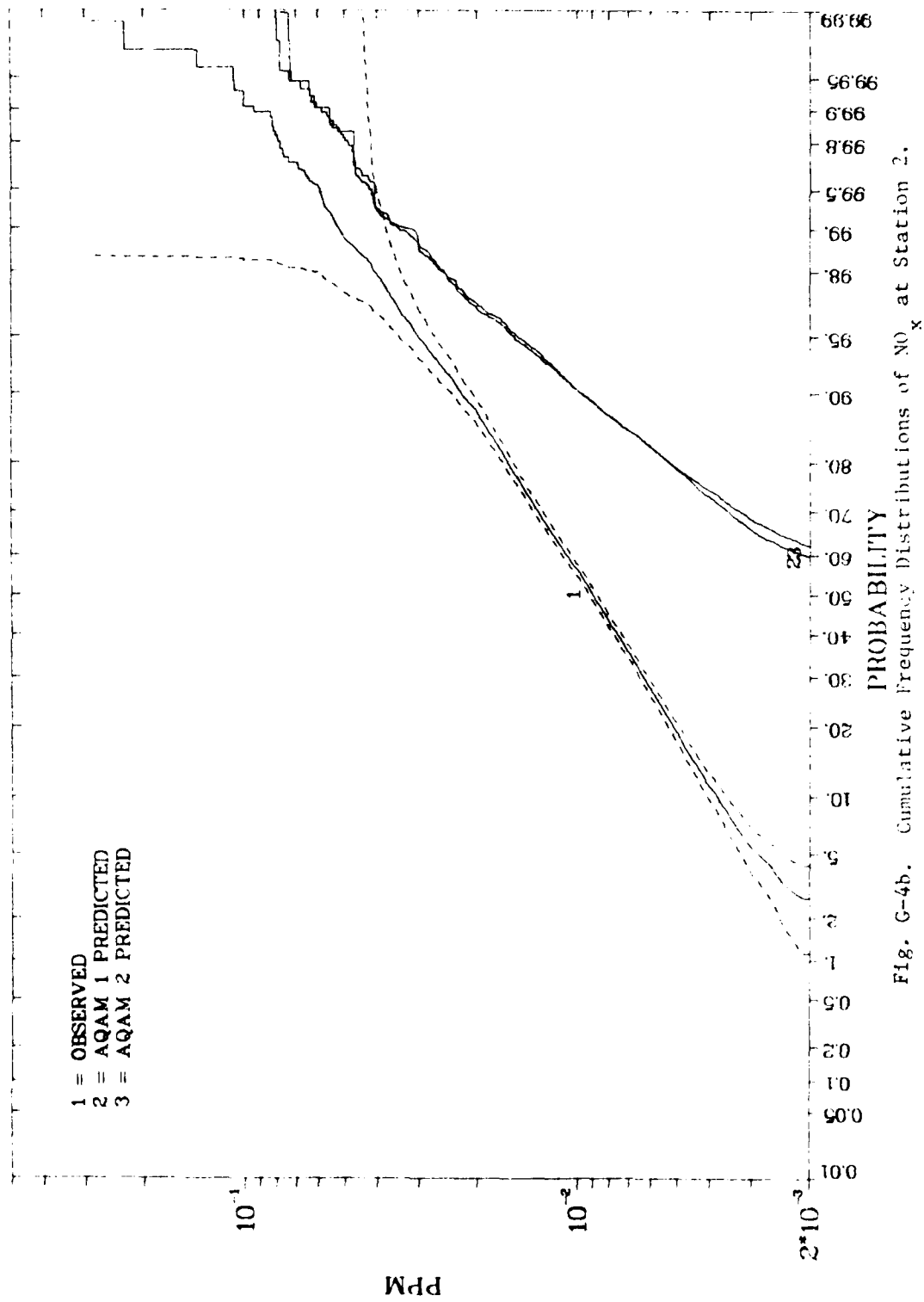


Fig. G-4b. Cumulative Frequency Distributions of NO_x at Station 2.

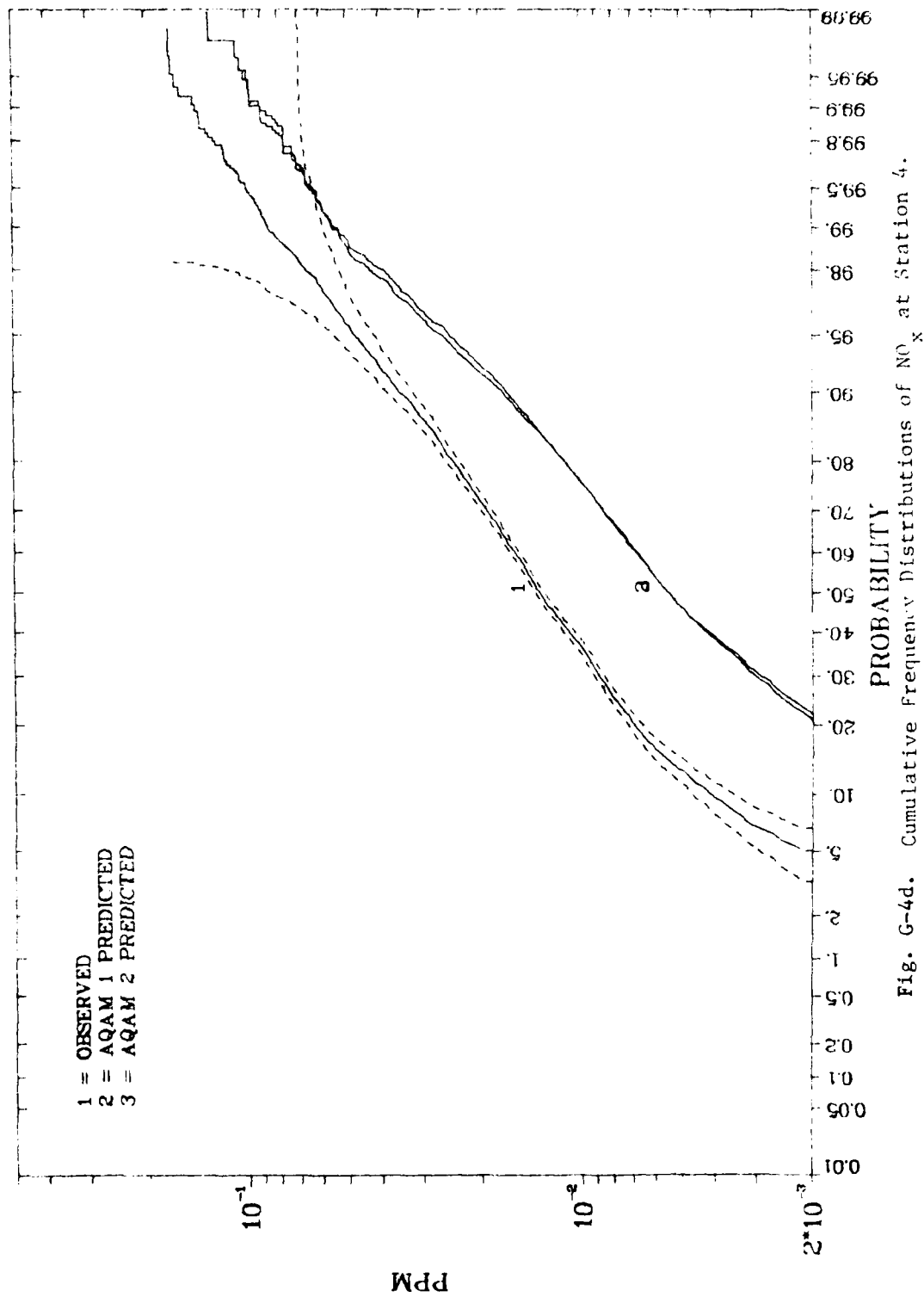


Fig. G-4d. Cumulative Frequency Distributions of NO_x at Station 4.

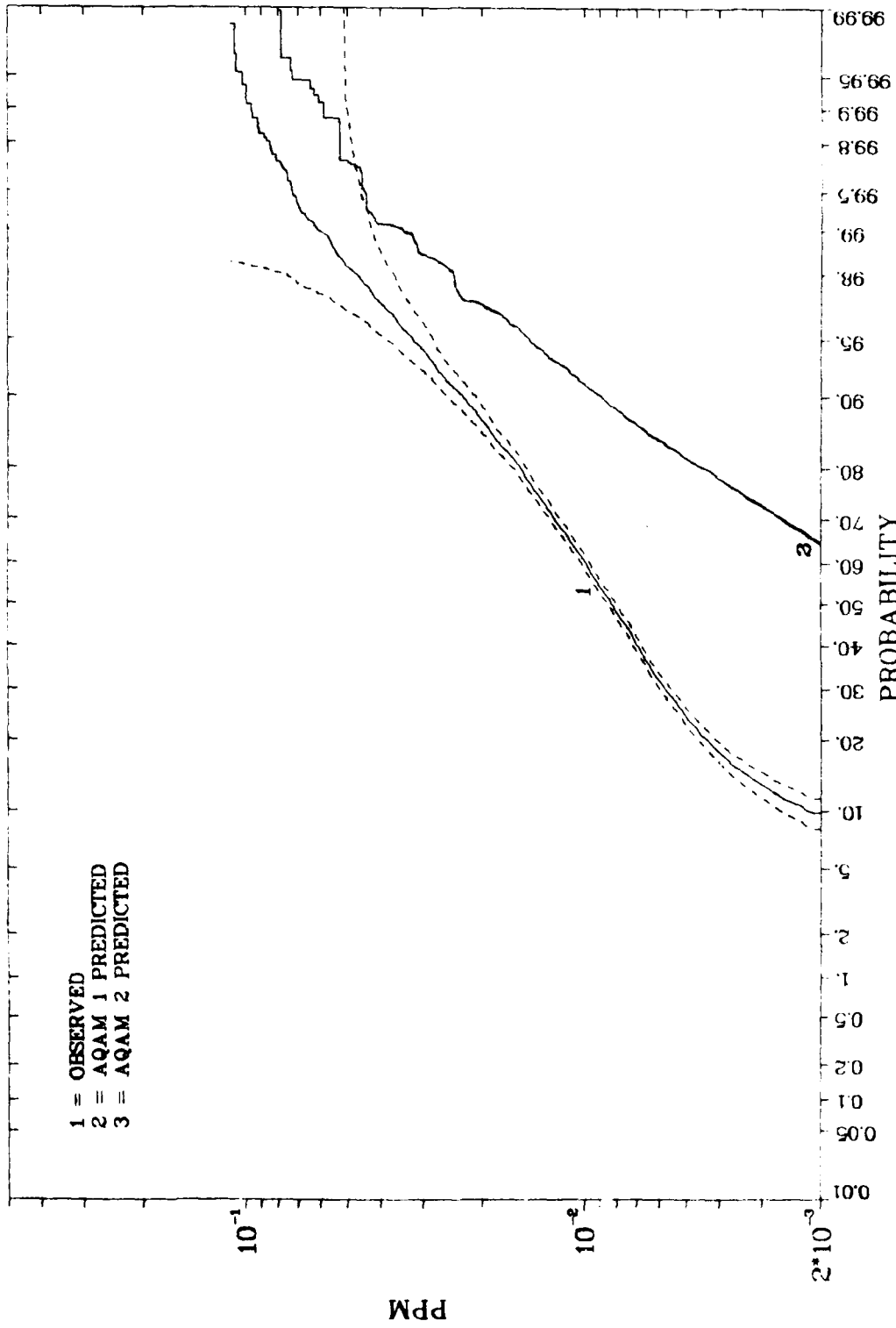


Fig. G-4e. Cumulative Frequency Distributions of NO_x at Station 5.

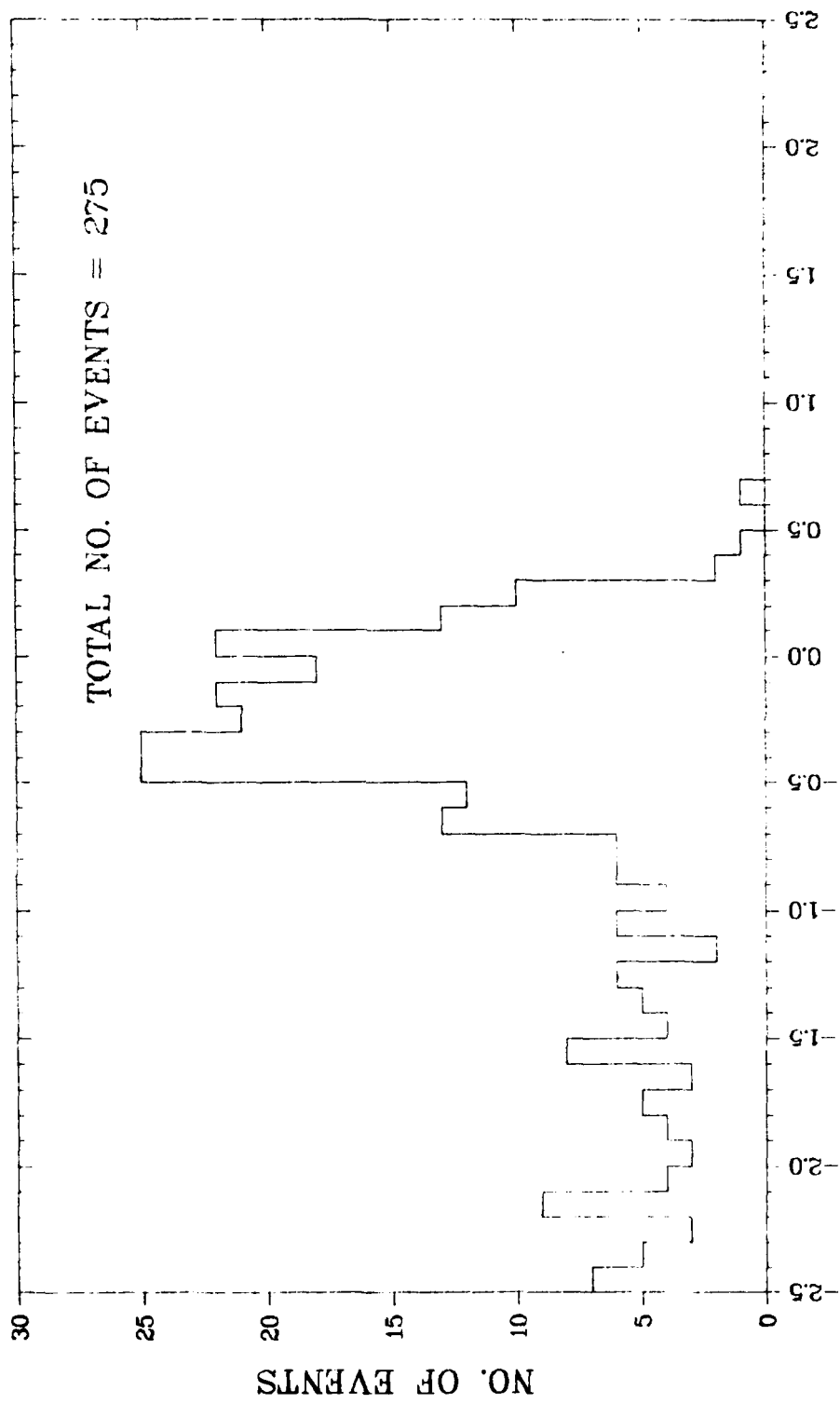


Fig. G-5a. Frequency Distribution for the Upper 10% of Observed CO Concentrations at Station 1.
Williams AFB Hourly Data

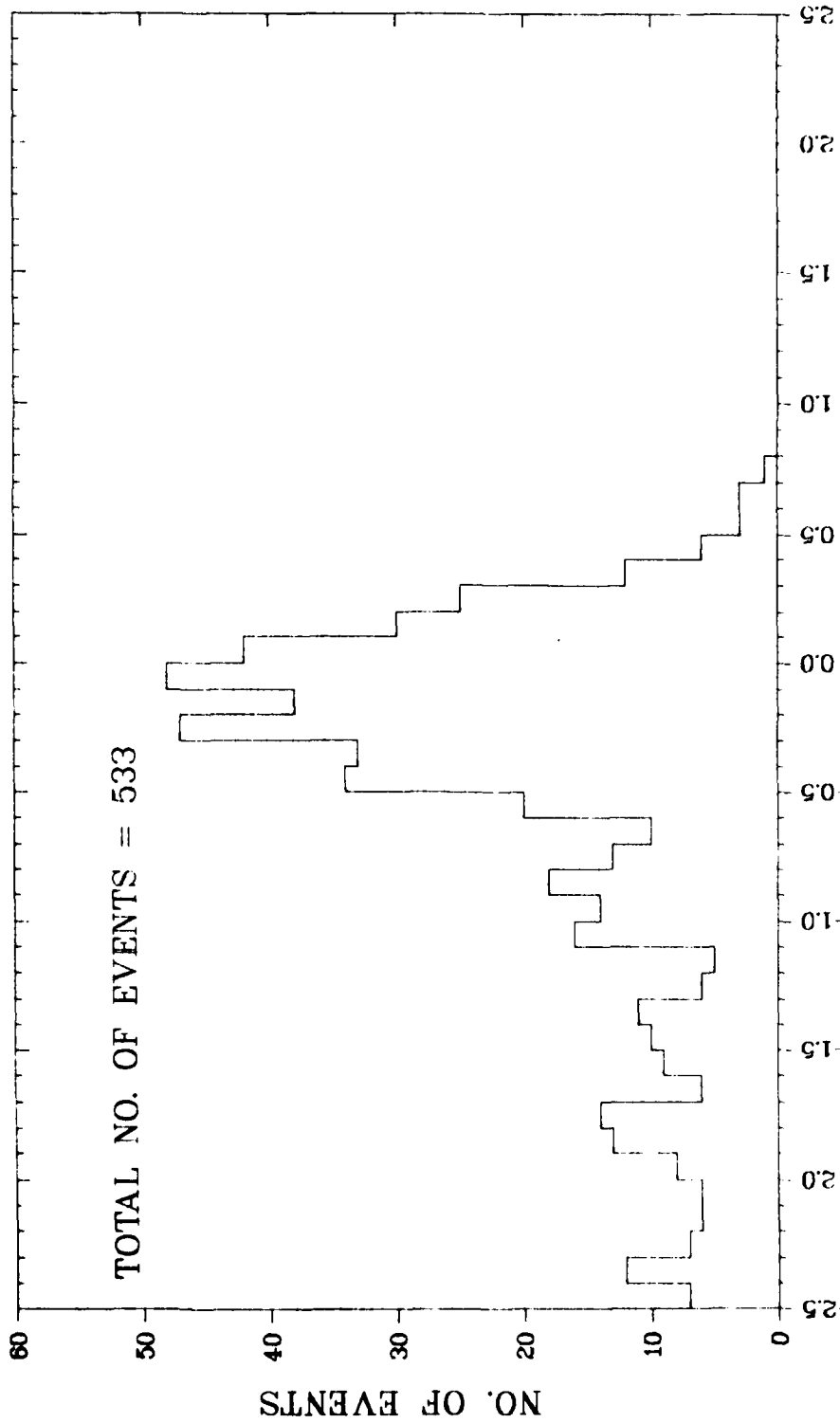


Fig. 6-5b. Frequency Distribution for the Upper 10% of Observed CO Concentrations at Station 2.
Williams AFB Hourly Data

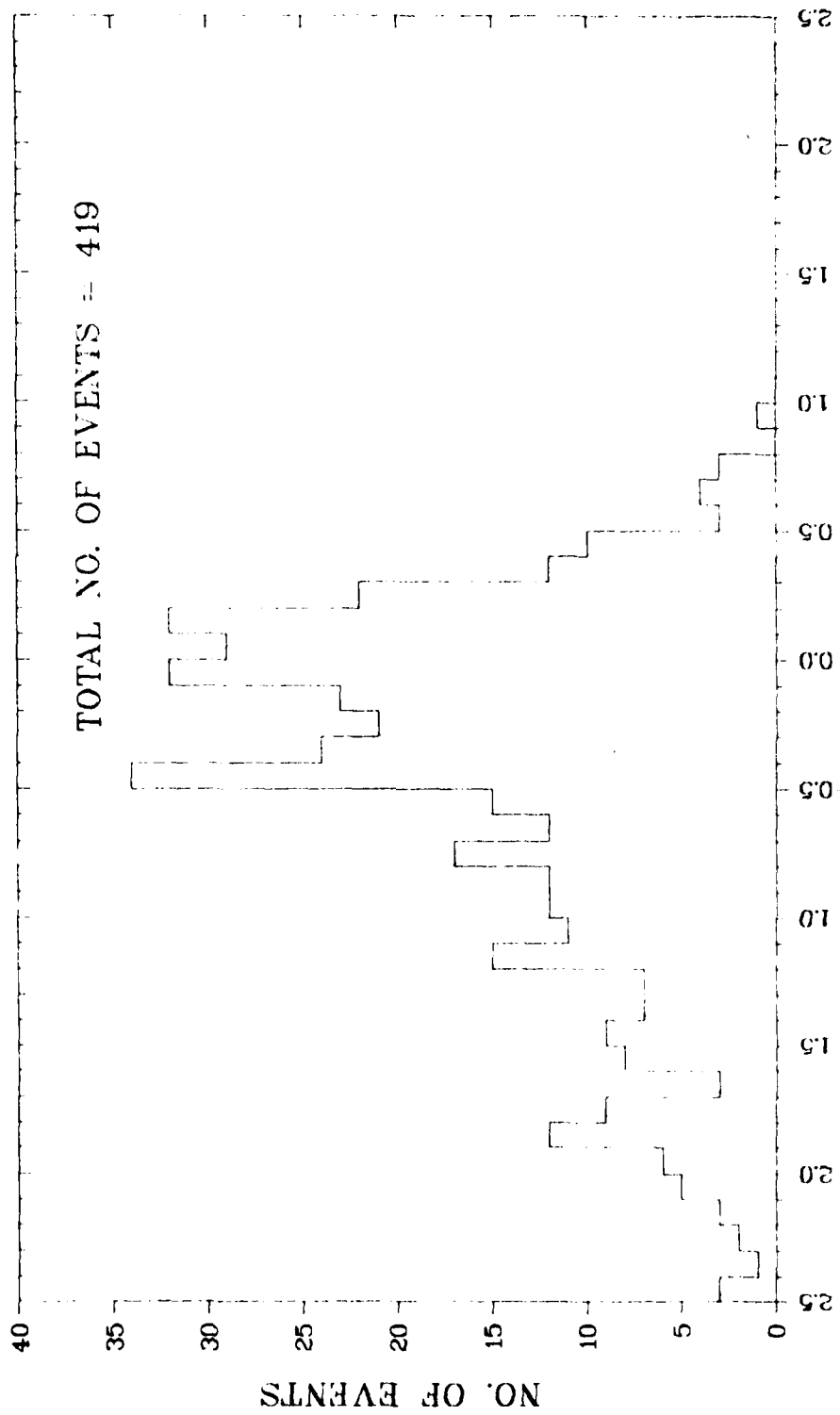


Fig. G-5c. Frequency Distribution for the Upper 9105 of Observed CO Concentrations at Station 3.
Williams AFB Hourly Data

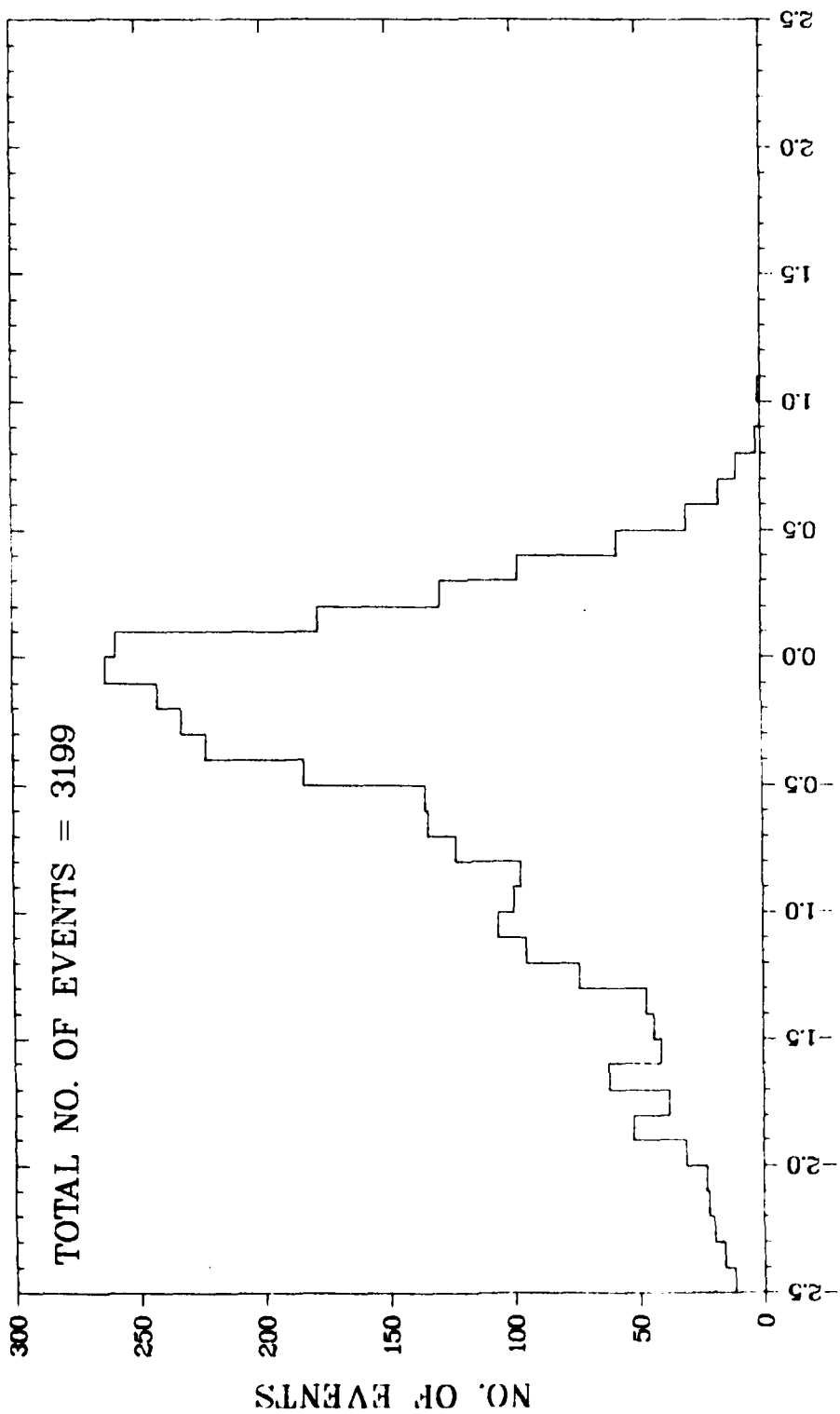


Fig. G-5d. Frequency Distribution for the Upper 10% of Observed CO Concentrations at Station 4.
Williams AFB Hourly Data

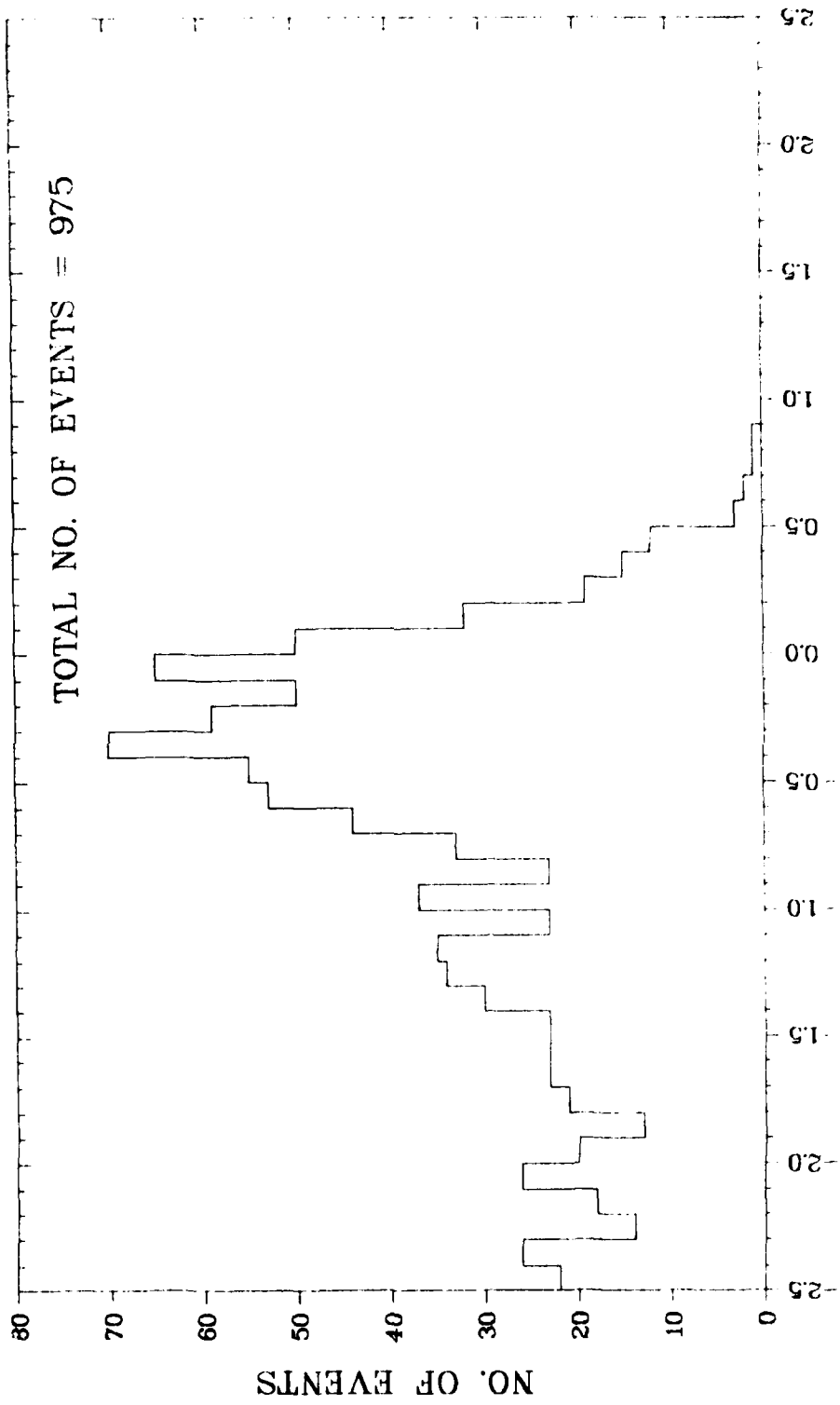


Fig. C-5e. Frequency Distribution for the Upper 10% of Observed CO Concentrations at Station 5.
Williams AFB Hourly Data

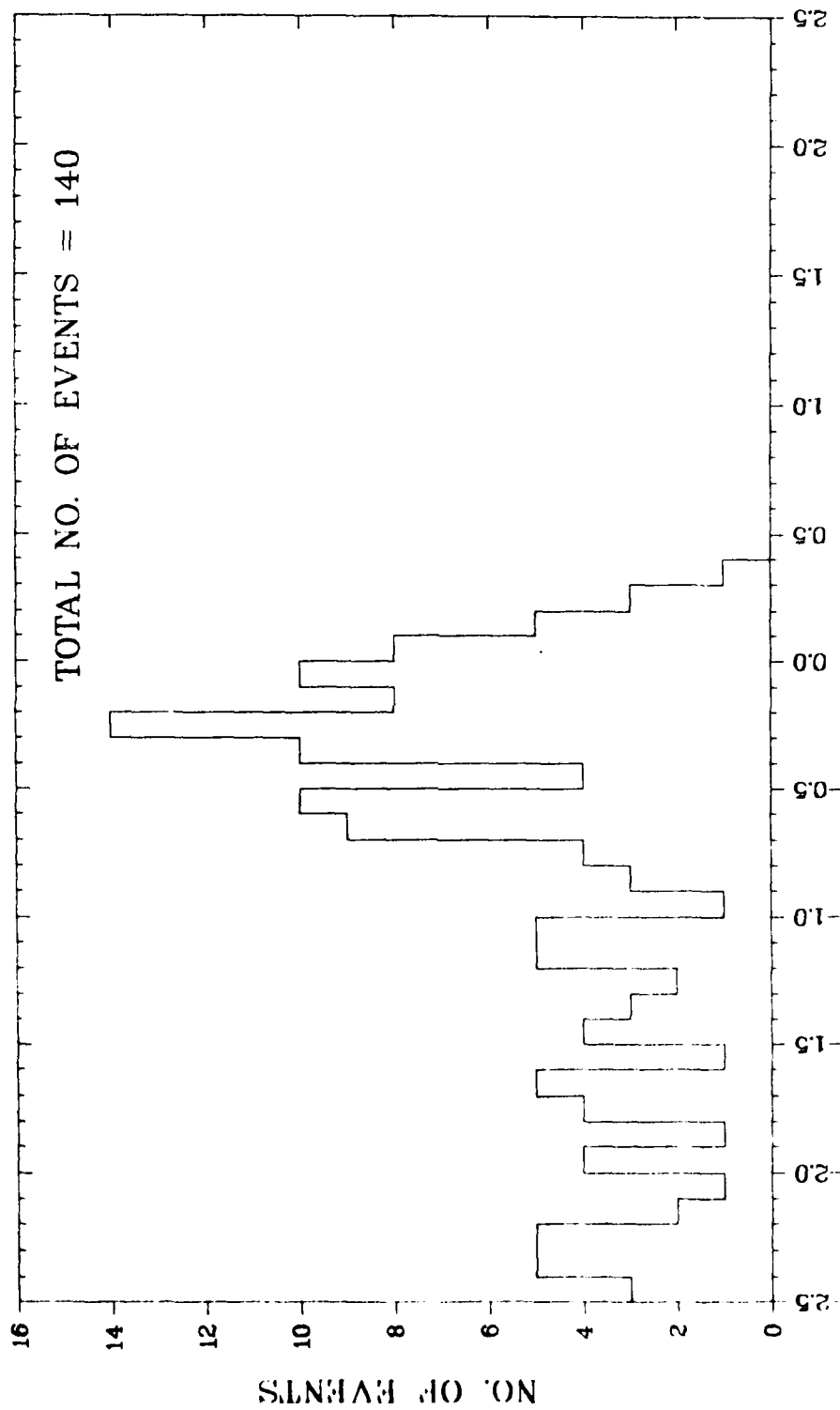


Fig. G-6a. Frequency Distribution for the Upper 10% of Observed NMHC Concentrations at Station 1.
Williams AFB Hourly Data

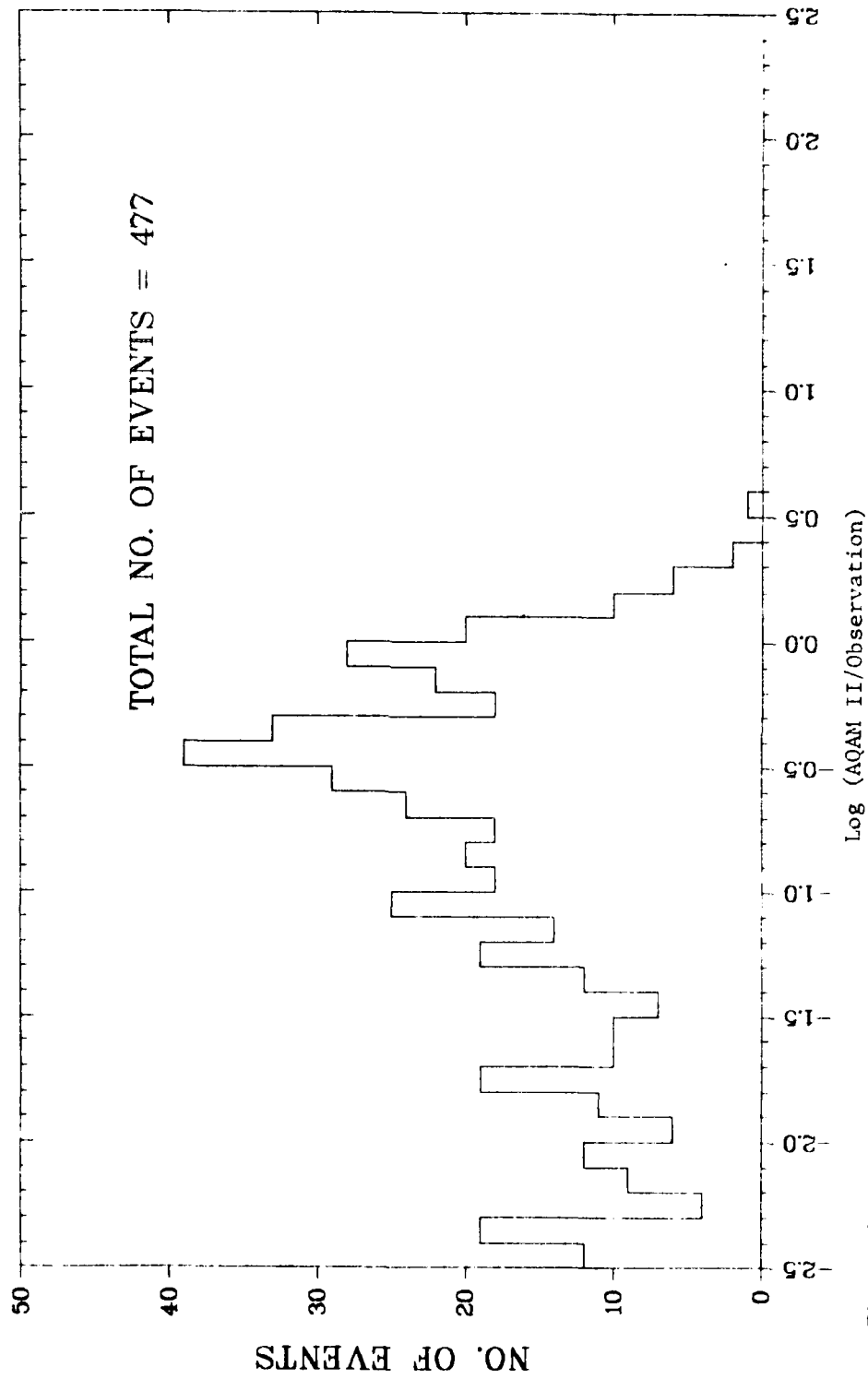


Fig. G-6b. Frequency Distribution for the Upper 10% of Observed NEMC Concentrations at Station 2.
Williams AFB Hourly Data

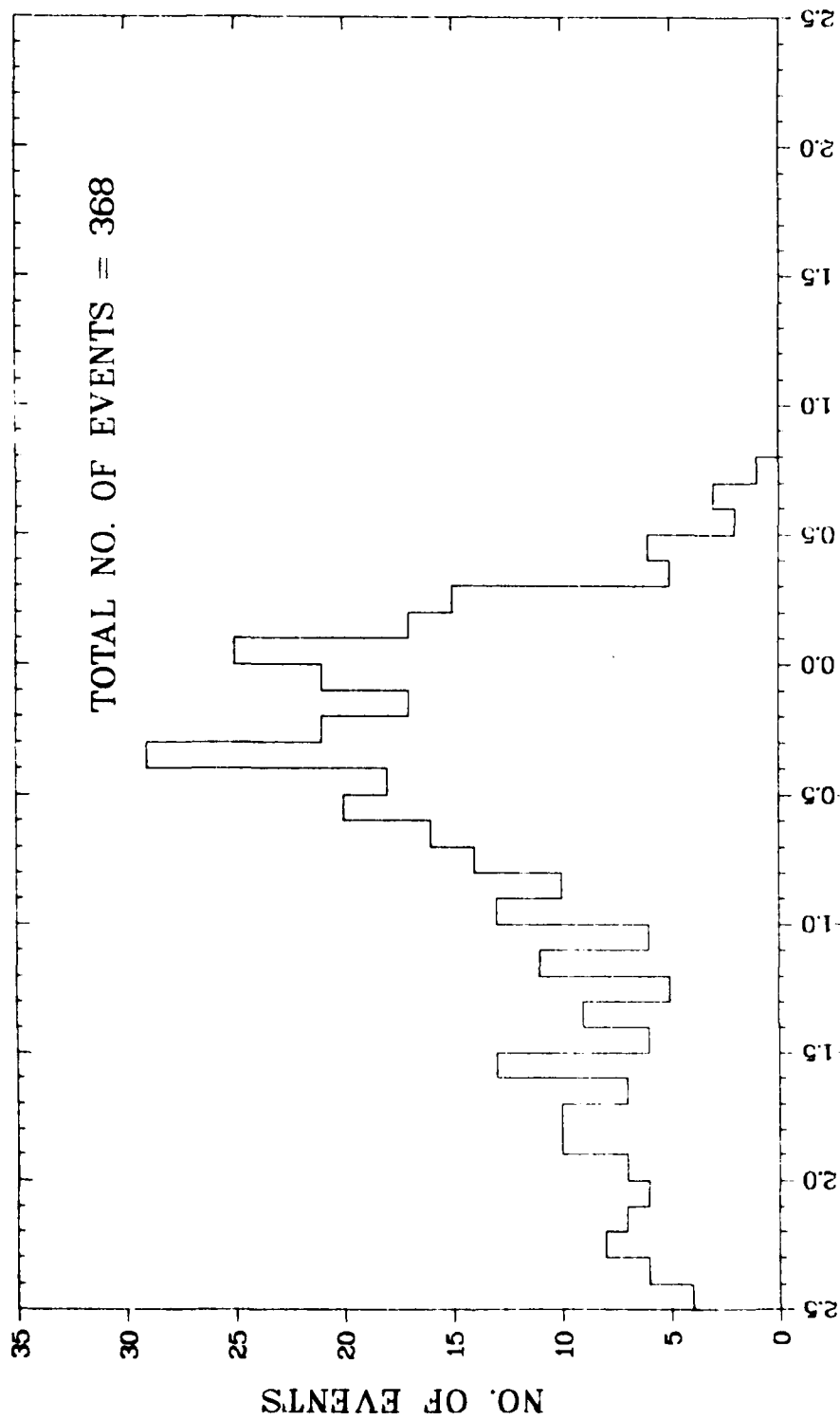


Fig. G-6c. Frequency Distribution for the Upper 10% of Observed NMHC Concentrations at Station 3.
Williams AFB Hourly Data

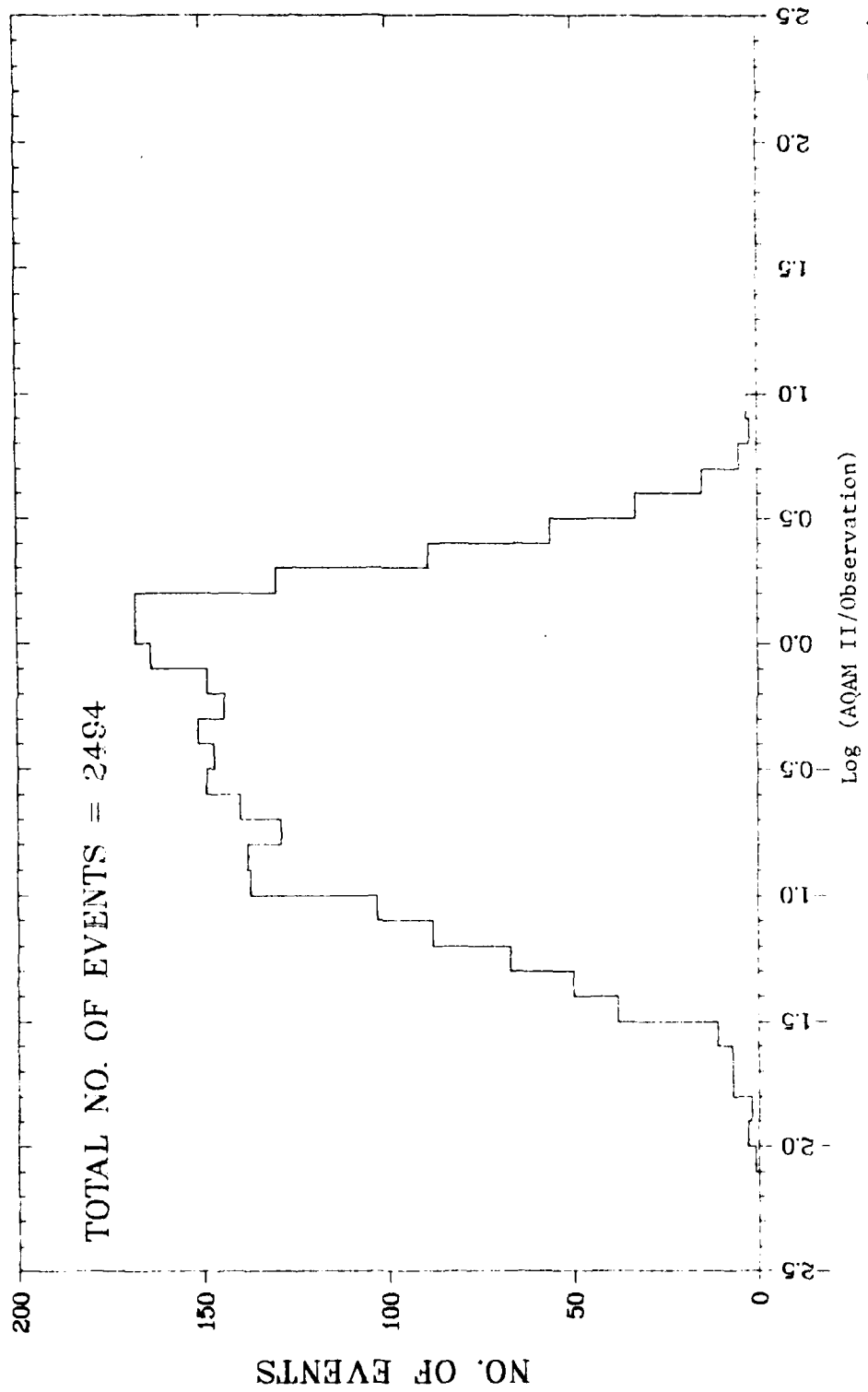


Fig. G-6d. Frequency Distribution for the Upper 10% of Observed NHC Concentrations at Station 4.
Williams AFB Hourly Data

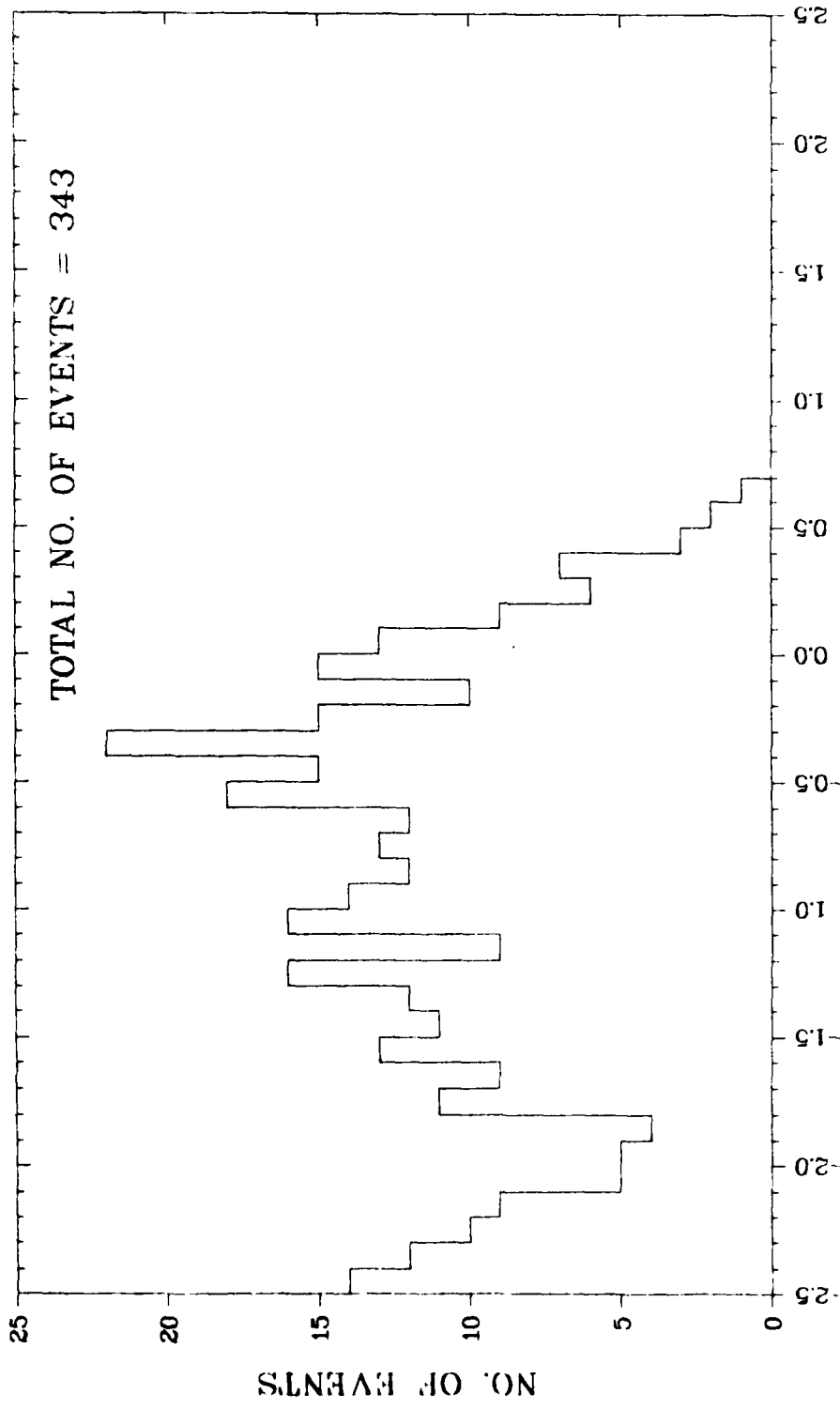


Fig. G-6e. Frequency Distribution for the Upper 10% of Observed NMHC Concentrations at Station 5.
Williams AFB Hourly Data

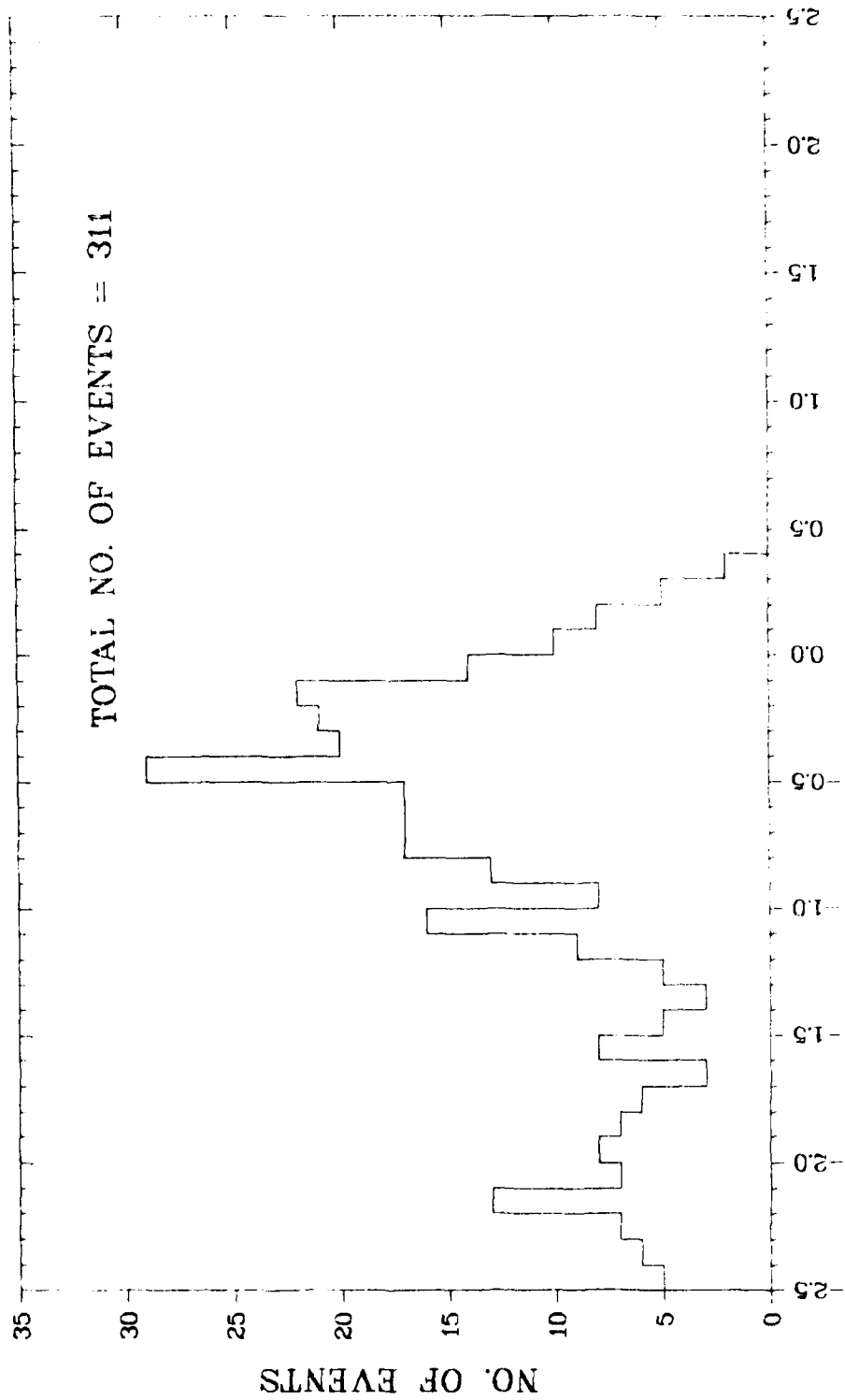


Fig. G-7a. Frequency Distribution for the Upper 10% of Observed NO_x Concentrations at Station 1.
Williams AFB Hourly Data

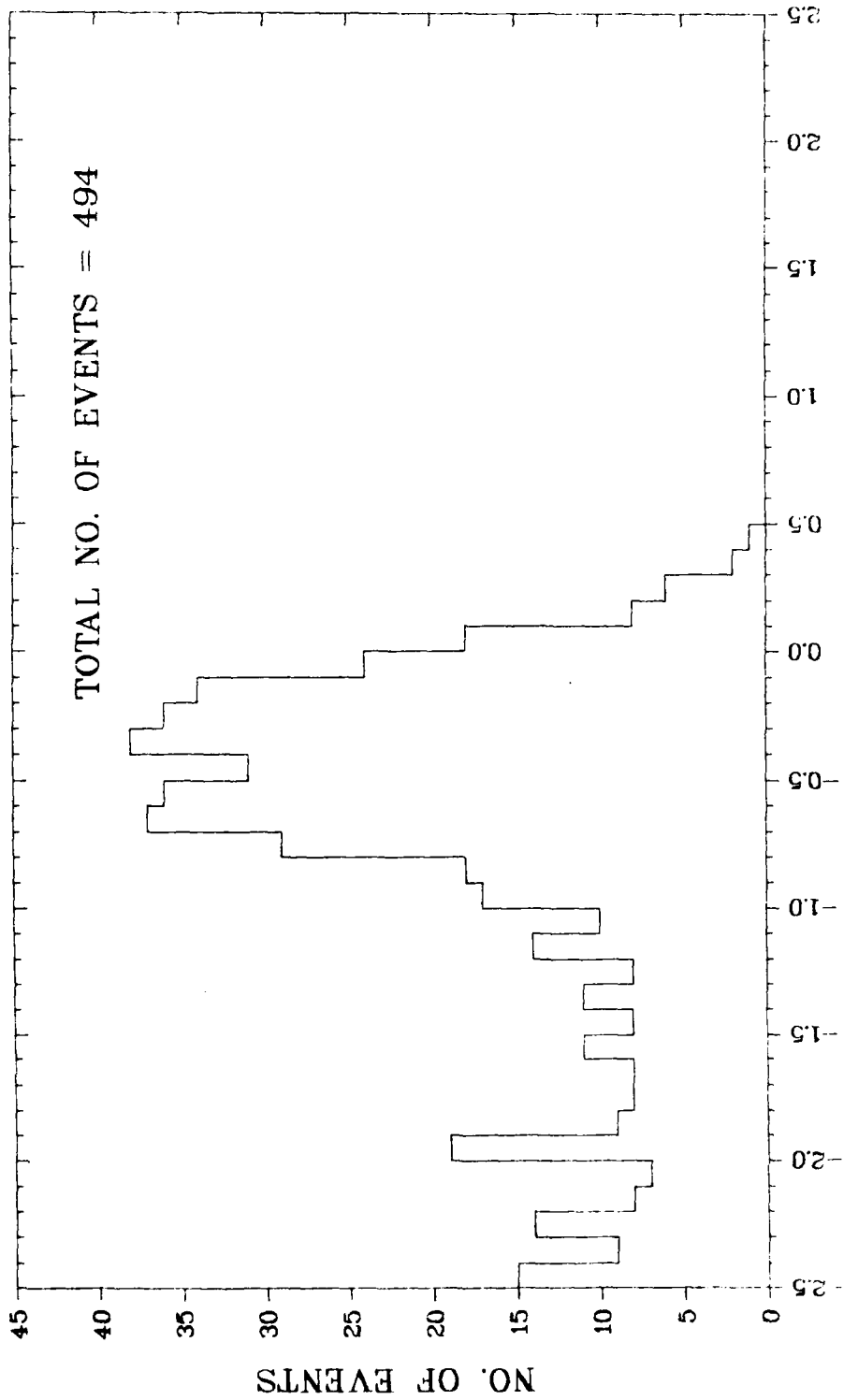


Fig. G-7b. Frequency Distribution for the Upper 10% of Observed NO_x Concentrations at Station 2.
Williams AFB Hourly Data

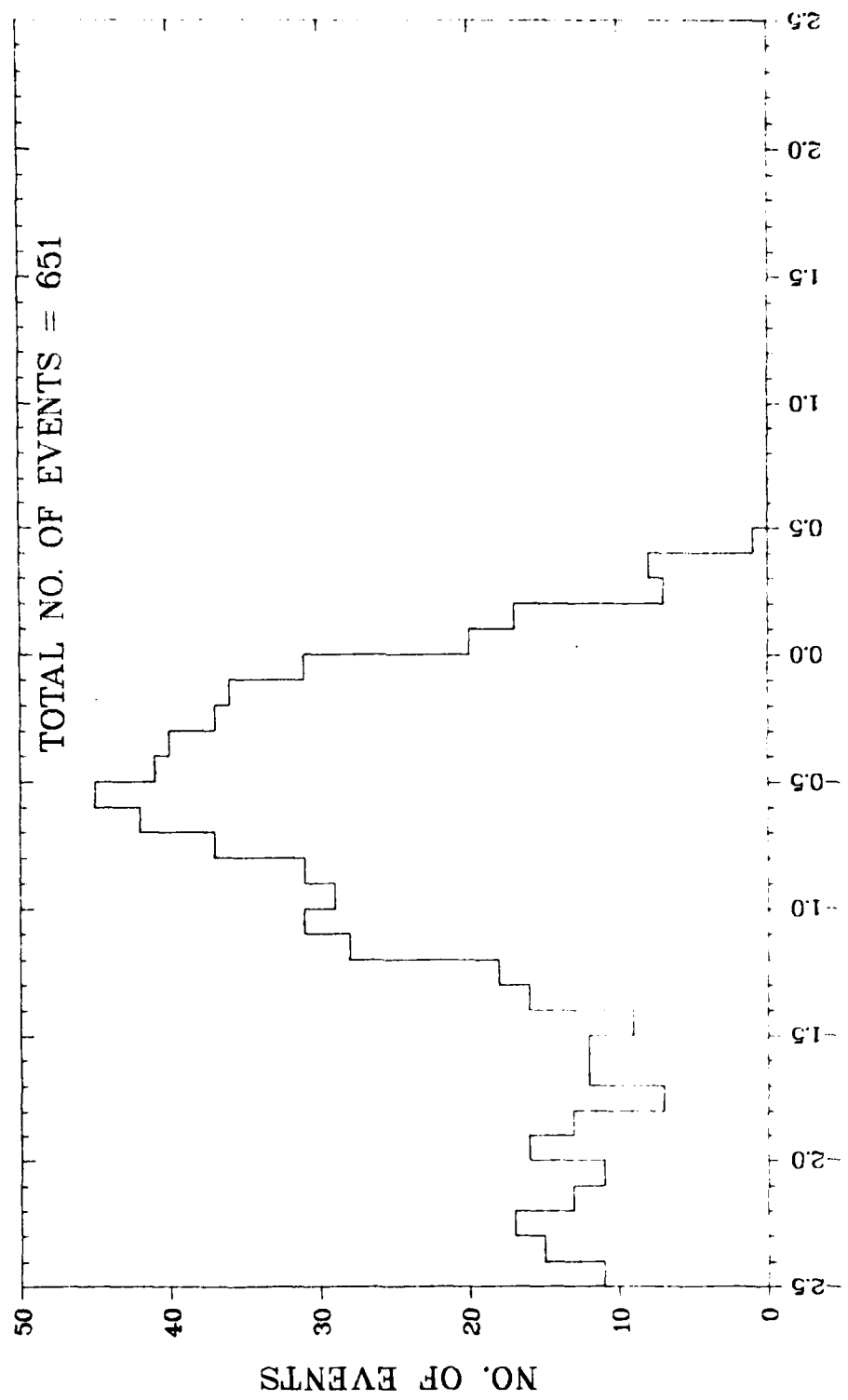


Fig. G-7c. Frequency Distribution for the Upper 10% of Observed NO_x Concentrations at Station 3.
Williams AFB Hourly Data

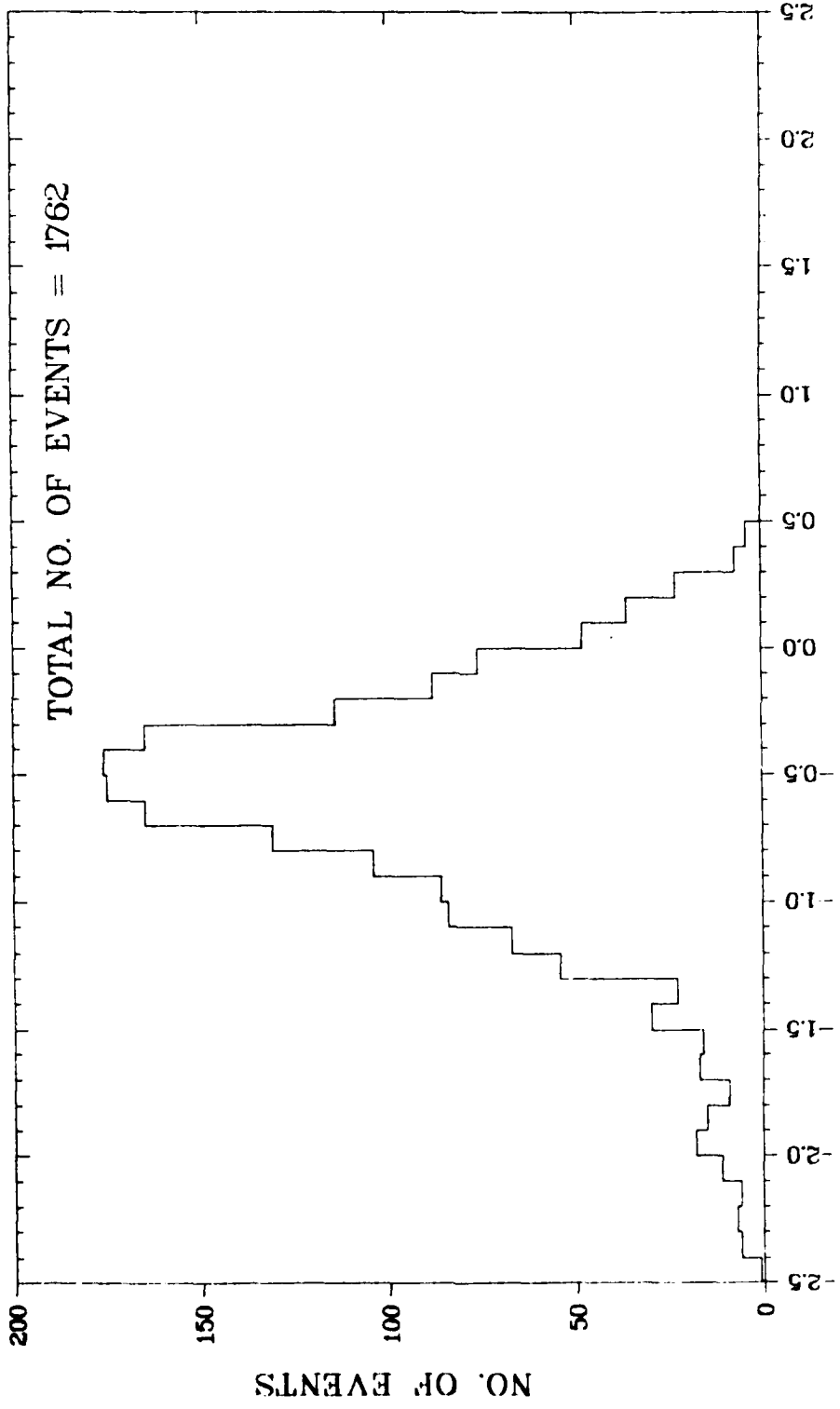


Fig. C-7d. Frequency Distribution for the Upper ~10% of Observed NO_x Concentrations at Station 4.
Williams AFB Hourly Data

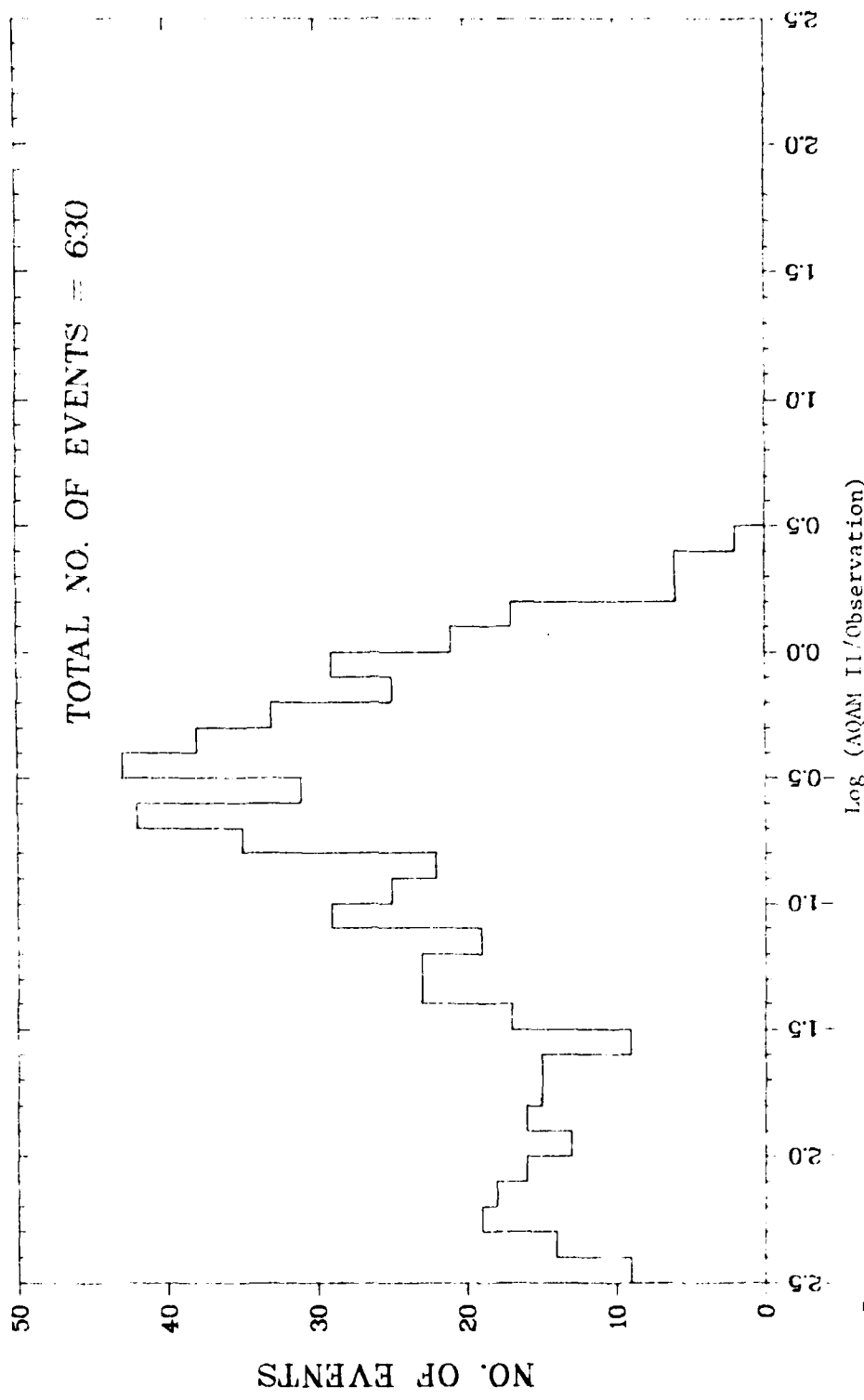


Fig. G-7e. Frequency Distribution for the Upper 10% of Observed NO_x Concentrations at Station 5.
Williams AFR Hourly Data

APPENDIX H
ANALYSIS OF HIGHER REPETITION RATE DATA

1. INTRODUCTION

During normal operations of the meteorological and aerometric monitoring facility at Williams AFB, each station and thus each experimentally measured quantity was sampled once per minute. This repetition rate was, at first, considered questionably low, especially in view of the short time scales associated with aircraft operations or atmospheric turbulence. Thus, the question was investigated of how hourly averages of once per minute compare with hourly averages computed on the basis of higher repetition rate data.

The data sample for this comparison was obtained during May 25-27, 1977, by operating the Monitor Labs 9400 Data Acquisition System at a higher sampling rate at the expense of number of channels sampled. The samples chosen for analysis consist of 17 hr of wind speed (WS), wind direction (WD), NO and NO_x data taken at 6-sec intervals, and 5 hr of vertical wind speed data taken at sampling rates as high as once per 2 sec.

The basic analysis approach was to:

- (1) calculate hourly averages using rapid scan data;
- (2) subdivide this rapid scan data into subsets containing data at 1-min intervals;
- (3) calculate hourly averages using the once-a-minute data in these subsets; and
- (4) compare the two calculations.

These data suggest that the following uncertainties related to sampling rate may be associated with the once-per-minute Williams AFB measurements.

Pollutants:	NO _x ≤ 2%
	NO ≤ 12% (usually ≤ 3%)
Meteorological quantities:	\overline{WS} ≤ 3%
	\overline{WD} ≤ 8% (of σ_θ)
	σ_θ ≤ 12% (usually ≤ 8%)
	σ_v ≤ 8%
	σ_w ≤ 17%

In the last section of this appendix, the "one-fifth" power law is investigated. This law, describing the time-dependent increase in σ_θ with averaging time raised to the power 0.2, is an assumption inherent in many air quality dispersion algorithms, including AQAM. These data suggest that between averaging times of 3-60 min this power is 0.27 ± 0.12 in agreement with the one-fifth hypothesis.

2. INDEPENDENCE OF COMPUTED HOURLY QUANTITIES FROM SAMPLING FREQUENCY

From the rapid scan data taken on days 145, 146, and 147 of the experiment, 17 hours of windspeed and wind direction measurements are available. This data, taken every six seconds, can be used to compute various hourly quantities such as hourly average windspeed, hourly σ_θ , etc. If all the 6-sec data values for 1 hr are used in these calculations, the sampling frequency of the data is once per 6 sec, whereas the sampling time (τ) is 1 hr, since hourly quantities are computed.

If, however, one only wanted data with a sampling frequency of $S=1 \text{ minute}^{-1}$, one could simply pick out every tenth data point from the $S=(6 \text{ sec})^{-1}$ data. However, because there are 10 of these data points every minute, there are 10 different times on which to start the first minute of the $S=1 \text{ min}^{-1}$ data. So, for the subsequent analyses, the $S=(6 \text{ sec})^{-1}$ data is broken up into 10 independent subsets of data for each of the 17 hr. Each subset of data therefore has a sampling frequency of once per minute.

Let

ϕ_i = the data points that make up the complete rapid scan data set, with sampling frequency $S=(6 \text{ sec})^{-1}$. i is an index.

and

ϕ_{jk}^* = the data points that make up the j^{th} subset of the $S=1 \text{ min}$ data. k is an index while j indicates the subset.

Then the process whereby the 10 subsets of $S=(1 \text{ min})^{-1}$ data are extracted from the $S=(6 \text{ sec})^{-1}$ data can be represented by:

$$\begin{aligned} \phi_{j1} &= \phi_j \\ \phi_{j2}^* &= \phi_{j+10} \\ \phi_{j3} &= \phi_{j+20} \\ &\vdots \\ \phi_{jk}^* &= \phi_{j+10(k-1)}, \\ &\vdots \\ &\vdots \end{aligned}$$

which can be repeated for each j , $j=1,2,\dots,10$. The asterisk indicates that the data has a sampling frequency of 1 min^{-1} .

The object of this part of the analysis is to compare the values of various hourly quantities obtained by using the $S=(6 \text{ sec})^{-1}$ data (all ϕ_j) to the values obtained by using the $S=1 \text{ min}^{-1}$ data (the ϕ_{jk}^*).

Let $S_{\tau}(X_i)$ be some statistical process that operates on the set of data points X_i for the sampling period τ . For example, $S_{\tau}(X_i)$ could represent an hourly average of the X_i , in which case:

$$S_{\tau}(X_i) = S_{1 \text{ hr}}(X_i) = \frac{1}{N} \sum_{i=1}^N X_i$$

where:

N = the number of X_i in 1 hr.

Then define the following operations on the meteorological data, and let the variables indicated represent the desired hourly quantities:

$\phi = S_{1 \text{ hr}}(\phi_i) =$ value obtained from the statistical process S_{τ} using the $S=(6 \text{ sec})^{-1}$ data during a 1-hr sampling interval ($\tau = 1 \text{ hr}$).

$\phi_j^* = S_{1 \text{ hr}}(\phi_{jk}^*) =$ value obtained from the statistical process S_{τ} using the $S=1 \text{ min}^{-1}$ data in the j^{th} subset during a 1-hr sampling interval.

To show the independence of $S_{1 \text{ hr}}(X_i)$ on sampling frequency S , one must compare the value ϕ (the hourly quantity computed from $S=(6 \text{ sec})^{-1}$ data) to the ϕ_j^* values (the hourly quantity computed from each of the $S=1 \text{ min}^{-1}$ data subsets). But because there are ten ϕ_j^* values (one for each subset of $S=1 \text{ min}^{-1}$ data), it is convenient to define some method for comparing these values without having to look at each ϕ_j^* . However, since each subset ϕ_{jk}^* has the same chance of being selected as a unique set of minute-averaged data (assuming a random start time for data collection), all ϕ_j^* values should be considered when comparisons with ϕ are made. Thus it is reasonable to define a "standard deviation" that measures the distribution of the ϕ_j^* values around the ϕ value:

$$\sigma(\phi) = \left[\frac{1}{10} \sum_{j=1}^{10} (\phi_j^* - \phi)^2 \right]^{1/2} \quad (B-1)$$

where:

$\sigma(X)$ = the standard deviation of the ϕ_j^* 's around the value X .

A low value for $\sigma(\phi)$ would imply that the hourly quantities computed from the $S=1 \text{ min}^{-1}$ data (ϕ_j^*) and the $S=(6 \text{ sec})^{-1}$ data (ϕ) are nearly the same, and therefore, that the operation $S_{1 \text{ hr}}(X_i)$ is independent of the averaging time of the data X_i .

One may further define the mean value of the ϕ_j^* 's

$$\bar{\phi}^* = \frac{1}{10} \sum_{j=1}^{10} \phi_j^* \quad (\text{H-2})$$

As a measure of how well the value $\bar{\phi}^*$ represents the individual quantities ϕ_j^* , use the standard deviation:

$$\sigma(\bar{\phi}^*) = \left[\frac{1}{10} \sum_{j=1}^{10} (\phi_j^* - \bar{\phi}^*)^2 \right]^{1/2} \quad (\text{H-3})$$

In cases where S defines an arithmetic average, ϕ will be exactly equal to $\bar{\phi}^*$. For other processes, however $\bar{\phi}^*$ can be used as a representative value for the individual ϕ_j^* 's and may differ from the value ϕ .

As an example of this approach, suppose that $S_{\tau}(X_i)$ represents the hourly average of X_i , and that the ϕ_i are the rapid scan measurements of wind speed.

Then

$$\phi_i = WS_i$$

$$\phi_{jk}^* = WS_{jk}^*$$

$$\phi = \overline{WS} = S_{1 \text{ hr}}(WS_i) = \frac{1}{600} \sum_{i=1}^{600} WS_i,$$

$$\phi_j^* = WS_j^* = S_{1 \text{ hr}}(WS_{jk}^*) = \frac{1}{60} \sum_{k=1}^{60} WS_{jk}^*,$$

$$\sigma(\phi) = \sigma(\overline{WS}) = \left[\frac{1}{10} \sum_{j=1}^{10} (\overline{WS}_j^* - \overline{WS})^2 \right]^{1/2},$$

$$\bar{\phi}^* = \overline{WS}^* = \frac{1}{10} \sum_{j=1}^{10} \overline{WS}_j^*, \text{ and}$$

$$\sigma(\bar{\phi}^*) = \sigma(\overline{WS}^*) = \left[\frac{1}{10} \sum_{j=1}^{10} (\overline{WS}_j^* - \overline{WS}^*)^2 \right]^{1/2}.$$

Or suppose that $S_{\tau}(X_i)$ represents the hourly standard deviation of the wind direction, σ_{θ} . Then:

$$\phi_i = WD_i,$$

$$\phi_{jk}^* = WD_{jk}^*,$$

$$\phi = \sigma_\theta = \left[\frac{1}{600} \sum_{i=1}^{600} (WD_i - \overline{WD})^2 \right]^{1/2},$$

$$\phi_j^* = \sigma_{\theta_j}^* = \left[\frac{1}{60} \sum_{k=1}^{60} (WD_{jk}^* - \overline{WD}_j^*)^2 \right]^{1/2},$$

$$\sigma(\phi) = \sigma(\sigma_\theta) = \left[\frac{1}{10} \sum_{j=1}^{10} (\sigma_{\theta_j}^* - \sigma_\theta)^2 \right]^{1/2},$$

$$\overline{\phi^*} = \overline{\sigma_\theta^*} = \frac{1}{10} \sum_{j=1}^{10} \sigma_{\theta_j}^*, \text{ and}$$

$$\sigma(\overline{\phi^*}) = \sigma(\overline{\sigma_\theta^*}) = \left[\frac{1}{10} \sum_{j=1}^{10} (\sigma_{\theta_j}^* - \overline{\sigma_\theta^*})^2 \right]^{1/2}.$$

If a computed quantity ϕ (such as WS, WD, σ_θ) is independent of the sampling frequency S (at least to the extent of S being either $(6 \text{ sec})^{-1}$ or 1 min^{-1}), then one would expect that $\sigma(\phi)$ will have a low value, indicating that the ϕ_j^* 's are very close in value to ϕ .

Let V_i represent each individual wind-speed measurement and let θ_i represent each individual wind-direction measurement. Then, the equations actually used to compute each of the hourly quantities are as follows:

average wind speeds:

$$\overline{WS} = \frac{1}{N} \sum_{i=1}^N V_i, \quad (\text{H-4})$$

average wind direction

$$\overline{WD} = \tan^{-1} \left[\frac{\sum_{i=1}^N \sin \theta_i}{\sum_{i=1}^N \cos \theta_i} \right] \quad (\text{H-5})$$

vector mean wind speed:

$$VMWS = \frac{1}{N} \left[\left(\sum_{i=1}^N v_i \sin \theta_i \right)^2 + \left(\sum_{i=1}^N v_i \cos \theta_i \right)^2 \right]^{1/2}, \text{ and} \quad (H-6)$$

vector mean wind direction:

$$VMWD = \tan^{-1} \left[\frac{\sum_{i=1}^N v_i \sin \theta_i}{\sum_{i=1}^N v_i \cos \theta_i} \right]. \quad (H-7)$$

The standard deviation is defined by:

$$\sigma_{\bar{X}} = \left[\frac{1}{N} \sum_{i=1}^N (X_i - \bar{X})^2 \right]^{1/2}.$$

In computing the standard deviations of the above quantities one should note that for wind directions the smallest angle between X_i and \bar{X} is used; that is, $X_i - \bar{X}$ is always less than or equal to π radians.

The results of these calculations for the 17 hr of rapid scan meteorological data are shown in Tables H-1 through H-6.* The important thing to notice in these tables is the low value of $\sigma(\phi)$ in most cases -- implying good agreement between the ϕ and ϕ_j^* values. In the case of the hourly average wind direction \overline{WD} , the largest value of $\sigma(\overline{WD})$ one encounters is 2.4° . For hourly \overline{VMWD} , the maximum $\sigma(\overline{VMWD})$ is 2.2° . Both values are well within the range of instrument error. For \overline{WS} the largest percentage deviation ($\sigma(\phi_0)/\phi \times 100\%$) is 3% and for \overline{VMWS} is 4%, but most values of $\sigma(\phi)$ are less than or equal to 2% of the value of ϕ itself. In the case of σ_{θ} , the relative values of $\sigma(\theta_0)$ are larger, ranging between 1 and 12% but with over 1/2 of the values at or below 6%. Therefore, the value one computes for a quantity during a given hour will not depend greatly on whether the data used for the computations was taken at six-second intervals or one-min intervals during that hour.

In addition, from the values of the standard deviation of $\sigma(\overline{\phi^*})$, it is apparent that the values computed from the $S=1 \text{ min}^{-1}$ data subsets (ϕ_j^*) do not differ widely from their mean. This lack of spread implies that $\overline{\phi^*}$ is representative of the individual ϕ_j^* and that the starting time of the first minute is not important -- any set of minute-averaged data recorded during an hour is just as valid for computational purposes as any other set that starts at a different time.

So it is apparent that any minute-averaged data, regardless of the starting point during an hour, is just as acceptable for use in computing

*Tables and figures appear consecutively at the end of this appendix.

hourly quantities as data taken with a higher scan rate, at least down to $S = (6 \text{ sec})^{-1}$. Hence, if computations are to be done only for 1-hr sampling periods, nothing substantial is gained by using a scan interval of 6 sec instead of 1 min.

In the same manner, hourly average pollutant concentrations can be checked for dependence on the scan interval S . Along with the meteorological data, NO and NO_x were recorded at 6-sec intervals during the 17 hr on days 145, 146 and 147.

Tables H-7 and H-8 contain the results of the same calculations using this NO and NO_x data. Again, notice the good agreement indicated by the low values of $\sigma(\phi)$ for most hours. For NO_x , the value of $\sigma(\text{NO}_x)$ is never more than 2% of the value for NO_x itself. The values for $\sigma(\text{NO})$ are relatively larger, ranging from 1 to 12% of the value of NO . For most hours, however, the ratio is under 3%.

Therefore, as in the case for the hourly meteorological quantities, data taken with a scan interval of one minute as opposed to six seconds seems to make very little difference in the values computed for the hourly average concentration.

3. THE EFFECT OF SCAN RATE ON THE AVERAGE VERTICAL WIND SPEED AND THE STANDARD DEVIATION

Let W represent the vertical velocity of the air as measured by a vertical propeller. The data used to compute \bar{W} (the average vertical wind speed) and σ_W (the standard deviation of the vertical wind speed) comes from five hours of measurements taken at various sampling frequencies. The notation used here is the same as used in the previous section, with the exception that now there is more than one rapid sampling rate. However, the object still is to compare the results obtained using data with a short-scan interval (the computed quantity denoted by ϕ) to the results obtained using $S=1 \text{ min}^{-1}$ data (the quantities denoted by ϕ_j^*).

As before, the $S=1 \text{ min}^{-1}$ data is obtained by selecting points from the rapid-scan data at 1-min intervals. Because the shortest scan interval varies for different hours there will be a different number of subsets of minute-interval data in each case. In general, for this minute-interval data ϕ_{jk}^* , $j=1, 2, \dots, 60s$, where S is the sampling frequency. The use of the standard deviation $\sigma(\phi)$ to compare the ϕ_j^* values to ϕ is very helpful here because $\sigma(\phi)$ accounts for the different numbers of ϕ_j^* values.

Tables H-9 and H-10 show the values calculated for σ_W and \bar{W} . A sampling period of 1 hr is used here, and, as in the last section, the relation between ϕ and the ϕ_j^* is emphasized. In this case, however, notice that the agreement between the ϕ values and the ϕ_j^* values is very poor, as indicated by the large values of $\sigma(\phi)$. For σ_W , the values of $\sigma(\sigma_W)$ are on the order of 10% of the σ_W value itself. For \bar{W} , the relative values of $\sigma(\bar{W})$ are much higher, ranging between 13 and 73% of the value for \bar{W} . Thus, it is obvious that the scan rate for vertical wind speed data does influence the calculated hourly quantities. This influence could be due to the large deviations

encountered in the vertical wind speed -- notice that σ_w is always larger than \bar{W} . A one-minute-scan interval may not provide enough detail of the W trace for use in calculating an hourly quantity that is representative (i.e., one that is independent of the starting time of the first minute). So for vertical wind speeds, a scan rate higher than once per minute is desirable.

One other interesting point to notice is the diurnal variations of \bar{W} . Of course, no definite conclusions can be drawn from five hourly averages, but it is reassuring to see that the highest values of \bar{W} occur in the afternoon, when the temperature lapse rate is maximum; whereas at night and in the morning, when conditions are more stable, the \bar{W} values are lower.

4. THE STANDARD DEVIATION OF THE WIND DIRECTION AS A FUNCTION OF SAMPLING TIME

It has been suggested that the standard deviation of the wind direction, σ_θ , depends on the sampling time in the following way:

$$\frac{\sigma_\theta(\tau)}{\sigma_\theta(\tau_0)} = \left(\frac{\tau}{\tau_0}\right)^{0.2} \quad (\text{H-8})$$

where:

- τ_0 = a reference sampling time,
- $\sigma_\theta(\tau_0)$ = standard deviation of the wind direction calculated with sampling time τ_0 , and
- $\sigma_\theta(\tau)$ = standard deviation of the wind direction calculated with sampling time τ .

The 17 hr of rapid-scan meteorological data provide a data base with which to test this equation, since, even for short sampling times, there will still be a suitable number of data points available for the calculations of σ_θ .

Equation (H-8) will be tested for three sampling times: $\tau = 3$ min, 10 min, and 1 hr. In all comparisons, τ is taken as the shorter sampling time. However, to compare $\sigma_\theta(\tau)$ and $\sigma_\theta(\tau_0)$, the average of the $\sigma_\theta(\tau)$'s during the longer sampling period τ_0 is used as the value to be compared with $\sigma_\theta(\tau_0)$.

Assuming that the form of Eq. (H-8) is correct (i.e., that it is a power law relation), the exponent can be optimized with respect to our data in order to check the agreement. Generalize Eq. (H-8) by using a variable p as the exponent:

$$\frac{\sigma_\theta(\tau)}{\sigma_\theta(\tau_0)} = \left(\frac{\tau}{\tau_0}\right)^p \quad (\text{H-9})$$

Taking the log of both sides, rewrite Eq. (H-9) as:

$$p = \frac{\log \left(\frac{\sigma_{\theta}(\tau)}{\sigma_{\theta}(\tau_0)} \right)}{\log \left(\frac{\tau}{\tau_0} \right)} \quad (\text{H-10})$$

For each set of calculated σ_{θ} 's [$\sigma_{\theta}(\tau)$ and $\sigma_{\theta}(\tau_0)$] a value for p can be determined. The mean of these values for p , denoted as \bar{p} , can be used as the value for the exponent in Eq. (H-9). The standard deviation is then an indication of how representative \bar{p} is for different conditions.

In Tables H-11 to H-13 a value for p is calculated for each of the 17 hr of rapid-scan data using different combinations of sampling times. Note that the mean values for p determined from data are higher than the exponent value used in Eq. (H-8). For $\tau=3$ min and $\tau_0=60$ min, $\bar{p}=0.265$ with a standard deviation of 0.116. For $\tau=10$ min and $\tau_0=60$ min, $\bar{p}=0.227$ with a standard deviation of 0.125. For $\tau=3$ min and $\tau_0=10$ min, $\bar{p}=0.322$ with a standard deviation of 0.134. This last comparison, however, is between the averages of the σ_{θ} (3 min) values and σ_{θ} (10 min) values during each hour.

With such relatively large standard deviations, it is apparent that Eq. (H-9) is only a first approximation of the relationship between σ_{θ} and sampling time.

Instead of this power law relation, an exact identity can be derived that relates a σ_{θ} calculated for a given sampling period to the σ_{θ} 's calculated for a set of shorter sampling periods that lie within the longer period. Specifically, suppose one has a set of wind direction measurements taken with a scan interval of s seconds. If the longer sampling interval is denoted by τ_L and the shorter sampling interval by τ_S , then there are exactly $J=\tau_L/\tau_S$ short sampling periods contained in the long interval.

If j is an index that represents the position of the short sampling period during the longer one and i is an index that represents the position of a wind direction measurement during the shorter sampling period, then the individual wind direction measurements can be represented by θ_{ij} , where $i=1, 2, \dots, I$ and $j=1, 2, \dots, J$. I is the number of measurements taken during the short sampling interval τ_S . The mean wind direction during the longer sampling period is

$$\theta(\tau_L) = \frac{1}{IJ} \sum_i \sum_j \theta_{ij},$$

and the mean wind direction during each short sampling period is

$$\theta_j(\tau_S) = \frac{1}{I} \sum_i \theta_{ij}.$$

The standard deviation of the wind direction for the long and short sampling periods is defined as

$$\sigma_{\theta}(\tau_L) = \left[\frac{1}{I} \sum_i \sum_j (\bar{\theta}(\tau_L) - \theta_{ij})^2 \right]^{1/2},$$

$$\sigma_{\theta}(\tau_S) = \left[\frac{1}{I} \sum_i (\bar{\theta}_j(\tau_S) - \theta_{ij})^2 \right]^{1/2}.$$

By squaring and expanding the expression for $\sigma_{\theta}(\tau_L)$, adding and subtracting the second term, on the right hand side of Eq. (H-11), and substituting from the other equations, the following relationship can be obtained:

$$\sigma_{\theta}^2(\tau_L) = \frac{1}{J} \sum_j \sigma_{\theta j}^2(\tau_S) + \frac{1}{J} \sum_j (\bar{\theta}(\tau_L) - \bar{\theta}_j(\tau_S))^2. \quad (H-11)$$

This is an exact equation that relates the σ_{θ} 's calculated, over several short sampling periods to a σ_{θ} that would be calculated if these short periods were combined into one long sampling period.

Using one hour as the long sampling period τ_L and 3 and 10 minutes as two different short sampling periods τ_S , values for $\theta_j(\tau_S)$ and $\sigma_{\theta j}(\tau_S)$ can be computed from the rapid-scan, wind direction data using the same methods as in Sec. 2. Equation (H-11) can then be used to calculate a value for $\sigma_{\theta}(1 \text{ hr})$. Tables H-14 and H-15 compare the actual hourly σ_{θ} 's and the σ_{θ} 's predicted by Eq. (H-11) for short sampling times of 3 and 10 min.

Since Eq. (H-11) is exact, the close agreement between the calculated and observed σ_{θ} 's are not unexpected. With one exception, the two values for σ_{θ} are within 1.5 degrees of each other for the case $\tau_S=3$ min and within 0.6 degrees, for the case $\tau_S=10$ min. The exception in both cases is the hour starting at 0930 on day 147 where relatively large differences between the σ_{θ} values occur.

All these differences in the σ_{θ} values are probably due to the fact that $\bar{\theta}$ is calculated using Eq. (H-5) of Sec. 2 instead of the linear mean, for $\bar{\theta}$ used in this section to derive Eq. (H-11). The larger deviation occurs during an hour with low wind speed and a meandering wind direction.

5. MEAN SQUARE EDDY VELOCITIES AND FILTERING OF THE RAPID SCAN DATA

In order to define what one means by mean square along-wind and crosswind eddy velocities or fluctuations, one must first define the mean velocities from which the instantaneous quantities deviate. In the case of the along-wind component, the instantaneous velocity, u_i , is just the sum $\bar{u} + u_i'$, where \bar{u} is the mean or low frequency wind component and u_i' is the eddy or high frequency wind component.

At the time of the i^{th} sampling, let the instantaneous wind speed and direction be given as V_i and θ_i , respectively. (See Fig. H-1)* If the "mean" quantities are given as \bar{V} and $\bar{\theta}_i$, then the along-wind fluctuation is just

$$u_i' = \bar{V}_i - V_i \cos \theta_i' \quad (H-12a)$$

*Figures and tables appear consecutively at the end of this appendix.

while the cross-wind fluctuation is just

$$v_i' = -v_i \sin \theta_i' \quad (\text{H-12b})$$

where:

$$\theta_i' = \theta_i' - \theta_i.$$

The mean square eddy velocities are then given by the expressions

$$\overline{u'^2} = \frac{1}{N} \sum_{i=1}^N (u_i')^2 \quad (\text{H-13a})$$

$$\overline{v'^2} = \frac{1}{N} \sum_{i=1}^N (v_i')^2 \quad (\text{H-13b})$$

where:

N = the number of events available during the sampling period of interest.

To obtain the "mean" quantities \bar{v}_i and $\bar{\theta}_i$, a number of averaging (or filtering) techniques can be considered. One method, of course, is a straightforward linear average of the v_i and θ_i during the sampling period. The advantages of this scheme are:

- 1) it sets an upper bound on mean square eddy velocities;
- 2) it may be most indicative of what is actually happening to the pollutant; and
- 3) it is a standard statistical procedure and is easy to implement and interpret.

Some of the disadvantages, however, include:

- 1) The mean value depends strongly on the duration of the sampling period, which most likely is of arbitrarily selected length.
- 2) Poor connection with u v w results, especially under light, variable winds.

To overcome these problems, it is necessary to consider a moving mean for \bar{v}_i and $\bar{\theta}_i$. In this way, large, low frequency fluctuations during the sampling period do not introduce large deviations in the along-wind and cross-wind velocities (u_i' and v_i') because these low frequency components become part of the moving mean.

One way of obtaining such a moving mean is to borrow the techniques of electronic signal filtering and actually construct a low-pass filter. When

the individual θ_i and v_i are run through the filter, the output is a time series consisting of the frequency components below the cut-off frequency of the filter. The higher frequency components will have been removed, and therefore the output signal is suitable as a "moving mean" in that when it is subtracted from the complete signal, the remaining values are the true high frequency turbulence components of the wind speed or wind direction.

Consider the three stage low-pass Butterworth filter of Fig. H-2, where the output is taken across resistor R_5 . From analysis of the circuit, given an input voltage $V_{in}(t)$, the output current I through resistor R_5 is governed by the third order differential equation:

$$a \dddot{I} + b \ddot{I} + c \dot{I} = d I = V_{in}(t) \quad (H-14)$$

where:

the dot denotes a derivative with respect to time, and the coefficients have the following values:

$$\begin{aligned} a &= R_1 R_5 C_2 C_4 L_3 \\ b &= R_1 C_2 L_3 + R_5 C_4 L_3 \\ c &= R_1 R_5 C_2 + R_1 R_5 C_4 + L_3 \\ d &= R_1 + R_5 \end{aligned} \quad (H-15)$$

To make this filter have a cut-off angular frequency of ω_c (rad/s) the values of the components should be set to:*

$$R_1 = 1$$

$$C_2 = \frac{1}{\omega_c}$$

$$L_3 = \frac{2}{\omega_c}$$

$$C_4 = \frac{1}{\omega_c}$$

$$R_5 = 1$$

Actually, ω_c is the half-power point on the frequency response curve of the filter, which means that at ω_c , the output voltage is 71% of its value in the pass band. Because of the construction of the Butterworth filter, the output voltages even in the pass band are 50% of the input voltage. This condition can be corrected by simply doubling the output of the filter.

Using the above values for the filter components results in coefficients for the differential equation of the form:

*See A Handbook on Electrical Filters, White Electromagnetics, Inc., Rockville, Md., 1963.

$$a = \frac{2}{\omega_c^3}$$

$$b = \frac{4}{\omega_c^2} \tag{H-17}$$

$$c = \frac{4}{\omega_c}$$

$$d = 2$$

Thus, the differential Eq. (H-14) becomes:

$$\frac{2}{\omega_c^3} \ddot{i} + \frac{4}{\omega_c^2} \dot{i} + \frac{4}{\omega_c} i + 2I = v_{in}(t) \tag{H-18}$$

V_{out} is then obtained from the relation

$$V_{out}(t) = I(t) \cdot R_5 \cdot 2 \tag{H-19}$$

since the output voltage is developed across resistor R_5 and must be doubled to compensate for the unavoidable attenuation. But because $R_5 = 1$,

$$V_{out}(5) = 2I(t) \tag{H-20}$$

where:

$I(t)$ = the solution of the differential Eq. (H-18), and

V_{out} = the low pass filtered signal using cut-off frequency ω_c .

From steady-state analysis of the filter, the steady-state frequency response is determined to be

$$A_{out} = \frac{R_5 A_{in}}{S} \tag{H-21}$$

where:

A_{in} = amplitude of input voltage signal,

A_{out} = amplitude of output voltage,

$S = ||Z_t|| = (x^2 + y^2)^{1/2}$,

Z_t = Complex impedance = $x + iy$,

$x = -b\omega^2 + d$, and

$y = -a\omega^3 + c\omega$.

where:

ω = the angular frequency of the input signal, and

a, b, c, d are defined in Eqs. (H-15) and (H-17).

The phase angle of the filter circuit is given by:

$$\theta = \tan^{-1} \left(\frac{y}{x} \right). \quad (H-22)$$

The steady-state response of this 3-stage, low-pass Butterworth filter is shown in Fig. H-3 for a cut-off period $T_c = 10$ min. ($T_c = 2\pi/\omega_c$.) Notice that the filter effectively attenuates the frequency components greater than ω_c , even though the rolloff is not extremely sharp.

Now, instead of using strictly voltage levels as the input signal to the filter, use the wind speed and wind direction signals as if they were voltages. The output of the filter will then be the low-pass filtered wind speed and wind direction that is suitable for use as a "moving mean," since it only includes the low frequency components of the input signal. The advantages of using a filter to get a moving mean are:

- 1) the method ties in more closely with classical turbulence theory; and
- 2) the mean follows the low frequency components of the signal and therefore does not introduce arbitrarily large deviations into the eddy velocities.

However, some important disadvantages are:

- 1) The insight into total pollutant dispersal power is not as clear as with a fixed mean; and
- 2) The filter introduces a delay time into the output signal.

The last point is very important when the eddy velocities are to be computed, since a matchup must be made between the total signal and the filtered signal, if their difference is to represent only true deviations of the wind speed and wind direction. If the delay time, t_d , introduced by the filter is known, then the input signal $V_{in}(t)$ can be matched with the output signal $V_{out}(t + t_d)$ to get the desired moving average of $V_{in}(t)$ at time t .

Recall that Eq. (H-22) defines the phase angle introduced by the filter circuitry:

$$\theta = \tan^{-1} \left(\frac{y}{x} \right)$$

If t_d is the delay time, then at angular frequency ω , the phase angle (which is a function of ω) is:

$$\theta(\omega) = \omega t_d. \quad (H-23)$$

Substituting the values for a, b, c, and d from Eq. (H-17) into the values for x and y of Eq. (H-21), one obtains:

$$x = -4 \left(\frac{\omega}{\omega_c} \right)^2 + 2, \text{ and}$$

$$y = -2 \left(\frac{\omega}{\omega_c} \right)^3 + 4 \left(\frac{\omega}{\omega_c} \right).$$

If $\omega \ll \omega_c$ then

$$x \approx 2,$$

$$y \approx 4 \frac{\omega}{\omega_c},$$

and

$$\theta = \tan^{-1} \left(2 \frac{\omega}{\omega_c} \right).$$

Expanding this and neglecting higher order terms yields

$$\theta \approx 2 \frac{\omega}{\omega_c},$$

and substituting this into Eq. (H-23) yields

$$t_d = \frac{2}{\omega_c} \tag{H-24}$$

for the cases of $\omega \ll \omega_c$. Also note that t_d can be rewritten using the coefficients of the differential equation:

$$t_d = \frac{c}{d}. \tag{H-25}$$

This equation gives a simple approximation for t_d , but it is strictly valid only for the frequencies $\omega \ll \omega_c$. For frequencies greater than ω_c , this is not a problem because these frequencies will have been filtered out of the output signal. For frequencies around ω_c where attenuation is not complete, t_d is underestimated by Eq. (H-24).

The phase angle θ at $\omega = \omega_c$ is

$$\theta = 2.356 \text{ radians,}$$

so from Eq. (H-23), which gives the exact value of t_d , one obtains:

$$t_d = \frac{\theta}{\omega} = \frac{2.356}{\omega_c}$$

The approximate Eq. (H-24) would predict

$$t_d = \frac{2}{\omega_c},$$

which amounts to an 18% underestimate in t_d at ω_c .

For example, notice in Fig. H-4 how the filtered signal of the wind speeds (adjusted for t_d) contains only the low frequency components of the wind speed trace and serves as a moving average for the wind speed. Also notice that the approximation for t_d effectively compensates for the delay time introduced by the filter for almost every frequency component of the filtered signal.

Filtering the wind direction is more difficult because of the cut at 360° . So instead of directly filtering the θ_i values, $\sin\theta_i$ and $\cos\theta_i$ are filtered separately and then recombined to obtain θ_i via the expression:

$$\bar{\theta}_i = \tan^{-1} \frac{(\sin\theta_i)_f}{(\cos\theta_i)_f} \quad (\text{H-26})$$

where:

f denotes that the filtered values of $\sin\theta_i$ and $\cos\theta_i$ are used.

This is not strictly a correct procedure, but it is a useful and simple technique that gives reasonable results. In Fig. H-5, notice that this method returns a signal for $\bar{\theta}_i$ that corresponds well to what would be expected from a moving average of the individual θ_i . Results of filtering the wind speed and wind direction data from a different hour are shown in Figs. H-6 and H-7.

Values for $\bar{\theta}_i$ and \bar{V}_i , then, can be obtained by filtering the individual θ_i and V_i , using this low-pass Butterworth filter. The actual technique used involves numerically solving the Differential Eq. (H-18) with the wind speed signal (V_i) or the sine and cosine of the wind direction signal ($\sin\theta_i$ and $\cos\theta_i$) as the input forcing function $V_{in}(t)$. The filtered output V_{out} is then calculated from Eq. (H-20). The value for \bar{V}_i is obtained directly in this way, but $\bar{\theta}_i$ must be calculated from Eq. (H-26).

To solve the third-order Differential Eq. (H-18), it must be rewritten as three first-order differential equations that are then solved numerically by the Runge-Kutta method. This technique is desirable for obtaining the filter output because the input function $V_{in}(t)$ need only be known at certain time intervals. Hence, a sequence of data points can be used as input to the numerical method without knowledge of the continuous function these points represent. Moreover, this method produces a sequence of points as a filtered output that, when adjusted for delay time, can be used as a continuous moving mean for display purposes (Figs. H-4 through H-7) or for calculations.

Equations (H-12a and b) can now be used to calculate the u_i' and v_i' . The mean square eddy velocities ($\overline{u'^2}$ and $\overline{v'^2}$) are then calculated from Eqs. (H-13a and b). For a cut-off period of 10 min and a sampling time of one

hour, the $\overline{u'^2}$ and $\overline{v'^2}$ computed from the 17 hr of rapid-scan meteorological data appear in Tables H-16 and H-17. As in previous sections, the computations are done for both $s = (6 \text{ sec})^{-1}$ data and $s = 1 \text{ min}^{-1}$ data.

From the large values of $\sigma(\phi)$, it appears that the ϕ_j^* values are not necessarily the same as the value for ϕ . This factor indicates that averaging time has a noticeable effect on the calculation of $\overline{u'^2}$ and $\overline{v'^2}$; although the filter cut-off period T_c might also have an effect, since, an averaging time of one minute means that after removal of the moving average, only fluctuations with periods between 1 and 10 min are left. This band is not very wide, and it may not contain enough information to compute the R.M.S. eddy velocities.

The selection of the cut-off period for the low-pass filter $T_c = 10 \text{ min}$ was almost arbitrary, being based on the desire to center T_c between the sampling time ($\tau = 1 \text{ hr}$) and the sampling intervals (6 sec and 1 min). In this way, the filter eliminates fluctuations with periods between 10 min and 6 sec. These periods can be detected with an averaging time of 6 sec or 1 min and will contribute to the values for the mean square eddy velocities. Also, T_c is less than 1 hr so that the moving mean follows the fluctuations with periods between 1 hr and 10 min and does not become much like a fixed mean (which would happen if $T_c \gg 1 \text{ hr}$).

For comparison, Tables H-18 and H-19 show the mean square along wind ($\overline{u'^2}$) and cross wind ($\overline{v'^2}$) eddy velocities computed, using a fixed linear mean for θ_i and v_i . The hourly average wind direction (\overline{WD}) is used for θ_i and the hourly average wind speed (\overline{WS}) is used for v_i .

Notice that the values for $\overline{u'^2}$ and $\overline{v'^2}$ computed with a fixed mean are higher than those computed using a moving mean. However, the values of $\sigma(\phi)$ are just as large, indicating poorer agreement between the ϕ and ϕ_j^* values in the case of $\overline{u'^2}$ and $\overline{v'^2}$ than for other hourly quantities.

6. APPROXIMATE EQUATIONS RELATING VARIOUS COMPUTED PARAMETERS

Manipulating the equations used to define the hourly quantities WS , WD , $VMWS$, $VMWD$, $\overline{u'^2}$, and $\overline{v'^2}$ leads to some new equations that interrelate some of these quantities. Before starting, however, it is necessary to derive a method for determining the correlation between a set of wind speed measurements V_i and a set of wind direction measurements θ_i . It can be shown that the agreement between WD and $VMWD$ is an indication of how uncorrelated V_i and θ_i are.

From Eq. (H-7) in Section 2:

$$VMWD = \tan^{-1} \left[\frac{\sum_{i=1}^N V_i \sin \theta_i}{\sum_{i=1}^N V_i \cos \theta_i} \right].$$

If V_i and θ_i are uncorrelated, then

$$\begin{aligned} \text{VMWD} &= \tan^{-1} \frac{\left[\frac{\sum_{i=1}^N V_i \sin \theta_i}{\sum_{i=1}^N V_i \cos \theta_i} \right]}{\left[\frac{\sum_{i=1}^N \sin \theta_i}{\sum_{i=1}^N \cos \theta_i} \right]} \\ &= \tan^{-1} \frac{\left[\frac{\sum_{i=1}^N \sin \theta_i}{\sum_{i=1}^N \cos \theta_i} \right]}{\left[\frac{\sum_{i=1}^N \sin \theta_i}{\sum_{i=1}^N \cos \theta_i} \right]} = \overline{\text{WD}} \end{aligned}$$

as defined by Eq. (H-5) of Section 2.

Thus, if $\text{VMWD} = \overline{\text{WD}}$, then V_i and θ_i are uncorrelated. This result is important, because the separation is used many times in the subsequent derivations. From Table H-1, notice the closeness between VMWD and $\overline{\text{WD}}$; if one compares the differences in VMWD and $\overline{\text{WD}}$ to σ_θ , the largest difference as a percentage of σ_θ is found to be 13%, but most values fall below 10%.

A relationship between σ_θ , $\overline{\text{WS}}$, and VMWS can be derived as follows:

Given that

$$\sigma_\theta = \left[\frac{1}{N} \sum_i (\theta_i - \bar{\theta})^2 \right]^{1/2}, \text{ and}$$

$$\overline{\text{WS}} = \frac{1}{N} \sum_i V_i,$$

and

$$\text{VMWS} = \left[\left(\frac{1}{N} \sum_i V_i \sin \theta_i \right)^2 + \left(\frac{1}{N} \sum_i V_i \cos \theta_i \right)^2 \right]^{1/2}.$$

Since V_i and θ_i are uncorrelated

$$\text{VMWS} = \left(\frac{1}{N} \sum_i V_i \right) \left[\left(\frac{1}{N} \sum_i \sin \theta_i \right)^2 + \left(\frac{1}{N} \sum_i \cos \theta_i \right)^2 \right]^{1/2}$$

or

$$\left(\frac{\text{VMWS}}{\overline{\text{WS}}} \right)^2 = (\overline{\sin \theta})^2 + (\overline{\cos \theta})^2. \quad (\text{H-27})$$

If

$$\Delta\theta_i = \theta_i - \bar{\theta}. \text{ (Note that } \overline{\Delta\theta_i} = 0.\text{)}$$

then:

$$\sin\theta_i = \sin\bar{\theta} \cos(\Delta\theta_i) + \cos\bar{\theta} \sin(\Delta\theta_i),$$

and so:

$$\overline{\sin\theta} = \left[\frac{1}{N} \sum_i \sin\bar{\theta} \cos(\Delta\theta_i) + \cos\bar{\theta} \sin(\Delta\theta_i) \right].$$

Since $\sin\theta$ is an odd function, $\overline{\Delta\theta_i} = 0$ implies that $\sum_i \sin\Delta\theta_i = 0$ also.

Hence:

$$\overline{\sin\theta} = \sin\bar{\theta} \cdot \overline{\cos(\Delta\theta)}. \quad (\text{H-28})$$

Similarly:

$$\overline{\cos\theta} = \cos\bar{\theta} \cdot \overline{\cos(\Delta\theta)}. \quad (\text{H-29})$$

Substitution of Eqs. (H-28) and (H-29) into Eq. (H-27) yields

$$\begin{aligned} \left(\frac{\overline{VMWS}}{\overline{WS}} \right)^2 &= (\sin\bar{\theta})^2 \cdot (\overline{\cos(\Delta\theta)})^2 + (\cos\bar{\theta})^2 \cdot (\overline{\cos(\Delta\theta)})^2 \\ &= (\overline{\cos(\Delta\theta)})^2. \end{aligned}$$

If $\Delta\theta_i$ is small, then use of the small angle approximation gives

$$\begin{aligned} \left(\frac{\overline{VMWS}}{\overline{WS}} \right)^2 &= (\overline{\cos(\Delta\theta)})^2 = \left[\frac{1}{N} \sum_i \left(1 - \frac{(\Delta\theta_i)^2}{2} + \frac{(\Delta\theta_i)^4}{24} - \dots \right) \right]^2 \\ &= 1 - \frac{1}{N} \sum_i (\Delta\theta_i)^2. \end{aligned}$$

This equation can be rewritten by using the definition of σ_θ :

$$\left(\frac{\overline{VMWS}}{\overline{WS}} \right)^2 = 1 - \sigma_\theta^2, \quad (\text{H-30})$$

which is valid for small values of $\Delta\theta_i$ and, subsequently, σ_θ .

Rewriting Eq. (H-30) one obtains:

$$\sigma_{\theta} = \left[1 - \left(\frac{VMWS}{WS} \right)^2 \right]^{1/2}. \quad (H-31)$$

The validity of this equation is shown by Figs. H-8, H-9, and H-10 where σ_{θ} calculated from Eq. (H-31) is plotted against the σ_{θ} calculated directly from the wind direction data. In Fig. H-8, the hourly quantities used are those computed from the six-second-scan interval data (the quantities denoted by ϕ). In Fig. H-9, the means of the quantities computed from the one-minute-scan interval data are used (the quantities denoted by ϕ^*). In Fig. H-10, the individual quantities computed from the one-minute-scan interval data are used (the quantities denoted by ϕ_j^*).

Notice that for σ_{θ} values below 40° , Eq. (H-31) predicts a value for σ_{θ} that corresponds very well to what is actually observed. For σ_{θ} values smaller than 20° , Eq. (H-31) predicts a value that is within 10% of the observed σ_{θ} value. For σ_{θ} values of less than 40° , the predictions are good to within 20%. In almost all cases, however, Eq. (H-31) slightly underpredicts the σ_{θ} value. Figure H-10 shows that even the individual ϕ_j^* values give good results, and more important, that the scatter of points is along the one-to-one correspondence line. This shows that Eq. (H-31) is applicable to any set of hourly averaged quantities computed from minute-interval data.

Manipulating Eqs. (H-4) and (H-7) of Sec. 2 and Eqs. (H-13a) and (H-13b) of Sec. 5 in other ways leads to some different relationships between these quantities. Two of the more useful ones are listed here without derivation:

$$\sigma_{\theta} = \left[\frac{\overline{v'^2}}{\sigma_v^2 + \bar{v}^2} \right]^{1/2}, \text{ and} \quad (H-32)$$

$$\overline{u'^2} = \sigma_v^2 (1 - \sigma_{\theta}^2) \quad (H-33)$$

where:

\bar{v} = average wind speed (WS), and

σ_v = standard deviation of the wind speed.

These equations use the small angle approximation to simplify expressions with σ_{θ} and assume that $\overline{u'^2}$ and $\overline{v'^2}$ are computed using a fixed, linear mean, as was done in Tables H-15 and H-16.

In Fig. H-11, σ_{θ} calculated from Eq. (H-32) is plotted against the calculated directly from the wind direction data. In Fig. H-12, Eq. (H-33) is tested in the same manner. For both cases, the ϕ values are used in the calculations. Referring to Fig. H-11, notice that Eq. (H-32) is accurate to within 10% up to σ_{θ} values of 20° and is accurate to within 30% up to 40° . From Fig. H-12, however, it is apparent that Eq. (H-33) is valid over only a very narrow range. The calculated value for $\overline{u'^2}$ is within 10% of the actual value up to $0.2 \text{ m}^2/\text{s}^2$ and is accurate to within 40% up to $2.0 \text{ m}^2/\text{s}^2$ with one exception -- a point calculated during an hour with very low wind speed falls well out of the 40% band.

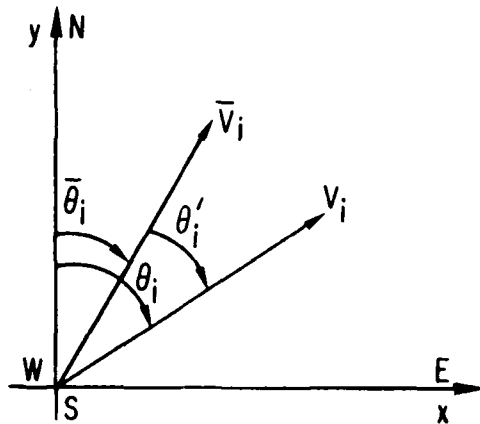


Fig. H-1. Definition of Coordinates

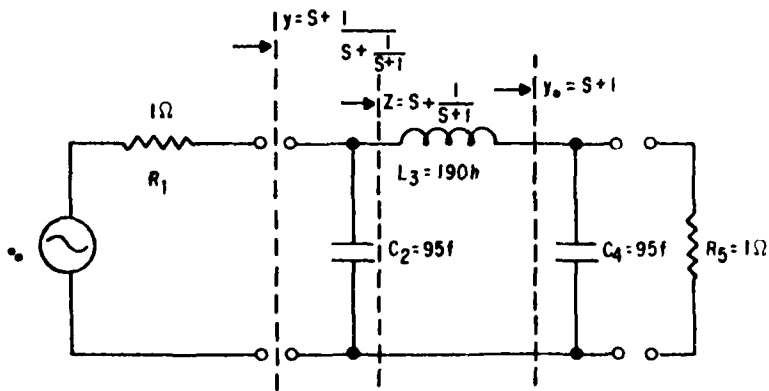


Fig. H-2. Synthesized Three-Stage,
Butterworth, Low-Pass Prototype
Values of Components Chosen to Give
 $f_c = 1.67 \times 10^{-3}$ Hz or $T_c = 10$ min

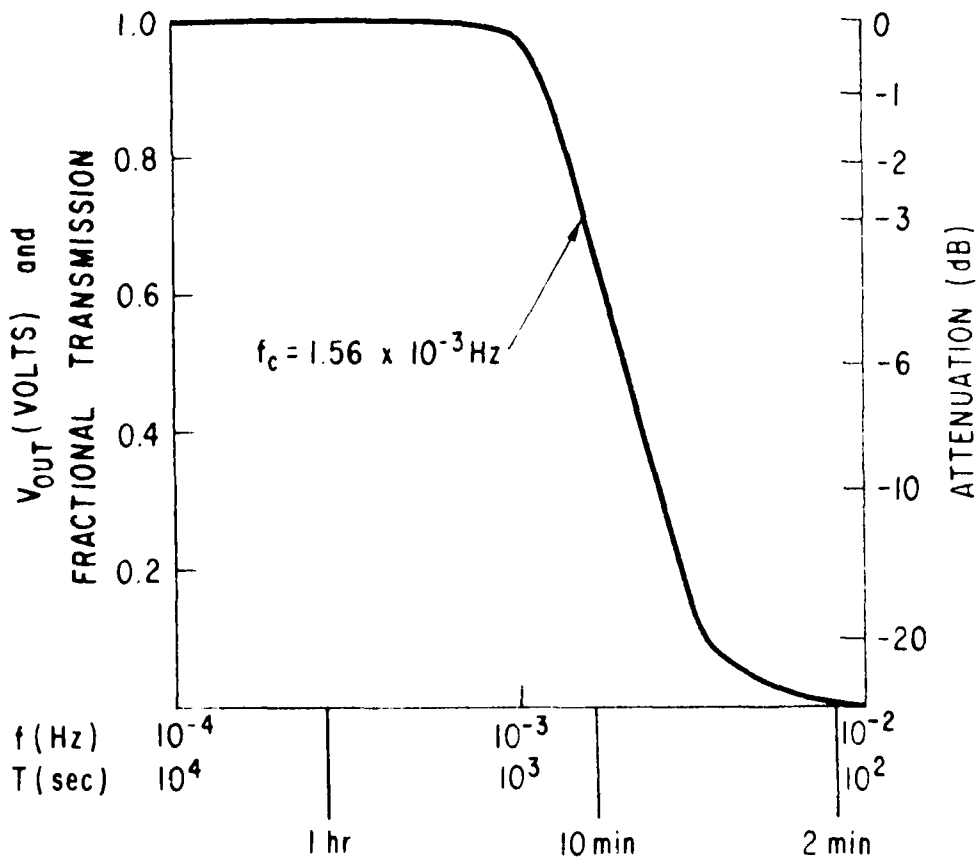


Fig. H-3. Frequency Response of 3-Stage Low-Pass Butterworth Filter

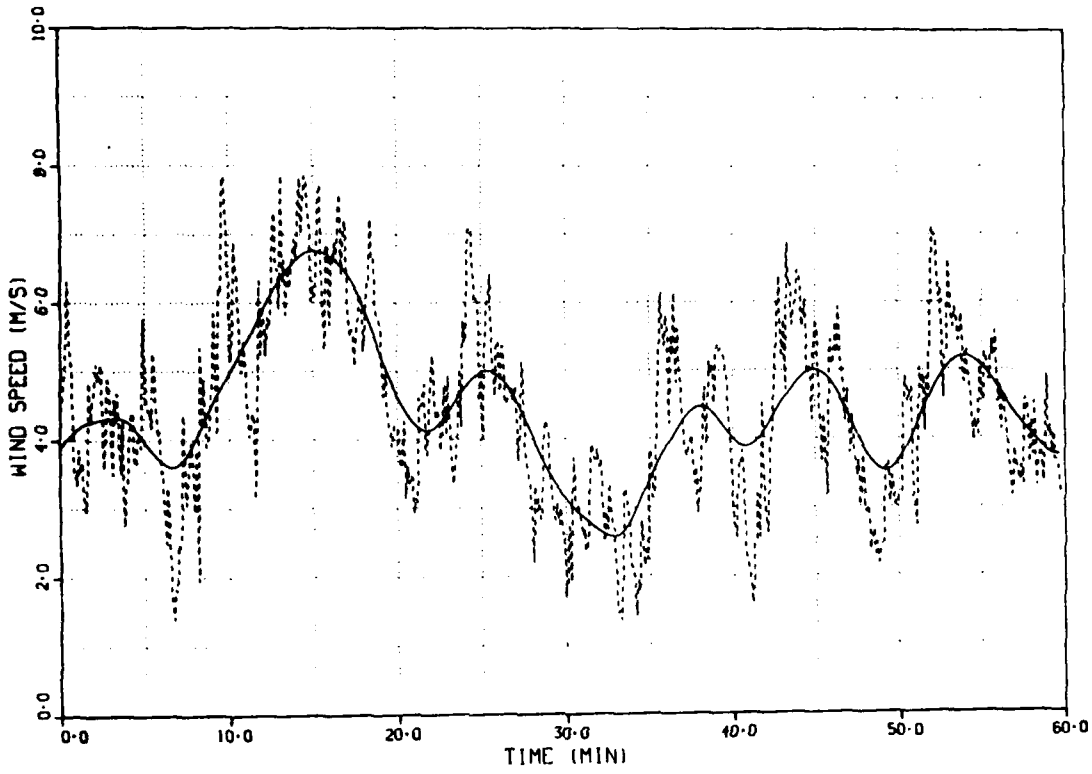


Fig. H-4. Filtered Wind Speed for Day 146, Hour 1650-1750

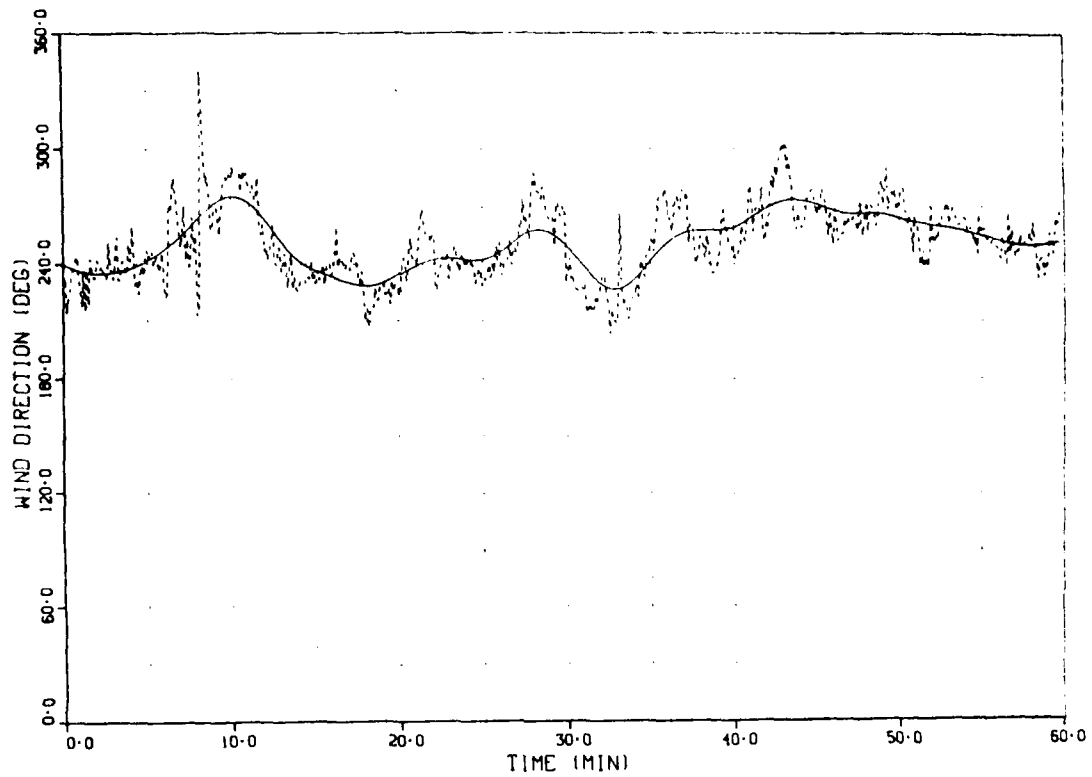


Fig. H-5. Filtered Wind Direction for Day 146, Hour 1650-1750

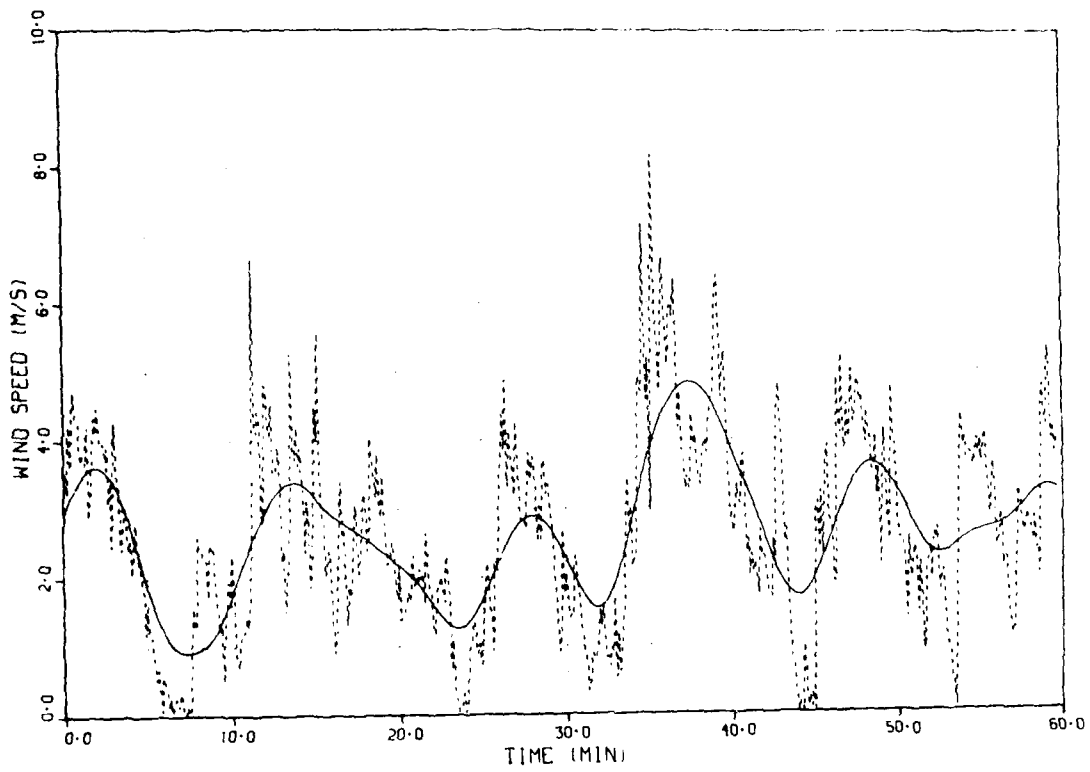


Fig. H-6. Filtered Wind Speed for Day 145, Hour 1200-1300

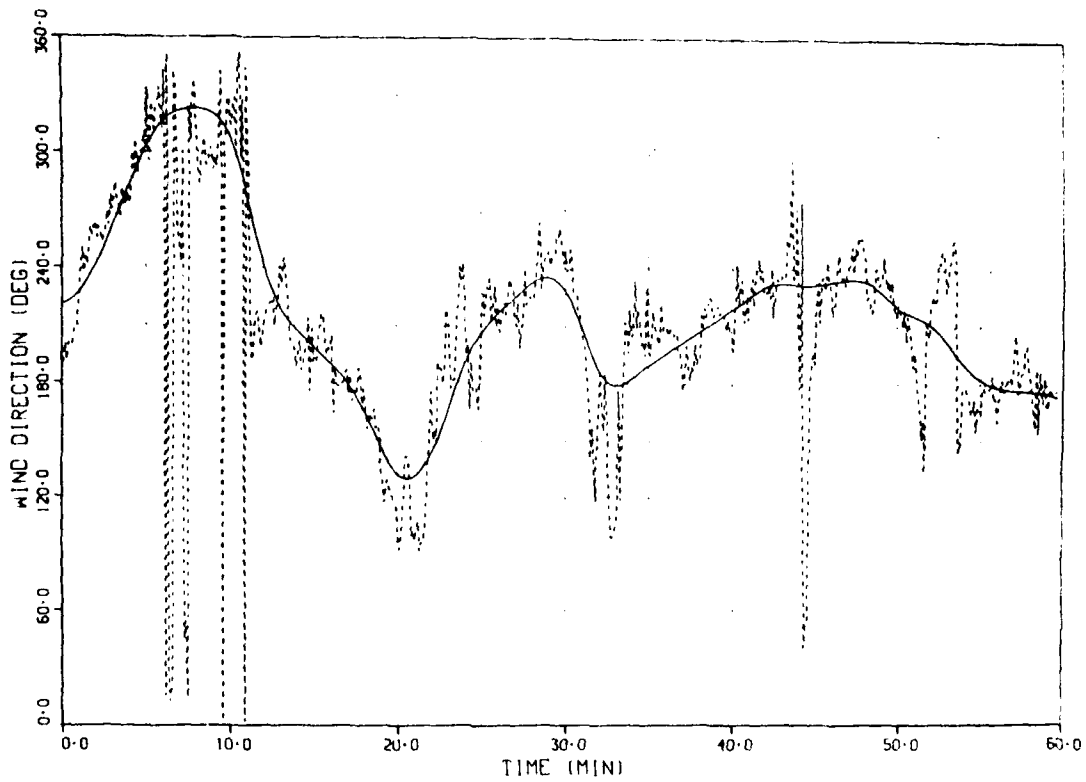


Fig. H-7. Filtered Wind Direction for Day 145, Hour 1200-1300

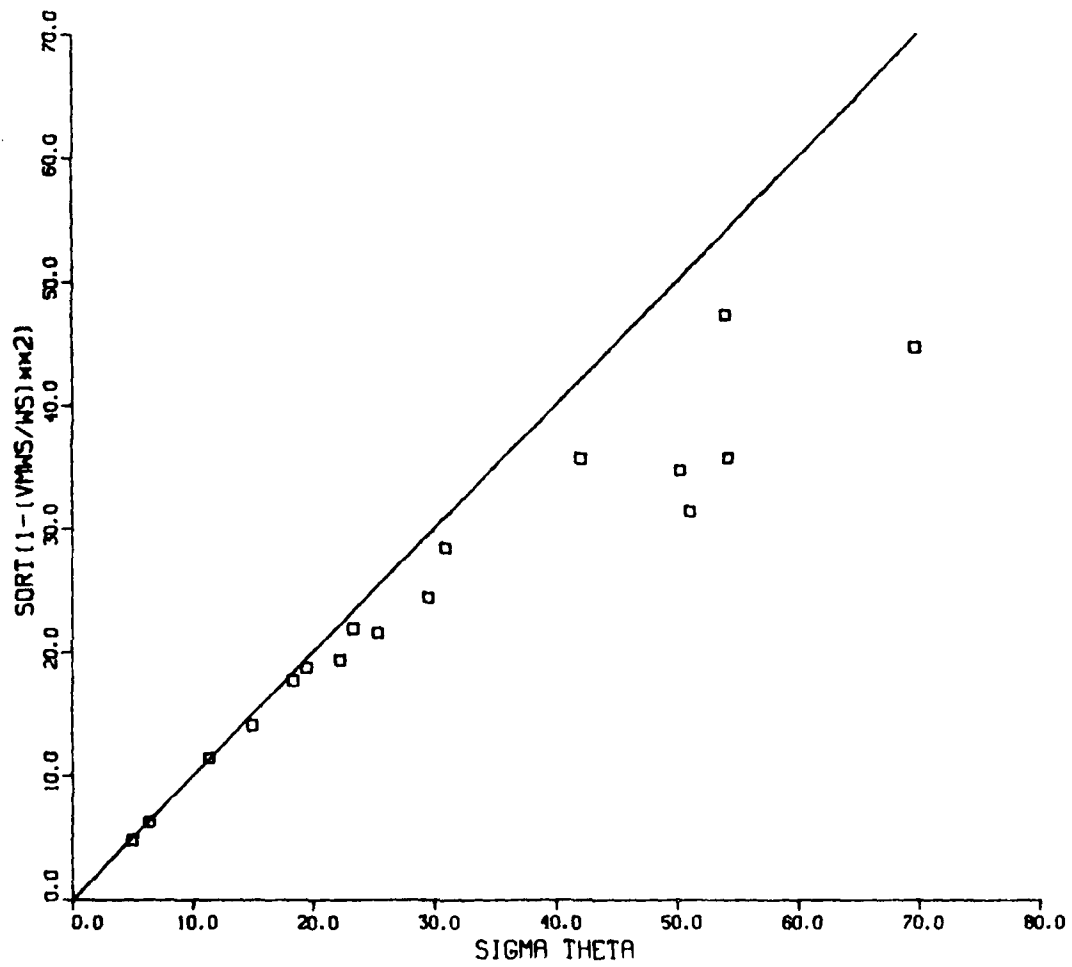


Fig. H.8. Calculated Eq. (H-31) versus Observed σ_{θ} : Global Values

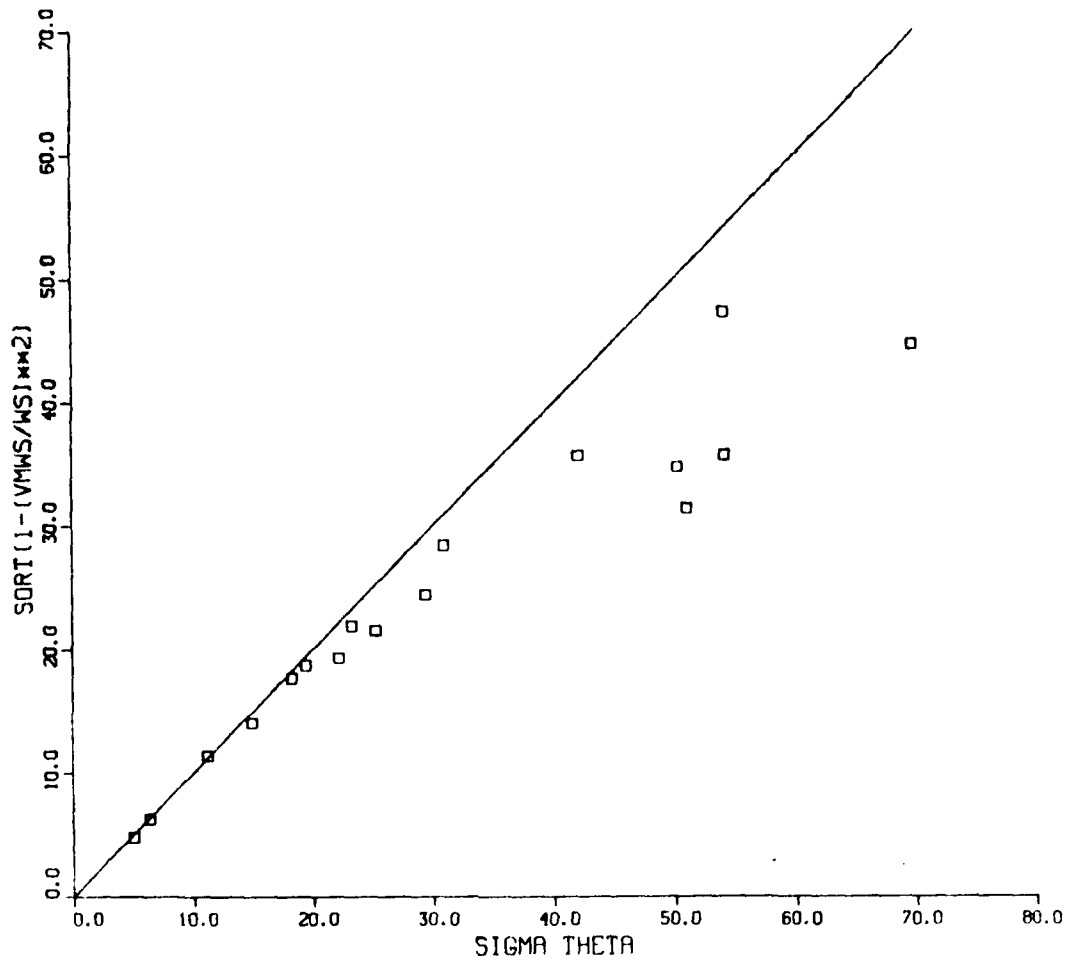


Fig. H.9. Calculated Eq. (H-31) versus Observed σ_0 :
Average of Minute Values

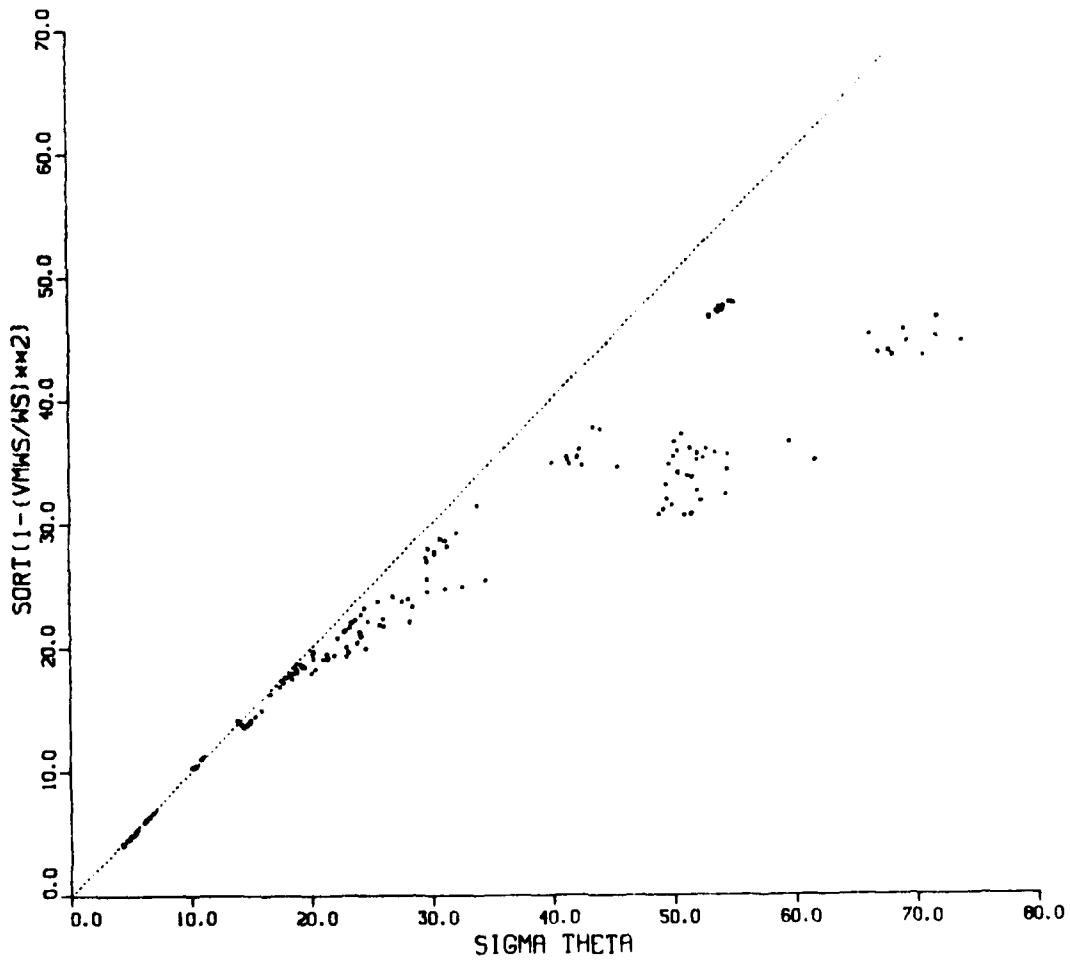


Fig. H-10. Calculated Eq. (H-31) versus Observed σ_a : Minute Values

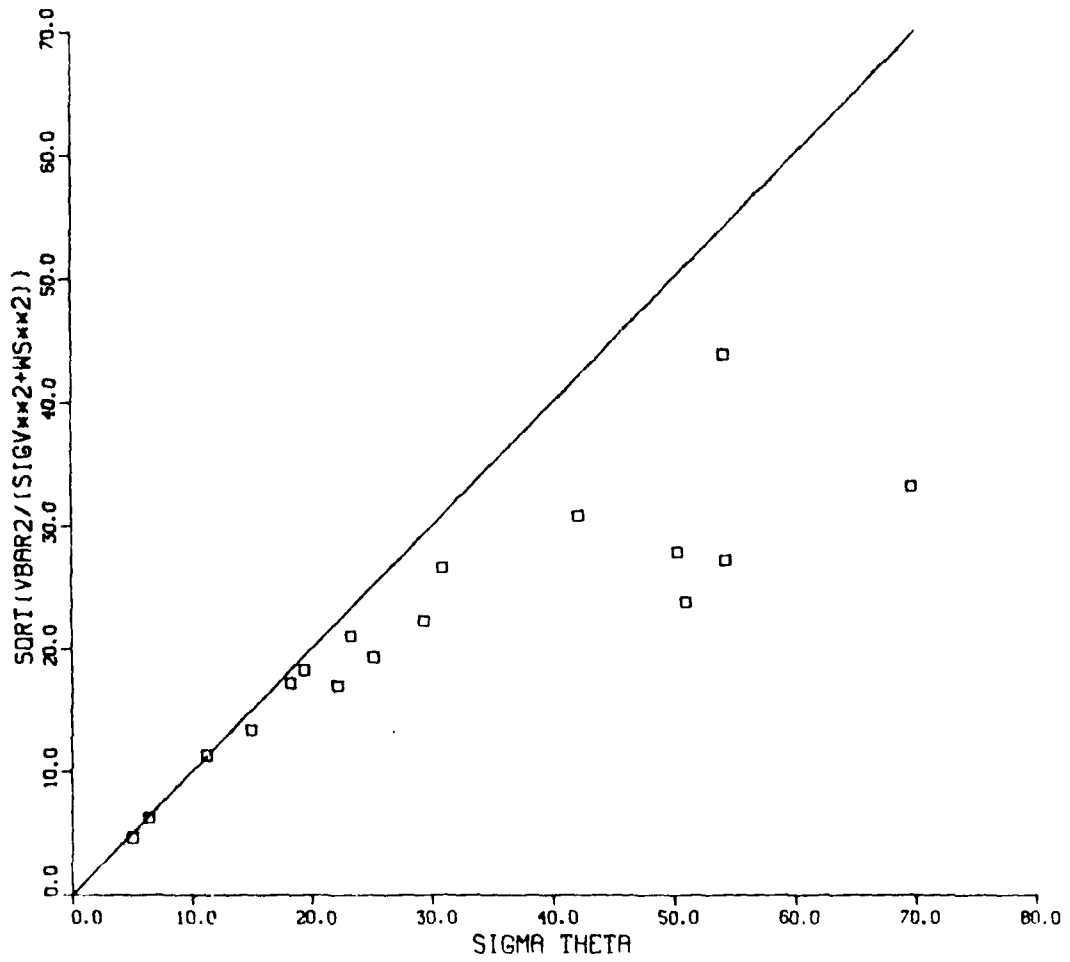


Fig. H.11. Calculated Eq. (H-32) versus Observed σ_θ :
Average of Minute Values

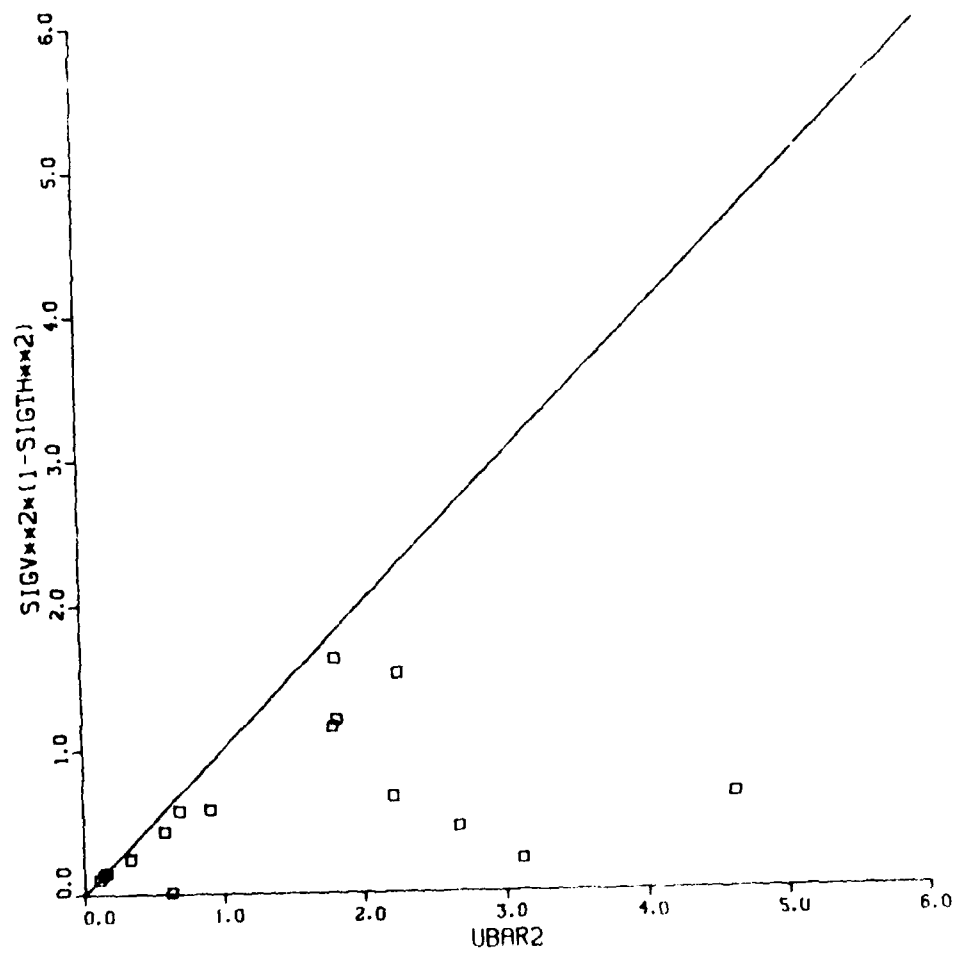


Fig. H-12. Calculated Eq. (H-33) versus Observed σ_a :
Average of Minute Values

Table H-1. Average Wind Direction ($\phi = \overline{WD}$)

Day	Hour	\overline{WD} (deg)	$\sigma(\overline{WD})$ (deg)	\overline{WD}^* (deg)	$\sigma(\overline{WD}^*)$ (deg)
145	1200	213.5	1.6	213.5	1.6
	1300	208.9	1.2	208.9	1.2
	1400	258.3	1.7	258.3	1.7
	1500	268.6	1.6	268.6	1.6
	1600	276.8	1.1	276.8	1.1
	1700	297.2	0.9	297.2	0.9
	1800	331.9	1.1	331.9	1.1
	1900	348.6	0.9	348.6	0.9
	2000	336.7	0.3	336.7	0.3
	2100	337.6	0.2	337.6	0.2
	2200	77.4	1.7	77.4	1.7
	146	1650	250.7	1.0	250.7
1750		268.7	0.4	268.7	0.4
1850		302.2	0.3	302.2	0.3
147	0830	141.7	1.1	141.7	1.1
	0930	168.9	2.4	168.9	2.4
	1030	223.8	2.0	223.8	2.0

Table H-2. Vector Mean Wind Direction ($\phi = \overline{VMWD}$)

Day	Hour	\overline{VMWD} (deg)	$\sigma(\overline{VMWD})$ (deg)	\overline{VMWD}^* (deg)	$\sigma(\overline{VMWD}^*)$ (deg)
145	1200	212.4	1.5	212.4	1.5
	1300	214.0	1.4	214.0	1.4
	1400	262.4	1.7	262.4	1.7
	1500	267.5	1.5	267.5	1.5
	1600	275.3	1.1	275.3	1.1
	1700	293.8	0.8	293.8	0.8
	1800	330.6	1.2	330.6	1.2
	1900	349.1	1.1	349.1	1.1
	2000	336.3	0.3	336.3	0.3
	2100	337.0	0.2	337.0	0.2
	2200	71.1	2.2	71.1	2.2
	146	1650	250.6	0.9	250.6
1750		266.8	0.6	266.8	0.6
1850		301.0	0.4	301.0	0.4
147	0830	140.9	1.1	140.9	1.1
	0930	167.3	1.9	167.3	1.9
	1030	229.5	1.6	229.5	1.6

Table H-3. Standard Deviation of the Wind Direction ($\phi = \sigma_{\theta}$)

Day	Hour	σ_{θ} (deg)	$\sigma(\sigma_{\theta})$ (deg)	$\overline{\sigma_{\theta}^*}$ (deg)	$\sigma(\overline{\sigma_{\theta}^*})$ (deg)
145	1200	54.3	3.6	54.1	3.6
	1300	50.3	1.8	50.3	1.8
	1400	51.1	1.6	51.0	1.6
	1500	25.3	2.0	25.2	2.0
	1600	29.5	2.6	29.4	2.6
	1700	30.9	1.2	30.9	1.2
	1800	18.3	0.8	18.3	0.8
	1900	11.4	1.4	11.2	1.4
	2000	5.1	0.4	5.0	0.4
	2100	6.4	0.2	6.4	0.2
	2200	54.0	0.6	54.0	0.6
146	1650	19.5	1.2	19.4	1.2
	1750	23.3	0.7	23.3	0.7
	1850	15.0	0.4	14.9	0.4
147	0830	22.2	1.4	22.1	1.4
	0930	69.7	2.3	69.6	2.3
	1030	42.1	1.1	42.0	1.1

Table H-4. Average Wind Speed ($\phi = \overline{WS}$)

Day	Hour	\overline{WS} (m/s)	$\sigma(\overline{WS})$ (m/s)	$\overline{WS^*}$ (m/s)	$\sigma(\overline{WS^*})$ (m/s)
145	1200	2.67	0.09	2.67	0.09
	1300	2.55	0.03	2.55	0.03
	1400	3.52	0.06	3.52	0.06
	1500	3.99	0.06	3.99	0.06
	1600	3.57	0.04	3.57	0.04
	1700	3.07	0.03	3.07	0.03
	1800	3.54	0.04	3.54	0.04
	1900	2.61	0.03	2.61	0.03
	2000	2.59	0.01	2.59	0.01
	2100	2.45	0.01	2.45	0.01
	2200	1.41	0.01	1.41	0.01
146	1650	4.46	0.09	4.46	0.09
	1750	4.07	0.03	4.07	0.03
	1850	3.37	0.03	3.37	0.03
147	0830	1.97	0.05	1.97	0.05
	0930	1.82	0.03	1.82	0.03
	1030	2.77	0.04	2.77	0.04

Table H-5. Vector Mean Wind Speed ($\phi = \text{VMWS}$)

Day	Hour	VMWS (m/s)	$\sigma(\text{VMWS})$ (m/s)	VMWS*	$\sigma(\text{VMWS}^*)$ (m/s)
145	1200	2.09	0.07	2.09	0.07
	1300	2.03	0.04	2.03	0.04
	1400	2.95	0.05	2.95	0.05
	1500	3.69	0.07	3.70	0.07
	1600	3.23	0.05	3.23	0.05
	1700	2.67	0.05	2.67	0.05
	1800	3.36	0.05	3.36	0.05
	1900	2.56	0.03	2.56	0.03
	2000	2.58	0.01	2.58	0.01
	2100	2.43	0.01	2.43	0.01
	2200	0.80	0.01	0.80	0.01
146	1650	4.22	0.10	4.22	0.10
	1750	3.76	0.04	3.76	0.04
	1850	3.27	0.03	3.27	0.03
147	0830	1.85	0.04	1.85	0.04
	0930	1.14	0.04	1.14	0.04
	1030	2.17	0.06	2.17	0.06

Table H-6. Standard Deviation of the Wind Speed ($\phi = \sigma_v$)

Day	Hour	σ_v (m/s)	$\sigma(\sigma_v)$ (m/s)	$\overline{\sigma_v^*}$ (m/s)	$\sigma(\overline{\sigma_v^*})$ (m/s)
145	1200	1.44	0.08	1.44	0.08
	1300	1.40	0.06	1.40	0.06
	1400	1.79	0.11	1.79	0.11
	1500	1.20	0.05	1.20	0.05
	1600	1.44	0.06	1.43	0.06
	1700	1.31	0.07	1.30	0.07
	1800	0.81	0.02	0.80	0.02
	1900	0.47	0.03	0.40	0.03
	2000	0.37	0.02	0.37	0.02
	2100	0.32	0.01	0.33	0.01
	2200	0.31	0.01	0.31	0.01
146	1650	1.36	0.08	1.36	0.08
	1750	0.84	0.04	0.84	0.04
	1850	0.52	0.03	0.51	0.03
147	0830	0.72	0.04	0.71	0.04
	0930	0.97	0.04	0.97	0.04
	1030	1.20	0.04	1.20	0.04

Table H-7. Hourly Average NO ($\phi = \text{NO}$)

Day	Hour	$\overline{\text{NO}}$ (ppb)	$\sigma(\overline{\text{NO}})$ (ppb)	$\overline{\text{NO}^*}$ (ppb)	$\sigma(\overline{\text{NO}^*})$ (ppb)
145	1200	3.66	0.04	3.66	0.04
	1300	3.53	0.08	3.53	0.08
	1400	3.68	0.05	3.68	0.05
	1500	3.62	0.08	3.62	0.08
	1600	4.13	0.07	4.13	0.07
	1700	3.40	0.06	3.40	0.06
	1800	3.52	0.07	3.52	0.07
	1900	3.11	0.05	3.11	0.05
	2000	3.35	0.03	3.35	0.03
	2100	3.57	0.03	3.57	0.03
	2200	3.68	0.04	3.68	0.04
146	1650	1.48	0.05	1.48	0.05
	1750	0.88	0.06	0.88	0.06
	1850	0.78	0.09	0.78	0.09
147	0830	0.75	0.09	0.75	0.09
	0930	1.13	0.08	1.13	0.08
	1030	1.07	0.07	1.07	0.07

Table H-8. Hourly Average NO_x ($\phi = \overline{(\text{NO}_x)}$)

Day	Hour	$\overline{\text{NO}_x}$ (ppb)	$\sigma(\overline{\text{NO}_x})$ (ppb)	$\overline{\text{NO}_x^*}$ (ppb)	$\sigma(\overline{\text{NO}_x^*})$ (ppb)
145	1200	8.56	0.11	8.56	0.11
	1300	8.81	0.07	8.81	0.07
	1400	8.98	0.05	8.98	0.05
	1500	9.46	0.10	9.46	0.10
	1600	10.00	0.07	10.00	0.07
	1700	8.54	0.06	8.54	0.06
	1800	7.45	0.04	7.45	0.04
	1900	8.42	0.06	8.42	0.06
	2000	17.79	0.07	17.79	0.07
	2100	28.84	0.03	28.84	0.03
	2200	26.79	0.07	26.79	0.07
146	1650	5.71	0.13	5.71	0.13
	1750	4.21	0.07	4.21	0.07
	1850	6.98	0.10	6.98	0.10
147	0830	6.24	0.07	6.24	0.07
	0930	6.48	0.06	6.48	0.06
	1030	4.77	0.11	4.77	0.11

Table H-9. Standard Deviation of the Vertical Wind Speed ($\phi = \sigma_W$)

Day	Hour	S (sec)	σ_W (m/s)	$\sigma(\sigma_W)$ (m/s)	σ_W^* (m/s)	$\sigma(\sigma_W^*)$ (m/s)
144	1200	2.4	0.535	0.055	0.528	0.055
	1300	2.4	0.429	0.042	0.423	0.041
	1430	3.3	0.372	0.025	0.369	0.025
145	2305	3.0	0.096	0.010	0.095	0.010
146	1130	3.0	0.722	0.052	0.717	0.052

Table H-10. Average Vertical Wind Speed ($\phi = \overline{W}$)

Day	Hour	S (sec)	\overline{W} (m/s)	$\sigma(\overline{W})$ (m/s)	$\overline{W^*}$ (m/s)	$\sigma(\overline{W^*})$ (m/s)
144	1200	2.4	0.166	0.064	0.166	0.064
	1300	2.4	0.184	0.058	0.184	0.058
	1430	3.3	0.209	0.044	0.209	0.044
145	2305	3.0	0.075	0.010	0.075	0.010
146	1130	3.0	0.096	0.071	0.096	0.071

Table H-11. Calculation of p for Sampling Times of 3 min and 60 min

Day	Hour	σ_0 (3 min)	σ_0 (60 min)	p
145	1200	26.903	54.266	0.244
	1300	23.690	50.309	0.251
	1400	24.422	51.092	0.246
	1500	15.592	25.309	0.162
	1600	17.097	29.487	0.182
	1700	18.033	30.891	0.180
	1800	9.061	18.304	0.235
	1900	5.493	11.359	0.243
	2000	2.837	5.054	0.193
	2100	2.121	6.407	0.369
	2200	8.343	54.046	0.624
	146	1650	11.063	19.454
1750		7.029	23.261	0.359
1850		4.950	14.954	0.369
147	0830	16.623	22.184	0.096
	0930	27.929	69.665	0.305
	1030	18.854	42.079	0.268

Mean Value for p = 0.265

Standard Deviation = 0.116

Table H-12. Calculation of p for Sampling Times of 10 min and 60 min

Day	Hour	σ_0 (10 min)	σ_0 (60 min)	p
145	1200	40.723	54.266	0.160
	1300	35.202	50.309	0.199
	1400	39.580	51.092	0.142
	1500	20.367	23.309	0.121
	1600	20.586	29.487	0.201
	1700	26.337	30.891	0.089
	1800	12.585	18.304	0.209
	1900	6.825	11.359	0.284
	2000	3.378	5.054	0.225
	2100	3.618	6.407	0.319
	2200	19.571	54.046	0.567
	146	1650	16.905	19.454
1750		12.357	23.261	0.353
1850		7.388	14.954	0.394
147	0830	19.768	22.184	0.064
	0930	44.445	69.665	0.251
	1030	29.405	42.079	0.200

Mean Value for p = 0.227

Standard Deviation = 0.125

Table H-13. Calculation of p for Sampling Times of 3 min and 10 min

Day	Hour	σ_0 (3 min)	σ_0 (10 min)	p
145	1200	26.903	40.723	0.344
	1300	23.690	35.202	0.329
	1400	24.422	39.580	0.241
	1500	15.592	20.367	0.222
	1600	17.097	20.586	0.154
	1700	18.033	26.337	0.315
	1800	9.061	12.585	0.273
	1900	5.493	6.825	0.180
	2000	2.837	3.378	0.145
	2100	2.121	3.618	0.444
	2200	8.343	19.571	0.708
	146	1650	11.063	16.905
1750		7.929	12.357	0.369
1850		4.950	7.388	0.333
147	0830	16.623	19.768	0.144
	0930	27.929	44.445	0.186
	1030	18.854	29.405	0.369

Mean Value for p = 0.322

Standard Deviation = 0.134

Table H-14. Comparison of the Actual σ_θ to the σ_θ Value Calculated from Eq. (H-11) using $\tau_S=3$ min

Day	Hour	σ_θ (deg.)	
		Actual	Calculated
145	1200	54.3	55.3
	1300	50.3	51.8
	1400	51.1	52.6
	1500	25.3	25.4
	1600	29.5	29.5
	1700	30.9	31.1
	1800	18.3	18.5
	1900	11.4	11.5
	2000	5.1	5.1
	2100	6.4	6.4
	2200	54.0	54.2
146	1650	19.5	19.5
	1750	23.3	23.3
	1850	15.0	15.0
147	0830	22.2	22.2
	0930	69.7	77.9
	1030	42.1	42.2

Table H-15. Comparison of the Actual σ_θ to the σ_θ Value Calculated from Eq. (H-11) using $\tau_S=10$ min

Day	Hour	σ_θ (deg.)	
		Actual	Calculated
145	1200	54.3	54.9
	1300	50.3	50.3
	1400	51.1	49.7
	1500	25.3	25.3
	1600	29.5	29.5
	1700	30.9	31.2
	1800	18.3	18.3
	1900	11.4	11.6
	2000	5.1	5.1
	2100	6.4	6.4
	2200	54.0	54.2
146	1650	19.5	19.5
	1750	23.3	23.3
	1850	15.0	14.9
147	0830	22.2	22.1
	0930	69.7	75.7
	1030	42.1	42.4

Table H-16. Mean Square Along Wind Eddy Velocity ($\phi = \overline{u'^2}$)

Day	Hour	$\overline{u'^2}$	$\sigma(\overline{u'^2})$	$\overline{u'^2*}$	$\sigma(\overline{u'^2*})$
		(m ² /s ²)			
145	1200	0.959	0.125	0.898	0.109
	1300	0.778	0.097	0.741	0.090
	1400	1.440	0.286	1.367	0.276
	1500	0.934	0.135	0.849	0.105
	1600	0.729	0.102	0.667	0.081
	1700	0.576	0.068	0.531	0.051
	1800	0.401	0.046	0.377	0.040
	1900	0.095	0.031	0.078	0.025
	2000	0.026	0.007	0.021	0.004
	2100	0.021	0.004	0.019	0.004
	2200	0.017	0.003	0.015	0.003
146	1650	0.776	0.134	0.697	0.108
	1750	0.356	0.066	0.305	0.043
	1850	0.093	0.015	0.082	0.011
147	0830	0.342	0.065	0.302	0.051
	0930	0.454	0.063	0.412	0.046
	1030	0.700	0.087	0.640	0.063

Table H-17. Mean Square Cross Wind Eddy Velocity ($\phi = \overline{v'^2}$)

Day	Hour	$\overline{v'^2}$ (m ² /s ²)	$\sigma(\overline{v'^2})$ (m ² /s ²)	$\overline{v'^2*}$ (m ² /s ²)	$\sigma(\overline{v'^2*})$ (m ² /s ²)
145	1200	0.764	0.263	0.823	0.256
	1300	0.703	0.168	0.711	0.168
	1400	1.757	0.208	1.830	0.195
	1500	1.026	0.092	1.012	0.091
	1600	0.899	0.102	0.853	0.090
	1700	0.963	0.180	0.991	0.178
	1800	0.308	0.025	0.298	0.023
	1900	0.088	0.061	0.081	0.060
	2000	0.016	0.005	0.013	0.004
	2100	0.007	0.002	0.006	0.001
	2200	0.032	0.007	0.035	0.007
	146	1650	0.840	0.124	0.840
1750		0.310	0.042	0.286	0.035
1850		0.092	0.018	0.080	0.013
147	0830	0.256	0.036	0.242	0.033
	0930	0.345	0.061	0.398	0.030
	1030	0.604	0.071	0.602	0.071

Table H-18. Mean Square Along Wind Eddy Velocity ($\phi = \overline{u'^2}$)
Computed Using a Fixed Mean

Day	Hour	$\overline{u'^2}$ (m ² /s ²)	$\sigma(\overline{u'^2})$ (m ² /s ²)	$\overline{u'^2*}$ (m ² /s ²)	$\sigma(\overline{u'^2*})$ (m ² /s ²)
145	1200	3.122	0.312	3.119	0.312
	1300	2.668	0.202	2.671	0.202
	1400	4.631	0.387	4.626	0.387
	1500	1.795	0.142	1.791	0.142
	1600	2.262	0.207	2.256	0.207
	1700	1.818	0.136	1.816	0.136
	1800	0.691	0.036	0.689	0.036
	1900	0.159	0.037	0.158	0.037
	2000	0.137	0.012	0.137	0.012
	2100	0.109	0.007	0.109	0.007
	2200	0.626	0.022	0.625	0.022
	146	1650	1.819	0.249	1.807
1750		0.910	0.058	0.919	0.058
1850		0.134	0.031	0.133	0.031
147	0830	0.584	0.062	0.582	0.062
	0930	2.000	0.149	1.997	0.149
	1030	2.223	0.196	2.217	0.196

Table H-19. Mean Square Cross Wind Eddy Velocity ($\phi = \overline{v'^2}$)
 Computed Using a Fixed Mean

Day	Hour	$\overline{v'^2}$ (m ² /s ²)	$\sigma(\overline{v'^2})$ (m ² /s ²)	$\overline{v'^2*}$ (m ² /s ²)	$\sigma(\overline{v'^2*})$ (m ² /s ²)
145	1200	2.066	0.203	2.065	0.203
	1300	2.003	0.223	1.999	0.223
	1400	2.686	0.239	2.683	0.239
	1500	1.197	0.159	1.965	0.159
	1600	2.233	0.128	2.235	0.128
	1700	2.393	0.326	2.392	0.326
	1800	1.184	0.065	1.178	0.065
	1900	0.275	0.057	0.273	0.057
	2000	0.045	0.008	0.045	0.008
	2100	0.073	0.005	0.073	0.005
	2200	1.225	0.048	1.224	0.048
	146	1650	2.211	0.139	2.210
1750		2.315	0.149	2.314	0.149
1850		0.633	0.041	0.633	0.041
147	0830	0.383	0.039	0.384	0.039
	0930	1.428	0.080	1.430	0.080
	1030	2.622	0.180	2.625	0.180

APPENDIX I
PRELIMINARY TIME SERIES ANALYSIS

1. INTRODUCTION

It is often possible to describe complex physical phenomena and mechanisms better in the frequency domain than in the time domain. The time dependent nature of air pollution and meteorological data and the likelihood of serial correlation in it makes obvious the need for analyzing such data in terms of its frequency composition.

Many statistical analysis methods that operate on the data in the time domain make no use of the time dependency therein. For example, in the estimation of the frequency or cumulative frequency distributions, the data are sorted into order, after which the time dependency information is no longer available. An important property of time series analysis, on the other hand, is that much of the time dependency in the data is preserved.

The use of time series in the analysis of air pollution monitoring has been suggested or carried out by several authors including: Barlow and Singpurwalla,^{I-1} Saltzman,^{I-2} Marcus,^{I-3} and Tiao and Hamming,^{I-4} to mention only a few.

Data reduction, harmonic analysis, and filtering of Williams air quality data was performed previously on raw data from the HP9825.^{I-8} Spectral analysis was instrumental in identifying certain instrumentation problems that were exhibited by a sawtooth pattern in the raw data. These problems, which were diagnosed early in the experimental program, were subsequently corrected.

An extensive treatment of spectral analysis of time series has been given by Koopmans;^{I-5} time series data analysis and theory are discussed extensively by Brillinger;^{I-6} and a bibliography of time series analysis papers has been given by Wold.^{I-7}

The principal goal of spectrum analysis is to decompose the power of the given time series into its harmonic components, that is, to estimate the power spectrum from the available data. The estimated spectrum can then be used to gain information about the mechanism that generated the data. The statistical theory of spectral analysis has been based on the hypotheses that the underlying process is stationary and Gaussian, that the process mean is zero, and that the spectrum is continuous. Some of the preprocessing operations performed on the data before spectrum analysis is done (for example, removal of the DC component of the series) are intended to bring the data into reasonable conformity with these hypotheses.

Two models of spectral analysis have been used here, univariate and bivariate. Univariate spectral analysis involves the computation of the power spectrum or, as it is also called, the spectral density. The power spectrum is the Fourier transform of the autocorrelation function. The Fourier transform of a sequence of autocorrelations contains precisely the same information found in the original autocorrelations themselves. The intensity of the spectrum at any given frequency provides an estimate of the power or

energy at that frequency. The accumulated spectrum is essentially the first integral of the spectral density and can be used to indicate the range of frequencies that contain a substantial proportion of the total power of the time series.

Similarities between the spectra of two series, such as peaks at similar frequencies, may raise the possibility that the series are related. To investigate such possibilities, the cross spectrum of two series may be computed. This computation is an extension of the definition of the spectrum and is usually estimated by smoothing the cross periodogram; this is performed in the bivariate spectral analysis of two series. Bivariate spectral analysis allows for the decomposition of two series into various spectral parameters, equivalent to descriptive statistics. These include: the estimated spectral density of each series; the phase function that indicates the relative shift of harmonic components of the two time series at the same frequency; the transfer function that indicates the linear relationship between the two series in the same way that regression coefficients relate the linear relationship between two variables; and the coherence function that provides an estimate of the frequency-dependent correlation between two series. It is interesting to note that if the phase angle is a rapidly varying function of frequency, the estimated coherence can be biased downward to an extent that a strong coherence will be masked.

In summary, spectral analysis provides a means of analyzing serial correlations in the data, as well as a method of examining frequency dependent correlations. It is indispensable when searching for periodicity and gross variations of power with frequency in the data.

Spectral analyses were performed on a continuous period of one-hour averages, covering approximately one month, starting August 1, 1976. Missing data and outliers identified by an interface program to the AQAM data tape were assigned values via a simple linear interpolation of adjacent values. Univariate and bivariate spectral analyses were performed using methods outlined by Koopmans.¹⁻⁵ Before spectrum analysis was applied to the data, the mean (DC component) was removed from the series to bring the data into conformity with stationarity.

Figure I-1* shows the time series for observed CO at station 2. While this series appears to exhibit a pronounced 24-hour period, one finds upon close examination that the daily period has slight relative shifts. Where the periodicity is in fact a combination of several other periodic phenomena, closer investigation is required. It is felt that the roughly 24-hour periods are actually beats, and unless the series is filtered, these will not exhibit themselves in the spectrum as at first anticipated.

Figure I-2 shows the spectrum for this time series; the peaks at 16-17 hours, 8 hours, and 6 hours, are of interest. The largest peak at approximately 16 hours is an artifact of the sunrise-sunset period. (Note that this data was drawn from summer months.) Periodicity reflected by peaks at higher frequencies appears to be an artifact of source emissions activity during the day. It is felt that the higher frequencies at 8 and 6 hours may

*Figures appear consecutively at the end of the appendix.

be related to aircraft activity. The x-axis of the spectrum has been replotted in terms of period but was originally computed as a frequency in terms of cycles in units of $1/(2*M*DT)$, where $DT=1$ hour, and M is the truncation parameter that has a value of 100. The truncation parameter, also referred to as the number of lags, controls the smoothing of the periodogram and has been chosen approximately equal to 10% of the data length.

Figure I-3 shows the accumulated spectrum for the CO series. It is interesting to note that the higher frequencies, above the frequencies related to diurnal fluctuation, appear to contribute significantly to the total power of the observed CO series.

Figure I-4 shows the time series for observed NO_x at station 2 during this same period. That the structure of this series is very similar to the CO series is confirmed by the locations of the peaks in the spectral density shown in Fig. I-5. Figure I-6 shows the coherence between the CO and NO_x series. It is interesting to note that while the peak coherence is associated with the diurnal cycle, the coherence remains strong at the higher frequencies, suggesting that these two pollutants may be associated with the same set of sources.

Figure I-7 shows the time series of aircraft CO emissions on ground level lines. This emission rate is computed in AQAM on the basis of the hour-by-hour records of aircraft activity. The spectrum of this series shows the strong diurnally induced peak at 16 hours along with small enhancements at 8 and 6 hours where significant peaks were observed in the observed CO concentration spectrum (Fig. I-2). The coherence between the spectra of observed CO concentrations and aircraft CO emission rate also shows peaks corresponding to these periodicities; however, the wildly oscillating magnitude of the coherence and accompanying phase (not shown) are suggestive of computational instabilities possibly being driven by the strong low-frequency peaking in both spectra.

2. CONCLUSIONS AND RECOMMENDATIONS

While the background concentrations due to strong natural cycles are significant, harmonics at higher frequencies thought to be associated with emissions source activity have been identified. The presence of large peaks in the spectrum, have the effect of badly biasing estimates in the low end of the spectrum due to the inevitable side lobe distortion of the spectral estimates (filter leakage). A quasi difference filter can be used to balance the spectrum of a time series with a large peak at low frequencies. The balancing process is called prewhitening by Blackman and Tukey (1959). I-9 A prewhitening filter can be used to help smooth the larger natural peaks, improving the resolution of the higher frequency spectra.

Spectral analysis can be used to study the effect of filters used on the air quality time series and also in the design of such filters. Filters are used for purposeful modification of a discrete time series. It is important to understand the operation of the filter, and to know how to select the "parameters" of the filter to achieve specific objectives of data modification.

The spectral analyses presented here illustrate the benefits of analyzing time-dependent air quality data in the frequency domain. Estimation of correlation vis a vis the coherence function between two series provides important insights into complex physical systems generating the data, and the ability of the AQAM to reproduce features prevalent in the observations.

REFERENCES

- I-1. Barlow, R.E., and N.D. Singpurwalla, *Averaging Time and Maxima for Dependent Observations*, Proc. of the Symposium on Statistical Aspects of Air Quality Data, EPA-650/4-74-038 (Oct. 1974).
- I-2. Saltzman, B.E., *Fourier Analysis of Air Monitoring Data*, Proc. of the Symposium on Statistical Aspects of Air Quality Data, EPA-605/74-038 (Oct. 1974).
- I-3. Marcus, A.H., *A Stochastic Model for Estimating Pollutant Exposure by Means of Air Quality Data*, Proc. of the Symposium on Statistical Aspects of Air Quality Data, EPA-650/4-74-038 (Oct. 1974).
- I-4. Tiao, G.C., and W.J. Hamming, *A Statistical Analysis of the Los Angeles Ambient Carbon Monoxide Data 1958-1972*, J. of the Air Pollution Control Association, 25:11 (Nov. 1975).
- I-5. Koopmans, L.H., *The Spectral Analysis of Time Series*, Academic Press, New York (1974).
- I-6. Brillinger, D.R., *Time Series Data Analysis and Theory*, Holt, Rinehart and Winston, Inc. (1975).
- I-7. Wold, H.O.A., *Bibliography of Time Series and Stochastic Processes*, Oliver and Boyd, London (1965).
- I-8. Dunphy, E.P., *Diagnostic Investigation of Three Air Pollution Data Tapes from Williams AFB, final report for period 1 June 1976 to 30 July 1976, Letter report for C.E.R.F. Technical Directive 4.04/01.*
- I-9. Blackman, R.B., and J.W. Tukey, *The Measurement of Power Spectra from the Viewpoint of Communications Engineering*, Dover, N.Y., reprinted from Bell System Tech. J 37 (1959).

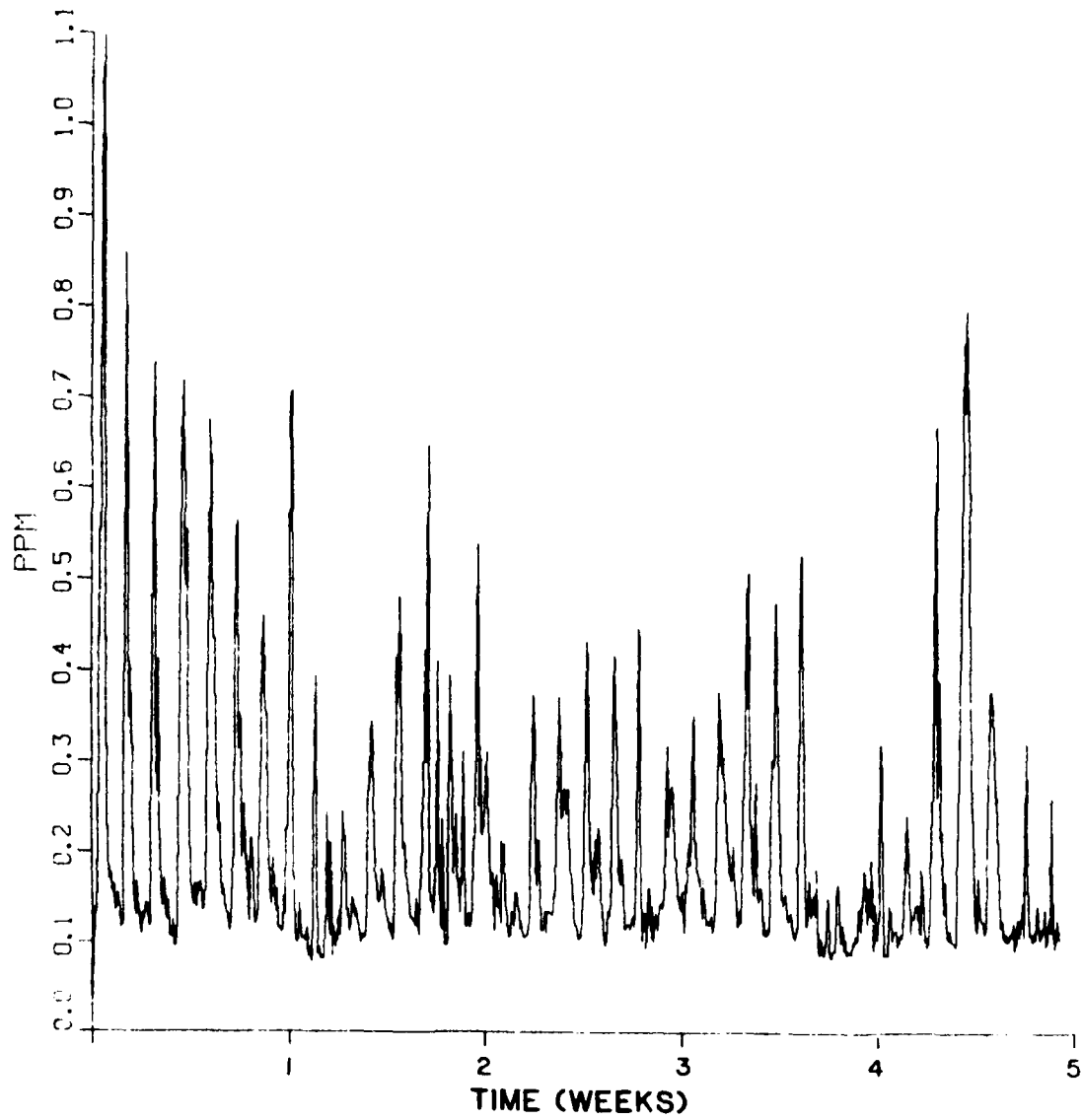


Fig. I-1. Time Series for Observed CO Concentrations at Station 2 during August 1976

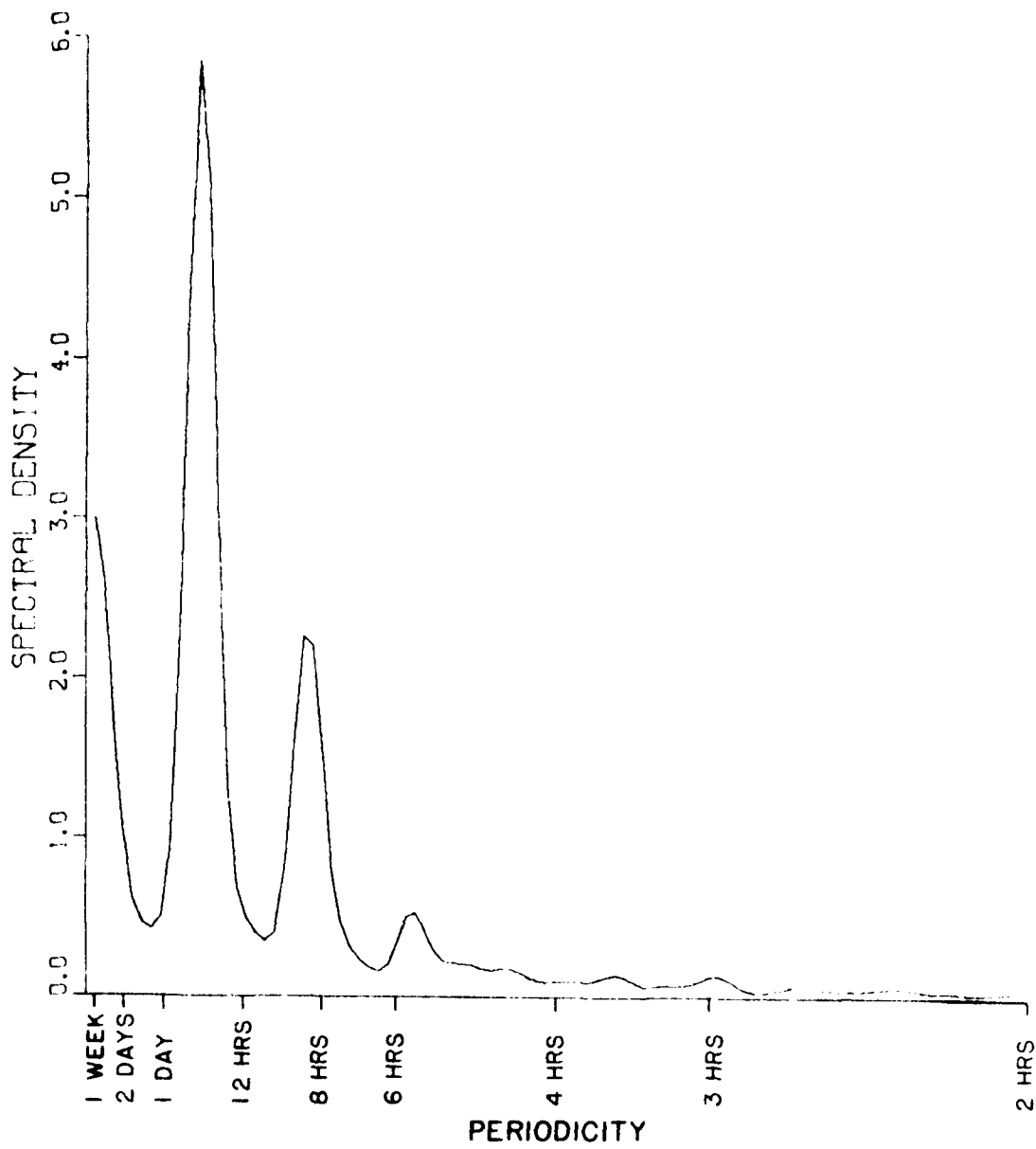


Fig. 1-2. Frequency Spectrum for the Time Series of Observed CO Concentrations at Station 2

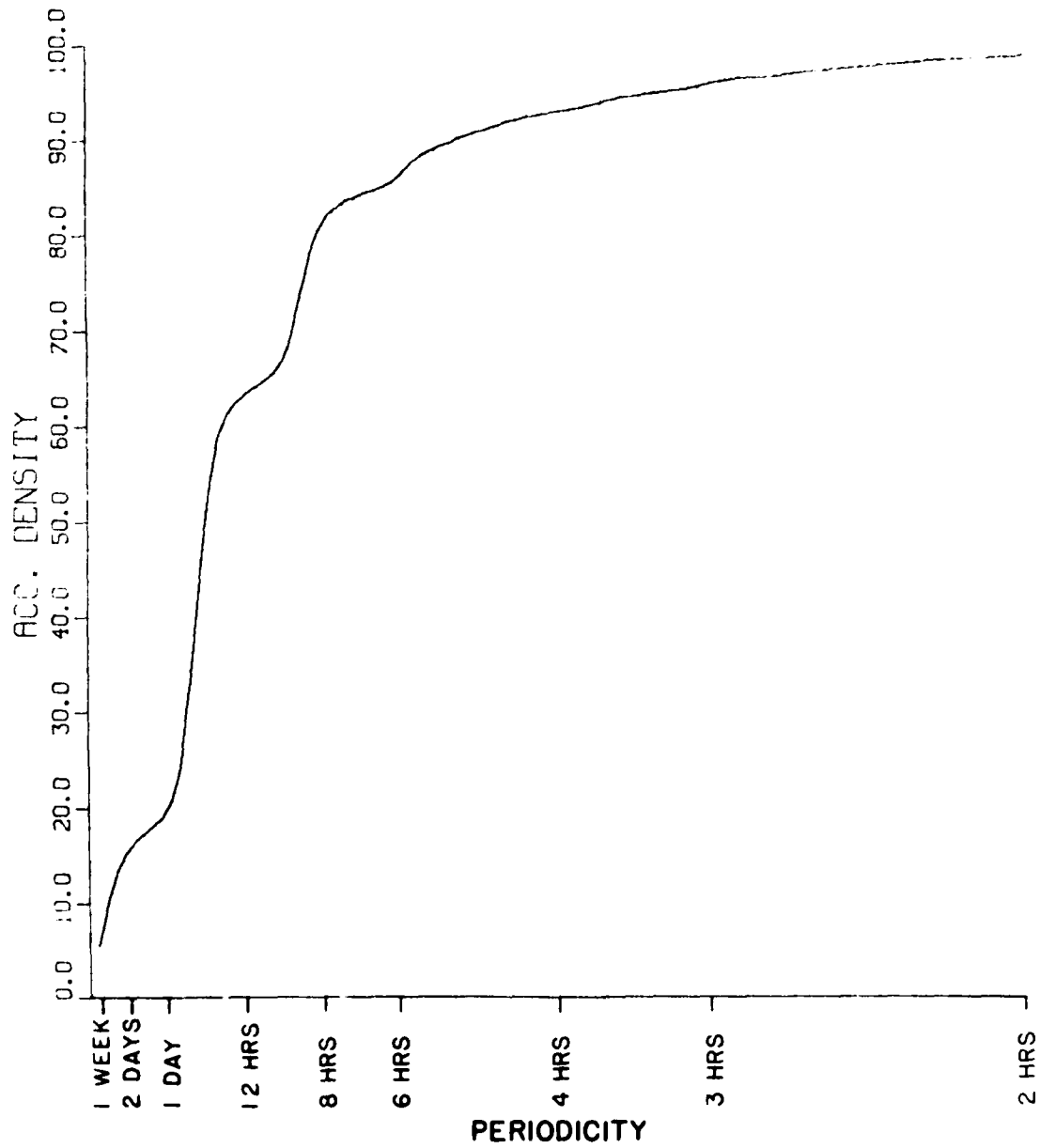


Fig. I-3. Integrated Spectral Density for Observed CO Concentrations at Station 2

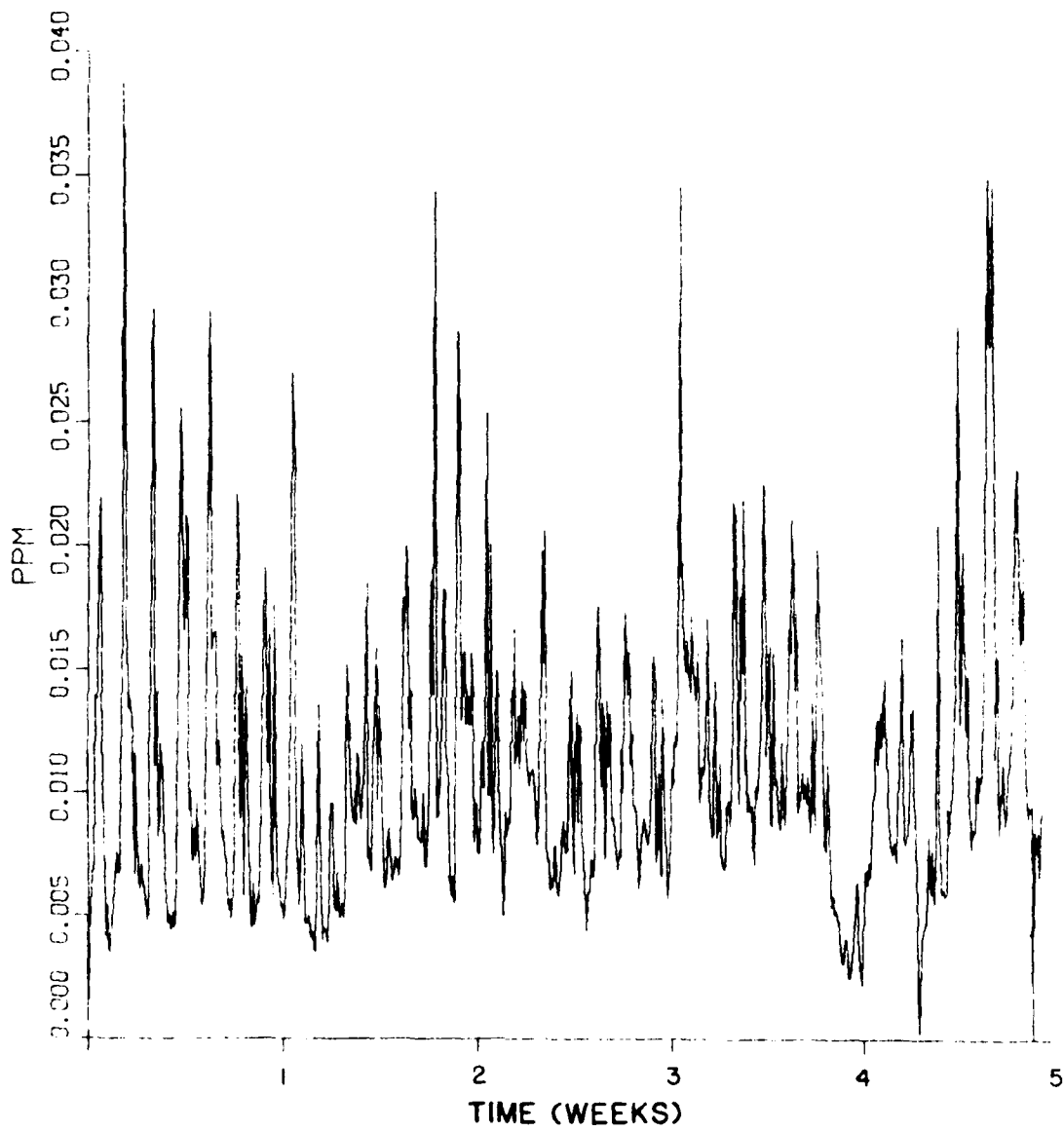


Fig. I-4. Time Series for Observed NO_x Concentrations at Station 2 During August 1976

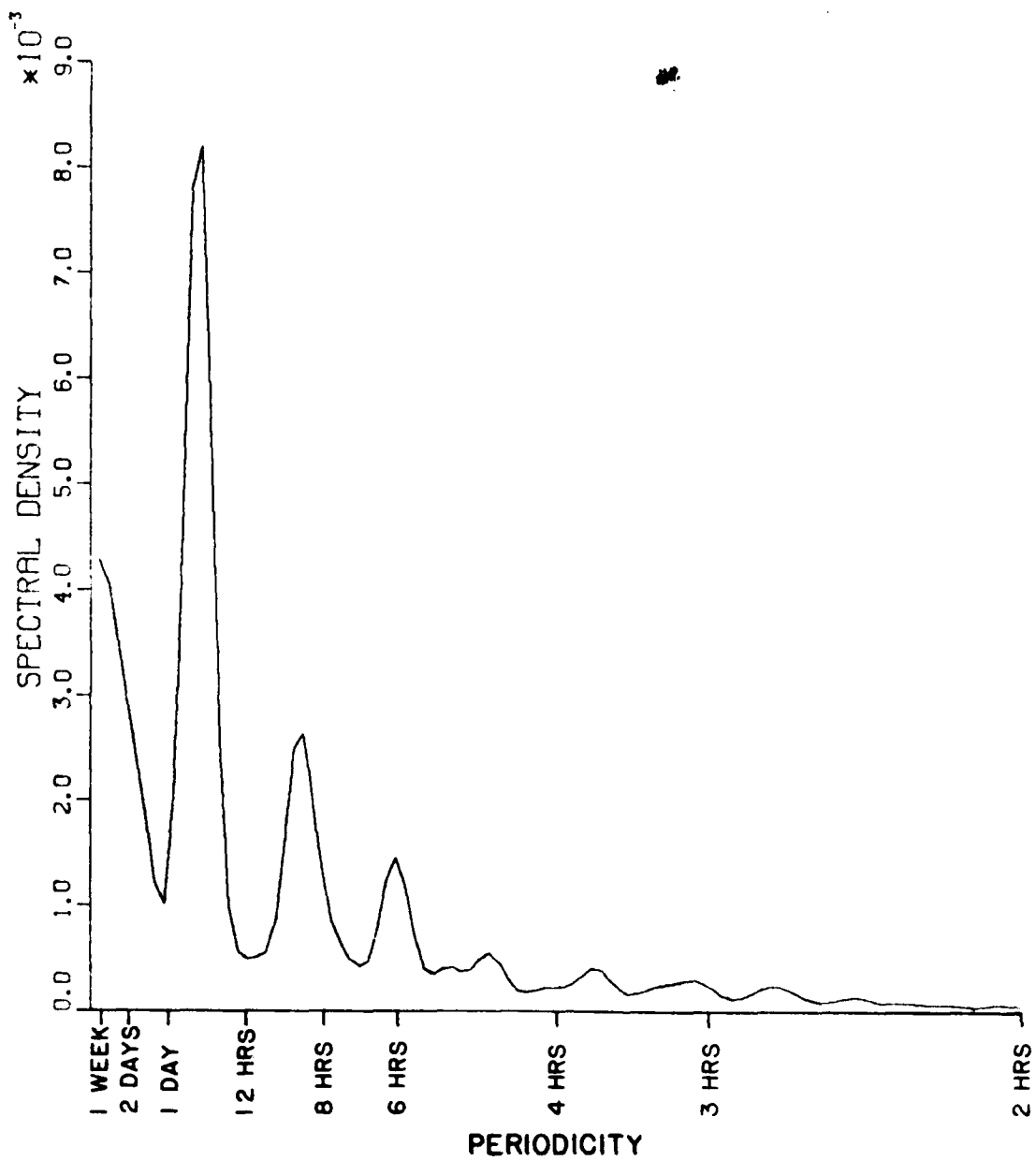


Fig. I-5. Frequency Spectrum for the Time Series of Observed NO_x Concentrations at Station 2

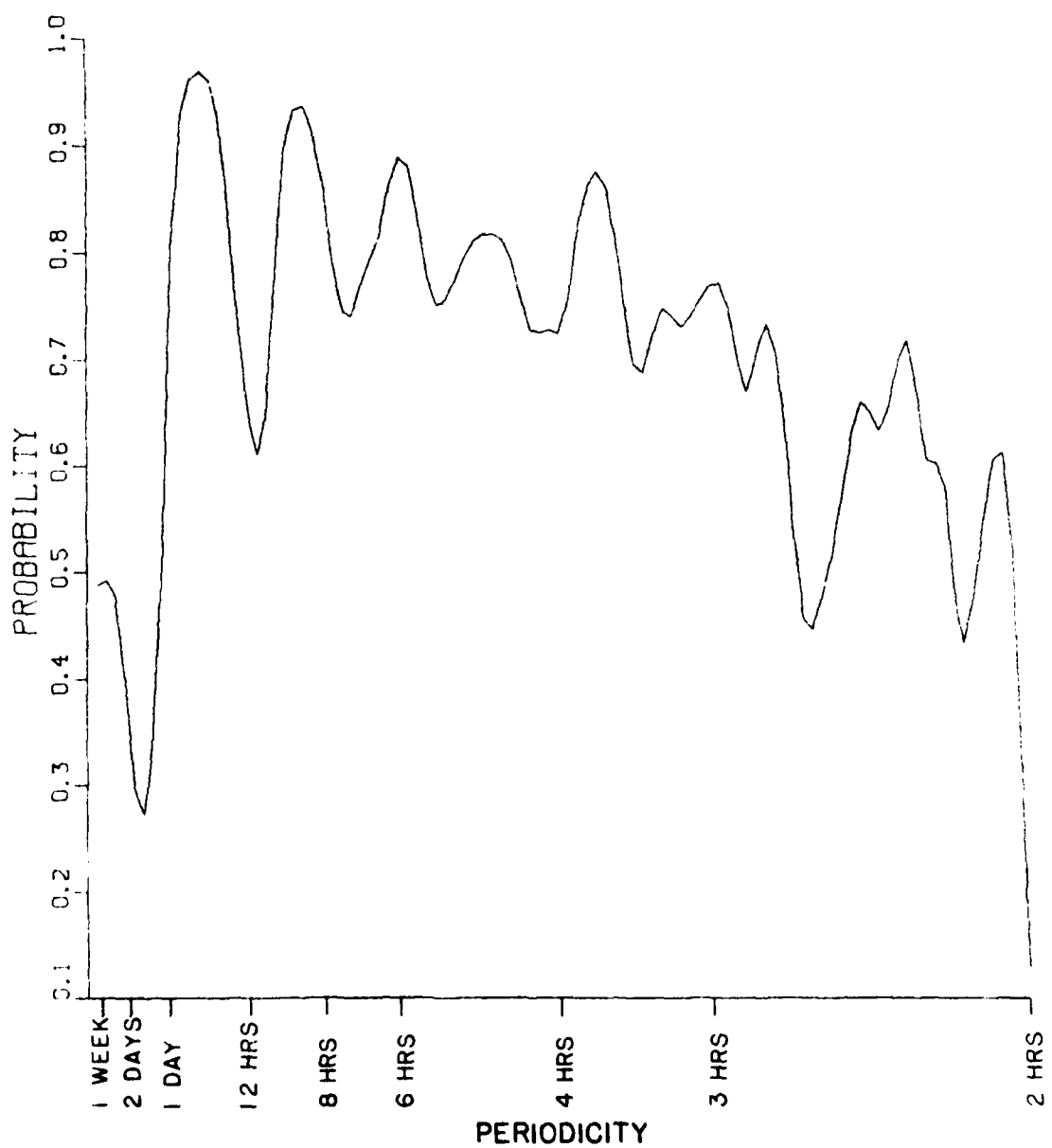


Fig. I-6. Coherence vs Periodicity of the Station 2 Observed CO and NO_x Time Series

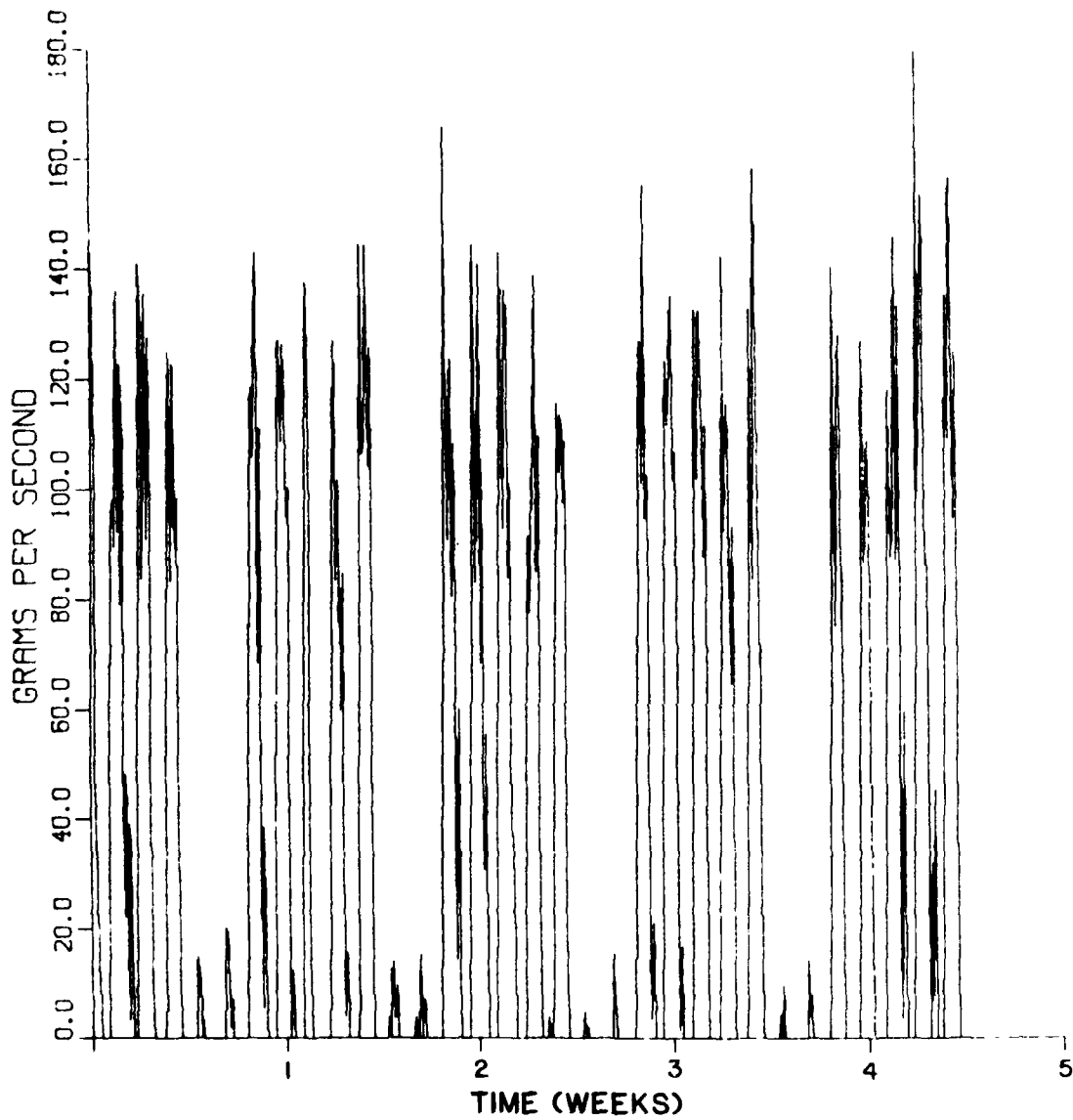


Fig. I-7. Time Series for Aircraft CO Emission Rates on All Ground-Level Lines Based on Actual Hourly Aircraft Operations for August 1976

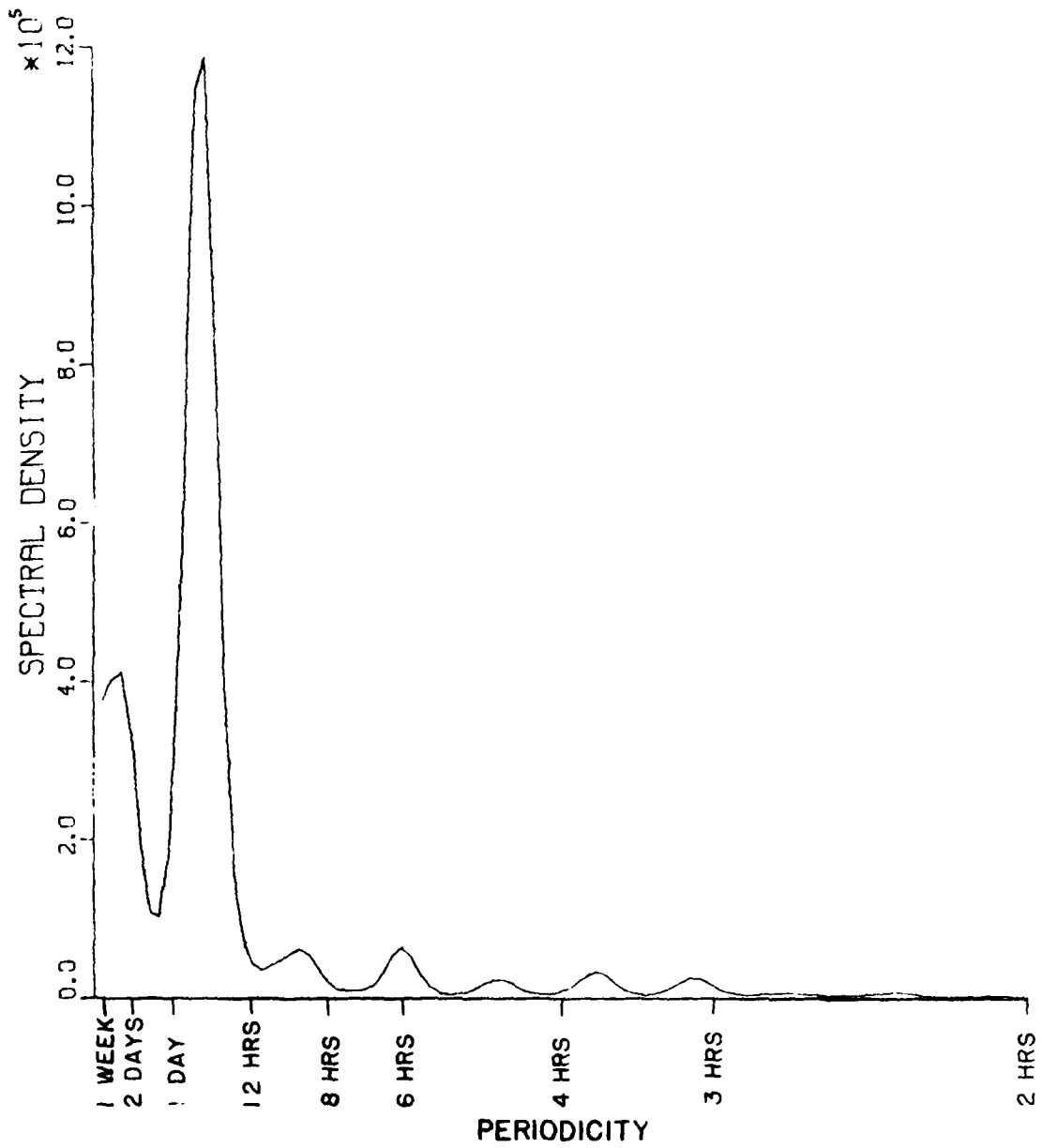


Fig. I-8. Frequency Spectrum for the Time Series of Aircraft CO Emission Rates

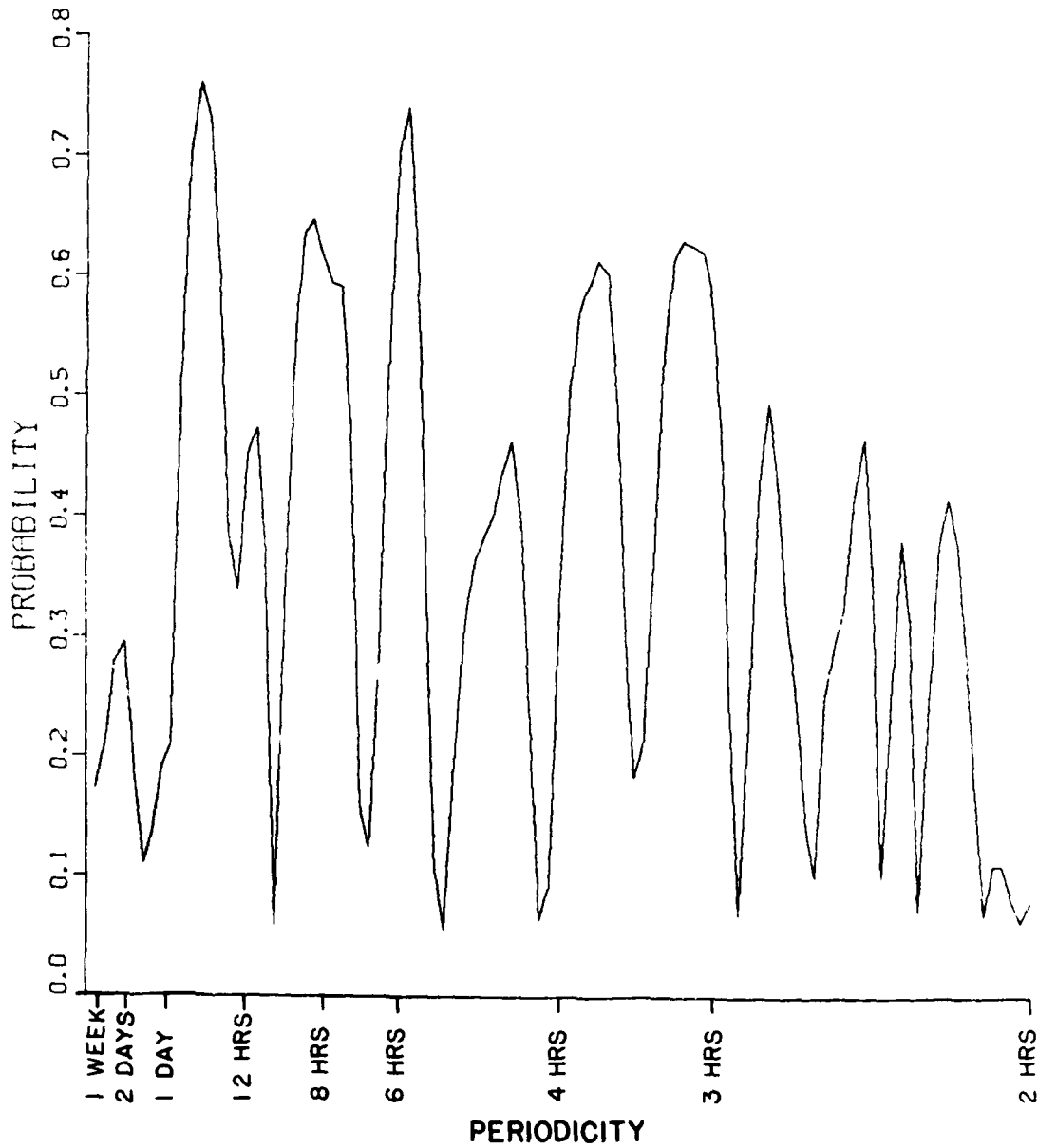


Fig. I-9. Coherence vs Periodicity of the Observed CO at Station 2 and the Aircraft CO Emission Rate Time Series

INITIAL DISTRIBUTION

HQ AFSC/DLW	1
HQ USAF/LEEV	1
HQ TAC/DEEV	1
HQ AFESC/DEV	1
HQ AFESC/TST	1
HQ AFESC/RDVA	4
AUL/LSE 71-249	1
AFATL/DLODL	1
DTIC/DDA	2
OSAF/MIQ	1
OSAF/OI	1
AFIT/Library	1
EPA/ORD	1
FAA (AEE-300)	1
Argonne National Laboratory	1
NAPC/Code PE71: AFK	1